

UNIVERSITY OF BELGRADE
FACULTY OF CIVIL ENGINEERING

Nikola S. Tanasić

**VULNERABILITY OF
REINFORCED CONCRETE BRIDGES TO LOCAL SCOUR
IN BRIDGE MANAGEMENT**

Doctoral dissertation

Belgrade, 2015

УНИВЕРЗИТЕТ У БЕОГРАДУ
ГРАЂЕВИНСКИ ФАКУЛТЕТ

Никола С. Танасић

**УПРАВЉАЊЕ АРМИРАНОБЕТОНСКИМ МОСТОВИМА
У КОНТЕКСТУ ЊИХОВЕ УГРОЖЕНОСТИ ЛОКАЛНОМ
ЕРОЗИЈОМ РЕЧНОГ ДНА**

Докторска дисертација

Београд, 2015

Supervisor: Associate prof. Rade Hajdin, PhD, civ.eng.
Faculty of Civil Engineering, University of Belgrade

Members of the jury: Prof. Miodrag Jovanović, PhD, civ.eng.
Faculty of Civil Engineering, University of Belgrade

Prof. Dan Frangopol, PhD, civ.eng.
Lehigh University, Betlehem, USA

Associate prof. Miloš Lazović, PhD, civ.eng.
Faculty of Civil Engineering, University of Belgrade

Associate prof. Rade Hajdin, PhD, civ.eng.
Faculty of Civil Engineering, University of Belgrade

Associate prof. Mirjana Vukićević, PhD, civ.eng.
Faculty of Civil Engineering, University of Belgrade

Defense date: _____

Ментор: Др. Раде Хајдин, дипл.инг.грађ, ванредни професор
Грађевински факултет, Универзитет у Београду

Чланови комисије: Др. Миодраг Јовановић, дипл.инг.грађ, редовни
професор у пензији, Грађевински факултет,
Универзитет у Београду

Др. Дан Франгопол, дипл.инг.грађ, редовни професор
Лихај Универзитет у Бетлејему, САД

Др. Милош Лазовић, дипл.инг.грађ, ванредни
професор у пензији, Грађевински факултет,
Универзитет у Београду

Др. Раде Хајдин, дипл.инг.грађ, ванредни професор
Грађевински факултет, Универзитет у Београду

Др. Мирјана Вукићевић, дипл.инг.грађ, доцент
Грађевински факултет, Универзитет у Београду

Датум одбране: _____

Acknowledgement

At the time I started the work on my thesis, I was a PhD student with a three-year engineering experience and employed as a teaching assistant at the Chair for concrete structures at the Faculty of Civil Engineering in Belgrade. However, I was inexperienced in research, and for some topics, which comprised my thesis, have had only elementary knowledge. Here the professional guidance of my supervisor Professor Rade Hajdin had significant contribution and helped me to cope up with the new matter. I am honestly grateful for his time, efforts, advices and patience over the four years as well as for a few books that I got as a present.

I am especially grateful to my parents for their unconditional support and to my wife Milja who followed me every step of the way, making sure I did not lack motivation in reaching the goal.

I would like to thank all members of the jury for the review of the thesis, their suggestions and comments.

The thesis was supported by the Serbian Ministry of Education, Science and Technological Development through the TR-36002 research project.

VULNERABILITY OF REINFORCED CONCRETE BRIDGES TO LOCAL SCOUR IN BRIDGE MANAGEMENT

Abstract

The road infrastructure around the world is impaired by natural hazards, in particular with extreme flooding, which sever the road links and lead to serious socio-economic consequences. The bridges, which are the most critical parts of road links, are threatened even by less extreme floods with high occurrence rates. The local scour at bridge substructures associated with floods is regarded as the predominant cause of hazard triggered failures. Although the management of bridges exposed to flooding is not a new topic and has been extensively elaborated in the last 20 years, the current Bridge Management Systems still cannot account for sudden events such as the local scour. The current procedures, which usually rest on qualitative approaches and regular inspections, do not give satisfactory results in scheduling the appropriate risk reducing interventions. The evaluation of real-time risk changes associated to this hazard is deemed necessary.

The topic of the thesis is to present the basis of the novel methodology for quantitative vulnerability assessment of reinforced concrete bridges with shallow foundations exposed to local scour. Here, the accent is set on the estimation of the conditional probability of a bridge failure due to a scouring event, while the related consequences are beyond the scope of the thesis. Based on the scour critical bridges in the Serbian road network, the reinforced concrete bridge types which are considered in the analysis have multiple span double-tee main girders on common pier-foundation systems.

In order to solve the multidisciplinary problem of local scour action at bridge piers and associated failures, it was essential to develop a typical bridge model and framework with a modest data set for its simple yet accurate analysis. As the general approach to analyze possible failure modes and consequently obtain the probability of bridge failure, the water-soil-bridge interaction is suggested. In addition, the perfectly rigid plastic behavior of soil and bridge is assumed to apply the upper bound theorem of the theory of plasticity.

The first step in the analysis is the approximation of the local scour action and here the choice of the appropriate local scour formula is discussed based on the state-of-the-art research on pier scour, giving the advantage to the formulas that may consider temporal aspect. The scour cavities beneath the common pier-foundation systems are given by the time-dependant local scour depth and their geometry is approximated in order to simplify the local scour action to a plane strain problem. The second step in the analysis is evaluation of supporting soil and bridge resistances to the approximated scour cavities. The cavities' influence on the decrease of a bearing capacity of the supporting soil at an affected pier is considered with basic kinematic mechanisms which are based on soil properties. The bridge resistance is given by plastic strengths of its elements, which is based on structural system properties and reinforcement detailing.

The soil-bridge model is defined, and separately for its longitudinal and lateral direction, the adopted kinematic mechanisms in the supporting soil are coupled with the possible failure modes of the bridge superstructure to reveal combined failure modes. These are consequently used in the optimization procedure, where the resistance of the model to local scour action is obtained as the ultimate horizontal scour extent beneath a shallow foundation.

The uncertainties related to parameters used in the local scour evaluation, soil properties and bridge elements' properties are discussed as the essential topic in calculation of the conditional probability of a bridge failure relying on the state-of-the-art research. In the example of a four span continuous bridge over a river channel, the conditional probabilities of the bridge failure are estimated in Monte Carlo simulations for four scenarios. Here, the limit state function accounts time-dependant local scour depths and the resistance of the assumed soil-bridge model to local scour action at the affected bridge pier.

The presented soil-bridge model clarifies the behavior of multiple span reinforced concrete girder bridges with shallow foundations in a scouring event. It sets the upper bound of the local scour extent at bridge piers necessary to trigger a failure. Here, in the calculation of the conditional probability of a bridge failure due to local scour, the combined resistance of the supporting soil and the bridge structure to local scour action is included as the essential ingredient, which has not been done in the

up-to-date research. The suggested methodology for quantitative vulnerability assessment provides a basis for development of vulnerability maps for road networks in respect to extreme flooding. These maps are going to be especially useful for unambiguous allocation of resources for mitigating the threat from future flooding events and issuing timely warnings in the regions where intensive flooding is expected.

Keywords: local scour, reinforced concrete bridges, bridge database, vulnerability assessment, water-soil-bridge interaction, combined soil-bridge failure modes, conditional probability of a bridge failure, Bridge Management Systems

Field of science: Civil and Structural Engineering

Subdivision: Concrete structures

UDC number: 624.012.3/.4(043.3)

УПРАВЉАЊЕ АРМИРАНОБЕТОНСКИМ МОСТОВИМА У КОНТЕКСТУ ЊИХОВЕ УГРОЖЕНОСТИ ЛОКАЛНОМ ЕРОЗИЈОМ РЕЧНОГ ДНА

Резиме

Путна инфраструктура широм света је угрожена природним непогодама, посебно са екстремним поплавама, које доводе до прекида путних праваца а самим тим и до озбиљних социо-економских последица. Мостови као најкритичнији сегменти путних праваца су угрожени чак и са не тако екстремним поплавама које имају велику учесталост догађања. Локална ерозија речног дна код доњег строја мостова која се догађа у поплавама је највећи узрок отказа и оштећења мостова изазваних природним непогодама. Иако тема управљања мостовима који су изложени поплавама није нова и значајно је обрађивана у предходних 20 година, данашњи Системи Управљања Мостовима и даље не узимају у обзир изненадне екстремне догађаје као што је локална ерозија речног дна. Овај проблем се у данашњој пракси углавном третира квалитативним приступом који се ослања на базу података мостова и регуларне инспекције, међутим то не даје задовољавајуће резултате и оцена промене ризика од екстремних поплава у реалном времену се сматра неопходним.

Тема ове тезе је представљање основе за нову методологију за квантитативну оцену угрожености армиранобетонских мостова са плитко фундираним темељима изложених локалној ерозији речног дна. Акцент је стављен на одређивање условне вероватноће лома моста услед локалне ерозије речног дна док последице оваквог догађаја нису разматране у оквирима тезе. Базирајући се на мостовима који су угрожени ерозијом речног дна у путној мрежи Србије, разматрани су континуални гредни армиранобетонски мостови са главним носачем који има попречни пресек дуплог слова Т.

Приликом решавања мултидисциплинарног проблема отказа моста услед локалне ерозије речног дна код стубова, било је неопходно дефинисати типични модел тло-мост и поступак са ограниченим бројем улазних података потребних за његову упрошћену али довољно прецизну анализу. Овде је као општи приступ за анализу могућих механизма лома модела и одређивање условне вероватноће лома разматрана интеракција вода-тло-мост и претпостављено је круто-пластично

понашање елемената модела како би се применила горња теорема теорије пластичности.

Први корак у анализи је поједностављење начина деловања локалне ерозије речног дна око мостовских стубова и овде је разматрана могућност примене формула за евалуацију локалне речне ерозије у оцени угрожености мостова, ослањајући се на савремена истраживања. Предност је дата оним формулама које могу узети у обзир раст дубине ерозије у току времена. Геометрија еродираног тла око и испод мостовских стубова је упрошћена тако да се начин деловања локалне ерозије на конструкцију може посматрати кроз равански проблем. Други корак у анализи је прорачун отпорности ослоначког тла и мостовске конструкције на усвојену упрошћену геометрију поткопавања код стубова. Овде је смањење граничне носивости тла моделирано уз помоћ основних кинематичких механизма који се заснивају на геотехничким својствима тла и узимају у обзир геометрију поткопавања. Отпорност мостовске конструкције је узета у обзир преко пластичне носивости њених елемената, одређене на основу карактеристика конструктивног система моста и детаља армирања.

За дефинисан модел тло-мост, посебно за подужни и попречни правац моста, одређују се комбиновани механизми отказа тако што се доводе у везу усвојени кинематички механизми за тло и механизми лома горњег строја моста. Комбиновани механизми се потом користе у оптимизационој процедури где је максимална отпорност модела тло-мост одређена као највећи хоризонтални домет поткопавања локалне ерозије речног дна код мостовског стуба.

Неизвесности код одређивања параметара потребних код евалуације локалне речне ерозије, карактеристика тла и носивости елемената мостовске конструкције су разматране на бази савремених истраживања као главна тема при прорачуну условне вероватноће отказа моста. На примеру континуалног моста на четири поља који прелази преко реке, срачунате су условне вероватноће лома моста у Монте Карло симулацијама за четири сценарија. Овде је у граничној функцији узета у обзир временски зависна дубина локалне ерозије и отпорност модела тло-мост на ширење зоне поткопавања код мостовског стуба.

Представљени модел тло-мост разјашњава понашање плитко фундираних континуалних гредних армиранобетонских мостова изложених деловању локалне ерозије речног дна и даје горњу границу простирања ерозије код мостовских стубова која доводи до отказа конструкције. Као есенцијална компонента за анализу угрожености, разматрана је комбинована отпорност ослоначког тла и мостовске конструкције на локалну ерозију речног дна, што није било тема предходних научних истраживања. Представљена методологија за квантитативну оцену угрожености представља основу за развој мапа угрожености путних мрежа у екстремним поплавама. Ове мапе ће посебно бити корисне код управљања ресурсима за ублажавање ризика од поплава као и за издавања раних упозорења на опасност у подручјима где се очекују поплаве великог интензитета.

Кључне речи: локална речна ерозија, армиранобетонски мостови, база података мостова, оцена угрожености, интеракција вода-тло-мост, комбиновани механизми лома тло-мост, условна вероватноћа отказа моста, системи управљања мостовима

Научна област: Грађевинарство

Ужа научна област: Бетонске конструкције

УДК број: 624.012.3/.4(043.3)

Table of Contents

Acknowledgement.....	i
Abstract.....	ii
Резиме.....	v
Table of Contents	viii
List of Figures.....	xi
Notation.....	xvi
Chapter 1. Introduction and literature review	1
1.1 Motivation	1
1.2 Existing methodologies for scour criticality assessment.....	10
1.2.1 The U.S. national scour evaluation program.....	12
1.2.2 The HYRISK methodology.....	15
1.2.3 Risk-Based Management Guidelines for Scour at Bridges with Unknown Foundations.....	16
1.2.4 New York state department of transportation – Hydraulic Vulnerability Manual.....	19
1.2.5 The software for risk assessment of bridges.....	21
1.3 Treatment of scour in bridge databases	22
1.3.1 Bridge information database in Serbia (“Baza Podataka Mostova”)	23
1.4 Literature review of the research on vulnerability and risk assessment of bridges exposed to local scour.....	25
1.4.1 Conclusion of the literature review	28
1.5 Thesis outline.....	29
Chapter 2. Vulnerability of bridges exposed to local scour and Water-Soil-Bridge interaction	31
2.1 The methodology for quantitative vulnerability assessment of bridges exposed to local scour.....	31
2.1.1 Bridge vulnerability to local scour	32
2.2 Bridge failure modes due to local scour	35
2.3 The analysis approach	40

2.3.1	The limit analysis method and the upper bound theorem.....	41
Chapter 3.	Local scour evaluation	46
3.1	The local scour action at bridge piers.....	46
3.1.1	The local scour evaluation formulas.....	48
3.1.2	Bridge site complications affecting local scour depth.....	57
3.1.3	Debris effect in the scouring event.....	58
3.1.4	Local scour cavity form.....	60
3.1.5	Temporal aspect of scour.....	62
3.2	The application of the state-of-the-art local scour formulas in the vulnerability assessment.....	63
Chapter 4.	Elements of the Soil-Bridge model and resistances of a bridge and supporting soil to local scour action	65
4.1	Scour critical bridges in the BPM.....	65
4.1.1	Pier-foundation systems	67
4.1.2	Bridge joints	68
4.2	Redistribution of forces in a soil-bridge system due to local scour action.....	70
4.3	The approximation of local scour cavities at bridge piers.....	72
4.4	The resistance of supporting soil to local scour action.....	73
4.5	The resistance of bridge elements to local scour action	81
Chapter 5.	Analysis of the Soil-Bridge Models	85
5.1	The soil-bridge model.....	85
5.2	Combined failure modes in the longitudinal direction	88
5.3	The optimization procedure.....	93
5.4	Analysis of a soil-bridge model in the longitudinal direction – An example.....	95
5.5	Additional comments on the <i>CFM</i> -s in longitudinal direction.....	104
5.6	Combined failure modes in the lateral direction	105
5.7	Analysis of a soil-bridge model in the lateral direction – An example.....	110
5.8	Failure modes without the soil failure	113
Chapter 6.	Probability of bridge failure due to local scour action.....	114
6.1	The crude Monte Carlo and quasi Monte Carlo analysis	114
6.2	The uncertainties in the vulnerability assessment of bridges to local scour.....	116

6.2.1	The uncertainties in the local scour evaluation	117
6.2.2	The uncertainties of soil geotechnical properties	120
6.2.3	The uncertainties related to the bridge structure	123
6.3	The limit state function.....	125
6.4	The probability of bridge failure due to local scour by considering the WSB interaction – An example	126
6.5	Review of the governing parameters in the procedure for estimation of the probability of a bridge failure due to local scour action.....	133
6.6	Application of the presented methodology for quantitative vulnerability assessment.....	135
Chapter 7. Conclusion		138
7.1	The summary of the realized work	138
7.2	Potential for further research	141
References.....		144

List of Figures

Fig. 1.1 Bridge failures in the Kanto region, Japan, 1998, [Fukui and Nishitani, 2002] .	1
Fig. 1.2 Gupo bridge on the Nakdong river, South Korea, 2003, [Ji and Julien 2005]....	2
Fig. 1.3 Bridge failures during the typhoon Morakot, Taiwan, 2009.....	2
Fig. 1.4 Bridge failures in the USA from 1966-2005, after [Briaud, 2006].....	3
Fig. 1.5 The collapses of the Schoharie Creek Bridge, 1987 (left) and Hatchie River Bridge, 1989 (right), USA	3
Fig. 1.6 Bridge failures in the UK from 1846 to 2003, [JBA, 2004]	4
Fig. 1.7 Northside Bridge prior and after the failure, Workington, UK, 2009.....	4
Fig. 1.8 Wairoa Bridge failure, New Zealand, 1988, [Wairoa, n.d.].....	5
Fig. 1.9 Collapse of the Hintze Ribeiro bridge, Portugal, 2001, [Figueiredo et al., 2013]	5
Fig. 1.11 Failure of the bridge on the river Filyos, northern Turkey, 2012	6
Fig. 1.10 Failure of the St.Adolph Bridge, Winnipeg, Canada, 2009	6
Fig. 1.12 Failure of the bridge across Rambla de Béjar, Spain, 2012.....	7
Fig. 1.13 Bonneybrook bridge collapse in Calgary, Canada, 2013.....	7
Fig. 1.14 Bridge failures near Dorgali (left) and Olbia (right), Sardinia, 2013	7
Fig. 1.15 Bridge failure, Lešak, southern Serbia, 2013.....	8
Fig. 1.16 Bridge failure near Kraljevo (left) and scour-critical bridge near Vranje (right), Serbia, 2014.....	8
Fig. 1.17 Damaged bridge pier, Lešak, southern Serbia, 2014	8
Fig. 1.18 Bridge failure, Topola, central Serbia, 2014.....	9
Fig. 1.19 Bridge failure, Draginac, central Serbia, 2014.....	9
Fig. 1.20 Bridge failure, Koceljeva, western Serbia, 2014.	9
Fig. 1.21 Evaluation of the vulnerability rating score, adapted from [NYSDOT, 2003]	21
Fig. 2.1 Scour reduces pier support, adapted from [Ettema et al., 2011].....	35
Fig. 2.2 Observed bridge failure modes, adapted from [Briaud et al., 2010].....	36
Fig. 2.3 Forces acting upon a river bridge pier, [Frederico, 2010]	37
Fig. 2.4 Pier sinking due to local scour, [Tanasic et al., 2013]	38
Fig. 2.5 Bridge failure due to local scour, [Tanasic et al., 2013].....	38
Fig. 2.6 The local scour cavity at a strip footing, [Tanasic and Hajdin, 2014].....	39
Fig. 2.7 WSB interaction- bridge pier model, [Tanasic and Hajdin, 2014]	39
Fig. 2.8 Stress-strain relationship for ideal and real soils, [Chen, 1975]	41
Fig. 2.9 Perfectly plastic material behavior.....	42
Fig. 2.10 Perfectly plastic assumption for RC behavior, [Monotti, 2004].....	43
Fig. 2.11 The flow rule i.e. normality condition for general soil, [Chen, 1975].....	44

Fig. 2.12 The yield criterion and normality conditions for RC plates, [Vrouwenvelder and Witteveen, 2003]	44
Fig. 3.1 Local scour at cylindrical pier, [FDOT, 2010]	47
Fig. 3.2 Local scour depth at pier in a sand-bed stream as a function of time, [Richardson and Davis, 2001]	48
Fig. 3.3 Variables influencing pier scour, [Ettema et al. 2011]	49
Fig. 3.4 Variables influencing erodibility (left), critical shear stress versus soil grain diameter (right), [Briaud et al., 2003]	50
Fig. 3.5 A result of an EFA-test, adapted from [Briaud et al., 2003].....	53
Fig. 3.6 Suggested erosion categories for soils and rocks based on velocity and shear stress, [Briaud et al., 2009].....	54
Fig. 3.7 EFA test data for low plasticity clays, based on velocity and plotted on the erosion function chart, [Briaud et al., 2009]	54
Fig. 3.8 Equilibrium scour depth with flow intensity ($y/a^* > 3$, $a^*/D50 = \text{const}$), [Sheppard et al, 2011]	56
Fig. 3.9 Scour depth variation in the four cases of non-uniform pier shape, [Melville and Coleman, 2000]	58
Fig. 3.11 Idealized flow patterns at pier, [Lagasse et al., 2010].....	59
Fig. 3.12 Differences in scour form at a cylindrical pier, [Ettema et al., 2011].....	60
Fig. 3.13 Bed hydraulic shear stress around rectangular pier B/L, [Briaud et al., 2003].....	61
Fig. 3.14 Model of a bridge pier (left) and the experiment setup (right), [Yao et al., 2010].....	61
Fig. 3.15 Local scour depth variation with flow intensity and time, [Melville and Coleman, 2000]	62
Fig. 4.1 Pier-foundation system configurations used in the analysis	67
Fig. 4.2 Observed typical footing failures due to scour [Agrawal et al., 2007]	68
Fig. 4.3 Two examples of bearing layouts for a two-span bridge	69
Fig. 4.4 Possible loading cases on steel reinforced elastomeric pads [Mtenga, 2007] ..	70
Fig. 4.5 Schematics of a double-neck concrete RC bearing at an abutment	70
Fig. 4.6 Case of a possible redistribution of forces in a soil-bridge system due to the local scour action at a pier	71
Fig. 4.7 Approximation of the local scour cavities for different types of pier/foundation system	72
Fig. 4.8 Kinematic mechanism in soil for centrally loaded strip footing	73
Fig. 4.9 Three-dimensional failure envelope for shallow foundations on cohesive soil under combined load and moments, [Tiebat and Carter, 2000]	75
Fig. 4.10 Upper-bound solutions for combined loading on footings on homogenous clay: a) Zero underbase suction and b), c) full underbase suction, [Ukrichton et al., 1998]	75

Fig. 4.11 Failure modes of a strip footing affected by combined loading, adapted from [Michailowski and You, 1998].....	76
Fig. 4.12 Assumed KMS at a strip footing affected by the local scour cavity.....	78
Fig. 4.13 Ultimate sagging and hogging plastic moments for the double-tee main girder	81
Fig. 4.14 Plastic bending strength of a RC circular section at a pier top	84
Fig. 5.1 The soil-bridge model	86
Fig. 5.2 Possible distributions of the bending moment resistance in the main girder....	87
Fig. 5.3 Superstructure failure modes in the longitudinal direction.....	89
Fig. 5.4 Connection of the KMS 2 and pier foundation system in a combined mechanism.....	90
Fig. 5.5 Combined soil/structure Failure Mechanisms (CFM) soil-bridge model in the longitudinal direction	93
Fig. 5.6 Combined failure modes for the BT 1	96
Fig. 5.7 Influence of soil internal friction angle on the results for the BT 1.....	97
Fig. 5.8 Influence of cohesion to results for the BT 1	97
Fig. 5.9 Combined failure modes for BT 2	98
Fig. 5.10 Influence of soil internal friction angle to results for BT 2	98
Fig. 5.11 Influence of cohesion to results for BT 2.....	98
Fig. 5.12 Combined failure modes for BT 3	99
Fig. 5.13 Influence of soil internal friction angle to results for BT 3	99
Fig. 5.14 Influence of cohesion to results for BT 3.....	99
Fig. 5.15 The resistances of the four bridge types to assumed local scour action	100
Fig. 5.16 The influence of the maximum assumed local scour cavity on the KMS 3- cases of frictional soil (left) and cohesive soil (right).....	102
Fig. 5.17 Influence of the maximum local scour cavity for BT 1	102
Fig. 5.18 Influence of the maximum local scour cavity for BT 1 and purely frictional soil.....	103
Fig. 5.19 The influence of the maximum local scour cavity for BT 1 and purely cohesive soil	103
Fig. 5.20 A possible combined failure mode for bridge with a pier on caisson foundation.....	104
Fig. 5.21 Failure modes of the pier frame	106
Fig. 5.22 Possible failure pattern of the superstructure - <i>DFP 1</i>	108
Fig. 5.23 Possible failure pattern of the superstructure - <i>DFP 2</i>	110
Fig. 5.24 The lateral combined failure modes.....	111
Fig. 5.25 The influence of internal friction angle on the lateral combined failure modes	112
Fig. 5.26 The influence of cohesion on the lateral combined failure modes	112

Fig. 5.27 The influence of the pier reinforcement ratio on the lateral combined failure modes	113
Fig. 5.28 Example of bridge failure solely governed by inadequate reinforcement	113
Fig. 6.1 Concept of generation of random variable x_j by uniform random number u_j based on the inverse transformation [Phoon, 2008].....	115
Fig. 6.2 Pseudo number generation (left) compared to quasi random number generation (right) for 1000 random numbers generated in two-dimensional space [Phoon, 2008]	116
Fig. 6.3 Example of an erosion plot based on velocity [Briaud, 2008] (left); Approximation of the experimental data - the erosion rate function (right) ...	119
Fig. 6.4 Inherent soil variability [Phoon and Kulhawy, 1999].....	121
Fig. 6.5 Comparison between finite element computations of bearing capacity for a uniform and heterogeneous soil deposit, adapted from [Popescu et al., 2005]	122
Fig. 6.6 Limit state function for estimation of the probability of bridge failure due to local scour action at shallow foundations.....	125
Fig. 6.7 The example of a multiple span continuous girder bridge crossing a trapezoidal water channel.....	127
Fig. 6.8 PDF-s and CDF-s of the local scour depths (FDOT) at the Pier 2, sub-case A1	129
Fig. 6.9 PDF-s and CDF-s of the local scour depths (FDOT) at the Pier 2, sub-case B1	129
Fig. 6.10 PDF-s and CDF-s of the local scour depths (HEC-18 clay) at the Pier 2, sub-case A2	129
Fig. 6.11 PDF-s and CDF-s of the local scour depths (HEC-18 clay) at the Pier 2, sub-case B2	129
Fig. 6.12 PDF-s and CDF-s of the soil-bridge model resistance at Pier 2, sub-case A1	130
Fig. 6.13 PDF-s and CDF-s of the soil-bridge model resistance at Pier 2, sub-case A2	130
Fig. 6.14 PDF-s and CDF-s of the soil-bridge model resistance at Pier 2, sub-case B1.....	130
Fig. 6.15 PDF-s and CDF-s of the soil-bridge model resistance at Pier 2, sub-case B2.....	130
Fig. 6.16 WSB interaction in evaluation of the probability of a bridge failure in a scouring event and interdependencies of the governing parameters	134
Fig. 6.17 Indirect failure consequences based on the Swiss National Transport Model [Erath et al., 2011].....	135
Fig. 6.18 Indirect failure consequences of closing the bridge Nišava 1, [Tanasic et al., 2013]	136
Fig. 6.19 Measured water levels at rivers Jadar (left) and Tamnava (right), during 4 days of flood, unofficial data from RHMS (Republic Hydrometeorological Service of Serbia)	137

List of Tables

Table 1.1 Manuals of practice and design guides for bridge scour by the year 2000, [Melville and Coleman, 2000].....	11
Table 1.2 Rating codes for NBI Item 113 – Scour Critical Bridges, [Pearson, 2002]... 14	
Table 1.3 The values of factors K_1 and K_2 in Eq. 1.1	15
Table 1.4 The status of Bridge Scour Program evaluation in the USA, [Arneson et al., 2012]	16
Table 1.5 Minimum performance levels, [Stein et al., 2006]	17
Table 1.6 Annual Probability of Scour Failure, adapted from [Stein et al., 2006]	18
Table 1.7 An example of condition rating for items in the BPM, [Mašović and Hajdin, 2014]	24
Table 2.1 Possible mechanisms of bridge failure due to scour, adapted from [May et al., 2002]	36
Table 3.1 Features review of the formulas for local scour evaluation.....	63
Table 4.1 Structural system and material in the BPM, [Mašović and Hajdin, 2014]	66
Table 4.2 Internal (INT) and external (EXT) work for the KMS in Fig. 4.12.....	80
Table 5.1 Four bridge types in longitudinal direction and associated <i>CFM</i> -s	90
Table 5.2 Input data and results of the optimization procedure for the four bridge types.....	95
Table 5.3 Effects of the joint and adjacent supports plastic strength on the results	101
Table 5.4 Input data and results of the optimization procedure for the lateral failure modes	111
Table 6.1 The COV for some common field measurements, adapted from [Phoon and Kulhawy, 1996].....	120
Table 6.2 Total measurement error for laboratory-measured properties, adapted from [Phoon and Kulhawy, 1999]	121
Table 6.3 The COV of geotechnical parameters, [Phoon et al., 2008]	123
Table 6.4 The deterministic input data used in the analysis (all cases)	126
Table 6.5 Probability models for the parameters used in the analysis (all cases).....	127
Table 6.6 Simple bounds of probability for sub-cases A1 and B1 (purely frictional soil).....	132
Table 6.7 Simple bounds of probability for sub-cases A2 and B2 (purely cohesive soil)	132

Notation

Abbreviations:

<i>AADT</i>	=	Average Automobile Daily Traffic
<i>ADT</i>	=	Average Daily Traffic
<i>ADTT</i>	=	Average Daily Truck Traffic
<i>BMS</i>	=	Bridge Management System
<i>BPM</i>	=	Serbian bridge database “Baza Podataka Mostova”
<i>CFM</i>	=	Combined Failure Modes for the bridge longitudinal direction
<i>COV</i>	=	Coefficient of variation
<i>DFP</i>	=	Bridge deck failure pattern
<i>GIS</i>	=	Geographic Information System
<i>FDOT</i>	=	Florida department of Transportation
<i>FHWA</i>	=	Federal Highway Administration (USA)
<i>KMS</i>	=	Kinematic Mechanism in Soil
<i>L_rCFM</i>	=	Combined Failure Modes for the bridge LaTeral direction
<i>NBI</i>	=	National Bridge Inventory (USA)
<i>NCHRP</i>	=	National Cooperative Highway Research Program (USA)
<i>NYS DOT</i>	=	New York State Department of Transportation
<i>PFM</i>	=	Pier Failure Mode
<i>PRS</i>	=	Priority Rating Score (BPM)
<i>SFM</i>	=	Superstructure Failure Mode
<i>USCS</i>	=	Unified Soil Classification System
<i>WSB</i>	=	Water-Soil-Bridge (interaction)

Roman upper case letters:

A_{ch}	=	channel flow cross-section area [m ²]
A_d	=	area of a bridge deck [m ²]
A_{DT}	=	ADT (NBI item 29)
A_{ab}	=	area of bottom longitudinal reinforcement in a bridge deck [m ²]
A_{dt}	=	area of top longitudinal reinforcement in a bridge deck [m ²]
A_h	=	area of top reinforcement in a main girder beam [m ²]

- A_s = area of bottom reinforcement in a main girder beam [m²]
 B = width of a strip foundation [m]
 B^* = effective width of a strip foundation (effect of load eccentricity) [m]
 B_{ch} = bottom width of a river channel [m]
 C = total consequences of a bridge failure with respect to a flooding event of a specific magnitude [€, \$, etc.]
 C_l = unit rebuilding cost [\$/year]
 C_2 = cost of running vehicle [\$/mile]
 C_{2a} = cost of running automobile [\$/mile]
 C_{2t} = cost of running truck [\$/mile]
 C_3 = value of time per adult in a passenger car [\$/h]
 C_4 = value of time for a truck [\$/h]
 C_{fn}^x = total consequences of a bridge failing in a mode n with respect to a flooding parameter intensity x
 D = bridge deck width [m]
 D_{50} = median soil sediment diameter [m]
 D_f = height of uniform surcharge load at a shallow foundation [m]
 D_L = detour length (NBI item 19) [miles]
 D_d = dimensionless depth (ratio of water depth and full waterway opening)
 DC = direct consequences of a bridge failure with respect to a flooding event of a specific magnitude [€, \$, etc.]
 DC_n = direct financial consequences with respect to a chosen bridge failure mode n [€, \$, etc.]
 F = bridge failure occurrence
 F_{cr} = critical Froude number based on V_c
 F_r = Froude number directly upstream of the pier
 G = limit state function (probability of bridge failure due to scour) [m]
 I = indicator function equal to 1 for $g(x) \leq 0$ otherwise equal to 0
 H_{pos} = location of a plastic hinge in a bridge main girder
 IC = indirect consequences of a bridge failure with the respect to a flooding event of a specific magnitude
 IC_n = indirect traffic related consequences with respect to the chosen bridge failure mode n (€, \$, etc.)
 K = risk adjustment factor based on K_1 and K_2 in HYRISK formula

- K_1 = risk adjustment factor based on a type of span
 K_2 = risk adjustment risk factor based on a foundation type
 K_t = factor used to evaluate the scour evolution in time (FDOT formula)
 $K_{d1,d2}$ = empirical factors used for evaluating scour in the case of rectangular and triangular debris
 L = width of a strip foundation [m]
 L_B = bridge length (NBI item 49) [ft]
 L_D = length of debris upstream from pier face [m]
 M_{pj} = ultimate plastic moment of the monolithic joint at the pier top [kNm]
 M_{ph} = ultimate hogging plastic moment at middle bridge supports [kNm]
 M_{ps} = ultimate sagging plastic moment in a bridge span [kNm]
 $N_{\gamma,c,q}$ = bearing capacity factors for soil self-weight, cohesion and surcharge load respectively
 O = average occupancy rate [number of adults]
 OT = overtopping frequency (NBI Items 26 and 71)
 P = probability of bridge failure due to the flooding event of a specific magnitude
 P_a = probability of failure each year (NBI items 26, 71 and 113)
 P_i = probability integral
 P_f = probability of the bridge failure in the local scour event
 P_n^s = conditional probability of specific bridge failure in a chosen failure mode n , with the respect to a scouring event of a specific magnitude s
 P_{fn}^x = probability of bridge failing in a mode n with the respect to a flooding parameter intensity x
 PF_g = pier-foundation system self-weight [kN]
 Ps_i = self-weight of the soil region i in the KMS [kN/m']
 Q_{ext} = extreme discharge [m³/s]
 $R(S_zmax, h_{cov})$ = resistance of a soil-bridge model to local scour action at affected pier [m]
 R_{bf} = risk of bridge failure with respect to a flooding event of a specific magnitude
 R_r = ratio of bottom beam reinforcement area to top beam reinforcement area
 R_h = hydraulic radius of the flow cross-section [m]
 $Risk$ = risk of scour failure [\$/year]

- R_s = total rating score of a bridge in BPM
 R_k = PRS for safety items (BPM)
 R_{d1} = PRS for expected further deterioration items (BPM)
 R_f = PRS for serviceability items (BPM)
 R_{d2} = PRS for additional prioritization items (BPM)
 R^{fp} = risk of a bridge failure with respect to an adopted respective flooding parameter
 S = slope of a river channel bottom [m/m]
 S_c = horizontal scour extent associated to $Z_{sc}(t)$
 S_z = scour depth below the foundation base associated to $Z_{sc}(t)$
 S_d = average detour speed [miles/h]
 SV = scour vulnerability (NBI Item 113)
 T = ADTT (% of ADT) (NBI 109)
 T_D = thickness of debris at a pier [m]
 T_i = external surface loads acting on a displacement boundary of a body
 F_i = external body loads acting on a body volume
 T_{ch} = top width of the flowing water in a channel [m]
 V_n^s = vulnerability of a bridge with respect to a scouring event of a specific magnitude s and a chosen failure mode n
 V = average flow velocity [m/s]
 V^s = vulnerability of bridge with respect to all scour magnitudes at bridge substructures
 V_1 = mean velocity of flow directly upstream of a pier [m/s]
 V_{1p} = live bed peak velocity [m/s]
 V_{br} = volume enclosed by an undeformed and deformed bridge deck body in an assumed superstructure mechanism [m³]
 V_c = critical velocity for initiation of erosion of a soil material [m/s]
 V_{max} = maximum velocity in a hydrograph [m/s]
 W_D = width of debris at a pier normal to flow [m]
 W_B = bridge width from NBI item 52 [ft]
 W_γ = external work of soil self-weight [kNm]
 W_{sur} = external work of surcharge load [kNm]
 W_{coh} = internal work of cohesion in supporting soil [kNm]

- W_h = internal work of all plastic hinges in a bridge structure [kNm]
 W_{yl} = internal work of yield lines in a bridge deck [kNm]
 \dot{Z} = erosion rate of scour (HEC-18 clay formula) [mm/hour]
 $Z_{sc}(t)$ = time- dependant local scour depth at an affected pier [m]

Roman lower case letters:

- a = pier width without debris [m]
 a_1 = centroid of the bottom reinforcement area in a main girder beam
 a_i = condition rating score for an inspection item i in the BPM
 a^* = equivalent pier diameter width [m]
 a' = projected pier width perpendicular to flow (rectangular piers) [m]
 b = girder beam width
 b_i = impact factor for an inspection item in the BPM
 c = cohesion in soil [kN/m²]
 d = effective girder beam depth [m]
 d_t = duration of detour based on an ADT (days) (NBI item 29)
 $d_{\gamma,c,q}$ = correction factors for embedded strip foundation
 e = cost multiplier for early replacement based on an ADT
 f_{cp} = plastic compressive strength of concrete [MPa]
 $f_X(x)$ = joint probability density function of a basic random variable x
 f_y = tensile strength of reinforcement [MPa]
 $i_{\gamma,c,q}$ = correction factors for inclined loading at a strip foundation
 $g(x)$ = limit state function
 g = dead load of the superstructure [kN/m²]
 Δg = additional dead load on the superstructure [kN/m²]
 $k_{xx,yy,xy}$ = plastic curvatures derived from downward displacement of the center plane of a slab
 $m_{xx,yy,xy}$ = moments that satisfy the yield condition of a slab [kNm]
 n = Manning roughness coefficient [s/m^{1/3}]
 p = probability of occurrence of a flooding event with a specific magnitude
 p^x = probability of a flooding parameter intensity x affecting a bridge

- q = superstructure self-weight over a bridge deck area, [kN/m²]
- q^* = limit load acting on a superstructure [kN/m²]
- q_u = ultimate bearing capacity of soil [kN/m²]
- $s_{\gamma,c,q}$ = shape correction factors for a strip footing
- t = peak flood duration (days)
- t_e = time to reach equilibrium scour depth (days),
- $t_{e,p}$ = equivalent time rate of pier scour [hours]
- t_{hyd} = duration of a complete hydrograph [hours]
- t_{90} = time to reach 90% of equilibrium scour depth [days] (FDOT formula)
- $t(z)$ = deterministic trend component of soil property which varies with depth z
- \dot{u}_i^{p*} = real or virtual plastic displacement rates at points of application of T_i
- u_{*c} = critical shear velocity for soil particle entrainment [m/s]
- $w(z)$ = random component of soil property which varies with depth z
- y = flow depth directly upstream of an affected pier [m]
- y_0 = neutral axis depth for a girder beam [m]
- y_1, y_d = average water depth in the upstream main channel (i.e. unscoured water depth) [m]
- y_s = local scour depth [m]
- $y_{st}(t)$ = local scour evolution in time [m]

Greek upper and lower case letters

- τ = shear stress in soli [kN/m²]
- φ = angle of internal friction of soil [rad]
- ε_u = ultimate strain for materials (e.g. for concrete or reinforcement)
- $\dot{\varepsilon}_{ij}^{p*}$ = plastic strain rate
- σ_{ij}^p = plastic stress state
- $v(x, y)$ = virtual vertical displacement associated to a bridge deck [m]
- v = virtual vertical displacement associated to a pier-foundation system [m]
- v_i = virtual vertical displacement associated to the region i in an assumed *KMS* [m]
- γ = soil self-weight [kN/m³]
- $\xi(z)$ = insitu soil property which varies with depth z

Chapter 1. Introduction and literature review

1.1 Motivation

Efficient and affordable mobility of people and goods is essential foundation of a modern society fostering economic growth and enabling people to be involved in various activities that yield private and public benefits. In order to ensure required mobility, the transportation infrastructure and in particular roads have to provide adequate and reliable service to their users. The road infrastructure is exposed to various threats that may sever road links or reduce their capacity and lead to severe socio-economic consequences. Given the recent events in Serbia in 2014 and elsewhere around the world, threats due to natural disasters need to be addressed in more detail.

The bridges, which are the most critical parts of road links, are particularly vulnerable to natural hazards (e.g. flooding, rockfall and earthquake) in terms of both exposition and resistance. The flooding is, however, clearly the number one culprit for the damage on bridges ([Faber, 2007], [Imhof, 2004] and [Sullivan, 2005]). During flooding, the bridges are endangered by overtopping, scour and impact of floating debris, or combination of these. In following, some of the very large flooding events and their effect on bridges and transportation infrastructure are presented. Additionally, a few cases of bridge failures triggered by scour are considered individually.

In Japan, in the northern part of Kanto region, the concentrated intensive rainfall (cumulative rainfall of 1,200 mm and a maximum rainfall of 90 mm/hour) in August 1998 inflicted severe damages to the road traffic infrastructure at 645 locations and caused many casualties [Fukui and Nishitani, 2002]. There were 14 confirmed bridge failures triggered by pier scour, abutment scour and washing out of approaches (Fig. 1.1).



Fig. 1.1 Bridge failures in the Kanto region, Japan, 1998, [Fukui and Nishitani, 2002]

In September 2003, the super typhoon Maemi caused more than 100 fatalities as flood waters submerged over 40000 acres of farmland and inflicted severe damage to the transportation infrastructure in South Korea. Total of 27 bridges and 774 roads were impaired while the losses have been estimated to more than 1.4 billion US dollars [Disaster Relief, 2003]. During this event, the Gupo Bridge on the Nakdong River suffered a partial collapse after one pier on pile foundation had failed due to excessive scour as presented in Fig. 1.2.



Fig. 1.2 Gupo bridge on the Nakdong river, South Korea, 2003, [Ji and Julien 2005]

In August 2009, the typhoon Morakot had hit Taiwan and devastated the total of 52 highway bridges [Hsieh et al., 2010]. The outlined causes of bridge failures were associated with debris flows, landslides and scouring (Fig. 1.3)



Fig. 1.3 Bridge failures during the typhoon Morakot, Taiwan, 2009

In the USA, according to the Federal Highway Administration (FHWA) [Arneson et al., 2012], up to 1973 there had been 383 bridge failures due to pier and/or abutment scour in catastrophic floods. In the years 1985 and 1987, a total of 90 bridges were destroyed or damaged in floods due to scour in the states of Pennsylvania, Virginia and West Virginia (73 bridges), and in the states of New York and New England (17 bridges). The floods in 1994, caused by the tropical storm Alberto in Georgia, induced the total damage to the Georgia highway system of approximately 130 million

U.S. dollars for repairs and reconstruction of 73 bridges. The confirmed modes of bridge failures in this flooding event were pier and/or abutment scour, and debris load. As seen in Fig. 1.4, the most of the bridge failures in the USA from 1966 to 2005 occurred due to hydraulics causes, i.e. 58% from scour [Sullivan, 2005].

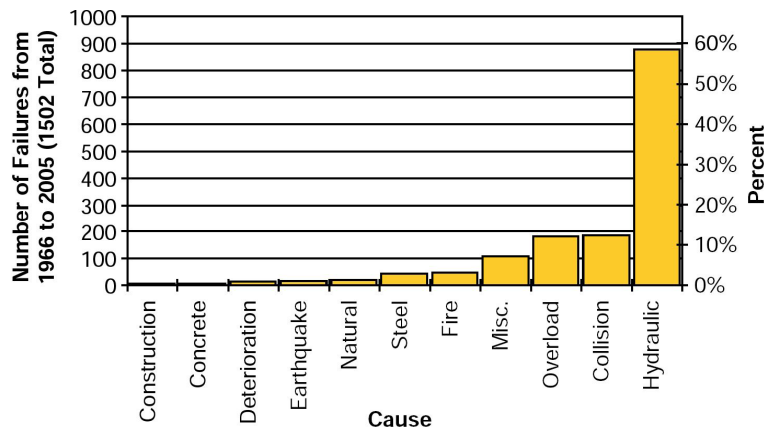


Fig. 1.4 Bridge failures in the USA from 1966-2005, after [Briaud, 2006]

In April 1987, Schoharie Creek Bridge had collapsed and there were several casualties (Fig. 1.5). The collapse was caused by the local scour (50-year flood event) at one of the bridge piers on strip footing that rests on the dense glacial till. The findings confirmed that inadequate rip-rap size, damage from prior flood events and lack of structure redundancy contributed to the collapse. Two years later, the 54-year old Hatchie River Bridge collapsed on the U.S. Highway 51 and eight people were killed (Fig. 1.5). The previous inspections found no abnormalities, but the general scour of the riverbed was observed. The flood level at the river and lack of structural redundancy contributed to this failure. After these accidents, the diving inspections became a routine in the USA.



Fig. 1.5 The collapses of the Schoharie Creek Bridge, 1987 (left) and Hatchie River Bridge, 1989 (right), USA

According to [JBA, 2004], highly localized storms were responsible for more fatalities than large scale flooding in the UK. This report states that on average there has been one railway bridge failure per 2.5 years in the UK since 1840 (Fig. 1.6), which in terms of financial consequences totals the loss of at least 1 million British pounds a year. The most common observed form of bridges failure is associated with undermining of abutments and piers. In 1987, during a period of heavy rain and flooding, the railroad bridge Glanthyd crossing Towy River collapsed killing 4 people. The cause of failure was local scour at a bridge pier and the investigation confirmed that remedial works previously carried out on a bridge increased the likelihood of scour damage because the piers were widened and the shape of the cutwaters was changed [Maddison, 2012]. The most recent cases of scour induced bridge failures in the UK occurred during 2009 at Feltham and Cumbria (Fig. 1.7). In the latter case, the flooding inflicted damage to 20 bridges and there was one casualty [Benn, 2013].

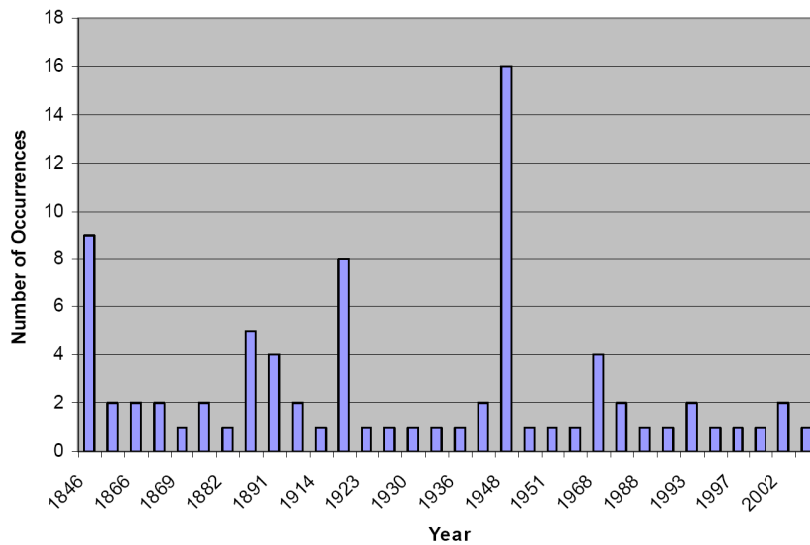


Fig. 1.6 Bridge failures in the UK from 1846 to 2003, [JBA, 2004]



Fig. 1.7 Northside Bridge prior and after the failure, Workington, UK, 2009

In New Zealand at least one bridge failure on average occurs each year due to flooding [Melville and Coleman, 2000]. The significant impact on the community had the failure of Wairoa River Bridge during the cyclone Bola in 1988 (Fig 1.8). The cause of bridge failure was associated to debris which had intensified scouring. The overall costs of the resulting traffic disruption were estimated to 50% greater than the replacement costs of the failed bridge.



Fig. 1.8 Wairoa Bridge failure, New Zealand, 1988, [Wairoa, n.d.]

In Portugal, the 116-year old Hintze Ribeiro Bridge over Douro River had collapsed in March 2001 killing 59 people travelling on a train, bus and three cars (Fig. 1.9). The river was rising for a few days due to intense rain and collapse was eventually triggered by scouring at a bridge pier founded on wooden piles, which was amplified by sand extraction. Additionally, the latest research in [Sousa and Bastos, 2013] showed that this steel truss bridge on masonry piers suffered significant deformation during the years that preceded the collapse.



Fig. 1.9 Collapse of the Hintze Ribeiro bridge, Portugal, 2001, [Figueiredo et al., 2013]

The 39-year old St. Adolph Bridge, near the Canadian city of Winnipeg, had suffered a partial collapse due to pier shifting and sinking as a result of scouring in August 2009 (Fig. 1.10). This RC bridge was partially closed for reconstruction, which lasted for 2 years and the costs totaled about 15 million U.S dollars [Curtiss, 2011].

The interesting fact is that the bridge had survived the 100-year flood in 1997, when the water levels were considerably higher than in 2009 [Manitoba, n.d.].



Fig. 1.10 Failure of the St. Adolph Bridge, Winnipeg, Canada, 2009

In April 2012, the 61-year old bridge over the Filyos River in northern Turkey partially collapsed and 15 people were killed (Fig. 1.11). The excessive scouring at one of the bridge piers, which were founded on wooden piles, eventually led to failure of this RC bridge [TKIC, n.d.].



Fig. 1.11 Failure of the bridge on the river Filyos, northern Turkey, 2012

In September 2012 in Spanish regions Murcia, Almeria and Malaga, the flash floods caused by torrential rain inflicted two bridge collapses on main arterial routes and there were several human fatalities. The collapsed bridges, which were 30 and 6 years old respectively, had to be demolished and replaced by new structures (Fig. 1.12).



Fig. 1.12 Failure of the bridge across Rambla de Béjar, Spain, 2012

In June 2013, the steel railroad Bonnybrook Bridge over the Bow River in the Canadian city of Calgary had suffered partial collapse. The failure happened suddenly, in spite of regular inspections during the flooding event. The sinking and rotation of the scour affected pier caused damage to the main girder and the bridge had to be closed (Fig. 1.13).



Fig. 1.13 Bonnybrook bridge collapse in Calgary, Canada, 2013

In November 2013 the catastrophic rainfall (450 mm of rain in 90 minutes overnight) caused by cyclone Cleopatra had hit Italian island of Sardinia. The direct consequences included several human fatalities and a few bridge failures near the cities Dorgali and Olbia. The failures were mainly associated with washing out of approaches (Fig. 1.14).



Fig. 1.14 Bridge failures near Dorgali (left) and Olbia (right), Sardinia, 2013

In Serbia, there have been substantial number of bridge failures due to flooding in the last 20 years and in following, only the most recent events are presented. The floods resulting from intensive snow melting in central and southern Serbia in 2013 (Fig. 1.15) and 2014 (Figs. 1.16 and 1.17) caused failures and damage to a few bridges.



Fig. 1.15 Bridge failure, Lešak, southern Serbia, 2013



Fig. 1.16 Bridge failure near Kraljevo (left) and scour-critical bridge near Vranje (right), Serbia, 2014



Fig. 1.17 Damaged bridge pier, Lešak, southern Serbia, 2014

In the western and central Serbia and in several regions of the neighboring countries Bosnia and Croatia, the severe flooding in May 2014 caused by cyclone Tamara inflicted dozens of fatalities, serious damage to crops, road infrastructure and industry. Almost one and a half million people were directly affected and more than 35,000 only in Serbia had to be evacuated as flood raised 5.0 m above the ground level at several urban areas. Subsequently, the numerous landslides had cut off settlements in

the flooded areas for several days. In Serbia alone, 50 bridges collapsed or were damaged on the state roads. The causes of these failures were mainly associated with pier and/or abutment local scour, and washing out of approaches (Figs. 1.18 to 1.20). The final toll of this extreme event is yet to be estimated.



Fig. 1.18 Bridge failure, Topola, central Serbia, 2014.



Fig. 1.19 Bridge failure, Draginac, central Serbia, 2014.



Fig. 1.20 Bridge failure, Koceljeva, western Serbia, 2014.

It may be concluded that floods in general represent the severe threat to bridges all around the world despite their age, static system or construction materials. It is the fact that the local scour associated with extreme flooding is widely recognized as the major cause of bridge failures triggered by a non-human factor and is often a topic of extensive research. Case studies (e.g. [Mlakar et al., 2000], [Coleman and Melville, 2001]) and forensic investigation reports (e.g. [Wu et al., 2012], [Lee et al. 2013]) on bridge failures in floods, contribute to the improvement of scour assessment

methodologies and identification of flaws in bridge design, construction and maintenance. Still, this hindsight does not provide satisfactory results in mitigating the threat of failure for existing bridges. The preventative interventions, which include monitoring and countermeasures installment at a bridge site although deemed useful, are costly and sometimes inapplicable especially in the cases that entail flash floods, fast flowing rivers and torrents. In such events, the influence of the local scour is dominant over the other scour processes at a bridge site. It is regarded as a sudden process and it is not easily possible to prevent the associated failures with adequate intercepting interventions. Unfortunately, the validation of bridge management practices in this case is only possible after the failures occur. The only suitable solution, which would focus on a bridge population in a road network, is a screening procedure that allows identification of vulnerable bridges to be examined in more detail. Thus, a new methodology for quantitative vulnerability assessment of bridges exposed to local scour is necessary, which implies estimation of both bridge failure probability for different intensity of floods and related consequences of failure. The main goal of the methodology is arranging timely maintenance interventions for bridges and issuing timely warnings in regions where extreme flooding is expected. Its integration in future Bridge Management Systems (BMS) will certainly aid in mitigating the consequences of oncoming extreme flooding events such as the recent one in Serbia.

The existing methodologies to assess scour criticality are discussed in section 1.2. The treatment of scour data in bridge databases and structure of the bridge database in Serbia – “Baza podataka mostova” (BPM) is given in section 1.3. The literature review of the up-to-date research on topics related to risk and vulnerability of bridges to local scour is presented in section 1.4. The motivation for development of a new methodology and the thesis outline are given in section 1.5.

1.2 Existing methodologies for scour criticality assessment

Many countries around the world developed methodologies and guidelines for evaluation of bridge scour and scour countermeasures installment by the year 2000 (Table 1.1). However, the most comprehensive research has been conducted in the USA. The U.S. Federal Highway Association (FHWA) has issued the three manuals: HEC-18, HEC-20 and HEC-23 (HEC-Hydraulic Engineering Circular), in

which respectively the subjects of bridge scour evaluation (section 1.2.1), stream stability at highway structures and selection of appropriate scour countermeasures are extensively elaborated. Based on the guidelines given in the manuals and the data in the National Bridge Inventory (NBI), the risk-based methodology has been developed and implemented in the software HYRISK (section 1.2.2).

Table 1.1 Manuals of practice and design guides for bridge scour by the year 2000, [Melville and Coleman, 2000]

Country	Agency	Document	Reference	Scour Coverage
USA	FHWA	Evaluating scour at bridges (HEC-18)	Richardson & Davis (1995)	Localized scour estimation procedures mandated for use in the USA
		Stream stability at highway structures (HEC-20)	Lagasse et al. (1995)	Geomorphic and hydraulic factors that affect stream stability at bridges, mandated for use in the USA
Canada	Road and Transportation Association of Canada (RTAC)	Guide to bridge hydraulics	Neill (1973, 1987)	General guidelines to bridge scour
	Ministry of transportation, Ontario	Hydraulic design for bridges, Chapter I, MTC Drainage Manual	Harris (1988)	Scour estimation procedures for use in Ontario, Canada
Australia	Austroroads	Waterway design	Austroroads (1994)	Guide to scour estimation methods in Australia based extensively on HEC-18
New Zealand	Ministry of Works and Development	Code of practice for the design of bridge waterways	Ministry of Works and Development (1979)	Guidelines for scour estimation and scour protection
	Ministry of Works and Development - Hamilton District Office	Waterway design procedures - Guidenotes	Georgious (1985)	Guidelines for scour estimation and scour protection
Sweden	Royal Institute of Technology, Stockholm	Local scour at bridge piers - A review of theory and practice	Dargahi (1982)	Review of pier scour estimation and scour protection
India	Central Board of Irrigation and Power, New Delhi	River behavior management and training	Central Board of Irrigation and Power (1989)	Comprehensive guidelines to scour estimation and scour contra-measures
	Indian Road Congress	Standard Specifications and code of practice for road bridges - Section VII. Foundations and substructure - Part I, General features of design	Indian Road Congress (1980)	General guidelines
Netherlands	Ministry of Transport, Pubic Works and Water Management, Delft, and Delft Hydraulics Laboratory	Scour manual	Hoffmans and Verheij (1997)	Chapters on abutment and pier scour
United Kingdom	Hydraulics Research, Wallingford	Hydraulics factors in bridge design	Farraday and Charlton (1983)	Chapters on local scour and bank protection and river training

In National Cooperative Highway Research Program (NCHRP) report (section 1.2.3), detail application of the HYRISK to bridges with unknown foundations is presented. Following the guidelines given by the FHWA, the States DOT (Department of Transportation) use their own bridge scour ranking systems and store necessary data for this purpose in bridge databases. Besides screening of scour prone bridges, these

databases support decision making process with regard to maintenance actions. An example of such ranking system, which is based on screening, classifying and rating procedures, is specified in the hydraulic vulnerability manual of New York State Department of Transportation (NYSDOT) (section 1.2.4). In section 1.2.5, the available software for risk assessment of bridges, which include flooding hazard, is briefly presented.

1.2.1 The U.S. national scour evaluation program

The U.S. Federal Highway Association (FHWA) has started scour evaluation program in the 1988 as a part of the National Bridge Inspection Standard (NBIS) with the primary goal to identify and evaluate existing bridge deficiencies and ultimately ensure the safety of traveling and transport. Within this program, all necessary data has been collected in the National Bridge Inventory database (NBI). This database represents a compilation of bridge data supplied by the States to the FHWA and contains detailed technical and engineering information about hundreds of thousands of bridges and tunnels in the U.S. on the public roads. The data is organized into elements (i.e. items) and is used for condition assessment of bridges and their prioritizing when corrective actions are needed. The descriptions of rating codes for the items in the NBI may be found in [Pearson et al., 2002]. For evaluation of scour at bridges the following items are used:

- NBI Item 60 – Substructures (describes physical condition of piers, abutments, piles, fenders, footings)
- NBI Item 61 – Channel and Channel Protection (describes the physical conditions associated with the flow of water under the bridge such as stream stability and the condition of the channel, riprap, slope protection, or stream control devices including spur dikes)
- NBI Item 71 – Waterway Adequacy (appraises the waterway opening with respect to passage of flow under the bridge), and
- NBI Item 113 – Scour Critical Bridges (Table 1.2)

Following items are also related to scour: the Item 92 – Critical Feature Inspection and the Item 93 – Critical Feature Inspection Date, in order to alert inspectors for previous scour problems.

Currently, the three manuals are used for a comprehensive scour analysis and structure stability evaluation: HEC-18, HEC-20 and HEC-23. The latest HEC-18 manual [Arneson et al., 2012] is the state-of-the-art document, which allow comprehensive bridge scour evaluation. It relies on the vast research performed by NCHRP and FHWA, technical resources and represents the updated version of the manual given by [Richardson and Davis, 2001]. The manual HEC-18 addresses:

- Designing new and improvement of existing bridges to resist scour
- Evaluating existing bridges for scour vulnerability
- Inspecting bridges for scour
- Improving the state-of-practice of estimating scour at bridges

According to FHWA, approximately 83 percent of the 583,000 bridges in the NBI are bridges built over waterways. By the November 2000, more than 90% of all bridges in the USA had been screened and evaluated for scour. The scour evaluation program is conducted by an interdisciplinary team consisted of: DOT's structural engineer, hydraulic, geotechnical and bridge engineers. The program comprises screening and evaluation procedures, and development of an action plan for bridges identified as scour critical. The screening procedures imply the identification of the scour risk at bridges (low risk, scour susceptible or scour critical), prioritizing (for necessary bridge scour evaluation), office review and, if needed, a field inspection. In the evaluation procedures, bridge plans, inspection reports and field reports are studied in order to assess potential problems, which may occur during a future flooding event. In addition, the necessary hydrologic and hydraulic information required for scour estimation at the bridge foundations are gathered and processed. A plan of action for scour critical bridges (NBI Item 113 rating from 0 to 3) implies establishing of bridge-specific inspection type and frequency, performing of scour countermeasures and providing other critical guidance such as identifying flood conditions that will trigger closing of the bridge to reduce the risk to the traveling public.

According to HEC-18 the monitoring as a preventative measure at a bridge site is not a long-term solution and does not render a scour critical bridge a non-scour critical bridge. Furthermore, it does not change the NBI Item 113 rating from a scour critical rating to a non-scour critical rating.

Table 1.2 Rating codes for NBI Item 113 – Scour Critical Bridges, [Pearson, 2002]

CODE	DESCRIPTION
N	Bridge not over waterway.
U	Bridge with "unknown" foundation that has not been evaluated for scour. Until risk can be determined, a plan of action should be developed and implemented to reduce the risk to users from a bridge failure during and immediately after a flood event (see HEC 23).
T	Bridge over "tidal" waters that has not been evaluated for scour, but considered low risk. Bridge will be monitored with regular inspection cycle and with appropriate underwater inspections until an evaluation is performed ("Unknown" foundations in "tidal" waters should be coded U.)
9	Bridge foundations (including piles) on dry land well above flood water elevations.
8	Bridge foundations determined to be stable for the assessed or calculated scour condition. Scour is determined to be above top of footing (Example A) by assessment (i.e., bridge foundations are on rock formations that have been determined to resist scour within the service life of the bridge), by calculation or by installation of properly designed countermeasures (see HEC 23).
7	Countermeasures have been installed to mitigate an existing problem with scour and to reduce the risk of bridge failure during a flood event. Instructions contained in a plan of action have been implemented to reduce the risk to users from a bridge failure during or immediately after a flood event.
6	Scour calculation/evaluation has not been made. (Use only to describe case where bridge has not yet been evaluated for scour potential.)
5	Bridge foundations determined to be stable for assessed or calculated scour condition. Scour is determined to be within the limits of footing or piles (Example B) by assessment (i.e., bridge foundations are on rock formations that have been determined to resist scour within the service life of the bridge), by calculations or by installation of properly designed countermeasures (see HEC 23).
4	Bridge foundations determined to be stable for assessed or calculated scour conditions; field review indicates action is required to protect exposed foundations (see HEC 23)
3	Bridge is scour critical; bridge foundations determined to be unstable for assessed or calculated scour conditions: - Scour within limits of footing or piles. (Example B) - Scour below spread-footing base or pile tips. (Example C)
2	Bridge is scour critical; field review indicates that extensive scour has occurred at bridge foundations, which are determined to be unstable by: - a comparison of calculated and observed scour during the bridge inspection, or - an engineering evaluation of the observed scour condition reported by the bridge inspector in Item 60.
1	Bridge is scour critical; field review indicates that failure of piers/abutments is imminent. Bridge is closed to traffic. Failure is imminent based on: - a comparison of calculated and observed scour during the bridge inspection, or - an engineering evaluation of the observed scour condition reported by the bridge inspector in Item 60.
0	Bridge is scour critical. Bridge has failed and is closed to traffic.

1.2.2 The HYRISK methodology

The HYRISK methodology is implemented as software with the same name that allows efficient estimation of relative annual risks of bridge damage or failure due to scour based on the FHWA guidelines. The risk is estimated as product of an annual probability (rate) of scour failure and the associated economic consequences by using pertinent items from the NBI database. The following equation is used [Pearson et al., 2002]:

$$Risk = KP_a[(RebuildCost) + (RunningCost) + (TimeCost)] \quad (1.1)$$

where:

$Risk$ = risk of scour failure (\$/year)

K = K_1K_2 – the risk adjustment factor based on the types of span and foundation (Table 1.3)

P_a = probability of failure each year (NBI items 26, 71 and 113)

The values of K_1 and K_2 are subjective (Table 1.3) and it is suggested that they should be adjusted using local experience or further forensic studies.

Table 1.3 The values of factors K_1 and K_2 in Eq. 1.1

K_1	1.00	simple spans less than 100 feet
	0.67	rigid continuous spans with lengths in excess of 100 feet
K_2	1.00	unknown foundations or spread footings on erodible soil above scour depth with pier footing top visible or 1 to 2 feet below stream bed
	0.80	pile foundations when length is unknown or is less than 19 feet, wood pile foundations
	0.20	foundations on massive rock

The probability of failure P_a is a function of overtopping frequency and scour vulnerability at bridge sites. It is adjusted based on the age of the bridge and estimated as follows:

$$P_a(F|(OT \text{ and } SV)) = \sum_D P_a(D_d|OT)P_a(F|(SV \text{ and } D_d)) \quad (1.2)$$

where:

F = bridge failure occurrence

OT = overtopping frequency (based on the NBI Items 26 and 71),

SV = scour vulnerability (based on the NBI Item 113), and

D_d = dimensionless depth (ratio of water depth and full waterway opening)

When the economic consequences of bridge failure i.e. *Rebuild Costs*, *Running Costs* and *Time Costs* are introduced in Eq.1.1 the risk can be expressed as:

$$Risk = KP \left\{ C_1 W_B L_B + C_2 D_L A_{DT} + \left[C_3 O \left(1 - \frac{T}{100} \right) + C_4 \frac{T}{100} \right] \frac{D_L A_{DT}}{S_d} \right\} \quad (1.3)$$

where:

C_1 = unit rebuilding cost (\$/year)

W_B = bridge width from NBI item 52 (ft)

L_B = bridge length from NBI item 49 (ft)

C_2 = cost of running vehicle (0.25\$/mile)

D_L = detour length from NBI item 19 (miles)

A_{DT} = average daily traffic (ADT) from NBI item 29

d_t = duration of detour based on the ADT from NBI item 29 (days)

C_3 = value of time per adult in passenger car (\$7.05h in 1991)

O = average occupancy rate (1.56 adults)

T = average daily truck traffic (ADTT) from NBI 109 (% of ADT)

C_4 = value of time for truck (\$20.56h in 1991)

S_d = average detour speed (40miles/h)

1.2.3 Risk-Based Management Guidelines for Scour at Bridges with Unknown Foundations

There is large number of bridges with unknown foundation in the USA (Table 1.4), and over 1500 of those were built after the year 2000 including 69 on arterials according to [Stein et al., 2006].

Table 1.4 The status of Bridge Scour Program evaluation in the USA, [Arneson et al., 2012]

Total Number of Bridges	Factor	Interstate Bridges	NHS Bridges	NON NHS Bridges	Total	Percent of Total
493,473	Needing Evaluation	80	136	3,701	3,917	0.80%
493,473	Foundation Unknown	55	703	40,067	40,825	8.30%
493,473	Scour Critical	937	1,936	20,181	23,034	4.70%

The proposed methodology, which is based on the HYRISK, includes guidelines for managing the bridges with unknown foundations. The requirement for these bridges is to satisfy the minimum performance levels (MPL-s). The MPL is defined as the probability of failure that a bridge with a certain functional classification must not exceed, given in NBI item 26 – Functional Classification of Inventory Route (Table 1.5). For investigated bridges that do not meet the MPL thresholds, the bridge inspection (i.e. foundation reconnaissance), quantitative scour evaluation and necessary scour countermeasures are suggested.

Table 1.5 Minimum performance levels, [Stein et al., 2006]

NBI Item 26	Description	Minimum Performance Level (Threshold Probability of Failure)
Rural		
01, 02	Principal Arterial - All	0.0001
06, 07	Minor Arterial or Major Collector	0.0005
08	Collector	0.001
09	Local	0.002
Urban		
11, 12, 14	Principal Arterial - All	0.0001
16	Minor Arterial	0.0002
17	Collector	0.0005
19	Local	0.002

The selection of the most appropriate management plan for the bridges with the unknown foundations follows three steps:

- The high priority bridges (high additional daily traffic (ADT) and/or principal arterials) should qualify for the most aggressive management plan
- The setting of the MPL for various functional classifications (Table 1.5)
- The comparison of estimated risk failure to the cost of installing automated monitoring and countermeasures.

Based on the preformed surveys and review of the available project documentation for the State bridges, the common assumptions that can be made for foundations are:

- Older structures (built before 1960) were usually built on timber piling
- Depth of piles can be assumed as at least 10 feet for unknown foundations
- If rock is near the surface, spread foundations can be assumed to support bridges with unknown foundations

- The top of a typical spread footing can be assumed 3 feet below the top of the soil and the bottom 7 feet below the top of the soil

The original HYRISK approach is developed primarily to prioritize bridges and cannot be used for risk assessment as it overestimates the number of annual failures. Thus, the original failure probabilities have been scaled down (Table 1.6) to a level corresponding to the approximate number of occurred failures in the USA, obtained from the State interviews. For unknown foundations, the Item 113 cannot be used and therefore the Items 60 and 61 are used instead as a closest potential measure of a bridge vulnerability to scour.

Table 1.6 Annual Probability of Scour Failure, adapted from [Stein et al., 2006]

Scour Vulnerability	Overtopping Frequency			
	Remote (R)	Slight (S)	Occasional (O)	Frequent (F)
(0) Failed	1	1	1	1
(1) Imminent failure	0.01	0.01	0.01	0.01
(2) Critical scour	0.005	0.006	0.008	0.009
(3) Serious scour	0.0011	0.0013	0.0016	0.002
(4) Advanced scour	0.0004	0.0005	0.0006	0.0007
(5) Minor scour	0.000007	0.000008	0.00004	0.00004
(6) Minor deterioration	0.00018	0.00025	0.0004	0.0005
(7) Good condition	0.00018	0.00025	0.0004	0.0005
(8) Very good condition	0.000004	0.000005	0.00002	0.00004
(9) Excellent condition	0.0000025	0.000003	0.000004	0.000007

The methodology uses the extended version of Eq. 1.3 (vehicles are distinguished between trucks and passenger cars) where the term in brackets (i.e. *Cost*) was updated by including the fatality costs:

$$\begin{aligned}
 Cost = C_1 e W_B L_B + \left[C_{2a} \left(1 - \frac{T}{100} \right) + C_{2t} \frac{T}{100} \right] D_L A_{DT} \\
 + \left[C_3 \left(1 - \frac{T}{100} \right) + C_4 \frac{T}{100} \right] \frac{D_L A_{DT}}{S_d} + C_6 X
 \end{aligned}
 \tag{1.4}$$

where in addition to Eq. 1.3:

- e = cost multiplier for early replacement based on the ADT
- C_{2a} = cost of running automobile (i.e. 0.45 \$/mile), or use local data
- C_{2t} = cost of running truck (i.e. 1.30 \$/mile), or use local data
- C_6 = cost of each life lost (typically \$500,000, or use local data), and
- X = number of deaths resulting from failure

For additional definition of the values for factors in Eq. 1.4 for the USA, refer to [Stein et al., 2006]. The recent application of this risk-based approach in the assessment of scour critical bridges in North Carolina confirms the benefits of the quantitative approaches. The savings from evaluation of 3752 bridges in comparison to the conventional method were estimated to nearly 7.0 million US dollars as reported by [Mulla, 2014].

1.2.4 New York state department of transportation – Hydraulic Vulnerability Manual

The NYSDOT started the Bridge Safety Assurance Program in the 1991 in order to eliminate or reduce the vulnerability of new and existing bridges predominantly due to floods. As a part of this program, the Hydraulic Vulnerability Manual [NYSDOT, 2003] is developed and applied to rate bridges with regard to their hydraulic vulnerability. The ultimate goal of the procedures is establishing urgency and priorities for undertaking corrective actions on the State's bridges. Depending on the rating score, these actions comprise flood monitoring program and/or protective hydraulic countermeasures. Additionally, it is used to prioritize the bridges for additional assessments based on hydraulic studies. The **hydraulic vulnerability assessment** consists of **screening, classifying and rating procedures**.

In the **screening procedure**, the bridges are placed into four susceptibility groups, which set the order of bridges entering the **classifying procedure**. The first step is the *inventory screen*, which represents preliminary screening of bridge inventory and inspection system data files for bridges over water. Then the two-phase *susceptibility screen* is performed. In the first phase, the bridges with low susceptibility to scour damage are identified as those which: do not have piers or abutments in a floodplain, span over static or controlled flows (e.g. lake, canal, etc.) are founded on scour-resistant soil (e.g. bedrock with slow rate of scour measured in terms of centuries). The second phase is *substructure foundation screening*, where the main criteria for placing of a bridge in the one of the susceptibility groups are based on the abutment and pier types. For example, the piers with spread footings on earth and piers with unknown foundations are placed in the first susceptibility group.

In the **classifying procedure**, the vulnerability of a bridge to scour damage is evaluated as the *classification score* based on geologic, hydraulic and

riverine conditions. The bridges are placed in high, medium or low hydraulic vulnerability class. The *classification score* is obtained as the sum of scores from *general hydraulic assessment* and *foundation assessment*. The score of the *general hydraulic assessment* is obtained by accounting for following parameters:

- river slope/velocity
- channel bottom and configuration
- debris/ice problem
- river confluence and backwater
- historic scour depth, and
- adequate opening and available overflow/relief

In the *foundation assessment*, both the abutments and the piers are assessed and the most critical element (i.e. with the highest scores) of these is used in the further score evaluation. Here, the factors that affect scour such as substructure geometry/type, location in the riverbed and existing scour countermeasures are accounted.

Finally, in the **rating procedure** the bridges are given one of the six vulnerability ratings by summation of the *likelihood score* and *consequences score*, which are evaluated through qualitative assessments (Fig. 1.21). The *likelihood score* is directly obtained from the *classification score*, while the *consequences score* is sum of the *failure type score* and *exposure score*. The *exposure score* is a measure of the effect that a failure of a structure will have on the road users. It is qualitatively based on the *traffic volume score* and *functional classification score* i.e. on the AADT (Average Automobile Daily Traffic) and road importance respectively.

The failures types are based on the extent of damage qualitatively, without analyzing specific failure modes:

- Catastrophic – structure is vulnerable to sudden and complete collapse of superstructure span/s, resulting from partial or total failure in the substructure or superstructure. (author`s remark: complete loss of traffic service and lives may be endangered)

- Partial collapse – structure is vulnerable to major deformation or discontinuities of a span (loss of traffic service and lives may be endangered), resulting from tipping or tilting of the substructure

- Structural Damage – structure is vulnerable to localized failures resulting from excessive deformation and cracking in bridge element/s (require repairs, no loss of service)

The manual suggests that following factors should be considered in evaluation of the *failure type score*: redundancy of the superstructure, simple span/continuous spans, bridge type, span length, support conditions, abutment/piers type & geometry. Besides the general discussion, the specific details on how this information affects the *failure type score* are not given.

LIKELIHOOD SCORE (LS)		
Vulnerability class		
HIGH	= 10	(classification score > 35)
MEDIUM	= 6	(classification score 20 - 40)
LOW	= 2	(classification score < 25)
NOT VULNERABLE	= 0	
CONSEQUENCE SCORE (CS)		
Failure Type		
Catastrophic	= 5	
Partial collapse	= 3	
Structural damage	= 1	
Exposure		
Traffic Volume Score		
> 25,000 AADT	= 2	
4000 - 25,000 AADT	= 1	
< 25,000 AADT	= 0	
Functional Classification Score		
Interstate and Freeway	= 3	
Arterial	= 2	
Collector	= 1	
Local Road & Below	= 0	
<hr/>		
VULNERABILITY RATING SCORE (VS= LS + CS)		
VS Rating		
> 15	1	Safety Priority
13 - 16	2	Safety Program
9 - 14	3	Capital Program
< 15	4	Inspection Program
< 9	5	No Action
-	-	Not Applicable

Fig. 1.21 Evaluation of the vulnerability rating score, adapted from [NYSDOT, 2003]

1.2.5 The software for risk assessment of bridges

Currently, there are only few software for risk analysis of bridges which account flooding hazard. The HAZUS-MH (HAZards U.S. Multi-Hazard) is risk assessment

software developed in the USA, which uses Geographic Information System (GIS). It distinguishes the effects of flooding hazards for two elements of transportation infrastructure:

- roadway sections, which can become submerged, and
- bridges, which may fail due to scour during a flooding event.

In both cases, it uses coincident analysis between the geographic extents of the flooding and the location of infrastructure. Here, the probability of failure of bridges exposed to local scour is based on the bridge's structural configuration, rating from the NBI and flood return period, while only the direct costs of failure are considered [FEMA, 2007].

The software CAESAR (Catalog And Expert evaluation of Scour risk and River Stability) is used for evaluating current and potential scour problems at bridges and identifying the urgency for appropriate countermeasures [Palmer et al., 1999]. It comprises bridge site characteristics, the geometry of bridge elements, soil properties, inspection data and independent scour risk evaluation by implementing Bayesian networks. It does not account bridge structural or soil geotechnical resistance in a local scour event.

The Swiss federal roads authority (ASTRA) developed the software Road Risk for evaluation of aggregate risks of road/traffic interruption [RoadRisk, n.d.]. It uses GIS and allows calculation of the probability of road links' failures for different intensities of hazards (flooding, rockfall and avalanche).

1.3 Treatment of scour in bridge databases

According to [Figuerido et al., 2013], a Bridge Management System (BMS) can be defined as an inspection-based decision-support tool developed to analyze engineering and economic factors and to assist the authorities in making timely decisions regarding maintenance, repair and rehabilitation of bridges. The oncoming development of the BMS around the world is mainly focused on the quantitative condition assessment of bridges i.e. structural health monitoring combined with destructive and non-destructive testing in situ. The advanced BMS today process the data stored in bridge databases to predict condition development over time using suitable deterioration models. For this purpose the stochastic models, in particular

discrete-time Markov chains are commonly applied. The Markov chains are used in several BMS such as PONTIS [Thompson et al. 1998] in the USA, KUBA [Hajdin, 2008] in Switzerland, and are recently applied to data stored in Serbian bridge database BPM [Mašović and Hajdin, 2014]. However, the analysis of the impact that natural hazards have on bridges and transportation infrastructure is yet to be included in the future BMS. Currently, only the qualitative assessments of the threat of flooding and associated local scour at bridges are included (e.g. PONTIS).

1.3.1 Bridge information database in Serbia (“Baza Podataka Mostova”)

The first version of the Serbian bridge database (BPM) “SR-01” was developed in 1988 and from 1990 to 1998 its electronic version “SR-02” was utilized. The version “SR-02” was updated and modified over the years to become the version “SR-03” [Bebić, 1998], which is operational since 1998. The main purpose of the BPM is to provide the concise information on properties and geometry of road bridges and their current condition. The qualitative assessments based on inspections give bridge rankings, which are used by Serbian Road Directory to determine an optimum maintenance program for bridges and road users. Still, the BPM is not a BMS, as it does not allow planning of future financial needs, treats bridges as individual objects in the road network and does not trace or predict the deterioration of bridge elements.

The two types of data are collected for the bridges in the Serbian road network: inventory data and inspection data. The *inventory data* comprises:

- Bridge identifiers (e.g. name/number) and location of the bridge in the network (e. g. road type/category, location (milepost), etc.)
- Bridge type and material
- Bridge geometry (e.g. spans, road and cantilever width, etc.)
- Identifiers and properties of bridge elements (e.g. abutments, piers, main girder, bearings etc.)
- Identifiers and properties of bridge equipment (e.g. pavement, bearings, hydro isolation, fence, etc.)
- The owner, operator and participants (designer, contractor, supervision, maintenance responsibility)

- Other data (year of construction, environment characteristics, barrier type etc.)

The bridge *inspection data* are classified in the four groups of items:

- Safety items (load-carrying elements: deck slab, main girder, piers, abutments, foundations, cross beams, bracings and bearings; corrosion presence)
- Expected further deterioration items (waterproofing, expansion joints, pavement, drainage, bridge opening etc.)
- Serviceability items (bridge equipment: signalization, lighting, fences, drainage system, etc.), and
- Additional prioritization items (ADT, location in the network, roadway/bridge alignment)

The total number of inspection items is 28 and the *condition rating score* for every item is evaluated by multiplying it's *condition rating* with an appropriate *impact factor*. The item's *condition rating* may have 5 to 8 values depending on the group (Table 1.7).

Table 1.7 An example of *condition rating* for items in the BPM, [Mašović and Hajdin, 2014]

State	Description of the condition	BPM rating	
		Load-carrying elements	Expansion Joints
1	Good	1	1
2	Satisfactory	5	2
3	Fair/unfavourable	10	4
4	Poor	15	6
5	Serious	20	8
6	Critical/dangerous	100	10

There are 6 values (11.3; 8.0; 5.65; 4.0; 2.82; 2.0) for the *impact factor* and their assignments to the *inspection items* are based on the item's importance. The load-carrying elements have the highest impact factor, while the lowest impact factor is for the bridge equipment. The *partial rating scores (PRS)* are evaluated for every group of inspection data as sum of *condition rating* scores for all items in one group. The *total rating score Rs* for a bridge is obtained as sum of all *PRS*:

$$Rs = R_k + R_{d1} + R_f + R_{d2} = \sum_k a_{ik}b_{ik} + \sum_{d1} a_{id1}b_{id1} + \sum_f a_{if}b_{if} + \sum_{d2} a_{id2}b_{id2} \quad (1.5)$$

where:

- R_k = *PRS* for safety items (max k = 10)
- R_{d1} = *PRS* for expected further deterioration items (max d1 = 6)
- R_f = *PRS* for serviceability items, (max f = 9)
- R_{d2} = *PRS* for additional prioritization items (max d2=3)
- a_i, b_i = *impact factor and condition rating* for an inspection item in a group

The type of static system in conjunction with the values of *PRS* and *Rs* is used for prioritizing of future maintenance actions. The envisaged maintenance actions in the BPM are dependent from the prescribed limit values of every *PRS* for 17 bridge types and imply:

- regular maintenance,
- regular maintenance and inspection,
- intensive regular maintenance,
- emergency maintenance,
- reconstruction plan, and
- urgent reconstruction

The information concerning special transport permits, repair and maintenance actions were intended to be collected as well, but only the *PRS* and *Rs* scores for a bridge from one or several inspections are available at the moment.

In order to perform screening of bridges endangered by scour in the BPM, firstly one should inquire for *PRS* and *Rs* scores. These give only the overall condition, and the additional indicators for flood/scour associated problems are found in entries for items related to bridge substructure (abutment foundation and pier foundation).

1.4 Literature review of the research on vulnerability and risk assessment of bridges exposed to local scour

As far as the existing bridges exposed to local scour are concerned, there is not much research done on the subject of quantitative risk and vulnerability assessments. Here the most relevant studies on this and related topics are presented.

The research in [Johnson and Ayyub, 1992] included the simulation of a local scour at a pier for a period of 35 years. Here the three parameters were varied: pier diameter, foundation depth and sediment grain size. The goal was to estimate the

parameters' impact on the probability of a bridge failure at various points of time. Here, the importance of including risk due to scour at existing bridges in decision-making process was recognized. In [Johnson and Dock, 1998], the CSU local scour evaluation formula (see section 3.1.1.1) was applied in Monte Carlo (MC) simulations for probabilistic estimation of scour at pile foundations. The Bonner Bridge in North Carolina was used in the example where 100 and 500-year hurricane events were simulated as the Poisson process.

In Serbia, the risk assessment of local scour at piers of the “Beška” Bridge over the river Danube has been performed in [Jovanović, 2006]. Here, the long-term hydrographic survey of the river bed was used as the basis for the probabilistic distributions of hydraulic parameters in the CSU formula for the MC simulations. The bridge failure was assumed for scour depths exceeding the pier's foundation depth.

The quantitative vulnerability analysis and bridge failure assessment procedure in accordance with the bridge exposition to the hazard of certain magnitude have been developed by [Birdsall, 2009]. In the case of a bridge pier on shallow foundation, the CSU local scour formula is used to obtain a deterministic maximum local scour depth, which is compared with a pier's foundation depth.

In [Apaydin, 2010], a risk of failure due to scour for a pilot bridge was calculated in order to present the applicability of the HYRISK methodology in Turkey. Here the water surface profile and scour depth calculations are performed with the software HEC-RAS (i.e. CSU formula). The study highlighted the necessity for establishing a bridge database as well as the need for development of a concept similar to HYRISK for different regions in Turkey.

Recently, the Observation Scour Method has been presented in [Govidasamy et al. 2013]. It is a new method for assessment of bridges to scour developed specifically for the state of Texas, which accounts for time-dependent scour in the erosion-resistant materials by using the HEC-18 clay method (section 3.1.1.2). In addition, it incorporates in situ measurements of scour depths and includes past observations of flow data at a bridge site to predict future scour depths.

The seismic performance of scour affected bridges in high seismic areas is also a current research topic. The multiple hazard reliability analysis, which considered local scour at a three-span RC bridge with pile foundations and earthquake loading, was a

part of the study presented in [Goshn et al., 2003]. The bridge failure was assumed for the soil failure due to lateral seismic loads and scour at a pile. Over the period of 75 years (i.e. design life of a bridge), the maximum local scour depths evaluated by the CSU formula, soil properties, strength of bridge elements and earthquake spectra were used in the MC simulations to obtain the probability of bridge failure and calibrate the partial load factors for multiple hazard loading. Recently, in [Alipour et al., 2013] a combined extreme event of scour and earthquake was considered for reliability-based calibration of Load Resistance Factors for Design (LRFD) for RC bridges on pile foundations. The probabilistic analysis of medium to long two-span bridges was conducted using the CSU formula in the MC simulations for the rivers with low-flow and high-flow discharge rates. The effects of scouring on the seismic performance of the investigated bridge types were assessed with the set of fragility curves, which associate ground motion intensity with probability of exceeding a specified damage state.

The effects of local scour on bridge stability in flooding events and related failure modes are rarely investigated. The research in [Ramey and Brown, 2004] was motivated by the fact that scour was not incorporated in the design of several hundreds of bridges in Alabama before 1990. The ultimate objective was to identify the primary parameters and develop a screening tool to evaluate the stability of simple pile bent supported bridges for a 50-year scour event. The analyzed failure modes consider pile buckling, pile cap failure and loss of friction force in the extreme scouring event where the critical depth of scour is the principal parameter governing failure. The automated screening tool, the outcome of this research, was presented by [Donnée, 2008].

The mechanism of a bridge failure due to local scour at shallow foundations has not been clarified in detail. To this end, the reduction of soil bearing capacity due to soil removal in the pier zone has not been thoroughly considered in up-to-date research. The CSU local scour formula has been adopted by [Frederico et al. 2003] to compute probability of a river bridge pier failure, which is assumed to be governed by the soil cover above the foundation level (i.e. surcharge load). Additionally in [Frederico, 2010] the dynamical effects of floods on river bridge foundations were discussed but the superstructure resistance was not considered (section 2.2). As in similar analyses, the pier failure was assumed for all scour depths exceeding the foundation depth.

In [Park et al., 2012], the vulnerability of bridges to local scour has been investigated on the case studies of 12 highway bridges with pile foundations in South Korea. The maximum local scour depths were calculated as an average value obtained by four local scour evaluation formulas for deterministic parameters and a 100-year flooding event. The reduction of a static bearing capacity of soil at bridges' piles due to scour and resulting safety factors were calculated (i.e. decrease of surcharge load and frictional resistance along the pile shaft). These results were suggested as the criterion in prioritization of bridges' maintenance interventions.

The idea to consider a local scour action as a degradation of elastic and plastic soil properties at a bridge pier was presented in [Tanasic et al., 2013]. The FDOT local scour evaluation formula (section 3.1.1.3) was used in the MC simulations to compute the probability of bridge failure at an actual site. Here, the pier sinking was adopted for the bridge failure mechanism in the scouring event (section 2.2). Also, as a part of this study, the application of the new methodology for quantitative vulnerability assessment of bridges to local scour was presented on the example of the road network in southern Serbia (section 6.6). Eventually, in [Tanasic and Hajdin, 2014], the bridge failure modes due to local scour action were discussed on a model which considers water-soil-bridge (WSB) interaction (section 2.2). Here, the main goals were clarification of the requirements for triggering of a specific bridge failure mode.

1.4.1 Conclusion of the literature review

The risk from local scour has been mostly assessed using qualitative approaches relying on: existing databases, surveys, monitoring and past experience. However, the applied scour evaluation procedures cannot adequately predict evolution of risk over time. The evaluation of risk evolution associated with floods is deemed necessary as emphasized in [Khelifa et al., 2013] and there is a need to enhance existing prioritizing procedures. The current quantitative risk-based assessment methods of bridges exposed to local scour are based on previous failure occurrences without appropriate consequence analysis, which are their main shortcomings. Furthermore, the up-to-date software for risk analysis does not account the resistance of bridges in extreme flooding events.

The review of the up-to-date research revealed that the scour evaluation is mostly based on the deterministic scour depths obtained from local scour formulas both in the design of new bridges and assessments of existing bridges. The rule of thumb criterion for bridge failure in a flooding event, according to which the failure occurs when the calculated scour depths reaches the bottom of the substructure's shallow foundation, is clearly too conservative. Furthermore, the temporal aspect of flooding event is often neglected, which leads to an overestimation of scour depths thus increasing the number of bridges designated as scour critical. The current vulnerability assessment procedures and up-to-date research do not account for the resistance of a bridge structure to local scour. It seems that the bridge failure modes (i.e. the way in which the bridge failure unfolds) caused by soil erosion and/or reduction of a soil bearing capacity in a scouring event have not been clarified up to date.

1.5 Thesis outline

The main objective of the thesis is to present the new comprehensive methodology for quantitative vulnerability assessment of bridges exposed to local scour that would allow timely decisions on risk reducing interventions. The motivation for development of such methodology arises from two insights. Firstly, in spite of well established practice of bridge site inspections, the local scour still represents a severe threat to bridges and transportation infrastructure. Secondly, the current procedures for evaluation of risk due to local scour lack the adequate approach for estimation of the probability of bridge failure, particularly in the cases of bridges with shallow foundations. Moreover, the existing quantitative analyses of bridge failures - to the author's knowledge- are not suitable for application to population of bridges as required in bridge management.

The approach of the new methodology is explained in the second chapter. For clarification of the possible bridge failure mechanisms due to local scour action, the approach which entangles water-soil-bridge (WSB) interaction is proposed. The upper bound theorem of theory of plasticity has been chosen for the failure analysis and the main concepts of this well-established theory are outlined.

The third chapter contains a review of the current approaches for local scour evaluation at bridge piers. The local scour processes for fine grained and coarse

grained soils are briefly presented followed by the established local scour evaluation formulas. The potential for application of the state-of-the-art research on local scour in the vulnerability analysis is discussed.

In the fourth chapter, the adopted the soil-bridge model and related assumptions are explained followed by a discussion of a bridge and supporting soil resistances due to local scour action at piers. The performed research in this thesis is based on the scour critical bridges in Serbian road network and their project documentation is reviewed. The estimation of the plastic strength of bridge elements and bearing capacity of the supporting soil affected by standardized local scour cavities is given.

In the fifth chapter, the soil-bridge models are analyzed to estimate the failure triggering extent of the local scour at shallow pier foundations. The combined failure modes are analyzed and the resistances of the models to local scour action are investigated separately for the longitudinal and lateral direction.

In the sixth chapter, the uncertainties related to the governing parameters are discussed and the limit state function for the estimation of the probability of bridge failure is defined. In the example, the quasi Monte Carlo simulation is used for estimation of the simple bounds of the probability of bridge failure in a scouring event. The WSB interaction approach in the vulnerability assessment is reviewed and the example of application of the presented methodology is presented.

The seventh chapter is the summary and critique of the realized work. Here the future research topics and possibilities for further development of the presented approach are given.

Chapter 2. Vulnerability of bridges exposed to local scour and Water-Soil-Bridge interaction

2.1 The methodology for quantitative vulnerability assessment of bridges exposed to local scour

One of the primary tasks for the future generations of civil engineers is certainly management of the aging transportation infrastructure. The threats to safety, functionality and availability of transportation infrastructure are related to gradual deterioration and to sudden events. The particularly virulent are the threats due to flooding, which are the main cause of bridge failures. Transportation infrastructure is not only endangered by low occurrence/extreme intensity floods but also by less extreme floods with relatively high occurrence rates impairing bridge performance and causing traffic interruptions. In the past years, regular inspections of bridges has been considered as an adequate measure for flood protection since, in the most cases, the scour induced in floods is a gradual process that can be observed allowing ample time to execute risk reduction interventions. The notable exception and the main culprit for bridge failures is the local scour, as it unfolds relatively fast and it is rarely possible to prevent the related threat by adequate intercepting interventions. In such cases, the up-to-date risk evaluation concepts do not give satisfactory results and thus a new comprehensive approach is necessary.

The aim is development of the methodology for quantitative vulnerability assessment, which will allow with a modest data set fast screening of bridges in road networks in respect to flooding. The input data for this assessment should comprise:

- information from an existing bridge database,
- bridges` project documentation,
- hydraulic and traffic studies

The availability, usability and reliability of data are governing the quality of the assessment (further discussed in Chapter 6.). Regarding bridge project documentation, the absence of information may be overcome by visual inspections, destructive and non-destructive testing in-situ, and laboratory experiments. The hydraulic and traffic data may be gathered by monitoring and thus providing the basis for stochastic modeling. Since the data collections are sometimes time-consuming and

entail significant resource spending, the identification of essential parameters for the assessment is of the utmost importance. Once recognized, these are going to be systematically collected for the update of existing bridge databases and integration in future Bridge Management Systems.

The new methodology should be applicable to road networks with various topologies and different bridge types with an ultimate goal to improve data driven decisions in the bridge management. Also, it should provide a valid basis for development of vulnerability maps which are going to be practically useful for issuing timely warnings in the regions where intensive flooding is expected. The basic of the new methodology is presented in the next section.

2.1.1 Bridge vulnerability to local scour

During their service life, the bridges are exposed to various loading events and severe weather conditions, which can accelerate their deterioration or cause failure process. In order to provide necessary information for overall risk reduction and optimization of resources allocation, methodologies for vulnerability assessment for bridge management are developed. For this purpose the quantitative approach is preferred as it allows rational assessments due to different threats and objective prioritization of risk reducing interventions. Prior to definition of a bridge vulnerability to local scour, the related terminology is discussed.

The natural hazards are naturally occurring events, which have a level of threat to life, health, property and environment. In engineering, every natural hazard may be defined as a function of two parameters:

- Magnitude i.e. severity represented by a respective variable intensity (or variables' intensities), which is site specific, and
- Frequency of occurrence i.e. how often a hazard of specific magnitude occurs at a particular location

In the case of flooding hazard, the discharge of a river (i.e. volume rate of water flow) at a bridge site commonly denoted as Q , may be considered as a parameter that represents a magnitude of flood. Alternatively, parameters such as flood depth or water velocity may be used. As the second parameter, usually the occurrence rate of a given

flood magnitude is adopted. With additional site specific hydraulic parameters the magnitude of flood can be directly related to the local scour depth at bridge piers by using local scour evaluation formulas, which are discussed in the Chapter 3.

Generally, the bridge failure is understood as inability of a bridge to perform as designed, which includes the total collapse. Here, the way in which bridge may fail (e.g. sinking or rotation of bridge piers due to soil failure, overload in the superstructure elements and washing out of approaches) is referred to as a failure mode. It must be clearly distinguished if a failure mode relates to partial damage of a bridge or total collapse in order to calculate corresponding consequences. The consequences of inadequate bridge performance according to [Birdsall, 2009] are:

- Direct consequences (DC) in the form of structural damage including repair costs required to return damaged bridge to its original state as well as a loss in life and limb, and
- Indirect consequences (IC) in the form of functional damage to the road network users by restricting or completely interrupting traffic flow including additional travel time and additional travel distance costs.

In general, the risk of bridge failure in a flooding event may be formulated as:

$$R_{bf} = p \cdot P \cdot C \quad (2.1)$$

where:

- R_{bf} = risk of bridge failure with respect to a flooding event of a specific magnitude
- p = probability of occurrence of the flooding event of a specific magnitude
- P = probability of bridge failure due to the flooding event of a specific magnitude
- C = $DC + IC$ = total consequences of a bridge failure with the respect to a flooding event of a specific magnitude

The total risk may be calculated if all possible flooding magnitudes and every possible bridge failure modes are accounted. In general, the bridge failure modes are strongly correlated, but if flooding magnitudes are predominantly related to only one failure mode, the modes may be considered as mutually exclusive. If the probability of bridge failure in one mode is much larger than for other modes, the formula in Eq.2.2

may be used for calculation of total risk giving negligible overestimation [Birdsall, 2009].

$$R^{fp} = \sum_{n=1}^N \int_0^{\infty} (p^x \cdot P_{fn}^x \cdot C_{fn}^x) dx \quad (2.2)$$

where:

R^{fp} = the risk of bridge failure with the respect to adopted respective flooding parameter (intensity range from 0 to infinity)

p^x = probability of the flooding parameter intensity x affecting the bridge

P_{fn}^x = probability of bridge failing in mode n with the respect to the flooding parameter intensity x

C_{fn}^x = total corresponding consequences of the bridge failing in mode n with the respect to the flooding parameter intensity x

Given this, bridge vulnerability to local scour can be quantified as the expected consequences to bridge, road link and general public of a scouring event of specific magnitude:

$$V_n^s = P_n^s \cdot (DC_n + IC_n) \quad (2.3)$$

where:

V_n^s = vulnerability of a bridge with respect to a scouring event of a specific magnitude s and a chosen failure mode n

P_n^s = conditional probability of specific bridge failure in the chosen failure mode n , with the respect to a scouring event of a specific magnitude s

DC_n = direct consequences with respect to the chosen bridge failure mode n

IC_n = indirect traffic related failure consequences with respect to the chosen bridge failure mode n

Similarly as for the total risk (Eq. 2.2), the total vulnerability with respect to all scouring event magnitudes and mutually exclusive failure modes (e.g. pier scour or abutment scour) may be estimated:

$$V^s = \sum_{n=1}^N \int_0^{\infty} P_{fn}^x \cdot C_{fn}^x dx \quad (2.4)$$

where:

V^s = vulnerability of bridge with the respect to all scour magnitudes at bridge substructures

P_{fn}^x = probability of bridge failing in mode **n** with the respect to the scouring event parameter intensity **x**

C_{fn}^x = total corresponding consequences of the bridge failing in mode **n** with the respect to the scouring event parameter intensity **x**

The probability of a bridge failing in a specific mode is governed by the interaction between the local scour action, supporting soil and the bridge structure. This water-soil-bridge interaction and the general approach for analysis of failure modes are discussed in the next sections. The consequences associated to specific bridge failures are briefly discussed in section 6.6, but their elaboration is beyond the scope of this thesis.

2.2 Bridge failure modes due to local scour

In the up-to-date literature, the limits of the scour extent necessary to trigger a bridge failure have not been sufficiently treated for the shallow foundations in particular. In practice, the bridge failure is assumed when predicted local scour depths reach a foundation base, which is a conservative assumption. The bridge failure modes are usually discussed based on the observed damage (Figs. 2.1 and 2.2, Table 2.1), but the way in which bridge fails in a scouring event has not been explained in detail. Currently there is no comprehensive approach that entangles water-soil-bridge (WSB) interaction in resolving this problem.

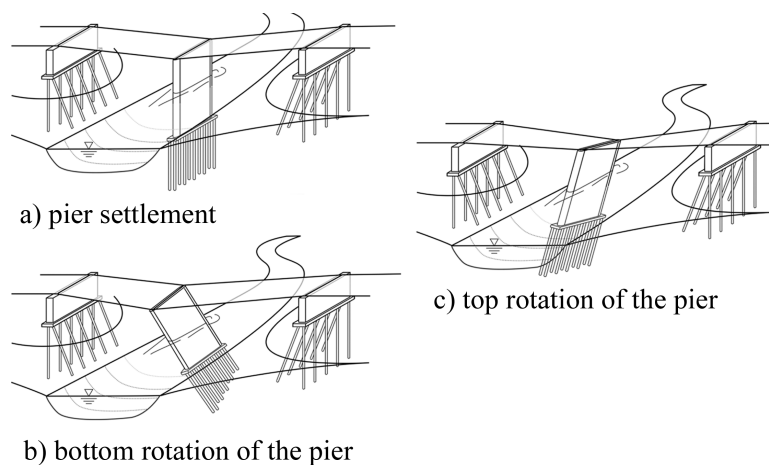


Fig. 2.1 Scour reduces pier support, adapted from [Ettema et al., 2011]

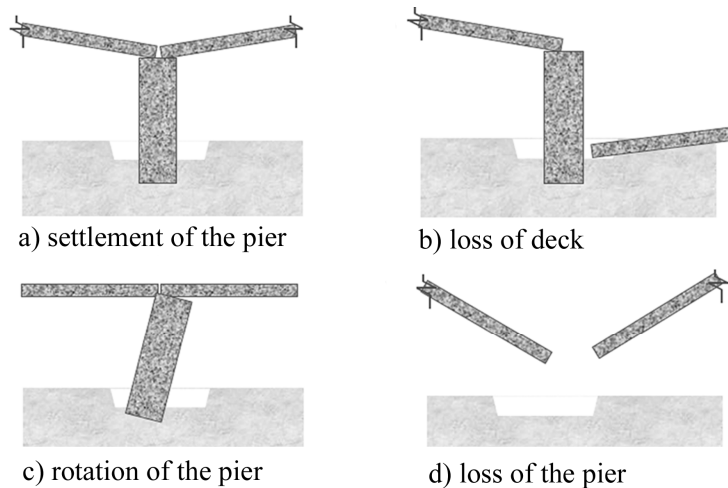


Fig. 2.2 Observed bridge failure modes, adapted from [Briaud et al., 2010]

Table 2.1 Possible mechanisms of bridge failure due to scour, adapted from [May et al., 2002]

General group	Possible mechanisms
Primary structural movement or failure	<ul style="list-style-type: none"> • pier settlement due to loss of support to foundation • pier tilting, or tilting of a group of piles • abutment settlement and/or tilting • piers, abutments or footings damaged by hydraulic loading, perhaps aggravated by debris accumulation • piers, abutments or footings damaged by collision sediment abrasion or impact from boulders • superstructure/deck sliding off supports due to hydraulic/debris loading and/or collision • superstructure/deck damaged by collision of debris or vessel • scour hole or washout of embankment behind abutment
Secondary structural movement or failure	<ul style="list-style-type: none"> • structural damage to superstructure/deck caused by twisting from differential settlement of piers and/or abutments • superstructure/deck falling off abutment or pier due to adverse tilt of support, increasing gap between supports • superstructure/deck buckling or riding up over support due to reduced gap between supports • superstructure/deck sliding off supports due to tilting of the supports • collapse of highway into embankment scour hole or washout

The WSB interaction implies establishing a simple yet sufficiently accurate relationship between a triggering event – local scour induced in a flood and a consequence – the possible failure mode. Considering all failure modes that can be triggered by a flood of certain magnitude, this relationship is defined in following two steps:

- Approximation of local scour action i.e. growth of scour cavity at bridge foundations
- Analysis of a soil-bridge model behavior for the assumed local scour action by considering both:
 - Bridge structure resistance to undermining of its foundations and,
 - Resistance of the supporting soil

In the research of [Frederico, 2010] a similar idea for this interaction was presented. The local scour action has been accounted as a decrease of the surcharge load at the foundation. In the soil-foundation constitutive model, the stability of a bridge pier to vertical loading and horizontal hydrodynamic force was discussed (Fig. 2.3). However, in such system the soil friction, contribution of a superstructure and scour depths exceeding foundation depth were not considered.

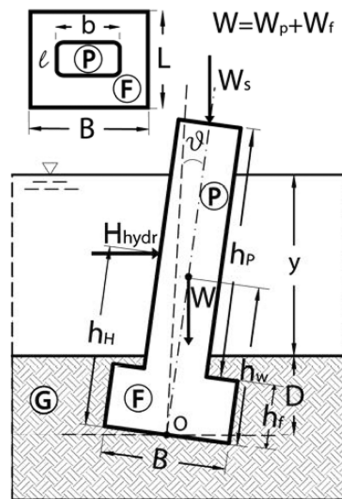


Fig. 2.3 Forces acting upon a river bridge pier, [Frederico, 2010]

In [Tanasic et al. 2013] the authors have adopted the local scour action as a degradation of elastic and plastic soil properties at the affected pier foundation S_3 (Fig. 2.4). The pier sinking was assumed as the bridge failure mechanism. Although the two types of failure modes were distinguished (Fig. 2.5), the reduction of the bearing

- The simplified triangular scour cavity cross-section for a ϕ -c soil is adopted (detail A in Fig. 2.6)

The redistribution of internal forces in the model is assumed to take place as a portion of the supporting soil is lost. This effect is simulated by introducing destabilizing moments M_{dx} and M_{dy} in the lateral and longitudinal direction respectively (Fig. 2.7). These are opposed by couples of horizontal forces B_x and S_x , B_y and S_y , which restrain horizontal displacement and act on superstructure and soil respectively:

- The magnitudes of forces B_x , B_y are given by the resistance of the superstructure or of the joint between pier & superstructure
- The magnitudes of forces S_x , S_y represent the soil resistance to friction at the foundation

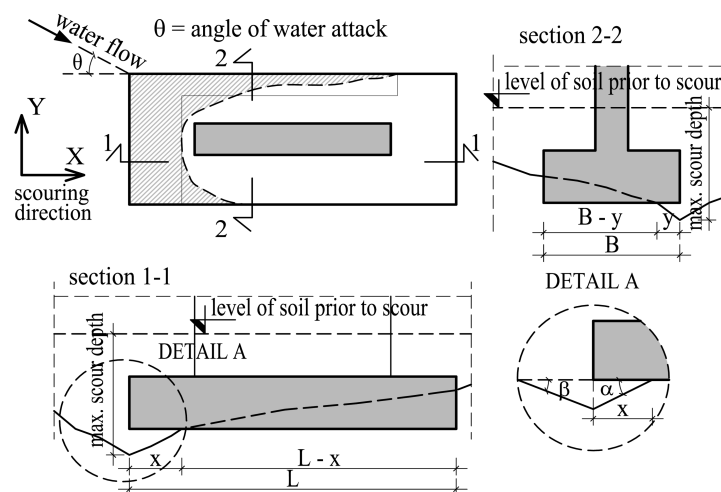


Fig. 2.6 The local scour cavity at a strip footing, [Tanasic and Hajdin, 2014]

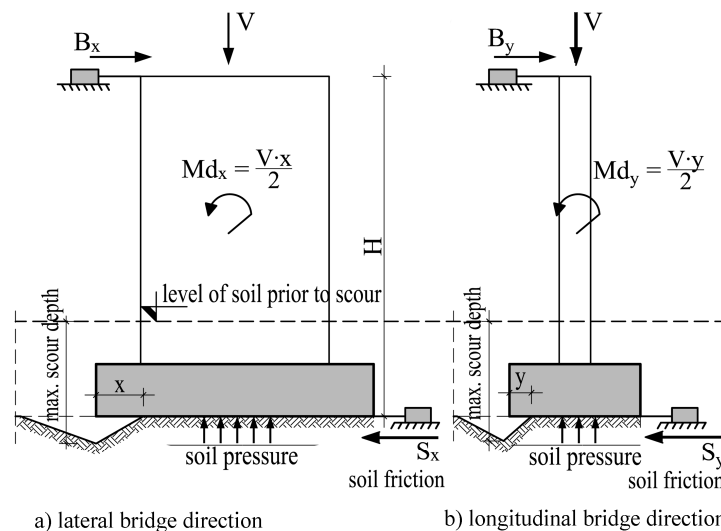


Fig. 2.7 WSB interaction- bridge pier model, [Tanasic and Hajdin, 2014]

The failure is assumed in the cases where the capacities of bridge structure and supporting soil to redistribute the internal forces are depleted. The conclusions drawn from the presented model point out that the assessment of the strengths of the superstructure (i.e. B_x , B_y) and the soil (i.e. S_x , S_y) are essential to determine possible bridge failure modes that may be triggered in a scouring event. Although the basics of the WSB interaction concept were used, this model lacks the ability to capture and explain the full interaction i.e. the combined failure mechanism of the bridge and the supporting soil.

The more comprehensive soil-bridge model for estimation of the probability of bridge failure in a scouring event is presented in Chapter 5, and in following the general approach used for failure analysis of this model is discussed.

2.3 The analysis approach

The data from the forensic investigation of previous bridge failures in scouring events may be used for developing of a comprehensive finite element model (FEM) for the collapsed bridge (e.g. [Ko et al., 2012]). Although the results of such analyses are useful, there are more than few restraints for their generalization to a population of bridges and application in bridge management.

The local scour around bridge foundations is a stochastic process and it may be considered as a time dependent degradation of soil bearing capacity, but the development of this degradation and the resulting safety factor still remains unknown. The redistribution of forces between a bridge structure and supporting soil due to local scour is governed by a significant number of parameters and generally unknown. It may be traced in a linear elastic-plastic FEM, where besides meticulous modeling of soil and bridge finite elements, a stochastic analysis in a time domain would be required. For the vulnerability assessment, the combined failure mode of a bridge and supporting soil is of interest and not the entire process of force redistribution, which make the FEM-s rather cumbersome for application.

The proposed methodology for quantitative vulnerability assessment of bridges exposed to local scour has emphasis on a simplified, yet sufficiently accurate approach, which may be readily used with current bridge databases. The limit analysis method has been chosen as the most convenient for analysis of the soil-bridge models that entangles

WSB interaction. This approach would clarify how the failure modes unfold and point out the governing parameters for their analysis. The basic concept of the related theory necessary for application of the limit analysis is outlined in the following sections.

2.3.1 The limit analysis method and the upper bound theorem

Due to its efficiency and simplicity, the limit analysis method is found in large number of applications such as resolving of soil stability problems e.g. in [Chen, 1975], design of reinforced concrete structures e.g. in [Nilsen, 1984] and other. The limit analysis is based on the law of conservation of an energy given by the lower and the upper bound theorem. Here the upper bound theorem is going to be used for soil-bridge model analysis and thus the main assumptions of the limit analysis are reviewed:

- The idealized stress-strain relation
- Yield condition and associated flow rule
- Small deformations (equilibrium can be computed on an undeformed system)

The stress-strain relationship for real soils as in Fig. 2.8 (solid line) may be observed in laboratory tests such as triaxial compression or shear stress tests. In the limit analysis, when the small amounts of work softening are neglected, the idealized elastic-perfectly plastic soil behavior may be assumed (line OAB in Fig. 2.8). For stability problems such as bearing capacity, it is justifiable to assume that general soil is perfectly plastic material i.e. experience continuing plastic flow at constant stress (Fig. 2.9) [Chen, 1975]. This is reasonable especially for the soft clays, which have large ratio of plastic to elastic deformation.

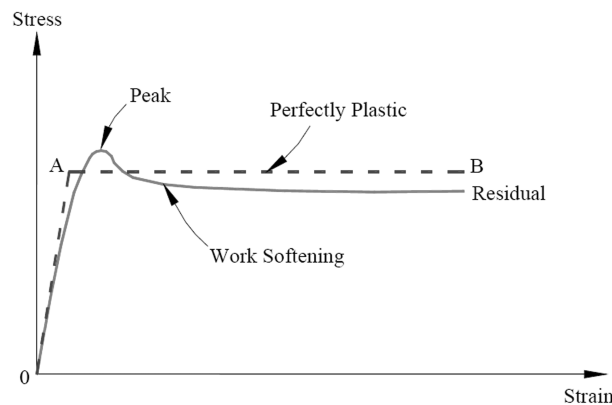


Fig. 2.8 Stress-strain relationship for ideal and real soils, [Chen, 1975]

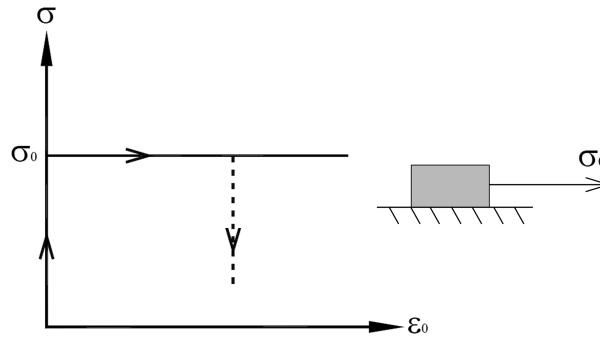


Fig. 2.9 Perfectly plastic material behavior

The perfectly plastic assumptions for RC behavior have been reviewed by [Monotti, 2004]. Here, the uniaxial responses (σ - ϵ diagrams) of concrete and steel are presented in Figs. 2.10a and 2.10b. The concrete is assumed to have no tensile strength and under compression it goes through few phases: linear elastic (OA), progressive loss of stiffness (AD) and softening (DE) before failure at ultimate strain ϵ_u (Fig. 2.10a). It is observed that the concrete in compression may be approximated by rigid-plastic material with somewhat conservative plastic strength f_c . The reinforcement in tension passes through linear elastic phase (OA) followed by yield plateau (AB) and hardening (BE) before failure at ultimate strain ϵ_u (Fig. 2.10b). Neglecting the elastic deformation and strain hardening in tension, the behavior of the reinforcement may be taken as rigid-plastic with plastic strength f_y . This assumption is also valid for compression.

The behavior (deflection u) of RC rectangular beam loaded at mid-span by a force F in Fig. 2.10c for normally reinforced beam ($A_s / (bd) = 0.5\%$) is presented in Fig. 2.10d. Here, the F_{cr} is associated with beam specimen cracking (point A) while the F_y is related to the yielding of reinforcement (i.e. plastic plateau). The beam behavior may be characterized by three ranges: elastic (OA), elastic cracked (AB) and plastic (BCD) denoted by dashed lines “1”, “2” and “3” respectively. The strong effect of reinforcement ratio on the plastic behavior of reinforced concrete is given by dotted lines “a”, “b” and “c”, which are respectively associated with the cases of over-reinforced, minimum reinforced and under-reinforced section. Nevertheless, even for the over reinforced and under-reinforced elements, the good correlation of plastic solutions to test results have been obtained when effective concrete strengths i.e. plastic strengths of concrete are applied [Nielsen, 1984].

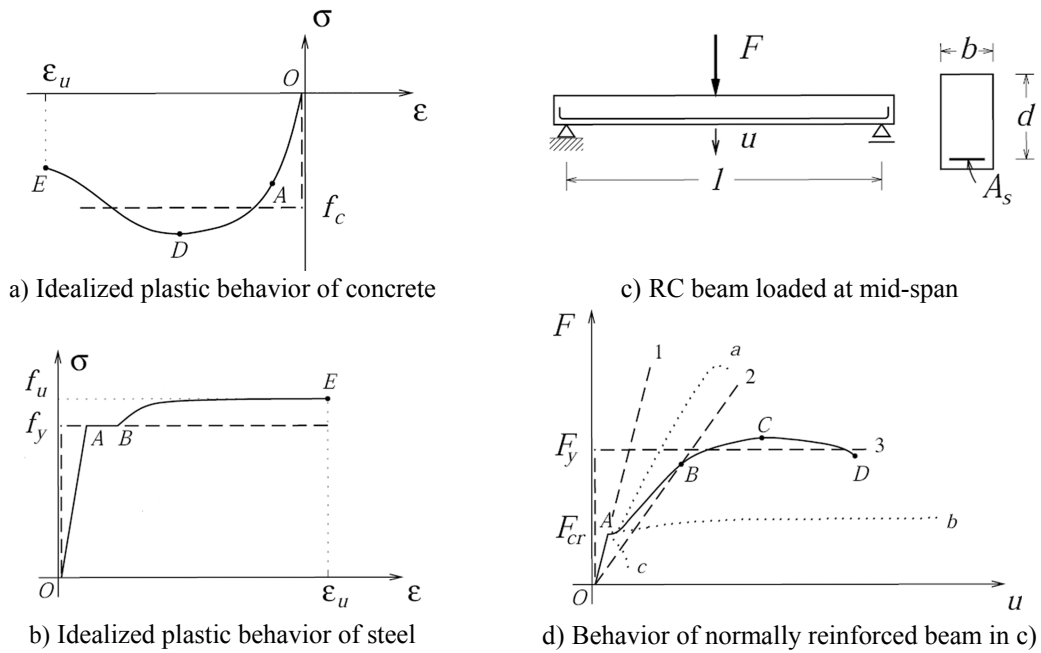


Fig. 2.10 Perfectly plastic assumption for RC behavior, [Monotti, 2004]

The condition that characterizes material behavior in transition from elastic state to yield state is given by the yield criterion. This condition expresses that for certain combinations of stresses in a point of the material the deformations increase without bounds (i.e. plastic yielding), and that for smaller stresses no plastic deformations occur.

The behavior of general soil to loading is dependent from the maximum shear stress τ before a collapse occurs. When the shear stress reaches an amount that depends linearly upon a cohesion stress c and a normal stress σ on any plane at any point in soil, the plastic flow commences. The Mohr-Coulomb failure criterion (Fig. 2.11) is used for general c - ϕ soils:

$$\tau = c + \sigma \tan \varphi \quad (2.5)$$

where:

- τ = shear stress [kN/m²]
- c = cohesion [kN/m²]
- φ = angle of internal friction [rad]

The flow rule (i.e. normality condition) assumes that plastic strain rate vector must be normal to the yield curve when the axes of plastic normal strain rate $\dot{\epsilon}^p$ and plastic shear strain $\dot{\gamma}^p$ are superimposed. In Fig. 2.11 this rule was presented for the Mohr-Coulomb failure criterion. The vector OB represents a stress state increased from zero to collapse.

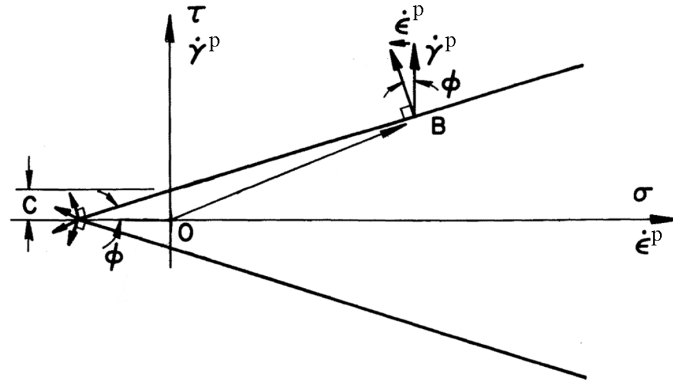


Fig. 2.11 The flow rule i.e. normality condition for general soil, [Chen, 1975]

For the orthotropic RC plates, the yield criterion (Fig. 2.12) is formulated in respect to bending moments in orthogonal directions m_{xx} , m_{yy} and a twisting moment m_{xy} . The values denoted with κ in Fig. 2.12 represent the plastic curvatures while the arrows represent the plastic strain rate vectors.

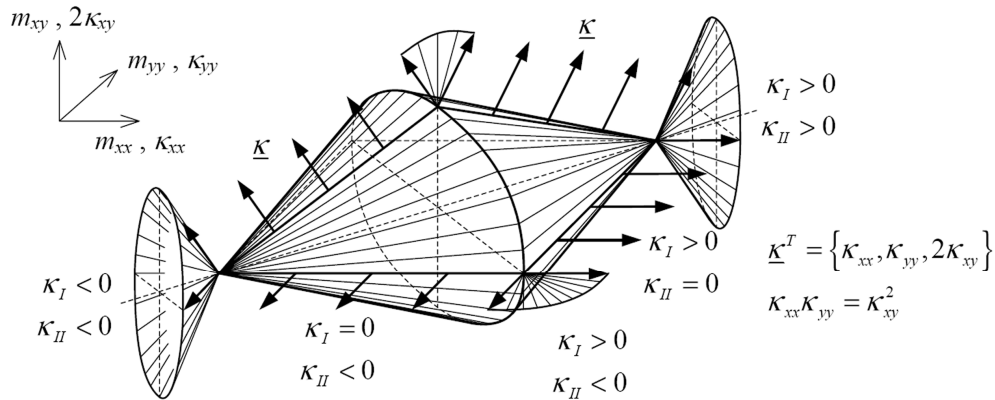


Fig. 2.12 The yield criterion and normality conditions for RC plates, [Vrouwenvelder and Witteveen, 2003]

The upper-bound theorem states that the loads, which are determined by applying the virtual work equation for a compatible mechanism of plastic deformation (Eq. 2.6), will be either equal or higher than the actual limit load.

$$\int_A T_i \dot{u}_i^{p*} dA + \int_V F_i \dot{u}_i^{p*} dV = \int_V \sigma_{ij}^p \dot{\epsilon}_{ij}^{p*} d \quad (2.6)$$

where:

- T_i = external surface loads acting on a displacement boundary A
- \dot{u}_i^{p*} = real or virtual plastic displacement rates at points of application of T_i
- F_i = external body loads acting on a body volume V

σ_{ij}^p = plastic stress state

$\dot{\epsilon}_{ij}^{p*}$ = plastic strain rate

For the obtained solution from Eq. 2.6, the stress distribution in the rigid parts of the structure in an assumed mechanism need not be in equilibrium. Still, by applying the virtual work principle for a valid mechanism a realistic value of the collapse load can be obtained. The least upper bound of the limit load acting on the system is evaluated by trials with various possible kinematically admissible failure mechanisms, and to minimize the upper-bound solutions, the optimization procedures are commonly applied.

Chapter 3. Local scour evaluation

The first step in the application of the WSB interaction is modeling of the local scour action at bridge foundations, which is here based on the state-of-the-art research on scour evaluation. The local scour action at bridge abutments is not considered and will be part of the future research. The parameters that govern the magnitude of local scour at bridge piers as well as the problems related to the local scour evaluation are presented. The possibility for application of the state-of-the-art local scour formulas in modeling of the local scour action at bridge piers for the vulnerability assessment is discussed.

3.1 The local scour action at bridge piers

The pier scour in coarse-grained and fine-grained soils are considered, and the scour in rock was not in the scope of this research. For more detailed explanations and further formulas, the reader is directed to [Melville and Coleman, 2000], [Richardson and Davis, 2001], [Briaud et al. 2003] and [FDOT, 2010]. In addition, the significant contribution to the research on local scour has been given in [Lagasse et al., 2010], [Sheppard et al., 2011], [Ettema et al, 2011], [Briaud et al., 2011] and [Lagasse et al., 2013]. The most of the above mentioned research has been reviewed in the latest HEC-18 manual [Arneson et al., 2012].

The scour is a hydraulic erosion process that entails lowering of a riverbed by flowing water. The bridge piers and abutments with their foundations in water or located in a floodplain may be exposed to this action. The total scour comprises several distinctive processes according to [FDOT, 2010]:

- General scour (due to lateral instability such as river meanders),
- Long term aggradation and degradation of river bed (due to channelization and deforestation),
- Contraction scour (e.g. due to presence of group of piers in the water),
- Bed form propagation through bridge site (due to currents and surface waves),
- Local scour at piers or abutments

Although every one of these processes contributes to the total scour depth, the local scour is commonly the ultimate cause of bridge failures in the extreme

flooding events. The mechanism of the local scour at piers involves formation of “horseshoe” vortex and the “wake” vortex (Fig. 3.1). Both types of vortices remove material from pier base as natural river flow is altered by obstruction. Eventually, if there is excessive lowering of the river bed near the piers, the stability of the bridge may be jeopardized. The local scour can be either clear-water scour or live-bed scour. Clear-water scour occurs when the bed material upstream of the scour cavity is at rest and the maximum scour depth is reached when the flow can no longer remove bed material from the scour cavity (Fig. 3.2). Live-bed scour occurs when sediment is continuously supplied to and transported out of the scour cavity. The equilibrium scour depth for live-bed scour is attained when these actions come in balance (Fig. 3.2).

The cohesionless (e.g. sand) and cohesive soils (e.g. clay) display diverse behavior in scouring. The erosion in cohesionless soils occurs particle by particle, and the maximum (or equilibrium) scour depth is reached within a time period of a few hours to a few days – usually during a single flooding event. The cohesive soils possess inherent resistance to erosion owing to electromagnetic and electrostatic interparticle forces, thus scouring can take place particle by particle but also block of particles by block of particles. For these soils it is common that the equilibrium scour depth is reached in weeks, months or even years as a result of accumulated scouring in multiple flooding events.

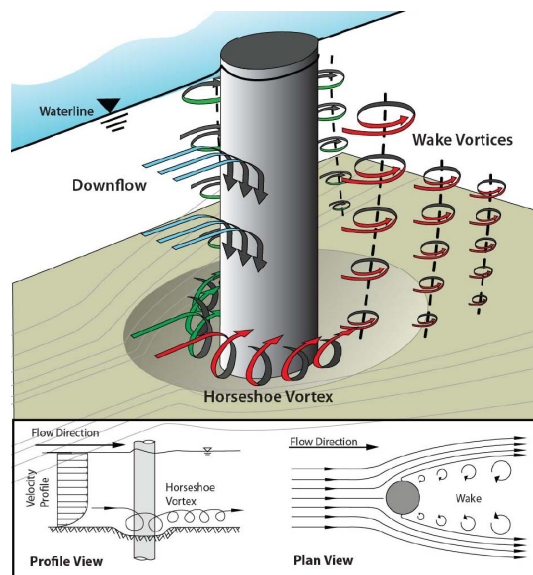


Fig. 3.1 Local scour at cylindrical pier, [FDOT, 2010]

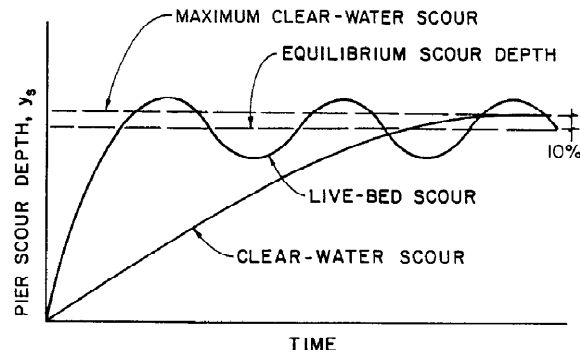


Fig. 3.2 Local scour depth at pier in a sand-bed stream as a function of time, [Richardson and Davis, 2001]

3.1.1 The local scour evaluation formulas

In addition to qualitative approach, the contemporary scour evaluation programs more or less rely on various hydraulic analyses in order to yield quantitative assessments. For computing of the water surface profiles and modeling the open channel flow at an investigated bridge site, commonly the software that perform one dimensional analysis (e.g. HEC-RAS, WSPRO) are used. When the variables such as approaching water velocity and unscoured water depth at a bridge pier/s are obtained, the scour evaluation formulas can be applied.

The local scour evaluation formulas have been derived on the basis of extensive hydraulics laboratory testing (flume tests), available field data and have been updated over the years. These formulas are empirical and considered conservative as the obtained results usually overestimate measured scour depths in situ. They are primarily developed for application in the design of new bridges as the information of possible maximum scour depth governs the selection of appropriate foundation type and depth. Although the mechanisms of local scour are thoroughly explained in the up-to-date literature and have been topic of many research in the past, the evaluation and prediction of local scour magnitude at the bridge piers still represents a difficult task. The large number of parameters, their interdependencies as well as scaling problems (e.g. soil properties) in the laboratory experiments, impede obtaining of the reliable results applicable in the field. The processes contributing to local scour at a cylindrical pier in cohesionless sediment (e.g. sand) involve basic parameters which are distinguished into primary and secondary based upon their influence on the maximum scour depth. They relate to river bed material & configuration, flow characteristics, fluid

properties, geometry of the pier and footing (Fig. 3.3) and the duration of a scour process [Ettema et al., 2011]:

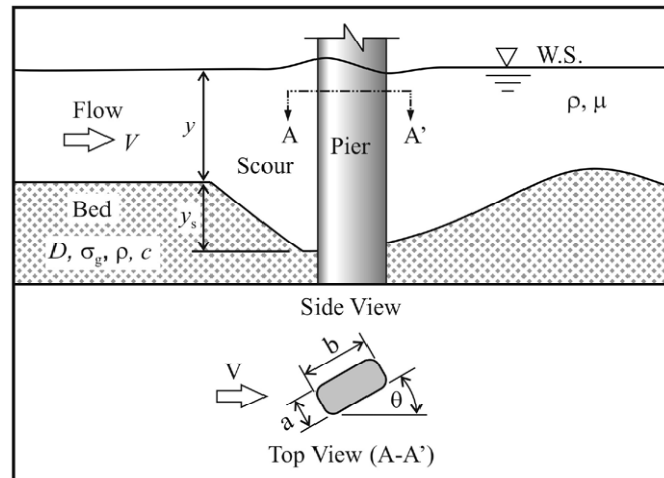


Fig. 3.3 Variables influencing pier scour, [Ettema et al. 2011]

1. The primary parameters, which relate directly to the pier flow field:

- y/a indicates the geometric ratio of the pier flow field in a vertical cross-sectional plane transverse to the pier, and streamwise to the pier; pier flow-field categories: narrow ($y/a > 1.4$), wide ($y/a < 0.2$), transition ($0.2 < y/a < 1.4$),
- a/D_{50} represents length ratio of pier width and median diameter of bed particle ratio
- Ω , a/b , and θ are respectively pier face shape, aspect ratio of pier cross-section, and approach flow alignment to pier

2. The secondary parameters have magnitudes derived from the primary parameters with regard to potential maximum scour depth:

- V/V_c is the flow intensity which distinguishes whether clear-water or live-bed scour conditions prevail in the approach flow to the pier (V_c is prescribed with sediment diameter D_{50})
- V^2/ga is an Euler number relating vorticity induced inertial forces in the pier flow field relative to gravity acceleration
- $\rho Va/\mu$ is the pier Reynolds number

- σ_s is geometric standard deviation of bed particles and characterizes soil uniformity
- tV/a characterizes the temporal development of scour associated with pier flow field and nature of foundation material (in conjunction with other parameters)

Unlike the cohesionless soils, the behavior of cohesive soils in scouring (e.g. clay) is greatly influenced by erodibility. The erodibility is tied to a number of factors (Fig. 3.4) and dependent from the critical shear stress τ_c on the water-soil interface at initiation of scour. The critical shear stress usually varies in the range from 0.1 N/mm^2 to 5 N/mm^2 both for cohesive and cohesionless soils (Fig. 3.4), but the major difference is the rate of erosion beyond this stress. For cohesive soils this rate is measured in mm/hour and in cohesionless soils the rate can be even 10^5 times higher [Briaud et al., 2003].

When this parameters increases	Erodibility
Soil water content	*
Soil unit weight	decreases
Soil plasticity index	decreases
Soil undrained shear strength	increases
Soil void ratio	increases
Soil swell	increases
Soil mean grain size	*
Soil percent passing sieve #200	decreases
Soil clay minerals	*
Soil dispersion ratio	increases
Soil cation exchange capacity	*
Soil sodium absorption ratio	increases
Soil pH	*
Soil temperature	increases
Water temperature	increases
Water chemical composition	*

*unknown

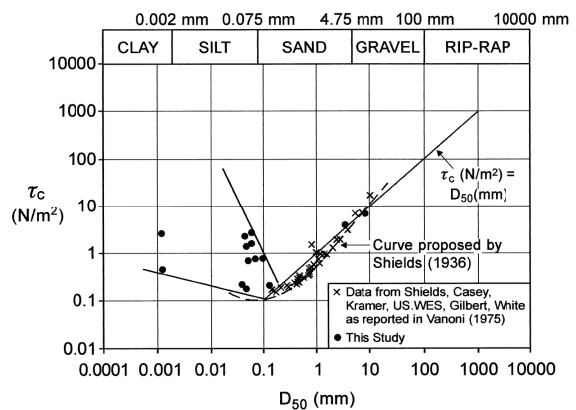


Fig. 3.4 Variables influencing erodibility (left), critical shear stress versus soil grain diameter (right), [Briaud et al., 2003]

In [Ettema et al. 2011], the two leading formulas for the local scour depth evaluation are analyzed. The first and widely utilized is the HEC-18 pier scour equation (the CSU formula) [Richardson and Davis, 2001]. The second is the Sheppard & Melville formula (i.e. FDOT formula) [Sheppard et al., 2011]. Both formulas are based on flume tests and local scouring around cylindrical shaped column in a cohesionless soil. The latest version of the method used for evaluation of scour in cohesive soils, termed SRICOS-EFA (Scour Rate In COhesive Soil – Erosion Function Apparatus), is given in [Briaud et al., 2011]. Here, the formulas of maximum scour

depth were developed on the basis of flume test results and dimensional analysis, while the maximum shear stress was developed on the basis of three-dimensional numerical computation results. The three above mentioned state-of-the-art formulas are now briefly presented.

3.1.1.1 HEC-18 pier scour evaluation method

This local scour formula (Eq. 3.1) is referred to as HEC-18 pier scour equation or commonly CSU formula as it stems from extensive research conducted at Colorado State University. Its latest form is given in the HEC-18 manuals [Richardson and Davis, 2001] and [Arneson et al., 2012]:

$$\frac{y_s}{y_1} = 2.0K_1K_2K_3K_4 \left(\frac{a^*}{y_1}\right)^{0.65} F_r^{0.43} \quad (3.1)$$

where:

y_s = local scour depth [m]

y_1 = flow depth directly upstream of the pier i.e. unscoured water depth [m]

a^* = equivalent pier diameter width [m]

$F_r = \frac{V_1}{\sqrt{g \cdot y_1}}$ = Froude number directly upstream of the pier

V_1 = Mean velocity of flow directly upstream of the pier [m/s]

g = acceleration of gravity [9.81 m/s²]

The K_1 , K_2 , K_3 , K_4 are correction factors respectively for pier nose shape, angle of attack flow, bed condition and armoring by bed material size. For their definition and values reader is directed to [Arneson et al., 2012]. The Eq. 3.1 has predefined upper bound values for round-nose pier aligned with the flow: $y_s(\max) = 2.4y_1$ for $F_r \leq 0.8$ and $y_s(\max) = 3y_1$ for $F_r > 0.8$.

This method is the predominant method for design estimation of pier scour in the U.S and recommended by American Association of State Highway and Transportation Officials (AASHTO). It is suggested both for clear water scour and live bed scour conditions as well as for non-cohesive and cohesive soil.

3.1.1.2 HEC-18 clay formula

The studies of bridge scour depths in cohesive soils with consideration of soil erodibility and time dependence have been performed at Texas A&M University since 1990. The motivation for this research came from the fact that the fine grained soils, such as clays, erode at a much slower rate than sand that was predominantly used to model local scour. The SRICOS-EFA method [Briaud et al. 2011], defines the time-dependent scour depth given as a function of the two main parameters, the maximum scour depth (Eq. 3.2) and the maximum shear stress at the water-soil interface (Eq. 3.3). Additional requirement in this method is the site-specific erosion testing - EFA apparatus [Briaud et al., 2003]. The EFA device utilizes site-specific, thin-walled tube soil samples extracted at foundations to acquire soil erosion rates which are subsequently used to estimate time-dependant scour depths (Eq. 3.4). The formula for evaluation of a maximum local scour depth at a bridge pier in cohesive soil, also referred to as HEC-18 clay formula, is:

$$\frac{y_s}{a} = 2.2K_w K_I K_L K_{sp} \left(2.6F_{r(pier)} - F_{rc(pier)} \right)^{0.7} \quad (3.2)$$

where:

- y_s = local scour depth [m]
- a = projected pier width (perpendicular to the flow for rectangular pier) [m]
- $F_{r(pier)}$ = Froude number based on V_1 and a
- $F_{rc(pier)}$ = critical Froude number based on V_c and a
- V_1 = approach average velocity [m/s]
- V_c = critical velocity for initiation of erosion of a soil material [m/s]

The K_w , K_I , K_L , K_{sp} are correction factors for water depth, pier shape, pier aspect ratio and pier spacing respectively. For their definition and values, the reader is directed to [Briaud et al., 2011]. Further, the formula for the evaluation of the maximum hydraulic shear stress exerted by the water on the riverbed around the pier is:

$$\tau_{max(pier)} = k_w k_{sh} k_{sp} k_{\theta} 0.094 \rho V_1^2 \left[\frac{1}{\log Re} - \frac{1}{10} \right] \quad (3.3)$$

where:

- $\tau_{max(pier)}$ = maximum shear stress around the pier [N/m²]
- V_1 = mean approach velocity of flow directly upstream of the pier [m/s]

- ρ = water density [1000 kg/m³]
 R_e = Reynolds number

The k_w , k_{sh} , k_{sp} , k_θ are correction factors for water depth, pier shape, pier spacing and attack angle respectively [Briaud et al., 2011]. The HEC-18 clay method is can be used to estimate the final scour at the end of the design life of a structure. The hyperbola is used to connect the erosion scour rate to the maximum scour depth:

$$y_s(t) = \frac{t}{\frac{1}{\dot{z}} + \frac{t}{y_s}} \quad (3.4)$$

where:

- $y_s(t)$ = depth of pier scour after a flood with duration t [m]
 t = flood duration [hours]
 y_s = maximum depth of pier scour (Eq. 3.2) [m]
 \dot{z} = erosion rate of scour [mm/hour]

It is not an easy task to obtain the \dot{z} (Eq. 3.4) as the relationship between soil properties and erodibility is complex and involves advanced understanding of combination of soil properties and environmental conditions (Fig. 3.4). Thus the direct testing and measurement is suggested in the EFA apparatus. Here, for τ_{max} calculated in Eq. 3.3, the related \dot{z} is obtained (e.g. Fig. 3.5 where τ_c denotes the critical shear stress for initiation of erosion of a soil material).

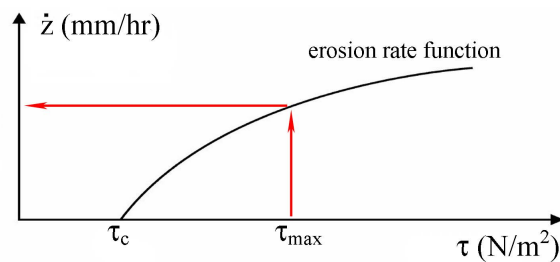


Fig. 3.5 A result of an EFA-test, adapted from [Briaud et al., 2003]

The idea to eliminate site-specific erosion testing led to the erosion function charts [Briaud et al., 2009]. These charts are based on velocity or shear stress for various soil types (Fig. 3.6). They in fact represent the EFA test data based on the six erosion categories of the Unified Soil Classification System (USCS).

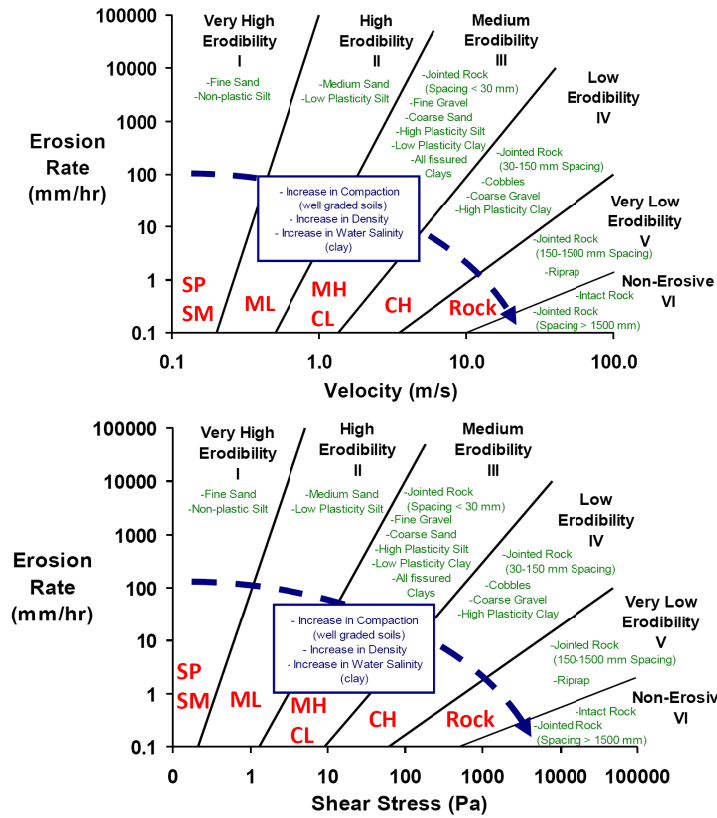


Fig. 3.6 Suggested erosion categories for soils and rocks based on velocity and shear stress, [Briaud et al., 2009]

Generally, it was observed that soil materials scatter approximately over two categories showing large covariance thus conservative values are suggested when selecting an erosion category (Fig 3.7).

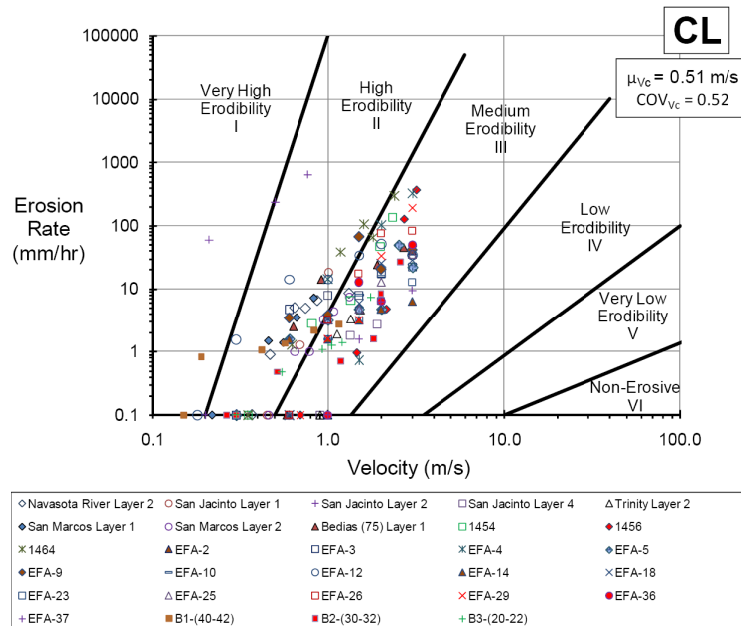


Fig. 3.7 EFA test data for low plasticity clays, based on velocity and plotted on the erosion function chart, [Briaud et al., 2009]

The SRICOS-EFA methodology accounts clear-water scour and does not simulate live bed scour nor include scour cavity infilling thus it gives a conservative prediction of scour depth.

3.1.1.3 Sheppard and Melville local scour evaluation method (FDOT method)

This method is developed on the basis of the work presented in [Melville and Coleman, 2000] and [Sheppard and Miller, 2006]. The six important dimensionless parameters comprised in the Sheppard and Melville formula (i.e. FDOT formula) [Sheppard et al., 2011] are: y/a , a/D_{50} , pier shape Ω , pier aspect ratio a/b , pier alignment θ and V/V_c . This method was primarily developed for estimating the scour at wide and long skewed piers ($y/a < 0.2$), but it gives fair results for narrow ($y/a > 1.4$) and transitional ($0.2 < y/a < 1.4$) pier flow-field categories. The both cases of local scour are distinguished, clear-water for $0.4 < V/V_c < 1$ and live bed for $V/V_c > 1$:

$$\frac{y_s}{a^*} = 2.5f_1f_2f_3 \quad (0.4 < V/V_c \leq 1.0) \quad (3.5)$$

$$\frac{y_s}{a^*} = f_1 \left[2.2 \left(\frac{V/V_c - 1}{V_{1p}/V_c - 1} \right) + 2.5f_3 \left(\frac{V_{1p}/V_c - V/V_c}{V_{1p}/V_c - 1} \right) \right] \quad \left(1 < \frac{V}{V_c} \leq \frac{V_{1p}}{V_c} \right) \quad (3.6)$$

$$\frac{y_s}{a^*} = 2.2f_1 \quad \left(\frac{V}{V_c} \geq \frac{V_{1p}}{V_c} \right) \quad (3.7)$$

where:

y_s = equilibrium local scour depth [m]

a^* = effective pier width [m]

$f_1 = \tanh\left(\frac{y}{a^*}\right)^{0.4}$

$f_2 = 1 - 1.2 \left(\ln\left(\frac{V}{V_c}\right)^2 \right)$

$f_3 = \frac{\frac{a^*}{D_{50}}}{0.4 \frac{a^*}{D_{50}}^{1.2} + 10.6 \frac{a^*}{D_{50}}^{-0.13}}$

y = flow depth directly upstream of the pier [m]

D_{50} = median sediment diameter [m]

V = average flow velocity at upstream main channel [m/s]

V_c = critical velocity for initiation of erosion of a soil material (D_{50}) [m/s]

$$V_{1p} = \max(5V_c, 0.6\sqrt{gy_1}) \quad \text{live bed peak velocity [m/s]}$$

$$y_1 = \text{average depth in the upstream main channel [m]}$$

$$g = \text{acceleration of gravity [9.81 m/s}^2\text{]}$$

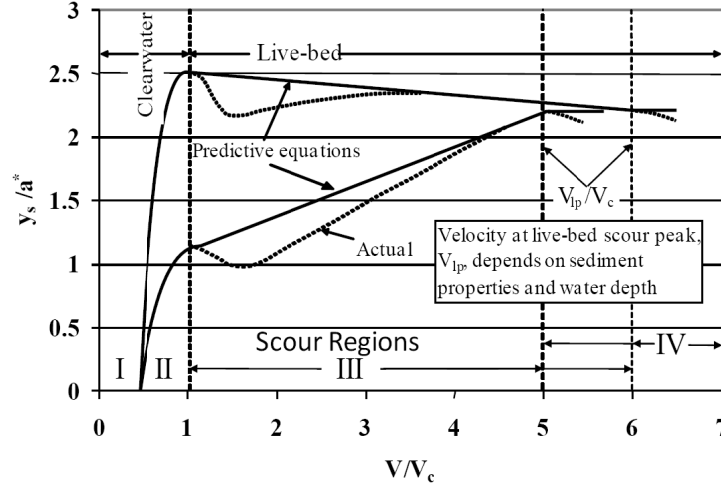


Fig. 3.8 Equilibrium scour depth with flow intensity ($y/a^* > 3$, $a^*/D_{50} = \text{const}$), [Sheppard et al, 2011]

In Fig. 3.8, the scour regions I, II, III and IV are related to the case of no scour, Eq. 3.5, Eq. 3.6 and Eq. 3.7, respectively. The critical velocity V_c may be calculated using the logarithmic law of velocity distribution:

$$\frac{V_c}{u_{*c}} = 5.75 \log \left(5.53 \frac{y}{D_{50}} \right) \quad (3.8)$$

where the critical shear velocity for soil particle entrainment u_{*c} may be evaluated as given in [Melville and Coleman, 2000]:

$$u_{*c} = 0.0115 + 0.0125D_{50}^{1.4} \quad [\text{m/s}] \text{ for } 0.1\text{mm} < D_{50} < 1\text{mm}$$

$$u_{*c} = 0.0305D_{50}^{0.5} - 0.0065D_{50}^{-1} \quad [\text{m/s}] \text{ for } 1\text{mm} < D_{50} < 100\text{mm}$$

In Eqs. 3.5 to 3.7, the factor K_t may be applied to obtain the scour evolution over time $y_{st}(t)$:

$$y_{st}(t) = y_s K_t \quad (3.9)$$

where:

$$K_t = e^{-0.04 \left| \frac{V_c}{V} \ln \left(\frac{t}{t_e} \right) \right|^{1.6}}$$

$$t_e = 200 \frac{a^*}{V} \left(\frac{V}{V_c} - 0.4 \right) \quad (\text{days}) \quad \left(\frac{y_1}{a} > 6, \frac{V}{V_c} > 0.4 \right)$$

$$t_e = 127.8 \frac{a^*}{V} \left(\frac{V}{V_c} - 0.4 \right) \left(\frac{y}{a^*} \right)^{0.25} \quad (\text{days}) \quad \left(\frac{y_1}{a} \leq 6, \frac{V}{V_c} > 0.4 \right)$$

t = peak flood duration (days),
 t_e = time to reach equilibrium scour depth (days), and additionally
 $t_{90} = e^{-1.83 \left(\frac{V}{V_c} \right)} t_e$ time to reach 90% of equilibrium scour depth (days)

The local scour depth approaches the equilibrium asymptotically (Fig. 3.2) thus t_{90} (see Eq. 3.9) is suggested to give a more realistic and practical value.

3.1.2 Bridge site complications affecting local scour depth

The leading methods for scour depth estimation are mostly based on laboratory data which involves simple cylindrical pier forms and usually does not coincide with common pier designs cases. Although various correction factors are applied in scour evaluation formulas, their accuracy reduces as pier form complexity increases.

In [Melville and Coleman, 2000], the scour depth variation at complex piers was discussed. It was observed that when the pier footing, cap or caisson with its top is below the river bed level, the local scour depth is reduced due to interception of the down-flow (Case II in Fig. 3.9). However, if the top of the wider foundation element comes to the bed level (in the undisturbed flow region away from the pier), or even above, the scour depth is increased.

The procedures for calculation of pier scour for complex pier geometries (pier stem, pile cap, pile group) is given for the CSU and FDOT methodologies in [Arneson et al., 2012] and [FDOT, 2010] respectively. The method of superposition of the scour depths for the pier components was used in both procedures. However, the summation of the scour attributable to individual parts of a pier lacks a physical basis as it does not relate to the actual flow field producing scour [Ettema et al., 2011]. The development of a formula, which will adequately consider the scour at shallow fundamentals, is still a critical research need.

The conditions at a bridge site that can adversely affect the flow field at a pier thus exacerbate scour depths, must be taken into consideration in the local scour evaluation. It is a fact that the proximity of an abutment and the case of bridge-deck submergence in flooding event introduce additional processes, which affect

the scour depth at a pier as reviewed in [Ettema et al., 2011]. Also, such scenario may arise from debris or ice presence in the river, which is further discussed below.

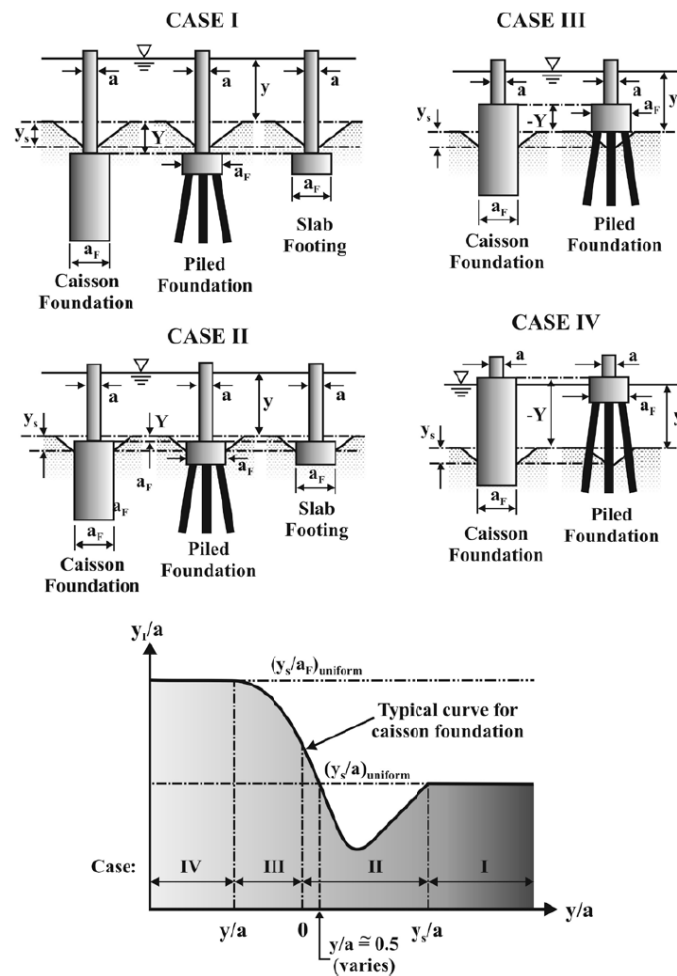


Fig. 3.9 Scour depth variation in the four cases of non-uniform pier shape, [Melville and Coleman, 2000]

3.1.3 Debris effect in the scouring event

Tree trunks, branches and other wood that fall into a river during a flood (i.e. wood debris) may eventually accumulate around bridge piers and thus obstruct, constrict or redirect river flow through bridge openings resulting in damaging load and/or excessive scour at bridge foundations (Fig. 3.10). Currently, the most comprehensive analysis of the potential for debris accumulation at the bridge substructures and its effects on the realized scour depths was presented in [Lagasse et al., 2010]. Here it was confirmed that debris cluster alter the flow pattern at a pier (Fig. 3.11) and significantly affects potential scour depth.

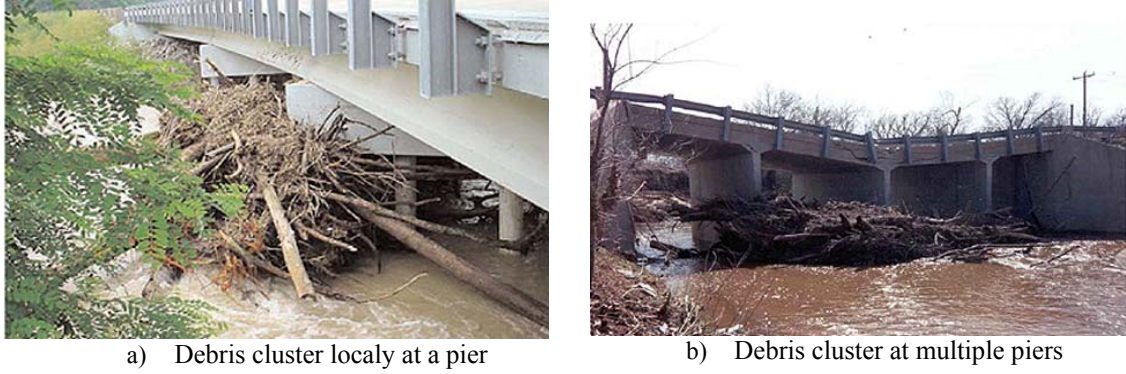


Fig. 3.10 Examples of debris clusters, [Lagasse et al., 2010]

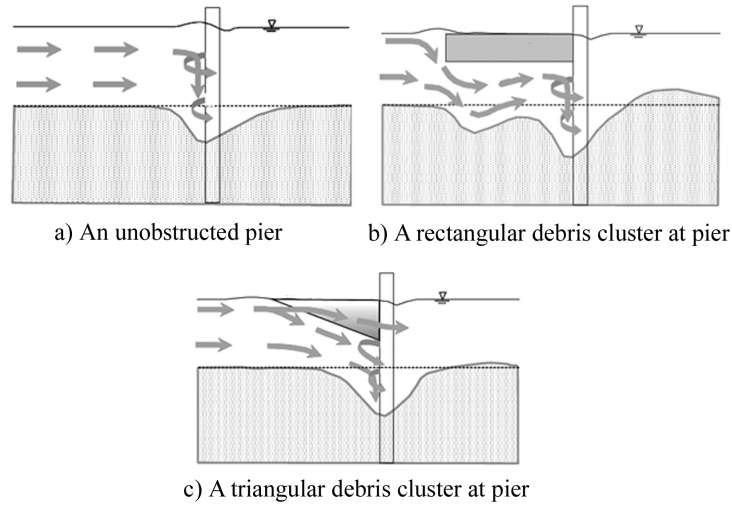


Fig. 3.11 Idealized flow patterns at pier, [Lagasse et al., 2010]

For the two types of debris clusters, rectangular and triangular, the formulas for calculating the effective pier width a_d^* are given:

$$\alpha_d^* = \frac{K_{d1}T_D W_D + (y - K_{d1}T_D)a}{y} \quad (L/y \leq 1.0) \quad (3.10)$$

$$\alpha_d^* = \frac{K_{d1}(T_D W_D) \left(\frac{L_D}{y}\right)^{K_{d2}} + (y - K_{d1}T_D)a}{y} \quad (L/y > 1.0) \quad (3.11)$$

where:

K_{d1} = 0.79 for rectangular debris, 0.21 for triangular debris

K_{d2} = -0.79 for rectangular debris, -0.17 for triangular debris

L_D = length of debris upstream from pier face [m]

y = depth of approach flow i.e. unscoured water depth [m]

T_D = thickness of debris [m]

W_D = width of debris normal to flow [m]

a = pier width without debris [m]

The examples given in [Lagasse et al., 2010] show that the accumulated debris at piers may adversely affect scour depths in comparison with a no debris case thus must not be neglected in the evaluation of the maximum local scour depths. The a_d^* obtained from Eq. 3.10 and 3.11 may be applied in the CSU formula (Eq. 3.1). The consideration of debris at a pier in the FDOT formula is a future research topic.

3.1.4 Local scour cavity form

Besides the maximum local scour depth, the feature that characterizes local scour action at bridge piers is the scour cavity form. The scour forms at a cylindrical pier in sand bed and clay bed were discussed by [Briaud et al., 2003] and the conclusion was that the maximum depth of scour is approximately similar for each material, but the location of the maximum depth differs. For the sand bed, the upstream side of the scour cavity slope is close to the angle of internal friction while for cohesive materials scour form is less regular and deepest at pier flanks (Fig. 3.12). Additionally, the scour forms may differ for various shapes of piers and are governed by the angle of water attack (e.g. Fig. 3.13) as discussed and considered in the local scour formulas by applying correction factors.

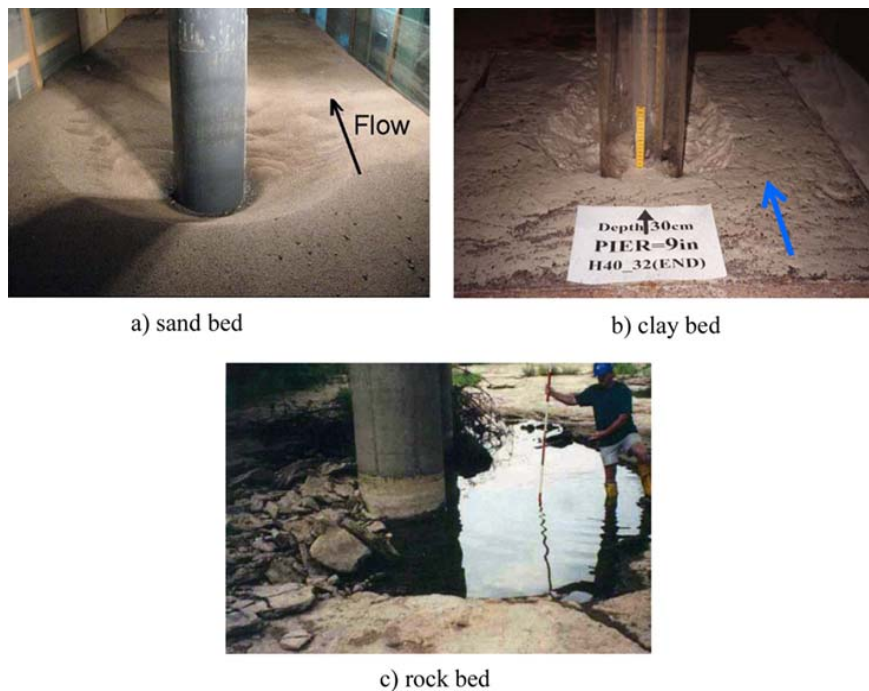


Fig. 3.12 Differences in scour form at a cylindrical pier, [Ettema et al., 2011]

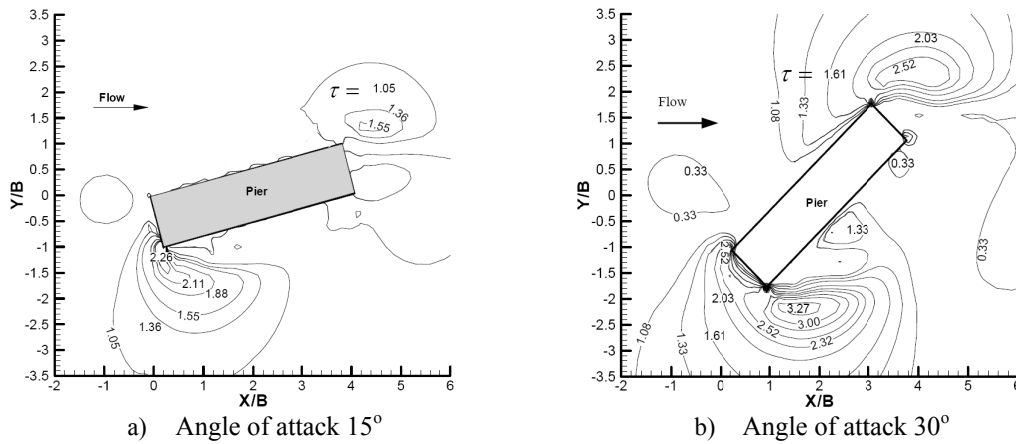


Fig. 3.13 Bed hydraulic shear stress around rectangular pier B/L, [Briaud et al., 2003]

The use of motion sensors as a monitoring tool in revealing the critical scour depth at a pier necessary to inflict collapse has been investigated by [Yao et al, 2010]. Here the large scale experiment has been performed to model the response of a bridge pier subjected to growth of progressive scour. The installed instruments gathered the data on the change in modal frequency of the 4 m-tall with 0.45 m-diameter embedded bridge pier (Fig 3.14). Since there was no restraint to horizontal displacement at the pier top, the pier started sinking and tilting as soon as the scour cavity reached the foundation base. The form of the scour cavity was not in the scope of the research.

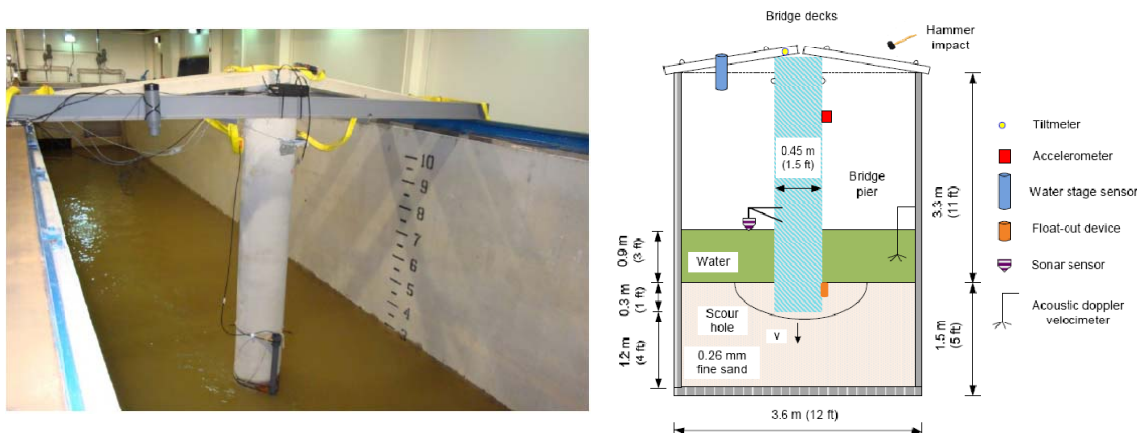


Fig. 3.14 Model of a bridge pier (left) and the experiment setup (right), [Yao et al., 2010]

The actual scour cavity form at a shallow pier foundation (i.e. spread footing), its connection to the maximum local scour depth obtained from local scour evaluation formulas and effect on a bridge stability has not been sufficiently clarified in the up-to-date research to the best knowledge of the author.

3.1.5 Temporal aspect of scour

The secondary parameters, such as the temporal aspect i.e. scour evolution (Fig. 3.15), are considered to be non-essential as they introduce considerable uncertainty in the scour depth calculation and therefore are omitted. As a consequence, the obtained results are conservative and suitable for the most pier design situations.

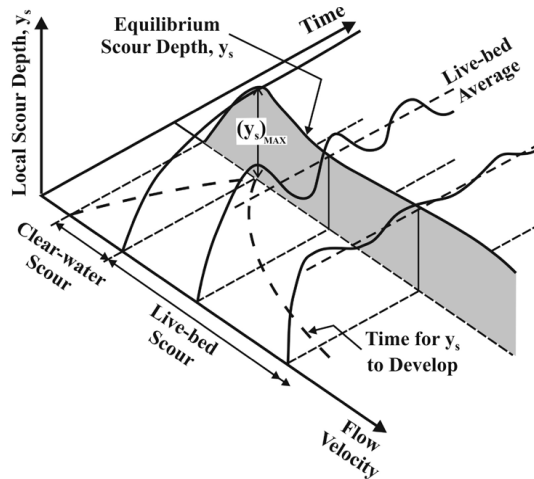


Fig. 3.15 Local scour depth variation with flow intensity and time, [Melville and Coleman, 2000]

Overall, there is not much research done on the scour evolution especially for the live bed conditions as they are difficult to model in the laboratory and currently there is no sufficient field data. Recently the time variation of scour was researched by [Yanmaz, 2006], [Olivieto et al, 2007], [Kothyhari et al, 2007]. Based on existing laboratory and field data, in [Sheppard et al., 2011] the several formulas, which model scour evolution, were compared. It was presented that the FDOT formula gives the least total error and nearly the lowest underestimation.

The duration of the highest flow conditions at a particular site has great influence on the local scour process at the piers. The shape of the flood flow hydrograph is important as well as the duration of flood recession period where live-bed scour turns into contraction scour and induce additional scouring around the pier [Melville and Coleman, 2000]. Additionally, for the live bed conditions the equilibrium scour depth may be reached in a single flooding event, while for the cohesive soils the scouring process may last longer and usually more than one flood is needed to reach the maximum local scour depths at piers. In fact, the local scour depths well below the maximum estimated using the scour evaluation formulas might be sufficient to trigger a

bridge failure. Thus in the vulnerability analysis, regardless of the soil type, the flood hydrographs for the investigated location should be applied in the estimation of the critical scour depths.

The concept of equivalent time required for the maximum velocity V_{max} in the known hydrograph to create the same scour depth as the one created by the complete hydrograph is given in the procedure for simplified scour estimation [Briaud et al, 2009]:

$$t_{e,p} = 73t_{hyd}^{0.126}V_{max}^{1.706}\dot{Z}^{-0.20} \quad (3.12)$$

where:

- $t_{e,p}$ = equivalent time of pier scour (hours)
- t_{hyd} = duration of the complete hydrograph (hours)
- V_{max} = maximum velocity in the complete hydrograph [m/s]
- \dot{Z} = erosion rate of scour (mm/hour)

The latter equation is limited to the database it was derived from, which include hydrographs for 7 rivers in Texas and EFA testing. However, the idea of equivalent time for pier scour is worth further consideration as it considerably simplifies complex hydrograph-based analysis.

3.2 The application of the state-of-the-art local scour formulas in the vulnerability assessment

Based on the previous sections and the mentioned literature, the features of the three presented local scour evaluation formulas are reviewed (Table 3.1) and the possibility for their application in the vulnerability assessment is discussed.

Table 3.1 Features review of the formulas for local scour evaluation

Local scour evaluation formula	Soli particles	Live bed scour	Complex pier geometry	Debris	Temporal aspect	Used for future hydrographs	Edrodibility testing
<i>CSU</i>	Coarse	YES	YES	YES	NO	NO	NO
<i>HEC-18 clay</i>	Fine*	NO	NO**	NO	YES	YES	YES
<i>FDOT</i>	Coarse	YES	YES	NO	YES	NO	NO

* may be used for scour evaluation in coarse-grained soil
 ** only the correction factors for column spacing are introduced

The CSU method is predominantly used in the up-to-date research and practice but in the light of most recent research on the parameters influencing the pier scour processes [Ettema et al., 2011], the advantage is given to the FDOT formula which is

considered as more robust and gives better results for transition and wide-pier categories. Furthermore, the CSU method does not account the temporal aspect of scour and overestimates the scour depths when used with erodible-resistant soils (e.g. clay, rock) [Govidasamy et al., 2013]. The advantages over the other two methods are the possibility to account for the debris at bridge substructures and somewhat simple approach in the case of complex pier-foundation systems.

Among the discussed formulas only the FDOT distinguishes the clear-water scour from live bed scour. In spite of good results for the live bed conditions, the research still needs more field confirmation [Sheppard et al., 2011]. The use of the FDOT method is limited to soils with D_{50} down to 0.1mm (Eq. 3.8).

The comparison of the HEC-18 clay method to the CSU method was presented in [Bolduc et al, 2008] and the conclusion was that the HEC-18 clay method may be used for cohesionless soils as well. The scour extent at complex pier geometries is not treated in this method. Furthermore, the additional testing of the soil specimens from the bridge site is necessary, which is a main drawback as it causes additional costs. This issue was addressed with erosion rate charts (Fig. 3.6), but there is non-negligible level of uncertainty when estimating the erosion category. This method is already being used for analysis of scour depths for future flood hydrographs and multiple-flood scenarios [Govidasamy et al., 2013].

Taking everything into consideration, the FDOT and HEC-18 clay formula are selected to be used in the following vulnerability analysis. The main criterions were consistency with the state-of-the-art research on the pier scour processes and possibility to account for scour evolution in different soil types. Considering its advantages in treating of the complex pier-foundation systems and debris accumulation, the application of the CSU method would certainly benefit the vulnerability assessment if it includes the temporal aspect in the future research.

Chapter 4. Elements of the Soil-Bridge model and resistances of a bridge and supporting soil to local scour action

4.1 Scour critical bridges in the BPM

The BPM database was screened for the bridges with shallow foundations, which are jeopardized by scour. Several multiple span RC girder bridges on the rivers Nišava (southern Serbia) and Crni Timok (eastern Serbia) were selected based on their database entries and the rating scores. The available project documentations were reviewed (e.g. [Bridge over Nišava II -reconstruction, 2010] and [Bridge over Crni Timok, 1968]) and the information related to the bridges` design and detailing is summarized in the following text.

The bridges were designed and built between 1965 and 1975. They have 3 or 4 spans ranging from 15 - 20 m. Their main girders have RC double-tee cross-sections and the girder beams are designed to be tapered towards the middle span supports (starting from approx. 3/4 of a span) to increase the shear and torsion resistance of the open cross section. The resistance of the main girders to arbitrary loading is supported by transverse beams which are located in thirds of spans (approx. every 5 to 7 m) and over supports. The bridge deck is designed as a continuous two-way slab supported by the girder beams and the transverse beams which are designed as simple span beams. The longitudinal reinforcement layout in the girder beams is based on the linear elastic analysis, implies splicing of the bottom rebar near middle supports (i.e. in the compression zones) and the minimal reinforcement ratios according to an applied design code. The shear reinforcement in all beams consists of “bent up” longitudinal bars and stirrups, which was the common practice in Serbia.

The monolithic joints between a superstructure and piers are not designed for the full-frame action (section 4.1.2) and pier reinforcement is anchored in a transverse beam. The supports at abutments are realized as double-neck RC bearings (Fig. 4.5). The substructures of the reviewed bridges are either single column piers or double column piers. The shallow foundations are strip footings, caissons or spread footings (Fig. 4.1). The reinforcement at the connection of a foundation and its pier is based on the minimum reinforcement ratios given by the applied code and the bending moment based on a braking force (the first seismic code in Serbia date from 1981 and it

does not apply to bridges). This force is adopted as 3% of the vertical force from superstructure at the pier including self-weight and live loading.

The bridge design, reinforcement layouts and detailing in Serbia were based on allowable stress design (ASD) up to 1987 and afterward on the limit state design (LSD). According to [Bebić, 2006], before 1932 there is no reliable data on the used bridge design codes. In addition, during the period between 1932 and 1941 the live loading regulations of Kingdom Yugoslavia were used, from 1941-1991 for highway bridges the regulations were based on the German DIN-1072, and the code used today dates from 1991 (in Serbian “Pravilnik o tehničkim normativima za određivanje veličina opterećenja mostova”). The project documentation is not available for every bridge in the BPM database, and in some cases, the years of bridge design and construction are not entered. This increases the uncertainty regarding the amounts of used reinforcement and detailing in these bridges.

According to the gathered information in the BPM, about 70% of bridges in Serbian road network are girder RC bridges (Table 4.1).

Table 4.1 Structural system and material in the BPM, [Mašović and Hajdin, 2014]

System	Material	%
Arch	Stone	0.3
	Masonry	0.9
	Concrete	4.2
	Σ	5.4
Frame	Reinforced concrete	16.2
	Prestressed concrete	0.3
	Σ	16.5
Beam	Reinforced concrete	53.3
	Prestressed concrete	17.9
	Steel	4.9
	Composite (steel girder with concrete deck)	2
	Σ	78.1

Depending on bridge design requirements (e.g. site characteristics, traffic demand) the most common RC main girders (i.e. superstructure) of a multiple span bridges in Serbia are:

- double-tee girder (spans > 15 - 30m),
- slab girder (spans < 15m),
- multiple pre-stressed I girders (spans 20 - 30m), and
- box girder (spans > 30m)

The information on the reviewed bridges was taken as a basis for development of the model, which represents a typical short to medium multiple span bridge in the BPM affected by local scour (Chapter 5.). The selected typical bridge is the RC double-tee main girder with transverse beams (e.g. in Fig 4.6).

4.1.1 Pier-foundation systems

The configurations of bridge piers and their shallow foundations (Fig. 4.1) considered in the analysis are:

- Single wide pier on a strip footing (i.e. wall type pier),
- Pier with double columns on a common strip footing,
- Pier with double columns each on a separate spread footing, and
- Single column pier on a caisson

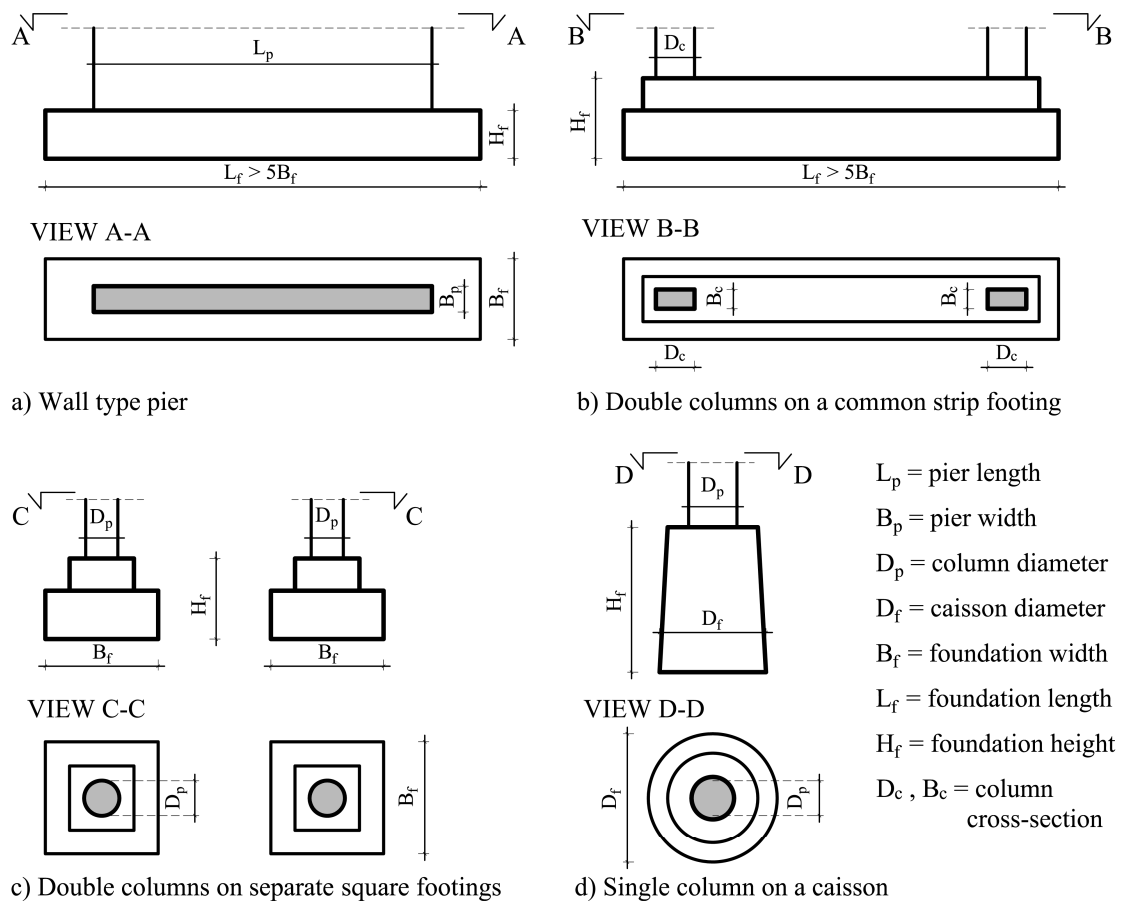


Fig. 4.1 Pier-foundation system configurations used in the analysis

Although the caisson foundation is classified as a deep foundation, the effects of multiple floods and general scour may reduce the soil cover at the foundation and expose it to the future local scour events. The susceptibility to scour and settlement of different pier-foundation systems were discussed in [Agrawal et al., 2007]. It was observed that the system that comprises two or more columns founded on the separate footings is the most vulnerable to local scour and uneven settlement (Fig. 4.2).

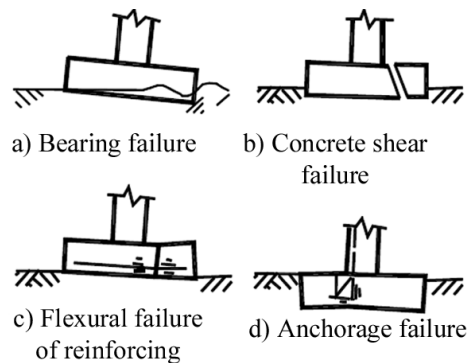


Fig. 4.2 Observed typical footing failures due to scour [Agrawal et al., 2007]

In general, the connection of RC bridge pier and its foundation may be considered as rigid as it is mostly oversized. Usually the minimum ratios of longitudinal and transverse reinforcement applied by design codes are sufficient to pass design checks. However, the loading case, which involves local scour action, is not a common design load combination and if there is poor detailing, the internal forces cannot be transferred between the pier and foundation leading to local failures, types of which are presented in Figs. 4.2*b*, 4.2*c* and 4.2*d*. Such failures may cause collapse of an entire bridge span (e.g. Fig. 1.5), thus it is essential to review the project documentation especially for pier-foundation system as in Fig. 4.1*b* (section 5.8).

4.1.2 Bridge joints

The joints between substructure and superstructure may have high impact on the overall bridge behavior in the scouring event. In general there are two types of joints depending on the bridge design requirements: monolithic and non-monolithic. The main difference between these, besides their bearing capacity, is the possibility to transfer shear forces, bending moments and torque between the main girder and piers. The monolithic joints restrain displacements and rotation in all directions. Unlike the full frame action joints, the constructive monolithic joints are those with inadequate

longitudinal or transverse reinforcement ratios and/or improper detailing according to official design codes. Nevertheless, their strength may be reliably estimated if the project documentation is available.

The non-monolithic joints physically separate the main girder from the substructure thus the transfer of forces, according to the design requirements (e.g. Fig. 4.3), is realized over a set of bearings which are fixed at the substructure (i.e. pier or abutment top). The most common types of bearings are:

- Elastomeric pad bearings, which accommodate displacement/rotation with elastic deformation (Fig. 4.4), but can also restrain translation with limiters
- Roller bearings, which allow rotation and translation in one direction
- Pot bearings, which allow rotation and restrain translation
- Rocker bearings, which allow rotation in one direction and restrain translation

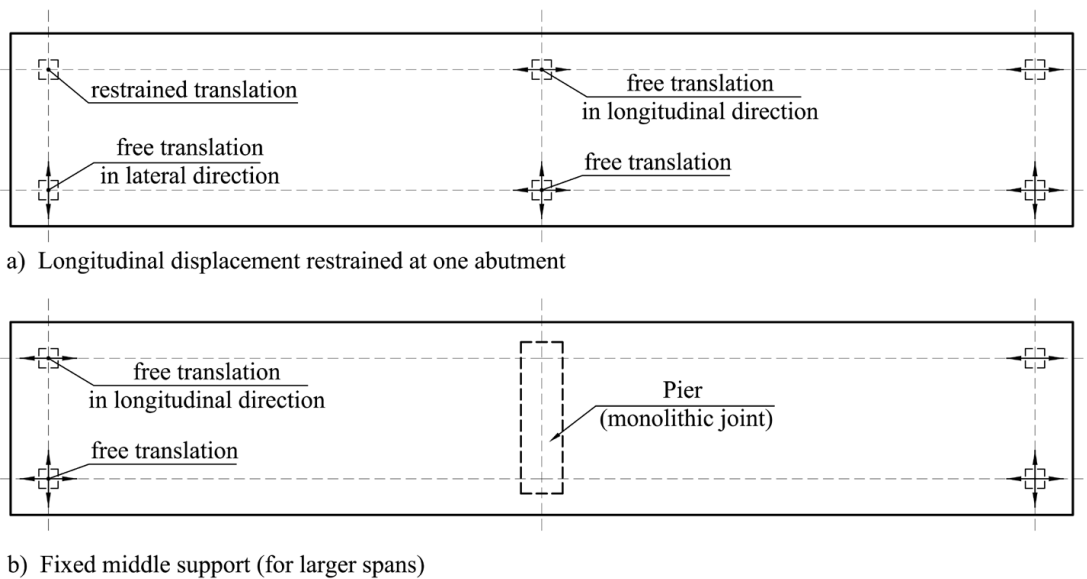


Fig. 4.3 Two examples of bearing layouts for a two-span bridge

The actual load transfer capacity of the bearings is generally unknown as these elements are prone to fatigue and decay. The manufacturer's data, if available, give the lower bound values. These uncertainties may lead to incorrect conclusions with regard to governing bridge failure mode and should be investigated in future. The behavior of bearings in combined loadings (e.g. Fig. 4.4) needs to be considered as well. This, however, is beyond the scope of this thesis.

The double-neck RC bearings (Fig. 4.5) at bridge abutments are common for aging bridges in Serbian road network. Although their detailing implies rebar

anchorages at an abutment and a superstructure, this support allows rotation and restrains translation by design (i.e. a pinned support).

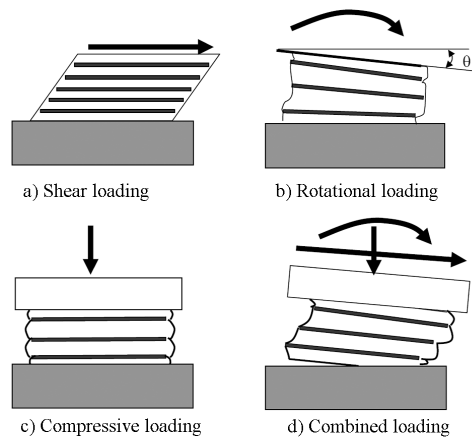


Fig. 4.4 Possible loading cases on steel reinforced elastomeric pads [Mtenga, 2007]

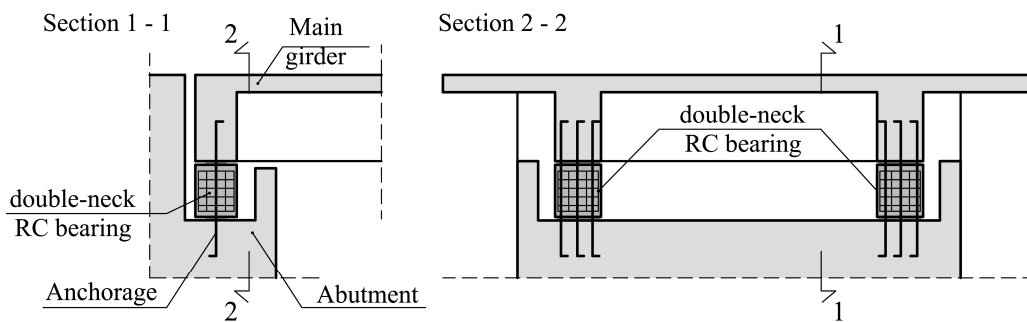


Fig. 4.5 Schematics of a double-neck concrete RC bearing at an abutment

For the sake of simplicity, the joints in the assumed bridge model are considered to be either fixed (i.e. restrained rotation and translation), pinned (i.e. allowed rotation, restrained translation) or free (i.e. allowed rotation and translation) (Fig. 5.1). For monolithic joints, the transition from fixed to pinned state due to force redistribution may be considered through perfectly plastic behavior. The mentioned types of bearings are assumed pinned with exception of roller bearings. The shear failure of bearings is neglected.

4.2 Redistribution of forces in a soil-bridge system due to local scour action

Bridge piers are usually aligned to the direction of a river flow and their local axes may differ from the axes of a main girder. Thus both longitudinal and lateral bridge direction contribute the bridge resistance to scouring.

The example of a multiple span bridge with a double-tee main girder and a wall type pier exposed to a local scour action is given in Fig. 4.6. Due to a force

redistribution, additional forces (i.e. bending M_y and tension B_y) act on the main girder in the longitudinal direction (Fig. 4.6a). As for the lateral direction, warping of the main girder introduces additional normal stresses (Fig. 4.6b). The double-tee main girder is quite robust for this type of loading and it restricts pier displacement (Fig. 4.6c) as long as the strength of the joints is not exhausted. Similarly, the supporting soil is affected by combined loading. The contact area is subjected to eccentric vertical force from the superstructure eventually accompanied by horizontal forces (S_x , S_y) and moments (M_{s_x} , M_{s_y}). The resistance of supporting soil to combined loading is rather high due to applied safety factors in the design. It is evident that a failure mode may be triggered only by reaching the combined resistance of the soil and superstructure.

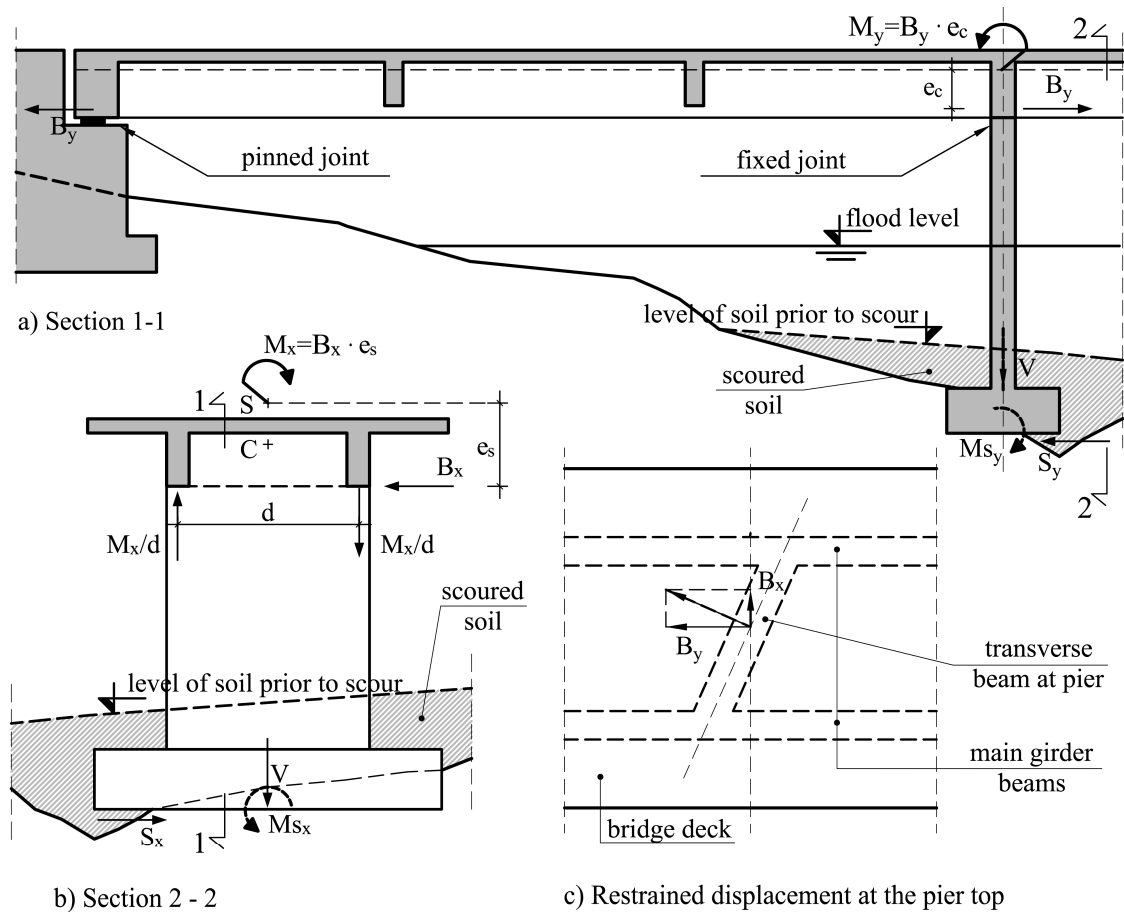


Fig. 4.6 Case of a possible redistribution of forces in a soil-bridge system due to the local scour action at a pier

The actual redistribution of forces between the bridge structure and supporting soil, which precedes the failure, is generally unknown. This is unimportant in the limit analysis approach, but the under-designed or deteriorated element/sections/joints must be pointed out (e.g. poor detailing) and accounted as they may govern the failure mode.

4.3 The approximation of local scour cavities at bridge piers

In Figure 4.7, the local scour cavities beneath a foundation base at different types of pier foundation system are presented with isohypses. The approximated 3D form of the cavities is an oblique cone with closed-curve basis. For the analysis, it is essential to model the scoured contact area between a foundation base and supporting soil, thus the cavities' geometries are approximated. The triangular cross-section of a scour cavity is adopted to be common for all cases (Fig. 4.7e). It is defined by the bottom vertex of the triangle i.e. the time-dependent maximum scour depth $Z_{sc}(t)$, obtained using local scour evaluation formulas, and the related maximum horizontal extent of scour beneath the foundation base S_c . The form of the triangle is adopted due to its simplicity but other cavity forms can be assumed if experimentally justified. Based on this cross-section, for the case of local scour at a wall type pier in Fig. 4.7a, it is assumed that the contact is lost over entire longitudinal side i.e. problem is simplified to plane strain. Similarly, this has been adopted for the other presented cases. Main idea here is the simplified calculation of internal and external work in supporting soil, which is discussed in the next section.

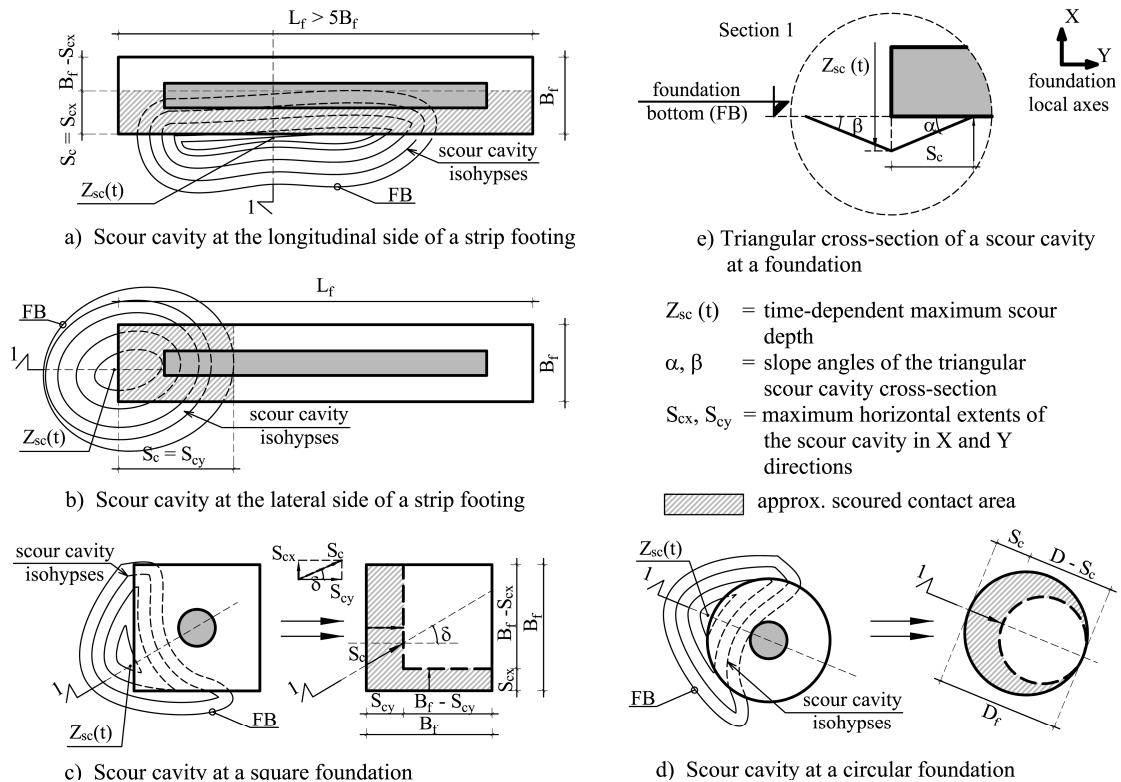


Fig. 4.7 Approximation of the local scour cavities for different types of pier/foundation system

4.4 The resistance of supporting soil to local scour action

The effects of soil erodibility and granular composition on the local scour magnitude at bridge piers were discussed in Chapter 3. Here the subject is geotechnical aspect of soil resistance to local scour, which is governed by the soil bearing capacity and friction at the soil-foundation interface. The basics for estimation of the bearing capacity are presented followed by brief review of the state-of-the-art research on the combined loading at shallow foundations. The effects of local scour cavity on kinematic mechanisms in soil yielding the lowest upper bound of limit load are discussed.

Based on the Prandtl solution [Prandtl, 1921] and using the principle of superposition, [Terzaghi, 1943] presented the formula for estimating ultimate bearing capacity for a general case of centric vertical loading on a rigid strip footing ($L/B > 10$) in a cohesive-frictional ($c - \phi$) soil including the uniform surcharge load (Fig. 4.8):

$$q_u = \frac{1}{2} B \gamma N_\gamma + c N_c + \gamma D_f N_q \quad (4.1)$$

where:

q_u = ultimate bearing capacity [kN/m^2]

B = width of the strip foundation [m]

γ = soil self-weight [kN/m^3]

D_f = height of the uniform surcharge load (Fig. 4.8) [m]

N_γ, N_c, N_q = bearing capacity factors for soil self-weight, cohesion and surcharge load, respectively

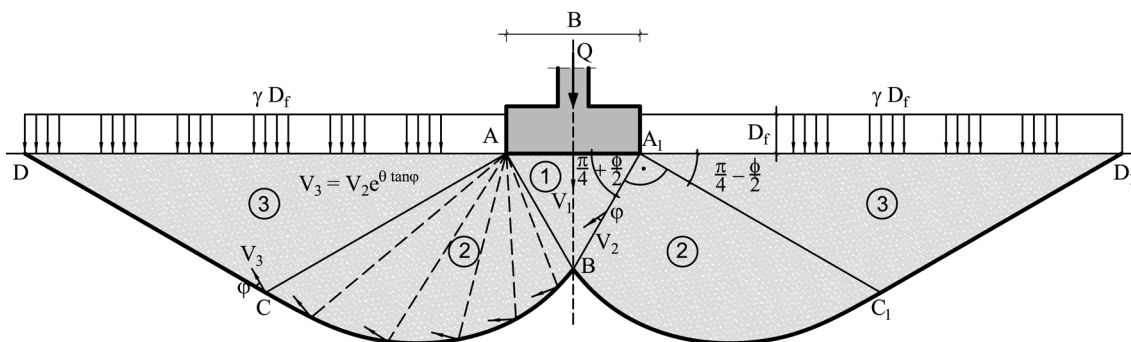


Fig. 4.8 Kinematic mechanism in soil for centrically loaded strip footing

The assumed kinematic mechanism is consisted from three region types. The region "1" is a triangular wedge (i.e. active Rankine zone), which is translating vertically as a rigid body with the same initial velocity V_1 as the footing.

This displacement causes the lateral movement in the regions “2” (i.e. radial shear zones), which are bounded by log spiral discontinuity curves, with starting velocity V_2 at the point B . The log-spiral curves BC and BC_1 have centers at the points A and A_1 . The lines A_1B , DC and AB , D_1C_1 are tangents of the log spiral curves. The regions “3” represent wedges that translate as rigid bodies (i.e. passive Rankine zones) with velocity V_3 . All velocity discontinuity vectors are inclined to lines of soil discontinuity at angle φ .

The non-dimensional bearing capacity factors in Eq. 4.1 are indeed derived from the principle of the virtual work for the assumed mechanism. It is a fact that the closed-form analytical solution to the bearing capacity problem including the effects of the soil self-weight beneath the footing is not possible. There is no general agreement on the precise value of the factors on an international level and even national standards give different values. In order to resolve this issue, different solutions were developed based on empirical relations, analytical derivations, or numerical analyses (e.g. [Michailowski, 1997]). To account the inclination of load, the ratios of $L/B < 5$ and embedment depth, the formula in Eq. 4.1 has been extended with correction factors, which in most cases are obtained as semi-empirical values. Widely used are the factors given by [Hansen, 1970] and [Vesic, 1975] and if there is eccentricity of the load, the “effective width concept” given by [Mayerhoff, 1953] is commonly applied. Thus, the general formula for estimating the bearing capacity of a strip footing is commonly given in the form:

$$q_u = i_\gamma s_\gamma d_\gamma \frac{1}{2} B^* \gamma N_\gamma + i_c s_c d_c c N_c + i_q s_q \gamma D_f N_q \quad (4.2)$$

where in addition to the Eq. 4.1:

i_γ, i_c, i_q = correction factors for inclined loading

s_γ, s_c, s_q = shape correction factors (shapes other than strip footing)

d_γ, d_c, d_q = embedded depth correction factors

B^* = effective width of the footing (effect of load eccentricity)

The common subject of the research in soil mechanics is oriented towards estimating the generalized yield criterion for combined loading at shallow foundations and associated kinematic failure mechanisms. The possible solutions to this problem are usually obtained by combining both FEM and limit analysis. The examples of such

analysis are the research of [Tiebat and Carter, 2000] (Fig. 4.9) and [Gouvernec, 2007]. The limit analysis was used in [Ukrichton et al., 1998] to evaluate undrained stability of surface footings on clay under combined loading. Here, in the focus were the effects of underbase suction (i.e. adhesion) and undrained non-homogenous soil profiles (Fig. 4.10). As a part of the research published in [Michailowski and You, 1998], the upper bound kinematic mechanisms for combined loading at shallow foundations for general (i.e. $c-\phi$) soil were computed (Fig. 4.11). Generally, the soil-superstructure interaction is not considered using the limit analysis approach, to the best knowledge of author.

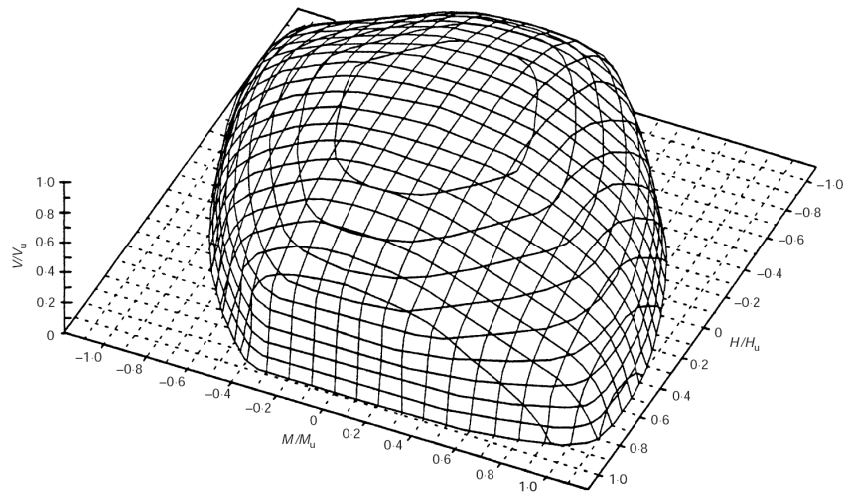


Fig. 4.9 Three-dimensional failure envelope for shallow foundations on cohesive soil under combined load and moments, [Tiebat and Carter, 2000]

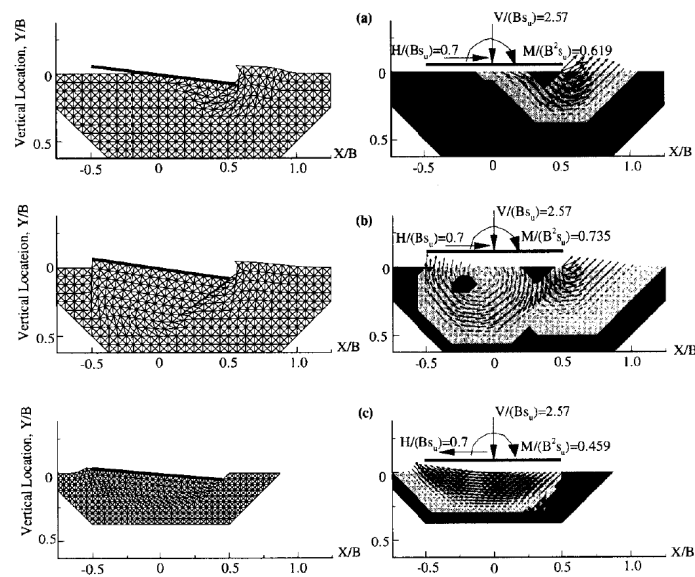
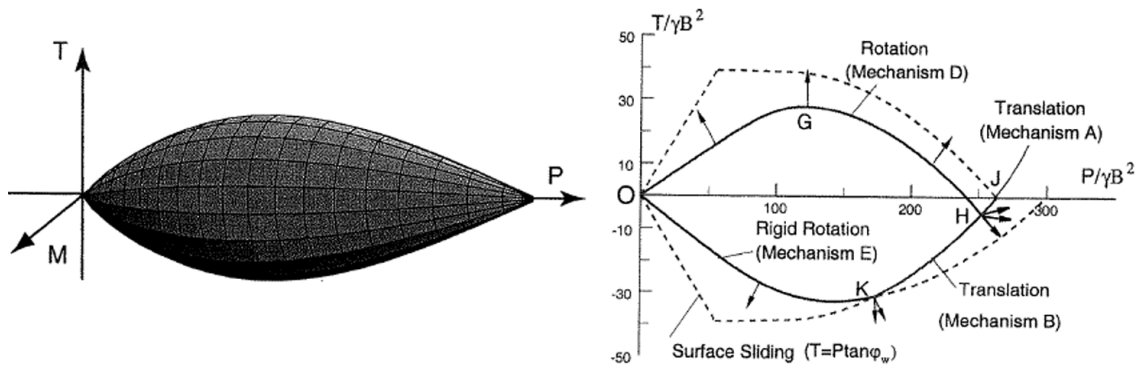
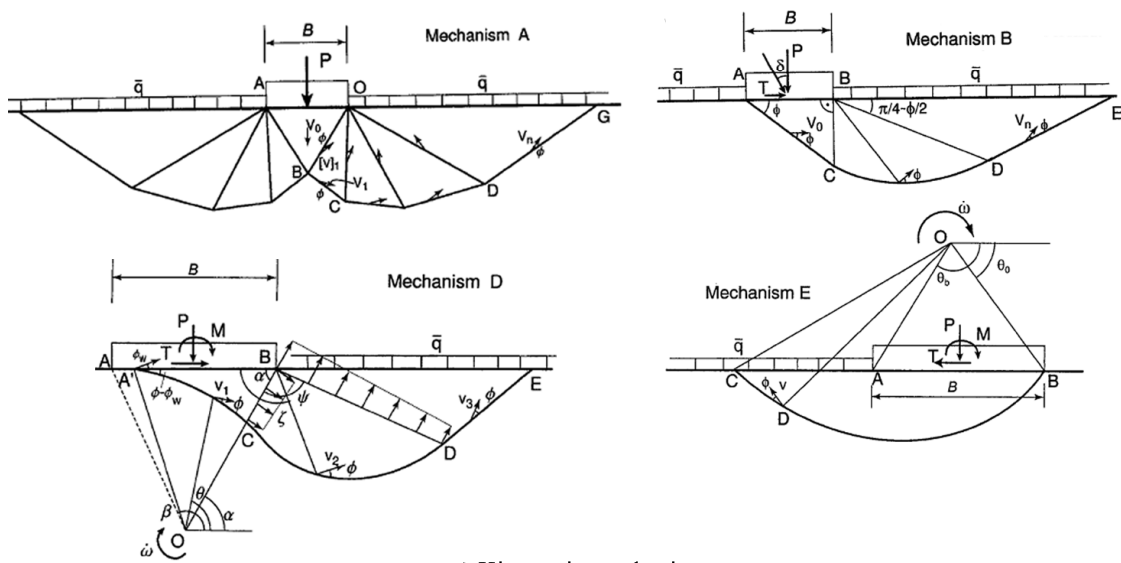


Fig. 4.10 Upper-bound solutions for combined loading on footings on homogenous clay:
a) Zero underbase suction and b), c) full underbase suction, [Ukrichton et al., 1998]



a) Schematics of a failure surface in the load space b) Cross-section of a failure surface for $M = \text{const}$



c) Kinematic mechanisms

Fig. 4.11 Failure modes of a strip footing affected by combined loading, adapted from [Michailowski and You, 1998]

The allowed contact pressure at the base of bridge pier foundation is typically designed to be 2.5 – 5.0 times lower than the soil bearing capacity based on the Eq. 4.2. The depletion of this safety margin due to local scour may be modeled as a decrease of the surcharge loading and foundation to soil contact followed by increase of the inclination and/or eccentricity of vertical force acting at the foundation base. However, the redistribution of internal forces in a hyperstatic soil-bridge system and the non-linear behavior of its elements deter straightforward evaluation of the magnitude of forces acting at a foundation base (Fig. 4.6). The existing solutions for correction factors and effective width concept are not suitable for the intended analysis.

Generally, the coefficient of friction between concrete and soil may be assumed between 0.2 and 0.4 for cohesive soil and frictional soil respectively. However, upon reaching the friction resistance, the sliding cannot occur until the horizontal

displacement of the pier is allowed by the superstructure and the joint at the pier top, as discussed in [Tanasic and Hajdin, 2014]. On many occasions, bridge piers have suffered rigid body rotation besides sinking, and to account this in the analysis, the appropriate kinematic mechanisms in soil (*KMS*) which allow horizontal translation and/or rotation should be applied. In addition, the mechanisms should consider geometry of a local scour cavity at a pier foundation, in order to capture the effect of the related bearing capacity reduction. The geometric simplicity and possibility to use the mechanisms for various types of soils and pier-foundation systems is essential for the analysis.

Many practical solutions in design of geotechnical structures are based on a plane strain assumption (i.e. long footing), which allows estimation of realistic limit loads even for complex geometries of foundations subjected to combined loading. With this assumption and the approximated local scour cavities (Fig. 4.7), the calculation of reduced bearing capacity for a strip footing is straightforward. However, in the case of square or circular footings, the three dimensional *KMS* would be more appropriate. In the thesis, these mechanisms were not considered in the light of the fact that they yield higher limit loads and have somewhat complex geometries compared to the associated plane strain problem. The bearing capacity reduction in the cases of spread footings (Figs. 4.7c and 4.7d) is treated similarly as for strip footings, solely governed by the assumed triangular cross-section of the cavity and related scoured contact area.

The basic mechanisms, which may account foundation sinking, translation and rotations, are accounted in the analysis. Inspired by research on the combined loading at foundations, the four mechanisms are chosen and discussed on the example of a strip footing of width B (i.e. 2D problem), where the favorable effect of the surcharge load is neglected (Fig. 4.12).

The mechanism *KMS 1a* (Fig. 4.12a) is the original Prandtl mechanism affected by a local scour cavity in the Rankine zones. It is defined by angles α and θ and their values, which minimize the limit load, are $\pi/4 + \phi/2$ and $\pi/2$ respectively. This failure mode will be associated to pier sinking in a scouring event. The non-symmetrical Prandtl mechanism, referred to as *KMS 1b* (Fig. 4.12b), is consisted from one active wedge, one log-spiral shear zone and one passive wedge. Generally, it yields better results for the frictional soils than *KMS 1a* due to lower values of the bearing capacity

factor N_γ , and besides sinking it involves horizontal translation. This fact restricts its use to cases where this displacement is allowed by a pier-foundation system and a superstructure. The *KMS 1b* mechanism is defined with three parameters (angles α , β and θ) and the local scour cavity can be introduced in Rankine zone at one side of the foundation.

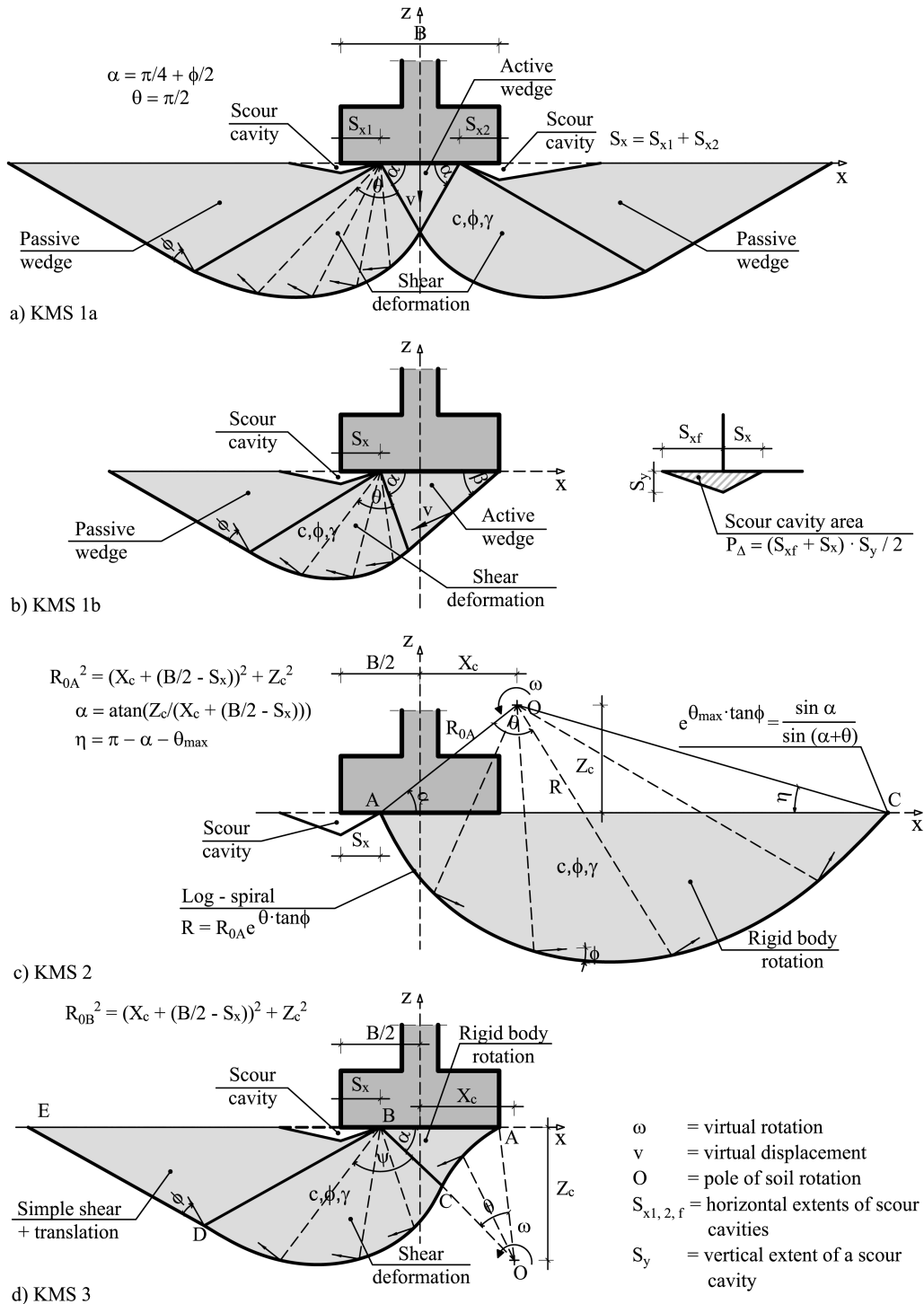


Fig. 4.12 Assumed KMS at a strip footing affected by the local scour cavity

The log-spiral kinematic mechanism, here referred as *KMS 2* and presented in [Narita and Yamaguchi, 1989], is a simple rigid body rotation mechanism defined with its center of rotation O located above the foundation and angle θ (Fig. 4.12c). The shape of the logarithmic spiral ensures the kinematic admissibility thus enabling application of this mechanism for different soil types. Overall it yields acceptable results when compared to other mechanisms except for frictional soils with $\phi > 20^\circ$ as the bearing capacity factor N_γ is over-predicted. For the purely cohesive soil this mechanism transforms into circular i.e. scoop mechanism. As seen in Fig. 4.12, the log-spiral mechanism, unlike the other presented mechanisms, is not affected by the area of the local scour cavity, but only by decrease of contact beneath the foundation. Besides its simplicity, the main reasons for choosing this mechanism for the analysis are:

- As presented in Fig. 4.11c (Mechanism E) it was applied for the case combined loading acting at the pier foundation, which is here assumed to be a consequence of force redistribution
- The variational calculus performed by [Li, 2013] confirmed that the log-spiral mechanism is suitable for solving problems where eccentricity of force at a strip foundation is involved

The mechanism *KMS 3* in Fig. 4.12d resembles the mechanism originally given in [Salençon and Pecker, 1995]. This rotational mechanism is consisted from the three regions. The footing and region ABC rotate as a one rigid body about the point O . The soil in the region BCD is subjected to the shear deformation (the log-spiral shear zone), while the region BDE undergoes a combination of translation and simple shear. This mechanism is defined with two parameters, the location of the center O and the angle ψ , and it involves displacement of the soil mass to the side where the scour cavity is formed (region BDE).

In general, the internal and external work done by a *KMS* depends on the assumed kinematic velocity field and the soil properties – soil weight, cohesion and internal friction angle. The internal work of the soil cohesion W_{coh} is calculated along the kinematic discontinuities of each region in a *KMS*. The calculation of the external work of soil weight W_γ and surcharge load considers the area bounded by regions in a *KMS* and associated velocities. Both internal and external works account the length of

the footing. It must be noted that every *KMS* has parameter constraints (e.g. point C for *KMS 2* in Fig. 4.12c) and they must be accounted when estimating the optimal solution for the bearing capacity.

The formulas for internal and external work in soil for the assumed mechanisms are summarized in Table 4.2. The local scour cavity area P_{Δ} in Fig. 4.12b, is accounted for in: *KMS 1a*, *KMS 1b* and *KMS 3*.

Table 4.2 Internal (INT) and external (EXT) work for the *KMS* in Fig. 4.12

<i>KMS 1a</i>	INT	$W_{coh} = \frac{c \cdot (B - S_x)(e^{2\theta \tan \phi} + 1) \cos \phi}{\cos \alpha} + \frac{c \cdot (B - S_x)(e^{2\theta \tan \phi} - 1)}{\tan \phi \cos \alpha}$
	EXT	$W_{\gamma} = \gamma \left(\frac{B - S_x}{2 \cos \alpha} \right)^2 \left(\cos \phi \cos \alpha + \int_0^{\frac{\pi}{2}} e^{3\theta \tan \phi} \sin(\alpha - \phi - \theta) d\theta \right) - \gamma \left(\left(\frac{B - S_x}{2 \cos \alpha} \right)^2 \cos \phi e^{\pi \tan \phi} - P_{\Delta} \right) \cos(\alpha - \phi) e^{\frac{\pi}{2} \tan \phi}$
<i>KMS 1b</i>	INT	$W_{coh} = \frac{c \cdot (B - S_x)(\sin \alpha \cos \phi + \sin \beta e^{2\theta \tan \phi} \cos \phi)}{\sin\left(\frac{\pi}{2} - \phi\right)} + \frac{c \cdot (B - S_x) \sin \beta (e^{2\theta \tan \phi} - 1)}{\tan \phi}$
	EXT	$W_{\gamma} = \frac{\gamma}{2} \left(\frac{B - S_x}{2 \cos \alpha} \right)^2 \left(2 \cos \phi \cos \alpha + \int_0^{\frac{\pi}{2}} e^{3\theta \tan \phi} \sin(\alpha - \phi - \theta) d\theta \right) - \frac{\gamma}{2} \left(\left(\frac{B - S_x}{2 \cos \alpha} \right)^2 \cos \phi e^{\pi \tan \phi} - P_{\Delta} \right) \cos(\alpha - \phi) e^{\frac{\pi}{2} \tan \phi}$
<i>KMS 2</i>	INT	$W_{coh} = \frac{c \cdot R_{OA}^2 \cdot (e^{2\theta \tan \phi} - 1)}{2 \tan \phi}$
	EXT	$W_{\gamma} = -\frac{\gamma}{3} \int_0^{\theta_{max}} R_{OA}^3 \cos(\alpha + \theta) d\theta + \frac{\gamma}{6} (R_{OA}^3 \cos^2 \alpha \sin \alpha - R_{OB}^3 \cos^2 \eta \sin \eta)$
<i>KMS 3</i>	INT	$W_{cohAC} = \frac{c \cdot R_{OC}^2 \cdot (e^{2\theta \tan \phi} - 1)}{2 \tan \phi}$ $W_{cohDC} = \frac{c \cdot R_{BC} \cdot (R_{OC} + R_{OB}) \cdot (e^{2\psi \tan \phi} - 1)}{2 \tan \phi}$ $W_{cohDE} = \frac{c \cdot (R_{OC} + R_{OB}) \cdot (e^{2\psi \tan \phi} - 1) \cdot (R_{OB}^2 \cos \beta \sin \beta - P_{\Delta})}{2 \cos \phi} + c \cdot e^{\psi \tan \phi} R_{OC} R_{BD} \cos \phi$
	EXT	$W_{\gamma ABC} = \gamma \cdot Z_C \cdot \left(\frac{B - S_x}{2} \right) - \gamma \cdot \int_0^{\theta} \frac{R_{OC}^3}{3} \cdot \cos(\alpha + \theta) d\theta$ $W_{\gamma CBD} = -\frac{\gamma}{4} \int_0^{\psi} R_{BC}^3 \cdot (e^{\psi \tan \phi} + 1) e^{2\psi \tan \phi} \cos(\alpha + \psi) d\psi$ $W_{\gamma BDE} = \gamma \frac{e^{\psi \tan \phi} (R_{OC} + R_{OB})}{2} \cos\left(\frac{\pi}{4} - \frac{\phi}{2}\right) \cdot \left(R_{BD}^2 \cos\left(\frac{\pi}{4} - \frac{\phi}{2}\right) \cdot \sin\left(\frac{\pi}{4} - \frac{\phi}{2}\right) - P_{\Delta} \right)$

4.5 The resistance of bridge elements to local scour action

The bridge resistance to local scour is governed by its ability to redistribute internal forces thus depends on structural system properties, joints between superstructure and substructure as well as on detailing. Since the upper bound theorem is going to be applied, it is necessary to estimate the rates of external and internal works for the bridge structure. The calculation of external work is given in Chapter 5, where possible modes of superstructure failure are discussed. In this section, the methods to estimate plastic strength of the bridge elements are presented.

In general, the plastic strength of RC elements is estimated based on the cross section geometry, acting forces and reinforcement detailing. The bending resistance for the case of double-tee cross section is given in (Fig. 4.13). Here, in the estimation of the ultimate sagging and hogging plastic moments it is assumed that the neutral axis lies in the deck and rib respectively. For the sagging moment, the top deck and the top beam reinforcement may be omitted as they are close to neutral axis.

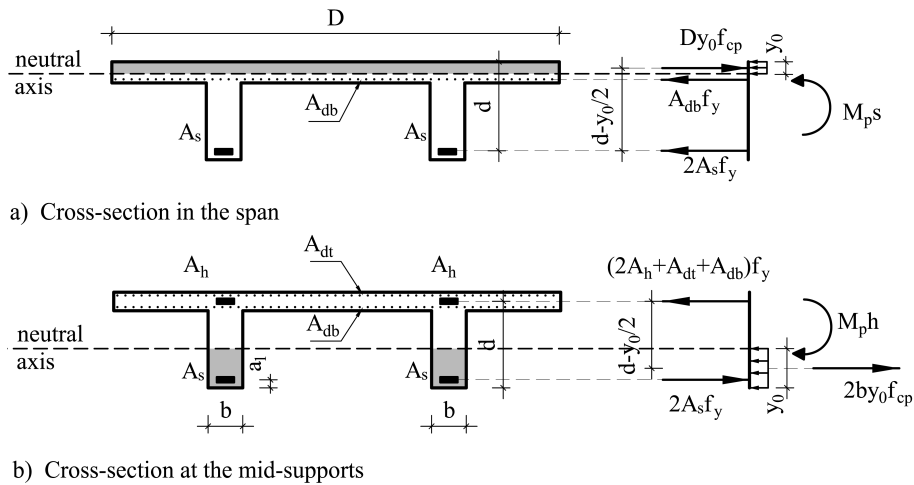


Fig. 4.13 Ultimate sagging and hogging plastic moments for the double-tee main girder

Based on the linear strain distribution, perfectly plastic RC element behavior and internal forces equilibrium, the following may be obtained from Fig. 4.13a:

$$y_0 = \frac{f_y}{f_{cp}} \frac{(2A_s + A_{db})}{D} \quad (4.3)$$

$$M_{ps} = D y_0 f_{cp} \left(d - \frac{y_0}{2} \right) - A_{db} f_y \left(d - \frac{y_0}{2} \right) \quad (4.4)$$

Similarly from Fig. 4.13b:

$$y_0 = \frac{f_y (2A_h + A_{ab} + A_{dt} - 2A_s)}{f_{cp}} \quad (4.5)$$

$$M_p h = 2by_0 f_{cp} \left(d - \frac{y_0}{2} \right) + 2A_s f_y (d - a_1) \quad (4.6)$$

where:

- y_0 = neutral axis depth (i.e. effective height of compression zone) [m]
- D = deck width [m]
- d = effective depth [m]
- b = beam width [m]
- a_1 = centroid of the bottom beam reinforcement area [m²]
- f_y = tensile strength of reinforcement [MPa]
- f_{cp} = plastic compressive strength of concrete [MPa]
- M_{ps} = ultimate sagging plastic moment in span [kNm]
- M_{ph} = ultimate hogging plastic moment at middle supports [kNm]
- A_h = area of girder beam top reinforcement [m²]
- A_s = area of girder beam bottom reinforcement [m²]
- A_{ab} = area of bottom longitudinal reinforcement in a bridge deck [m²]
- A_{dt} = area of top longitudinal reinforcement in a bridge deck [m²]

The plastic strength of a RC bridge deck is mostly governed by the top and bottom reinforcement in two orthogonal directions. The upper bound approach commonly used to calculate ultimate loading of slabs (here the deck) is the yield line method. The assumptions of this method are:

- The pattern of yield lines divide slab into regions which remain rigid
- Yield lines must end at slab boundaries and they form a mechanism in slab which allow unrestrained plastic deformation
- Elastic deformations are neglected and all plastic deformations are concentrated in zones in which the yield condition is satisfied
- Effect of shear forces on the failure of the plate may be neglected
- The effect of membrane (i.e. in plane) forces on slab collapse may be neglected
- Plate collapse is primarily governed by the reinforcement

The general procedure for upper-bound calculation of RC slabs with area A subjected to bending is applied as in [Vrouwenvelder and Witteveen, 2003]. With reference to Fig. 2.12, the total amount of dissipated energy E_d , is calculated as:

$$E_d = \int_A (m_{xx}k_{xx} + 2m_{xy}k_{xy} + m_{yy}k_{yy})dxdy \quad (4.7)$$

where:

- m_{xx}, m_{yy}, m_{xy} , = moments that satisfy the yield condition of the slab [kNm]
- k_{xx}, k_{yy}, k_{xy} , = plastic curvatures derived from $v(x,y)$
- $v(x,y)$ = the downward displacement of the center plane of a slab [m]

At the intersection of yield lines in a deck and superstructure beams, the plastic hinges must form. In general case, the beams are subjected to combined loading of bending moment and torsion. In the analysis, the beams will be treated as “hidden” in the deck. For a hogging yield line i.e. when the top beam reinforcement yields, the pair of internal forces M and M_t must satisfy the yield condition given in [Hsu and Mo, 2010]:

$$-\frac{M}{M_0 R_r} + \left(\frac{M_t}{M t_0}\right)^2 = 1 \quad (4.8)$$

where:

- M_0 = ultimate hogging plastic moment in pure bending [kNm]
- $M t_0$ = ultimate plastic moment in pure torsion [kNm]
- $R_r = \frac{A_{sb}}{A_{st}}$ ratio of bottom beam reinforcement area to top beam reinforcement area

For the common column cross-sections, the plastic bending strength of the joint at a pier top due to combined action of moment and normal force may be obtained from M-N interaction diagrams (i.e. generalized yield criterion). In practice, for the case of non-standard sections, these diagrams may be approximated with 5 points. These points distinguish five limit states of the analyzed section: pure tension, simultaneous failure of tensile reinforcement and concrete, balance point state (increase of the compressive normal force decreases the ultimate bending moment), the stress in tensile reinforcement equals zero and pure compression. In the case of a circular pier section in Fig. 4.14, the ultimate plastic bending moment M_{pj} is estimated for a known reinforcement area (Eq. 4.9). The mechanisms which imply the work of normal force at

the pier top (i.e. concrete crushing) yield large internal work thus are not considered in the analysis.

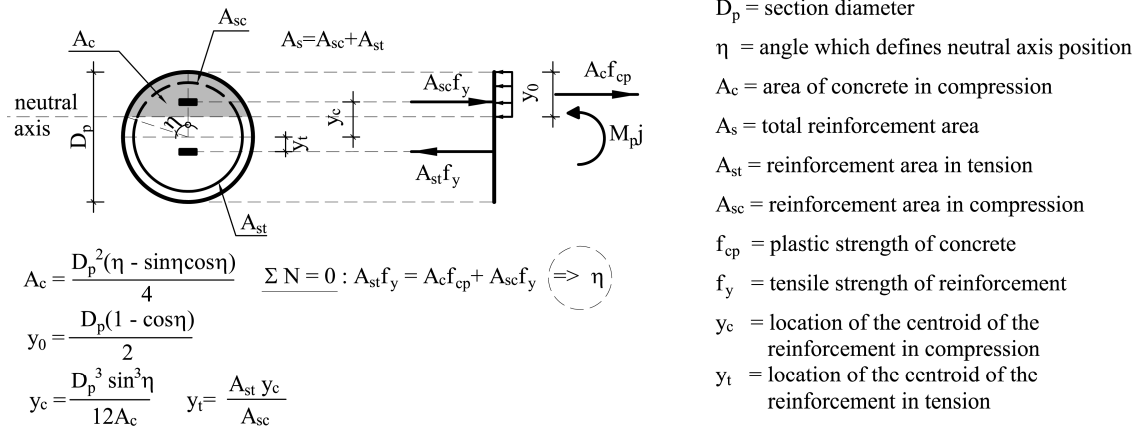


Fig. 4.14 Plastic bending strength of a RC circular section at a pier top

$$M_{pj} = (A_c y_0 f_{cp} + A_{sc} f_y) (y_c + y_t) \quad (4.9)$$

In the assumed kinematic mechanism of the superstructure, the internal work in a plastic hinge/yield line is obtained as the product of plastic strength (e.g. bending moment, normal force or combination of both) and virtual displacement (e.g. virtual rotation) associated to the flow rule.

Chapter 5. Analysis of the Soil-Bridge Models

In this chapter, the soil-bridge models affected by the idealized local scour cavities are analyzed. The combined soil-bridge failure modes in the longitudinal and lateral directions are separately investigated. The assumptions and constraints in the analysis and the parameters governing the failure modes are discussed. The upper-bound solutions for the ultimate local scour extents at bridge piers are obtained in the optimization procedure for various set of input data.

5.1 The soil-bridge model

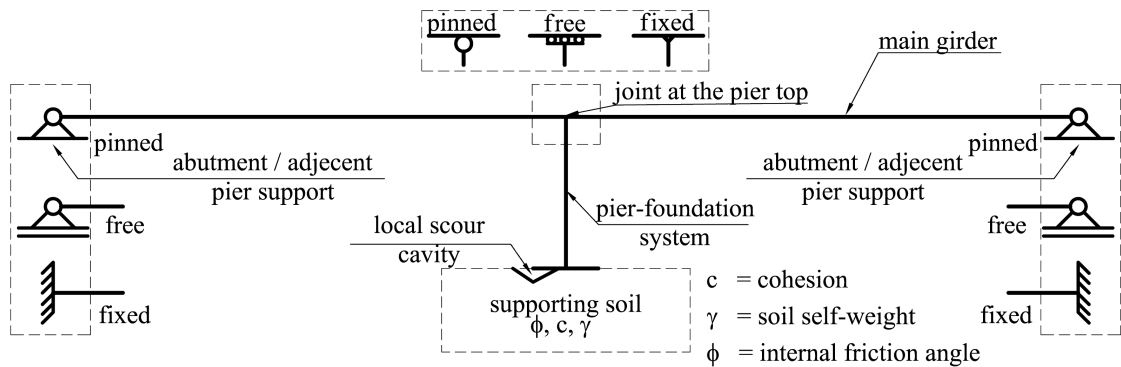
Based on Chapter 4, the elements and geometry of the soil-bridge model are given in Fig. 5.1 and its global assumptions are reviewed:

- Rigid – perfectly plastic behavior of the bridge structure and the supporting soil
- The superstructure is RC double-tee main girder
- The substructure is a rigid body RC pier-foundation system (Fig. 4.1)
- The local scour cavity at substructures is modeled with a triangular cross-section according to Fig. 4.7
- The active forces acting on the system are given by the superstructure self-weight q (main girder self-weight g and additional dead load on the bridge deck Δg), self-weight of the pier foundation system PF_g , and soil self-weight
- Local scour affects just one (i.e. middle) bridge pier (two spans and different adjacent support types are sufficient to model behavior of multiple span girder bridges)
- The second order (P- Δ) effects are neglected
- The plane strain approximation is adopted for evaluation of the ultimate bearing capacity of supporting soil
- The failure modes are defined for a combined soil-bridge kinematic mechanism

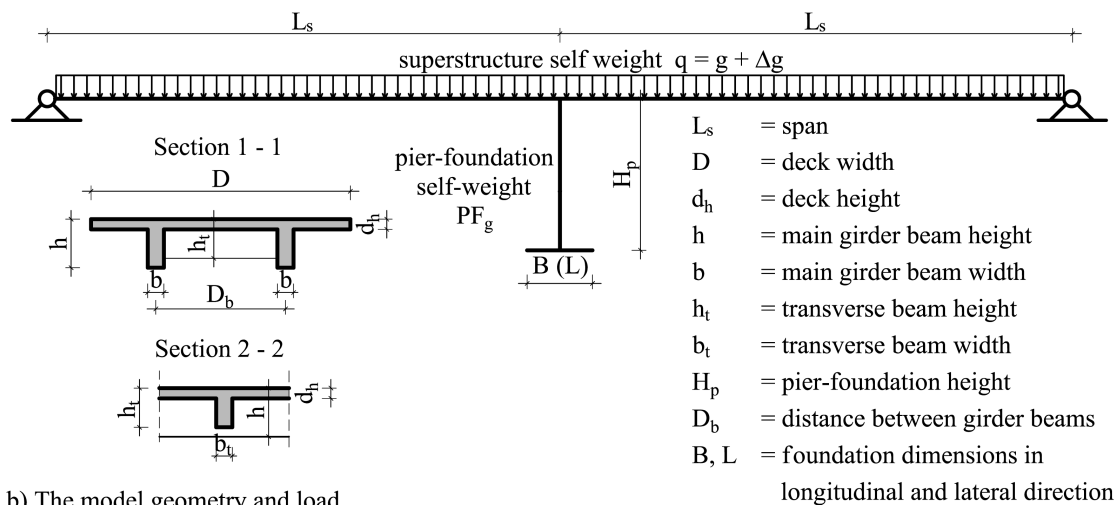
The following properties in the model are accounted for:

- The distribution of the bending moment resistance in the girder beams is given by the reinforcement layout, which is assumed to follow linear elastic analysis (e.g. Fig. 5.2).

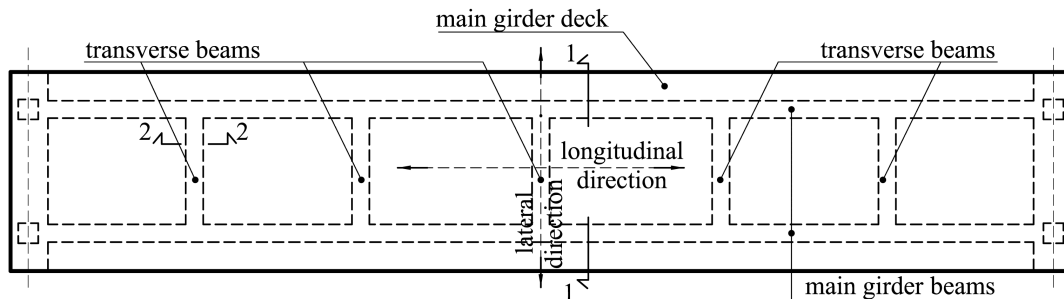
- The distribution of the bending moment resistance in the main girder deck is assumed based on the linear elastic analysis (based on the design for a two way slab).
- The joint at the pier top and the adjacent supports may be either free, pinned or fixed with an assumed strength with regard to bending and shear
- The supporting soil is either purely cohesive ($\phi = 0, c > 0$), cohesive-frictional ($\phi > 0, c > 0$) or purely frictional ($\phi > 0, c = 0$)



a) The model elements



b) The model geometry and load



c) The main girder top view

Fig. 5.1 The soil-bridge model

The ultimate hogging and sagging moments in girder sections are calculated as in Eq. 4.4 and Eq. 4.6. The girder beams' bottom reinforcement, which is designed for the critical section in a span, is in practice normally reduced near pier supports (H_{red} in Figs. 5.2a and 5.2c). However, the reinforcement may be designed as continuous, which is ensured by adequate splicing (Fig. 5.2b).

The location of possible plastic hinge/s in a span of the main girder is the parameter that is going to be varied in the analysis (H_{pos}). For the multiple span bridges, the hogging plastic hinges are assumed to develop in a failure mode at the sections over the piers.

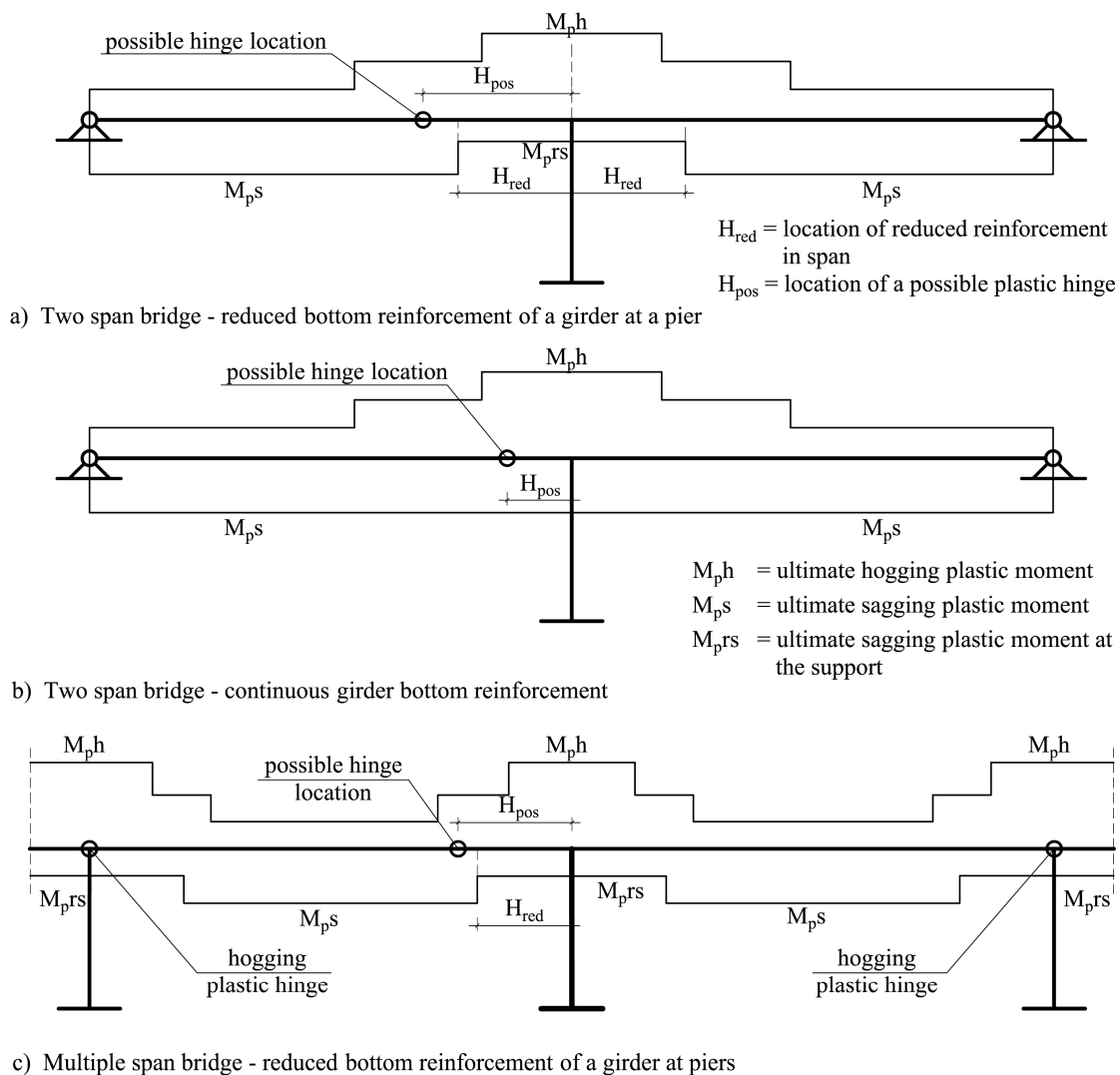
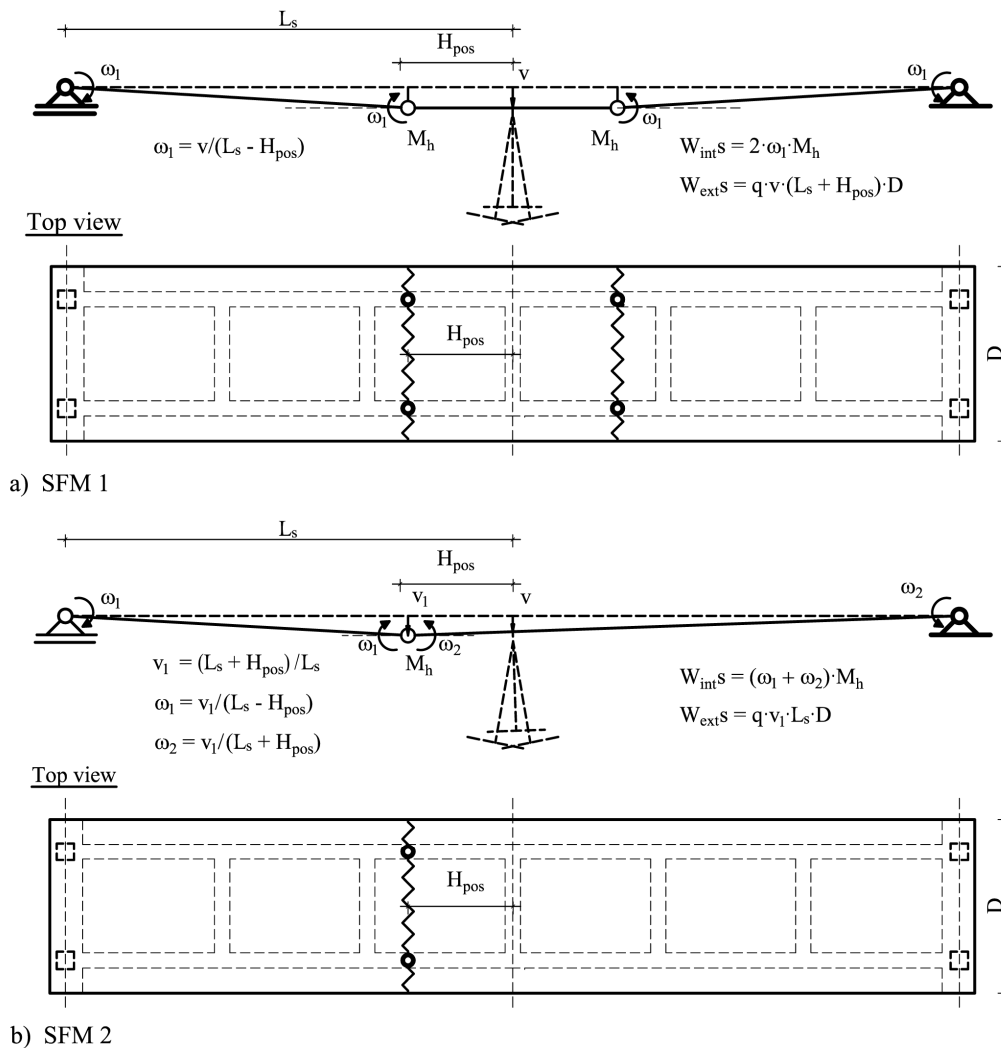


Fig. 5.2 Possible distributions of the bending moment resistance in the main girder

5.2 Combined failure modes in the longitudinal direction

With reference to Fig. 5.2, the possible modes of superstructure failure (SFM-s) for the longitudinal direction are presented in Fig. 5.3. The formulas for calculating the rates of internal and external work (W_{intS} , W_{extS}) are given. The properties of the joint at a pier top and possible displacement of a pier-foundation system are not considered for now, just the virtual vertical displacement at the pier (denoted as v). The mode *SFM 1* (Fig. 5.3a) has two symmetrical plastic hinges on girder beams and associated sagging yield lines in the deck. The *SFM 2* (Fig. 5.3b) represents a non-symmetric mechanism.

Depending on the adjacent supports type, failure modes may imply horizontal displacement of the main girder or additional hinges at fixed supports. For the latter, the difference to the presented modes is in the rate of internal work and thus they will be denoted with asterisk e.g. *SFM 1** in Fig. 5.3c. The example of such failure may be seen in Fig. 1.18.



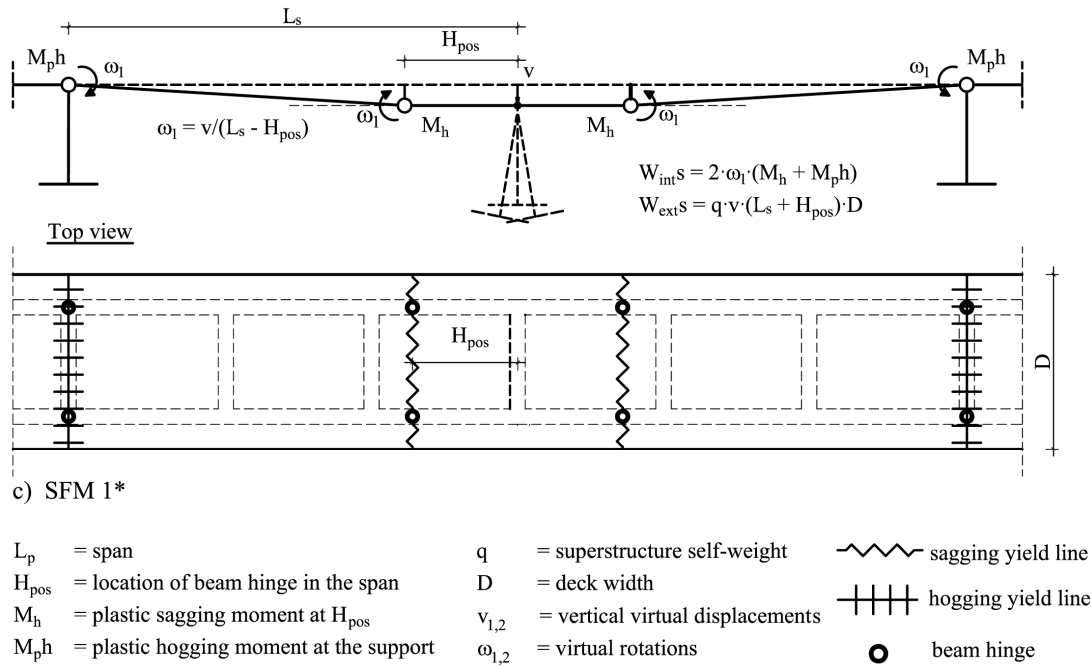


Fig. 5.3 Superstructure failure modes in the longitudinal direction

The horizontal translation of the main girder (i.e. for free adjacent joints) does not induce work of external forces since the only active force is self-weight. It should be noted that *SFM 1* and *SFM 2* have the identical rates of internal and external work for the matching vertical displacement at the pier top.

In order to define the combined soil-bridge mechanism, the discussed *SFM*-s must be in consistency with the *KMS* in Fig. 4.14. The straightforward case is when the joint at the pier top is considered as movable (i.e. free) – either as designed (e.g. roller bearing) or when it's plastic strength is reached resulting in the unrestricted horizontal displacement. Here, the center of rotation of a pier-foundation system coincides with the center of a *KMS* (Fig. 5.4a). The associated superstructure failure mode is independent from the type of the *KMS* and entails sinking (e.g. *SFM 1*). On the other hand, for the pinned or fixed joint at the pier top, the adequate consideration of the superstructure when evaluating the overall bridge resistance is required.

It is assumed that the center of a pier foundation is the connection between supporting soil and a bridge pier. For a pinned joint at the pier top and restrained horizontal displacement of the main girder (e.g. pinned adjacent supports), the pole of the rotation (O_1) for the pier-foundation system lays in the plane of the main girder (Fig. 5.4b). The given mechanism violates somewhat the compatibility condition as shown in Fig. 5.4c, *Detail A*. The rotation of foundation base does not follow exactly

the rotation of the soil underneath. However, this may be neglected assuming local crushing of soil and therefore underestimating the internal work.

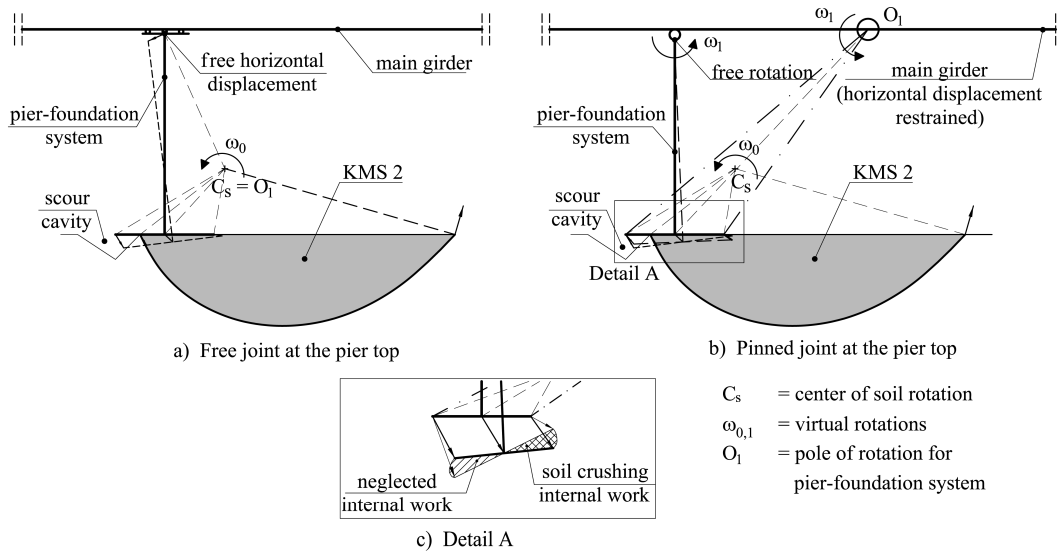


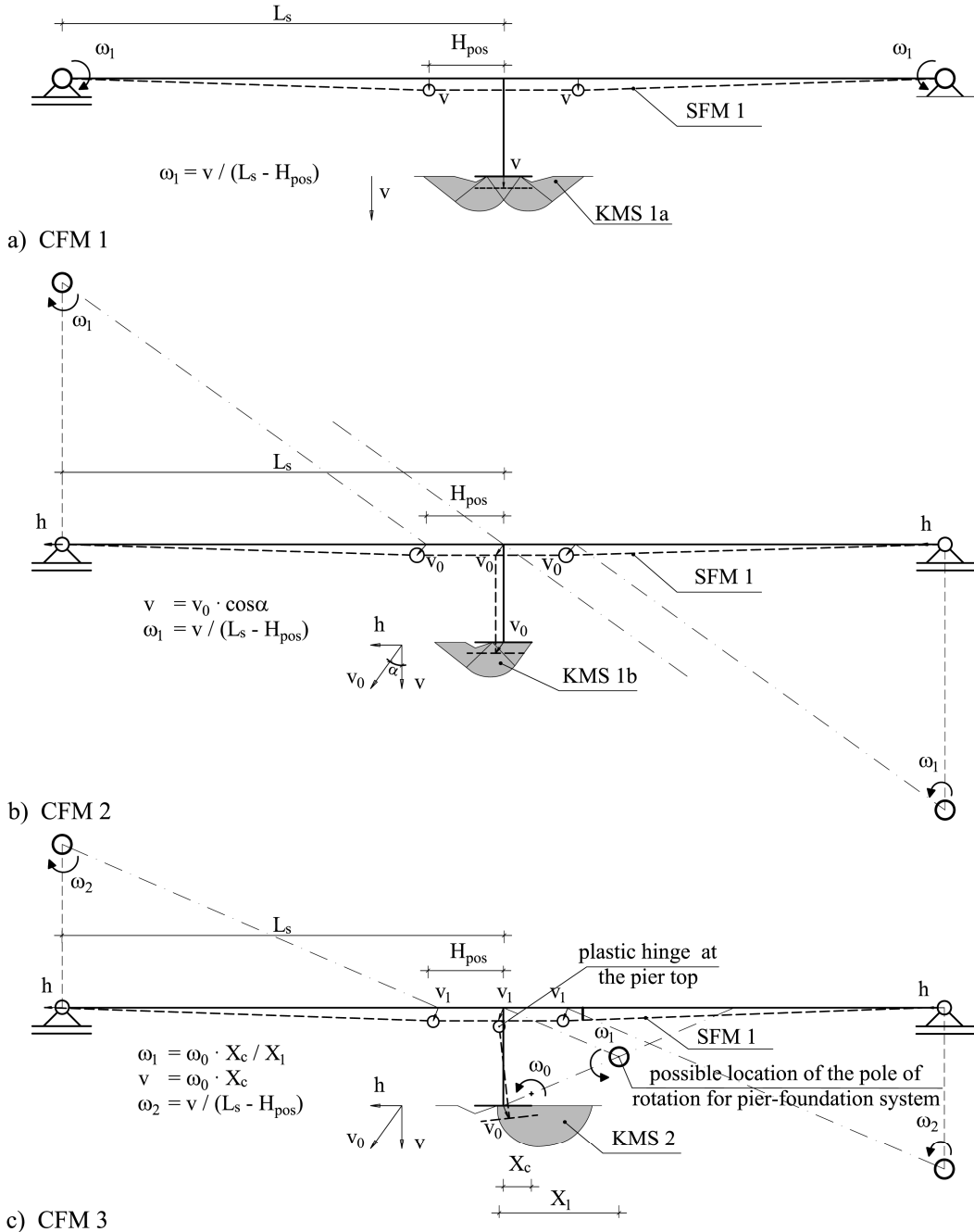
Fig. 5.4 Connection of the *KMS 2* and pier foundation system in a combined mechanism

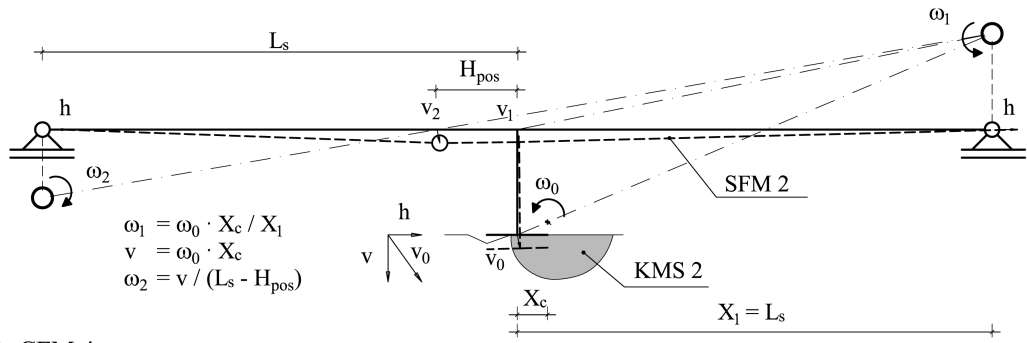
In respect to the type of the joint at the pier top and adjacent supports types, 27 different model types may be distinguished. However, the four chosen bridge model types (BT) are sufficient for the discussion (Table 5.1).

Table 5.1 Four bridge types in longitudinal direction and associated *CFM* -s

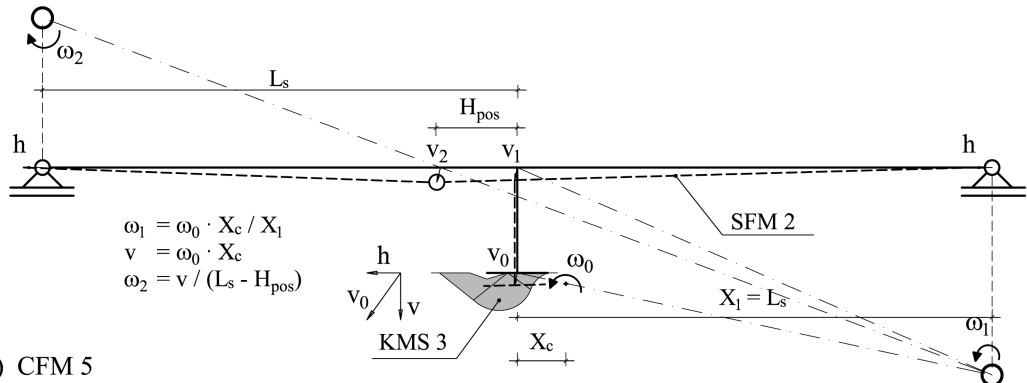
Bridge type	Adjacent supports	Joint at a pier top	Superstructure Failure Mode (Fig. 5.3)	Kinematic mechanism in soil (Fig. 4.12)	Combined Failure Mode	Figure
BT 1	Free	Fixed	<i>SFM 1</i>	<i>KMS 1a</i>	<i>CFM 1</i>	5.5a
			<i>SFM 1</i>	<i>KMS 1b</i>	<i>CFM 2</i>	5.5b
			<i>SFM 1</i>	<i>KMS 2</i>	<i>CFM 3</i>	5.5c
			<i>SFM 2</i>	<i>KMS 2</i>	<i>CFM 4</i>	5.5d
			<i>SFM 2</i>	<i>KMS 3</i>	<i>CFM 5</i>	5.5e
			<i>SFM 1</i>	<i>KMS 3</i>	<i>CFM 6</i>	5.5f
BT 2	Pinned	Fixed	<i>SFM 1</i>	<i>KMS 1a</i>	<i>CFM 1</i>	5.5a
			<i>SFM 1</i>	<i>KMS 2</i>	<i>CFM 3</i>	
			<i>SFM 2</i>	<i>KMS 2</i>	<i>CFM 7</i>	5.5g
BT 3	Fixed	Fixed	<i>SFM 1*</i>	<i>KMS 1a</i>	<i>CFM 1*</i>	
			<i>SFM 1*</i>	<i>KMS 2</i>	<i>CFM 3*</i>	5.5h
			<i>SFM 2*</i>	<i>KMS 2</i>	<i>CFM 7*</i>	
BT 4	Free Pinned Fixed	Free	Sinking at the pier support	<i>KMS 1a</i>	Governed by soil mech	
				<i>KMS 1b</i>		
				<i>KMS 2</i>		
				<i>KMS 3</i>		

Based on the presented *KMS*, *SFM*-s and simple kinematic constraints, the associated combined failure modes (*CFM*-s) for chosen bridge types are given in Fig. 5.5, and analyzed to find the least upper bound solution in the optimization procedure (section 5.3). The *CFM*-s listed in Table 5.1 with asterisks are those that include change of state for adjacent supports from fixed to pinned.

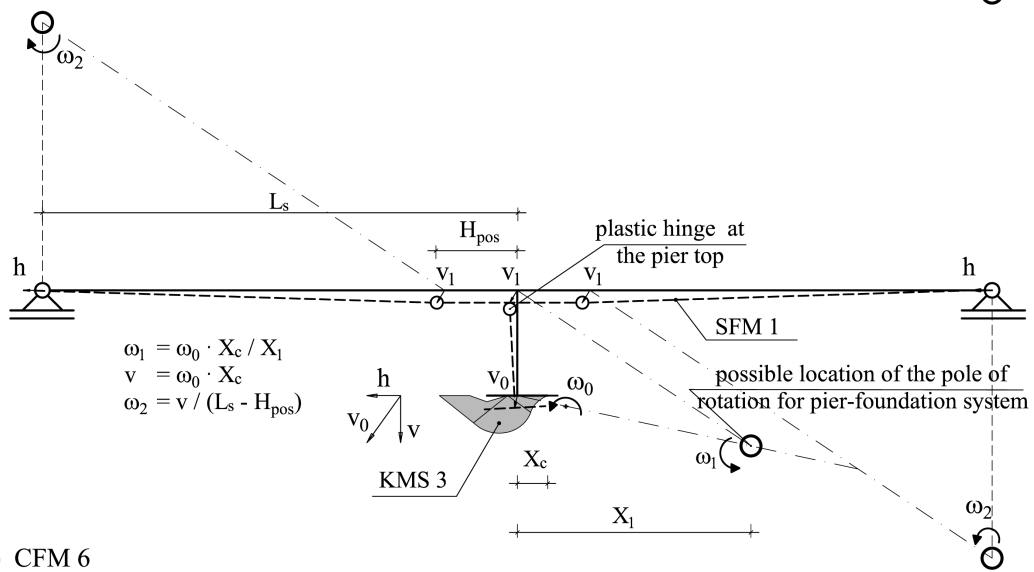




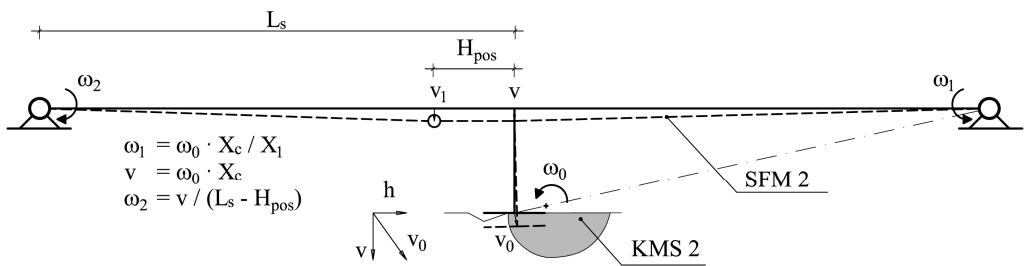
d) CFM 4



e) CFM 5



f) CFM 6



g) CFM 7

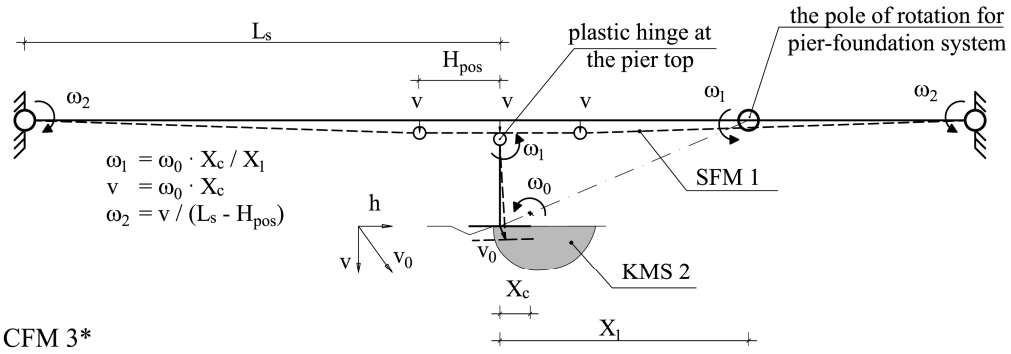


Fig. 5.5 Combined soil/structure Failure Mechanisms (*CFM*) soil-bridge model in the longitudinal direction

The location of the center of soil rotation for *KMS 3* restricts the application of this mechanism to the cases where the horizontal displacement of the joint at the pier top is free to move horizontally (Fig 5.5e and 5.5f). Otherwise, the assumption of the rigid behavior of a pier/foundation system would be violated. Generally, the center of rotation of a *KMS* directly above/beneath the foundation would lead to large dissipation of internal energy in the main girder and rather low external work rate as the combined mechanism would imply uplifting of the foundation. Such mechanisms are theoretically possible but yield unrealistic solutions. This does not account for the BT 4, and BT 1 for modes where plastic hinge forms at the pier top. These modes are *CFM 3* and *CFM 6* and for them the optimal location of the pole of rotation for pier-foundation is additional parameters in the optimization procedure.

The mode *CFM 7* resembles *CFM 4* with the exception that the pole of rotation for superstructure coincides with the pinned support.

5.3 The optimization procedure

The works of the internal and external forces (W_{int} , W_{ext}) are calculated for the *CFM*-s and the principle of the virtual work (Eq. 2.6) is applied:

$$W_{ext} = W_{int} \quad (5.1)$$

The total rate of external work W_{ext} done in a soil-bridge model is governed by assumed combined kinematic mechanism and self-weight of the model elements. It is calculated using the following formula:

$$W_{ext} = q \int_{A_d} v(x, y) dA_d + PF_g v + \sum_{i=1}^n v_i P S_i \quad (5.2)$$

where:

- q = superstructure self-weight given as constant continuous surface load over the bridge deck area, [kN/m²]
- PF_g = pier-foundation self-weight [kN]
- PS_i = self-weight of the soil region i in the KMS [kN/m³]
- A_d = area of the bridge deck [m²]
- x, y = local axes of the main girder [m]
- $v(x, y), v, v_i$ = virtual vertical displacements associated to the deck, the pier-foundation system and the region i in the assumed KMS [m]

The integral over area A_d in Eq. 5.2 actually represents the volume of the body enclosed by the plane of the undeformed deck and the deformed mode of the deck due to assigned virtual displacements. The third element on the right hand side of the Eq. 5.2 represents external work of a *KMS* (Table 4.2) and usually has negative values as the majority of the soil regions in a *KMS* have upward virtual displacement. This especially holds when the surcharge load is considered. The simplified form of the Eq. 5.2 is used:

$$W_{ext} = q^* \cdot V_{br} + PF_g \cdot v + W_\gamma + W_{sur} \quad (5.3)$$

where:

- q^* = limit load acting on the superstructure [kN/m²]
- V_{br} = volume enclosed by the undeformed and deformed deck mode in the assumed superstructure mechanism [m³]
- W_γ = external work of soil self-weight [kNm] (Table 4.2)
- W_{sur} = external work of the surcharge load [kNm]

The W_{int} comprises the total work of internal forces in the supporting soil and bridge structure:

$$W_{int} = W_{coh} + W_h + W_{yl} \quad (5.4)$$

where:

- W_{coh} = internal work of the cohesion in the supporting soil [kNm] (Table. 4.2)
- W_h = internal work of all plastic hinges in the bridge structure [kNm]
- W_{yl} = internal work of the yield lines in the bridge deck [kNm]

The effects of local scour on the reduction of bearing capacity of the supporting soil are considered by altering the geometry of the assumed kinematic mechanisms.

This is done by increasing the extent of local scour cavity directly beneath the foundation and changing the mechanism geometry accordingly. Eventually, the change in mechanisms due to scour cavity will result in q^* (Eq. 5.5) becoming equal to the superstructure self-weight q i.e. the combined soil-bridge failure mode sets in:

$$q^* = \frac{W_{int} - W_\gamma - W_{sur} - PF_g \cdot v}{V_{br}} \geq q \quad (5.5)$$

It may not be clear instantly from Eq. 5.5 which of the applied mechanisms yields better solution. Still, the impact of every element in the soil-bridge model on the resistance to the assumed local scour cavity may be observed. Evidently, in order to obtain the least upper bound, the combined kinematic mechanism should engage as much as possible of the structure's self-weight and at the same time dissipate the least possible amount of internal energy.

5.4 Analysis of a soil-bridge model in the longitudinal direction – An example

The soil-bridge model with wall type pier-foundation system (Fig. 4.1a) affected by the local scour cavity as in Fig. 4.7a is analyzed. The Matlab script was written and for the set-up of input data given in Table 5.2, the results of the optimization procedure for the four bridge types (Table. 5.1) are presented. The parameters in the applied *KMS* and position of the hinge in the main girder span were varied to obtain the optimal solutions. This problem of nonlinear-constrained optimization was solved using Matlab function *fmincon*.

Table 5.2 Input data and results of the optimization procedure for the four bridge types

Input data								Results			
Main girder		Pier-Foundation system		Plastic strength of bridge elements [kNm] *		Soil Properties		Bridge type ***	Least upper bound	Scour extent Sc (m)	Figure
Span L_s (m)	20.0	Pier height H_p (m)	8.0	Joint at the pier top M_{pj}	1020.6	friction angle ϕ [°]	25.0	BT 1	CFM 5	0.77	5.6
Deck width D (m)	8.0	Pier length L_p (m)	7.0	Adjacent support M_{ph}	5618.2	cohesion c [kN/m ²]	10.0	BT 2	CFM 3	0.85	5.9
Deck height d_h (m)	0.2	Pier width B_p (m)	0.5	Main girder $M_{ps}=2 \cdot M_{prs}$	1404.3	weight γ [kN/m ³]	18.0	BT 3	CFM 3*	0.97	5.11
Beam height h (m)	1.7	Foundation width B_f (m)	2.0	Deck in both directions M_{xy}	19.8	FS**	3.9	BT 4	KMS 3	0.53	5.15
Beam width b (m)	0.5	Foundation length L_f (m)	10.0	* Based on section 4.5 and minimum reinforcement requirements of a design code; The reinforcement layout according to Fig 5.2a/5.2c; $f_{pc}=2.0$ kN/cm ² , $f_v=24.0$ kN/cm ²							
Dead load g (kN/m ²)	7.6	Foundation height H_f (m)	1.5	** The initial factor of safety (FS) is based on the Eq. 4.1 without the surcharge load							
Add. dead load Δg (kN/m ²)	2.0	Self-weight PF_g (kN)	1450.0	*** Refer to Table 5.1 for bridge types and Fig. 5.8 for combined mechanisms							

In the Figs. 5.6, 5.9, 5.12 the lines on graphs represent the decrease of the limit load q^* (vertical axis) with the change in the horizontal scour extent S_c (horizontal axis) for the analyzed failure modes and associated bridge types. These may be interpreted as the decrease of the safety factor at the foundation due to local scour growth. The influence of the soil mechanical properties, given by ϕ and c , on the ultimate horizontal scour extent may be observed in Figs. 5.7, 5.10 and 5.13, and Figs 5.8, 5.11 and 5.14 respectively. Here, the different initial safety factors (FS) of bearing capacity are based on the Eq. 4.1 without the soil surcharge load, and the plastic strengths of superstructure elements are not varied. In these analyses, the influence of the slope angles of the triangular cavity cross-section and related weight of soil flushed away were neglected. Their maximum influence on the results is separately discussed (Fig. 5.15) and presented in Figs. 5.16 to 5.18.

For the BT 1 the *CFM 5* yields the least upper bound (Fig. 5.6). In the case of the pure frictional soil and the pure cohesive soil, the most critical mechanism is also *CFM 5* for the common design factors of safety ($FS > 2$). For purely cohesive soils, the *CFM 1* and *CFM 2* give identical results. The modes *CFM 3* and *CFM 6* are not presented here. For them, the optimal solution for the center of rotation of the pier-foundation system is in infinity. This leads to translational mechanisms, which are no longer consistent with the assumed rotational *KMS* and these modes may only be treated in a special case of BT 1 i.e. for the pinned joint at the pier top (Table 5.3).

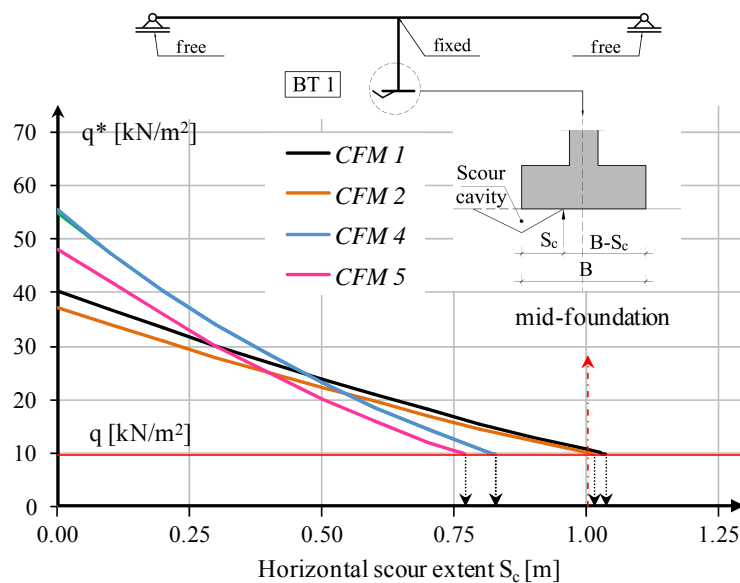


Fig. 5.6 Combined failure modes for the BT 1

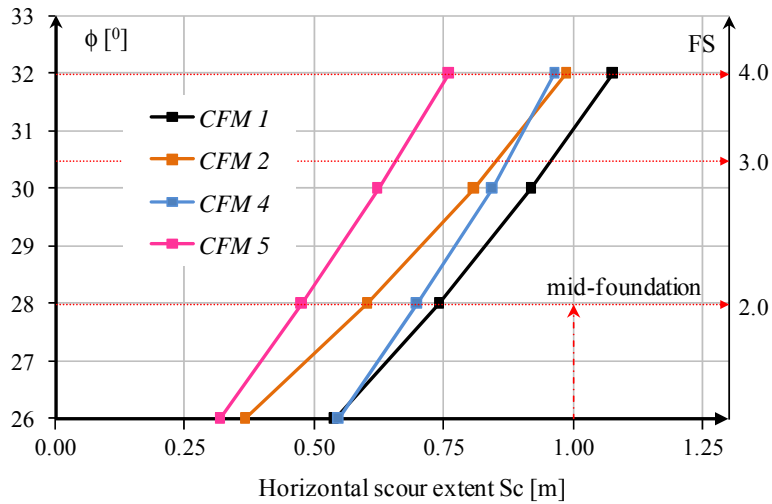


Fig. 5.7 Influence of soil internal friction angle on the results for the BT 1

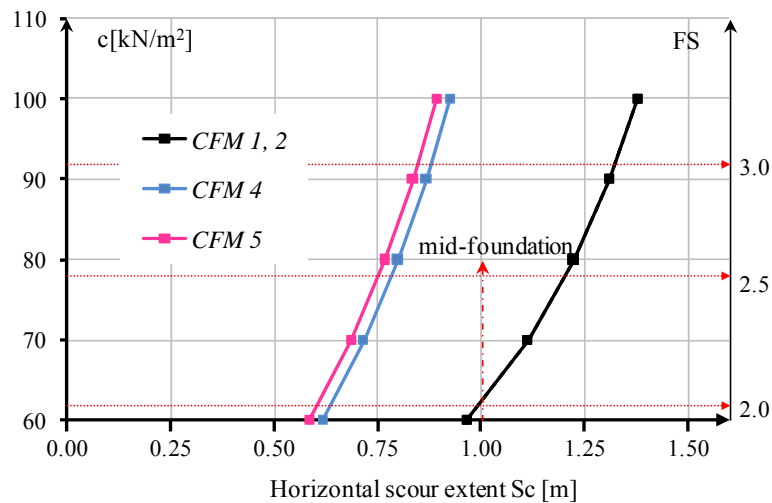


Fig. 5.8 Influence of cohesion to results for the BT 1

The pinned adjacent supports in the case of BT 2, restrain horizontal translation and therefore the three mechanisms are admissible (CFM 1, CFM 3 and CFM 7). The most critical for the adopted data set is the *CFM 3* (Fig. 5.9). This is evident also for purely frictional soils and common values of safety factors. In the case of purely cohesive soils, the *CFM 7* becomes critical mechanism.

The combined mechanisms for the BT 3 resembles to those of the BT 2 with the exception of additional internal work in adjacent joints. Here, the *CFM 3** becomes the critical mechanism. Similar as for BT 2, here for the purely cohesive soil the *CFM 7** yields lowest upper bound.

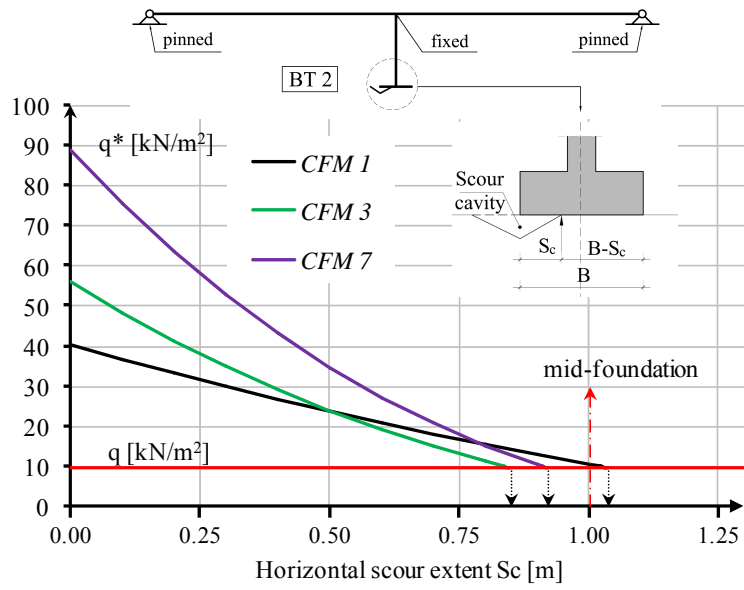


Fig. 5.9 Combined failure modes for BT 2

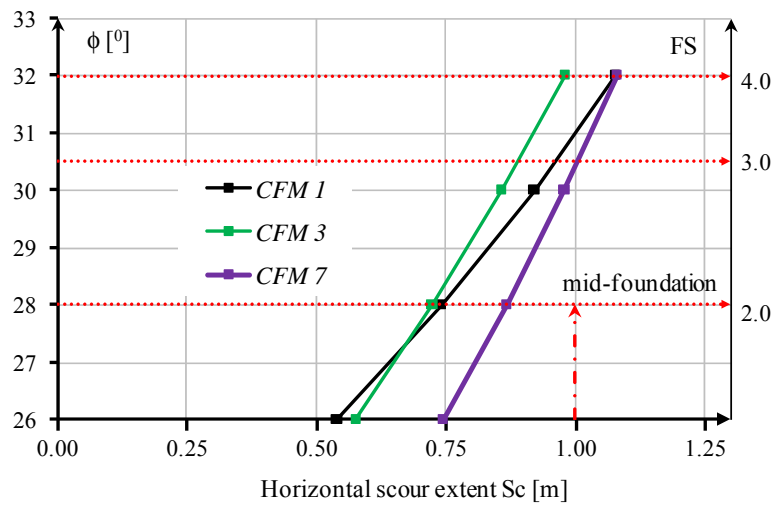


Fig. 5.10 Influence of soil internal friction angle to results for BT 2

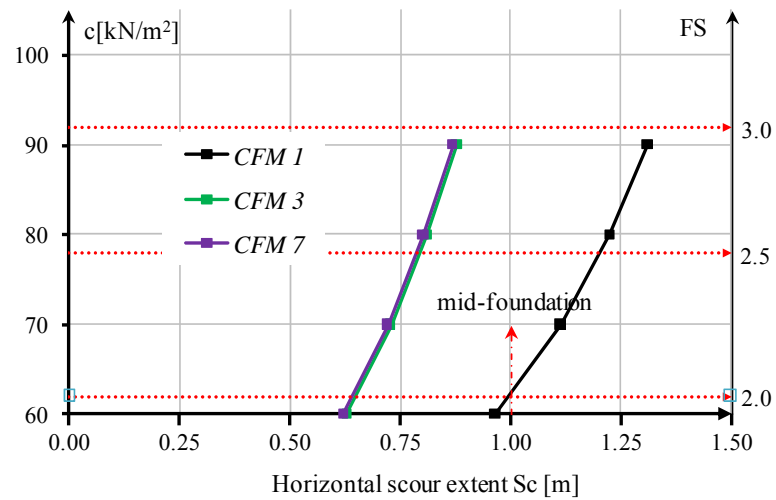


Fig. 5.11 Influence of cohesion to results for BT 2

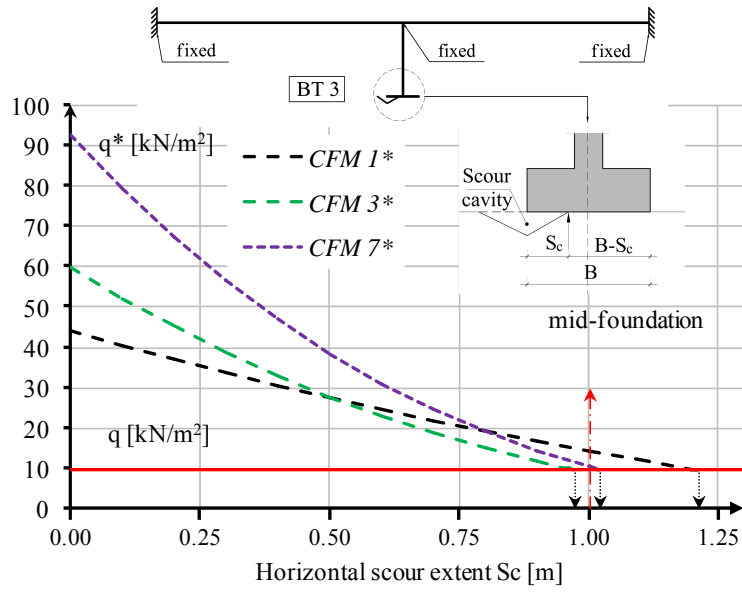


Fig. 5.12 Combined failure modes for BT 3

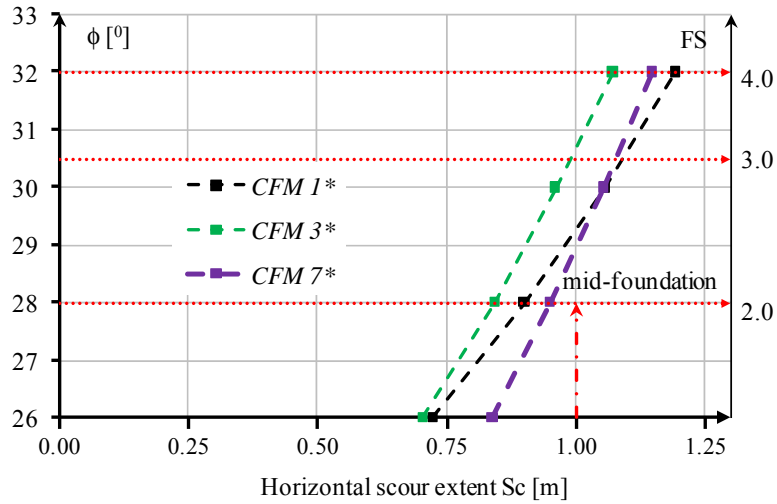


Fig. 5.13 Influence of soil internal friction angle to results for BT 3

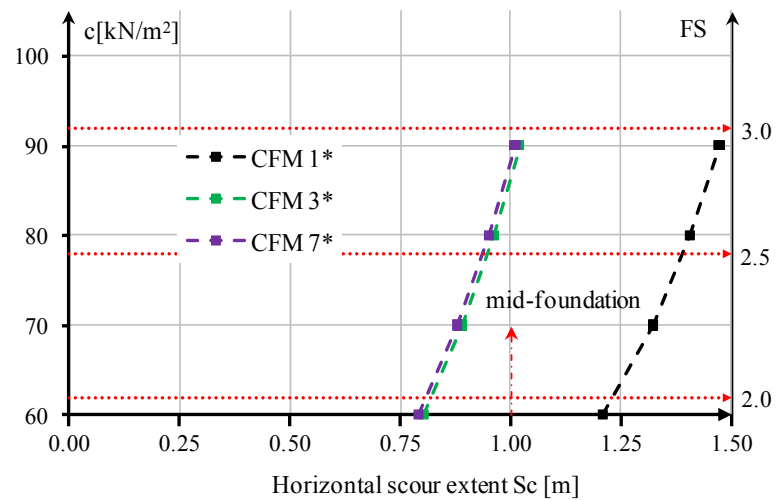


Fig. 5.14 Influence of cohesion to results for BT 3

In the case of BT 4, there is no combined failure mode. A *KMS* is sufficient to trigger a bridge failure. Here, the lifting of the foundation is not constrained by the bridge structure, thus the *KMS 3* (Fig. 4.12d) yields the least upper bound as centers of rotation are allowed in the area directly beneath the foundation. The zero-tension interface at the foundation base was assumed in this situation. Here, the Eq. 5.5 was applied in which the internal work of a bridge structure is omitted and the pier force from the superstructure was taken based on the elastic analysis. Alternatively, in this case the existing correction factors may be applied (Eq. 4.2).

The ultimate scour extents at the pier for the four bridge types are summarized in the Table 5.2 and the decrease of limit load for the related critical mechanisms is given in Fig. 5.15. Here, the impact of the superstructure type and properties in the resistance of a soil-bridge model to the assumed local scour action is clearly seen.

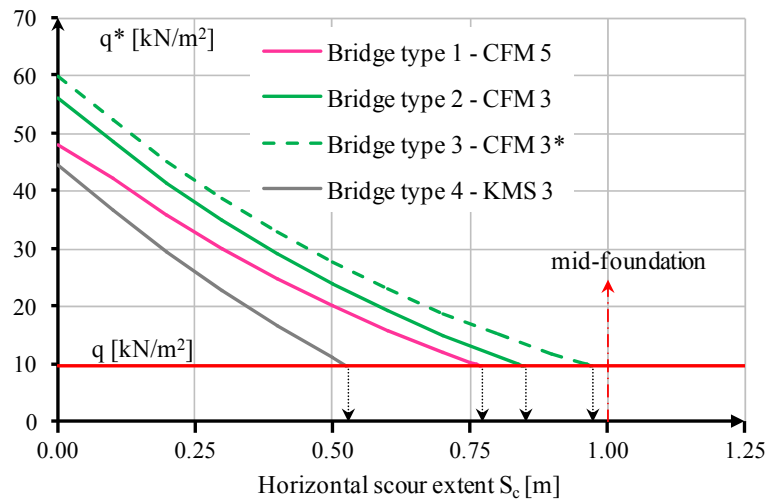


Fig. 5.15 The resistances of the four bridge types to assumed local scour action

The bridges with the pinned joint at the pier top may be considered as special cases of the given bridge types by setting the plastic bending strength of the joint to zero. Additionally, the case of a continuous multiple span girder bridge where the horizontal translation is allowed (e.g. roller bearings) may be considered by restricting rotation at adjacent supports in the BT 1. The crucial mechanisms in this case are the *CFM 5** and the *CFM 6** for the pinned joint at the pier top (i.e. *CFM 5* and *CFM 6* with additional work in the adjacent supports). In Table 5.3, the strengths of the joint at the pier top and the adjacent supports are varied to investigate their effect on the ultimate scour extent for discussed bridge types. Here, both the soil properties ($\phi = 25^\circ$, $c = 10 \text{ kN/m}^2$) and the sagging plastic strengths of girder were not changed.

Table 5.3 Effects of the joint and adjacent supports plastic strength on the results

Bridge Type	Plastic strength ^x		Combined failure mode	S _c (m)	%B
	Joint at the pier top	Adjacent Supports			
BT 1	0	0	<i>CFM 6</i>	0.55	27.5
	0	M _p h	<i>CFM 6*</i>	0.63	31.5
	M _p j	0	<i>CFM 5</i>	0.77	38.5
	M _p j	M _p h	<i>CFM 5*</i>	0.90	45.0
BT 2	0	0	<i>CFM 3</i>	0.83	41.5
	M _p j	0	<i>CFM 3</i>	0.85	42.5
	2M _p j	0	<i>CFM 3</i>	0.87	43.5
BT 3	0	M _p h	<i>CFM 3*</i>	0.95	47.5
	M _p j	M _p h	<i>CFM 3*</i>	0.97	48.5
	2M _p j	M _p h	<i>CFM 3*</i>	0.99	49.5
	4M _p j	2M _p h	<i>CFM 7*</i>	1.13	56.5
BT 4	/	/	<i>KMS 3</i>	0.53	26.5
^x see input data in Table 5.2					
/ these values are not important for BT 4					

The BT 1 with pinned joint gives similar result as the BT 4. This is because the optimal position for center of pier-foundation rotation coincides with the center of rotation for the applied *KMS 3* in *CFM 6*. The plastic strength of adjacent supports has a significant effect on all bridge types. For the BT 3 it may affect the critical mechanism (*CFM 7** instead of *CFM 3**), but in this case this would imply large (i.e. unrealistic) reinforcement ratios over supports. The plastic strength of the joint at the pier top has largest influence on the BT 1, but its variation has minor effect on the critical mechanisms for all bridge types.

For BT 3, the optimized solution involves plastic hinges at the sections where the strength was reduced (Figs. 5.2c). This does not apply in general for various reinforcement ratios and discussed bridge types. Actually, for the ratios in the span approaching the simple beam case, the optimal position of the hinge moves towards the middle support, whilst for lower ratios it moves towards the mid-span. Similar holds for the strength of the adjacent supports. For all bridge cases, the location of the reduced girder strength in the span (i.e. splicing location) did not significantly affect the results. It is concluded that the layout of the reinforcement and plastic sagging strength of girder affect the optimal position of the hinge, but the results are mostly governed by the ratio of internal works done in the *KMS* and the superstructure.

With reference to Fig. 4.7e, the influences of the cavity slope and the weight of soil flushed away on the assumed *KMS* was investigated. Here, the maximum scour

cavities are adopted as symmetrical ($\alpha = \beta$). Furthermore, for purely frictional soil, the maximum decrease in bearing capacities for *KMS 1a*, *KMS 1b* and *KMS 3* occurs when the angle α equals ϕ , whereas for purely cohesive soil or cohesive-frictional soil, the angle α is set to 45° (Fig. 5.16).

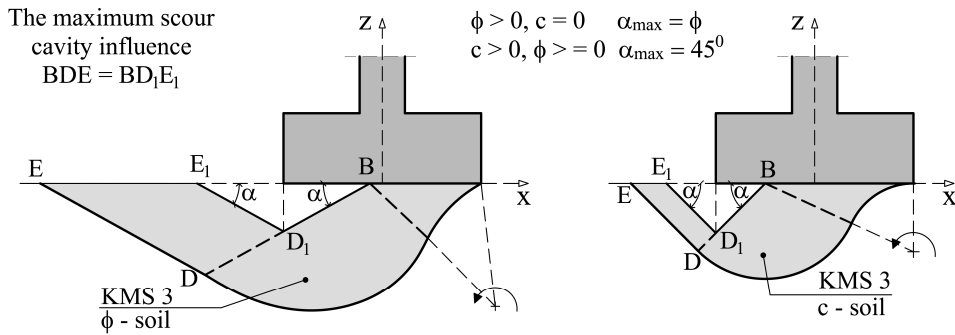


Fig. 5.16 The influence of the maximum assumed local scour cavity on the *KMS 3*- cases of frictional soil (left) and cohesive soil (right)

The BT-s are re-analyzed to include the maximum scour cavities. The updated mechanisms are denoted with letter ν in the index of a *CFM*. In the case of BT 1 the *CFM 5 ν* becomes critical (Fig. 5.17). The influence of the maximum local scour cavity is as high as 20% and 5% for purely cohesive and purely frictional soils, respectively (Figs. 5.18 and 5.19). For the other bridge types, the critical mechanisms involve the *KMS 2*, which is not affected by the weight of soil flushed from scour cavity. However, in the cases of BT 2 and BT 3 with purely frictional soils, the *CFM 1 ν* is the critical mechanism for $1 < FS < 2$.

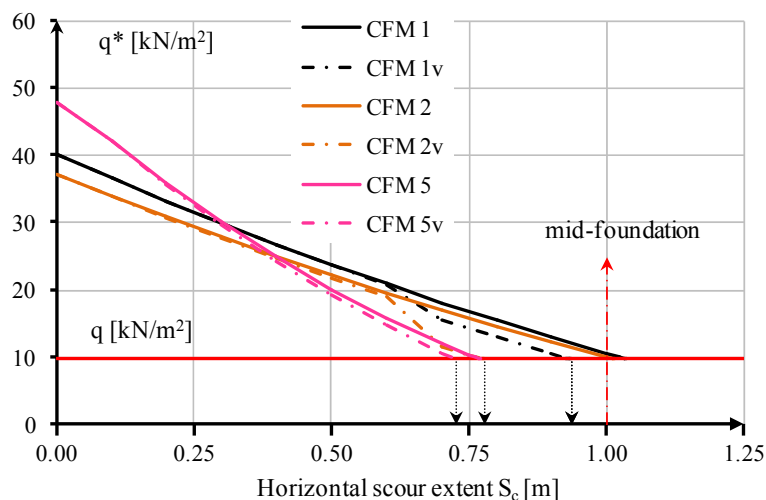


Fig. 5.17 Influence of the maximum local scour cavity for BT 1

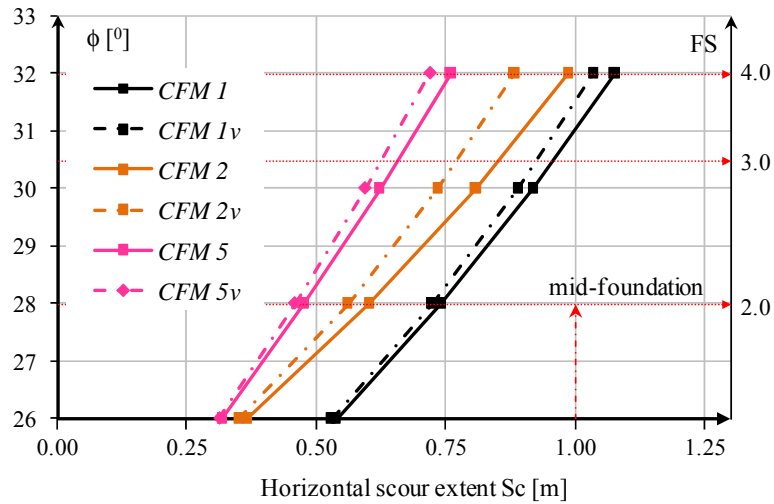


Fig. 5.18 Influence of the maximum local scour cavity for BT 1 and purely frictional soil

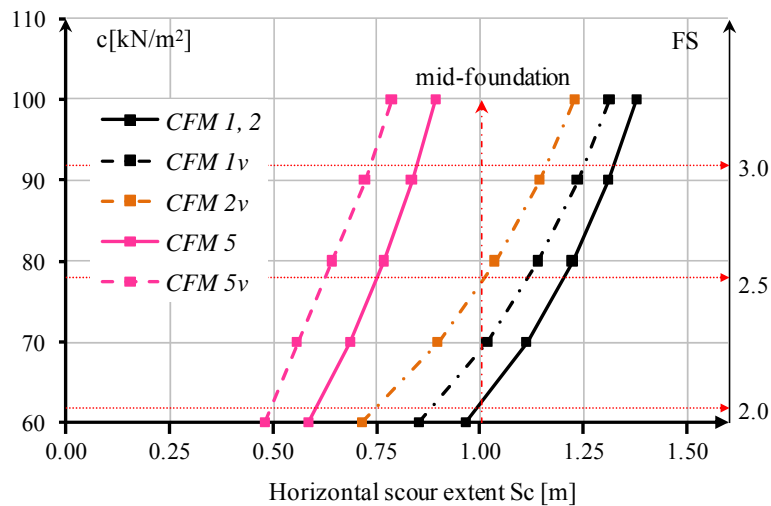


Fig. 5.19 The influence of the maximum local scour cavity for BT 1 and purely cohesive soil

In the case for a pier with one column founded on a caisson, the scour cavity given in Fig. 4.7d is considered with no surcharge load. Due to possible arbitrary location of the cavity, the failure mode may involve displacement of the pier-foundation system in a plane which does not coincide with the bridge longitudinal direction. Requirement for this scenario is the combined mechanism, which involves plastic hinge at the pier top. This type of mechanism resembles the presented *CFM 3* (Fig. 5.5c) with a difference in the direction of the plane in which the associated *KMS* forms (Fig. 5.20). Additionally, the mechanisms that only include sinking of the superstructure at the pier top are plausible (e.g. *CFM 1*), due to substantial lateral strength of the superstructure. This type of pier-foundation system is going to be considered in section 6.4.

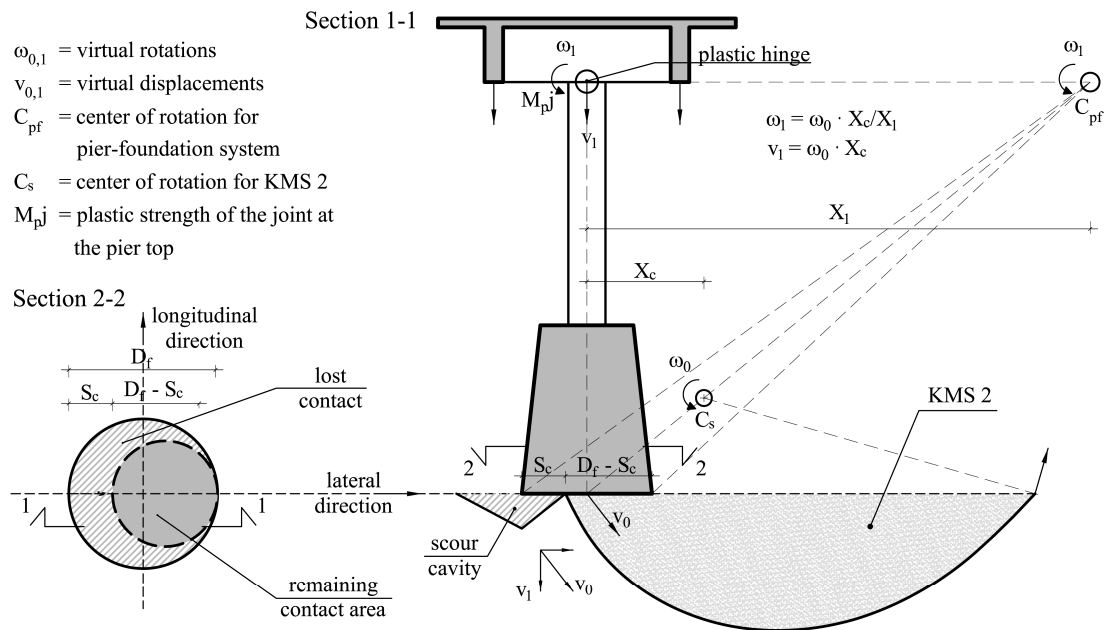


Fig. 5.20 A possible combined failure mode for bridge with a pier on caisson foundation

5.5 Additional comments on the CFM-s in longitudinal direction

According to the obtained results for a wall type pier, it may be concluded that the soil properties and the chosen *KMS* mostly govern the combined failure mode in the bridge longitudinal direction. However, it is essential to account the superstructure type (i.e. BT-s) in the analysis as seen in Fig. 5.15 and Table 5.3. Here, the variation of the plastic strength of elements has minor influence.

The *CFM*-s that include *KMS 1a* and *KMS 1b* give the least upper-bound solution for the initial state i.e. when scour has just reached the bottom of the shallow foundation. However, the combined mechanisms, which include *KMS 2* or *KMS 3* (i.e. rotational mechanisms), are proven to be more sensitive to the effects of the assumed local scour cavity, yielding considerable lower values of critical horizontal scour extent for the case BT 1 and cohesive soils in general.

The centers of soil rotation, which yield optimized solutions for the rotational mechanisms, are on the vertical line that passes through the foundation side unaffected by scour, with exception of *CFM 6**, where an uplift of the foundation is allowed.

The surcharge load has to be considered in scenarios as in Fig. 4.6, where one side of a river bank at the pier foundation may become severely affected by local scour. This gives advantage to mechanisms which involve soil displacement to the side of scour cavity, or simple sinking mechanisms.

It is noticed that the errors of $\pm 10\%$ in estimation of bridge self-weight affect the results $\pm 10\%$. Thus, any maintenance actions or rehabilitation measures that have been carried out or are planned in the future should be accounted. The pier height does not have significant effect on the results for owing to assumed kinematics and geometry of the *CFM*-s.

The geometry of a scour cavity and weight of soil flushed away have adverse effect on the bearing capacity of supporting soil, especially for purely frictional soils and the cases in which horizontal displacement of the pier top is restrained while $FS < 2$. Also, the obtained results suggest that assumed maximum local scour cavities (Fig. 5.16) may not only alter the geometric scale of an applied KMS, but it may transform the KMS into a different one. This transformation was not included in the analysis and will be considered in the future work.

5.6 Combined failure modes in the lateral direction

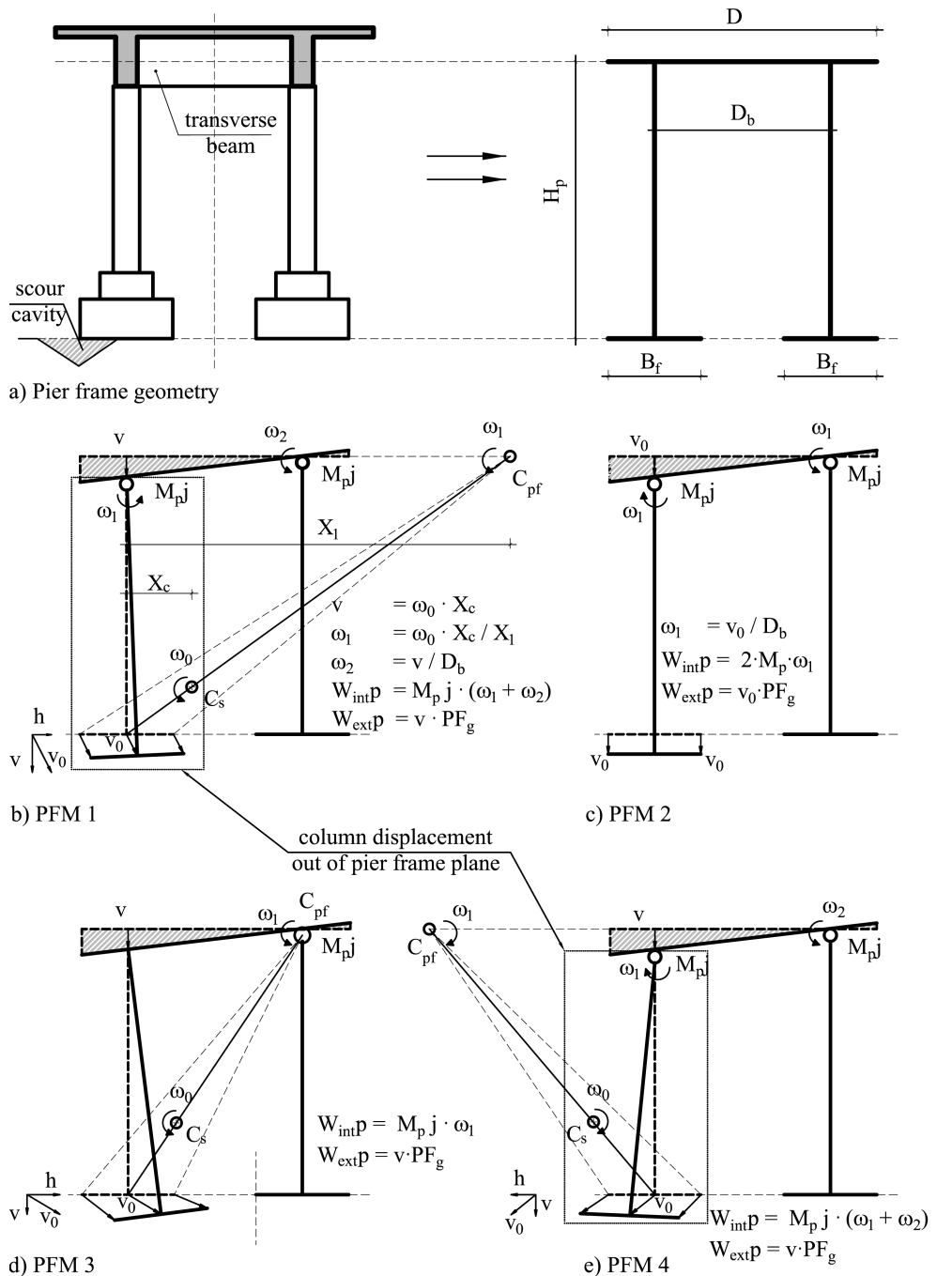
Considering the previous sections and the presented optimization procedure, the failure modes of a bridge in the lateral direction due to local scour action are discussed. In addition to the assumptions and constraints of the soil-bridge model given in section 5.1:

- There is no lateral displacement of the main girder due to the substantial strength in the lateral direction
- There is no lifting of the adjacent supports

For the pier with double columns on the separate spread foundations (Fig. 4.1c), there are two possible scenarios of local scour action. If it is assumed that both foundations are equally affected, the approach presented for the longitudinal bridge direction may be applied. However, the more realistic scenario is that one of the foundations is more affected than the other one is, due to their location with respect to the river flow direction, which is further analyzed.

Generally, the lateral combined failure modes (L_iCFM -s) are triggered by failure of the pier frame (Fig. 5.21). Here, it is adopted that the column unaffected by scour and its foundation have to resist additional vertical force resulting from a pier failure mode (*PFM*). For the *PFM 2* the uniform sinking is adopted, while in the other modes

the center of rotation of the scour-affected column is located in the plane of the deck (C_{pf} in Fig. 5.21). At least two plastic hinges in a pier frame are required for a failure mechanism, except in the *PFM 3* where the affected column and transverse beam jointly rotate as a rigid body in the plane of the pier frame.

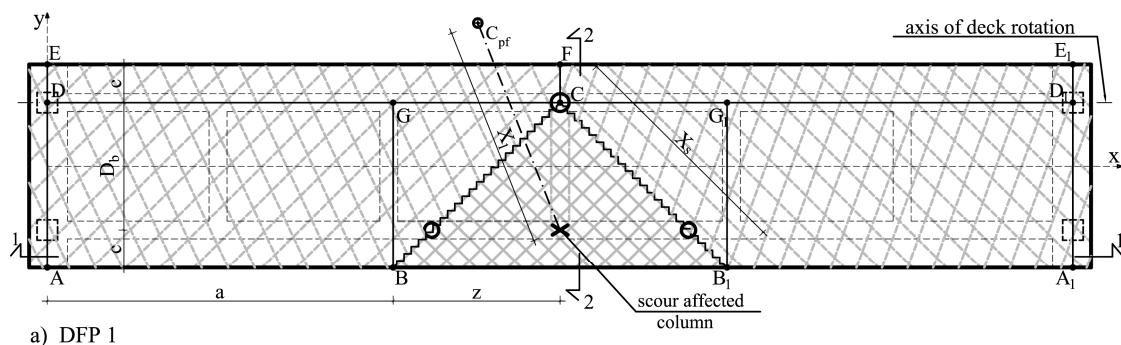


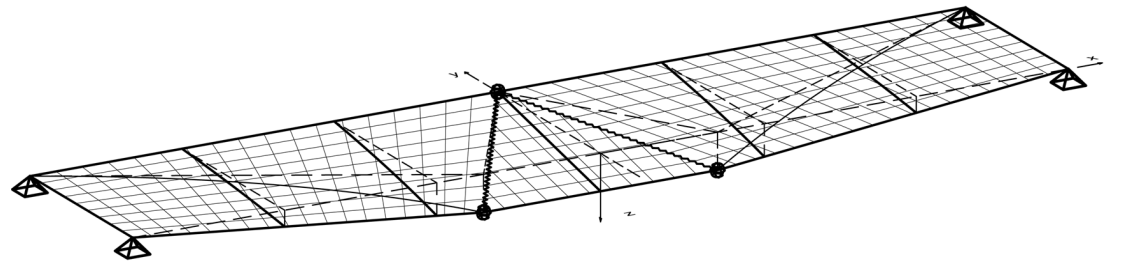
D = deck width B_f = foundation width M_{pj} = plastic strength of the joint at the column top
 H_p = pier height $\omega_{0,1,2}$ = virtual rotations C_{pf} = center of the affected column rotation
 $v_{0,1}$ = vertical virtual displacement at the affected column C_s = center of the rotation for a KMS
 D_b = distance between girder beams

Fig. 5.21 Failure modes of the pier frame

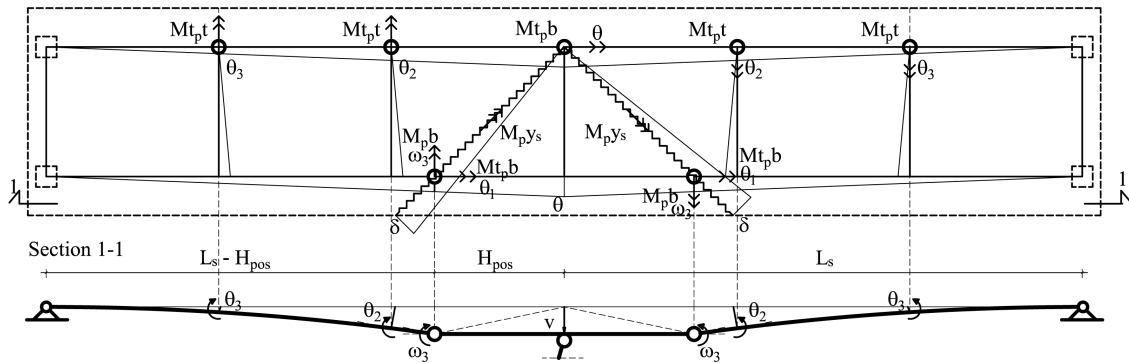
In that case, the extent of an assumed *KMS* beneath the affected foundation is limited by neighboring, unaffected foundation. This mode yields large upper-bound solution for bearing capacity and is not further discussed. In the modes *PFM 1* and *PFM 4*, the displacement of the affected column is out of the pier frame plane, which entails consistent rotational *KMS*. Since the appropriate *KMS* affected by the local scour cavity which involves displacement of soil mass to the side of the cavity is not yet found, the *PFM 4* is not considered and will be part of the further research. Thus, in the analysis the *KMS 1a* and *KMS 2* (Fig. 4.12) are applied in cases *PFM 2* and *PFM 1* respectively. The internal and external work (W_{intp} , W_{extp}) for the PFM-s are given in Fig. 5.21.

The superstructure failure has to be compatible with vertical displacement of the deck at the supporting point (i.e. affected column). The possible failure pattern in the main girder deck *DFP 1* is given in Fig. 5.22. The main girder beam, which is supported by the compromised column, suffers failure as two plastic hinges form in the span. Simultaneously, the bridge deck rotates around the axis that coincides with the axis of the opposite girder beam. The prerequisite for this rotation is the plastic hinge at the pier top of the unaffected column and pure torsion in the beam above it. This leads to the failure pattern consisted from two mirror hyper-surfaces (*ADCB* and $A_1D_1CB_1$ in Fig. 5.22a). In order to fulfill the compatibility of the assumed displacements, in the plane of the deck there is compression in the triangular zone (BCB_1). Here, the sagging yield lines have uneven rotation due to the variable angle between the adjacent surfaces. The rotation of the yield lines of deforming regions in the deck have been estimated based on the assumed geometry.

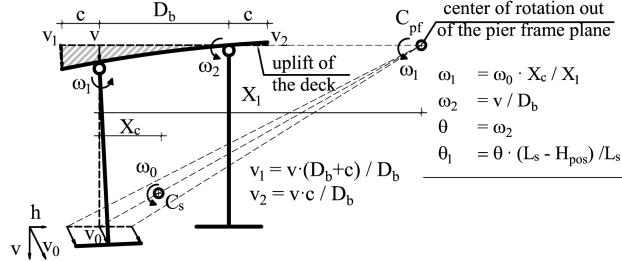




b) Isometry (the cantilevers are omitted)



Section 2-2 (PFM 1)



- $v_{1,2}$ = vertical displacements of the deck
- δ = rotation in the sagging yield lines
- $\omega_{1,2,3}$ = rotations of the pier and girder beams
- $\theta_{1,2,3}$ = torsional rotations of beams
- $M_{p,xy}$ = plastic bending strength of the deck
- M_{p,y_s} = plastic sagging moment of the yield line
- $M_{t_p,b}$ = plastic torsional moment of the girder beam
- $M_{p,b}$ = plastic sagging moment of the girder beam
- $M_{t_p,t}$ = plastic torsional moment of a transverse beam

$$W_{int,s} = 2 \cdot (M_{p,b} \cdot \omega_3 + M_{t_p,b} \cdot \theta_1) + M_{t_p,b} \cdot \theta + 2 \cdot 2 \cdot M_{p,xy} \cdot v_1 + 2 \cdot M_{p,y_s} \cdot X_s \cdot \delta / 2 + 2 \cdot M_{t_p,t} \cdot \theta_2 + 2 \cdot M_{t_p,t} \cdot \theta_3$$

c) Rotations of girder beams, transverse beams and sagging yield lines

- yield line-pattern (hypar-surface)
- triangular zone BCB_1
- sagging yield lines
- beam hinge

Fig. 5.22 Possible failure pattern of the superstructure - DFP 1

Thus, the internal energy dissipation in the superstructure $W_{int,s}$ considers the following (Fig. 5.22c):

- Plastic hinges in the compromised main girder beam (combined loading - bending and torsion)
- Plastic hinge in the uncompromised main girder beam (pure torsion)
- Pure torsion in the deck (hypar-surfaces)
- Sagging yield lines (uneven rotation)
- Transverse beams are subjected to pure torsion (hidden deck beams)

The work of external forces of the superstructure $W_{ext,s}$, for the displacement at the affected pier v , is calculated based on the assumed surface failure geometry taking

into consideration the uplift of zones DCFE and D_1FCE_1 (Fig. 5.22):

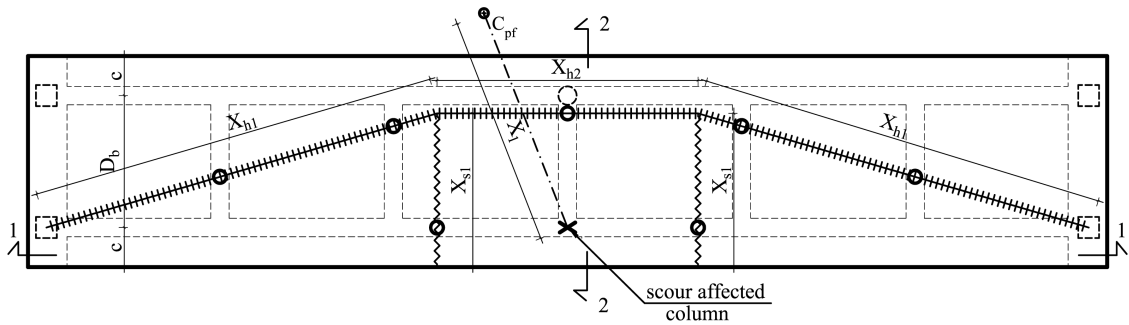
$$W_{extS} = 2 \left(v_1 \iint_{ABGD} \frac{xy}{a(D_b + c)} dx dy + v_1 \frac{z(D_b + c)}{3} - 3v_2 \iint_{DCFE} \frac{xy}{(a + z)c} dx dy \right) \quad (5.6)$$

where:

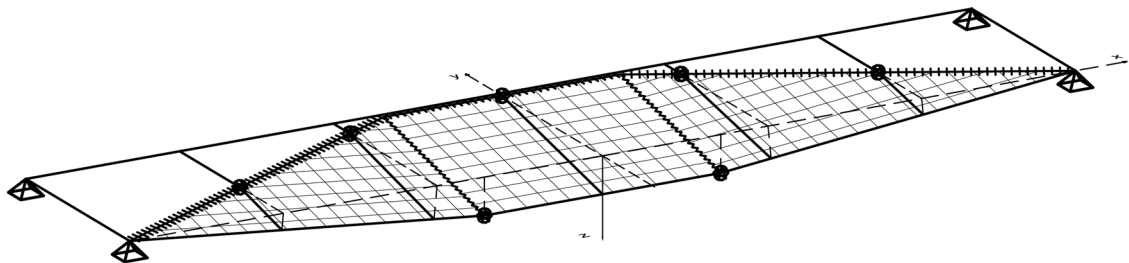
- x, y = longitudinal and lateral direction of the deforming regions in the deck
- v_1, v_2 = virtual vertical displacements of the deck (Fig. 5.22c)
- a, D_b, c, z = dimensions associated to the deforming regions of the deck

Inspired by research in [Barnard et al, 2010], a similar pattern, here denoted as *DFP 2*, is presented in the Fig. 5.23. In difference to the previously explained *DFP1*, there is no torsion of the deck, just the rotation of the assumed rigid body plates along the hogging and sagging yield lines. At the intersection of the yield lines and the transverse beams the plastic hinges must form. Thus, the work of the internal forces for the deck in this case consider (Fig. 5.23c):

- The compromised main girder beam subjected to bending
- Transverse beams subjected to combined bending and torsion
- Hogging and sagging yield lines



a) DFP 2



b) Isometry

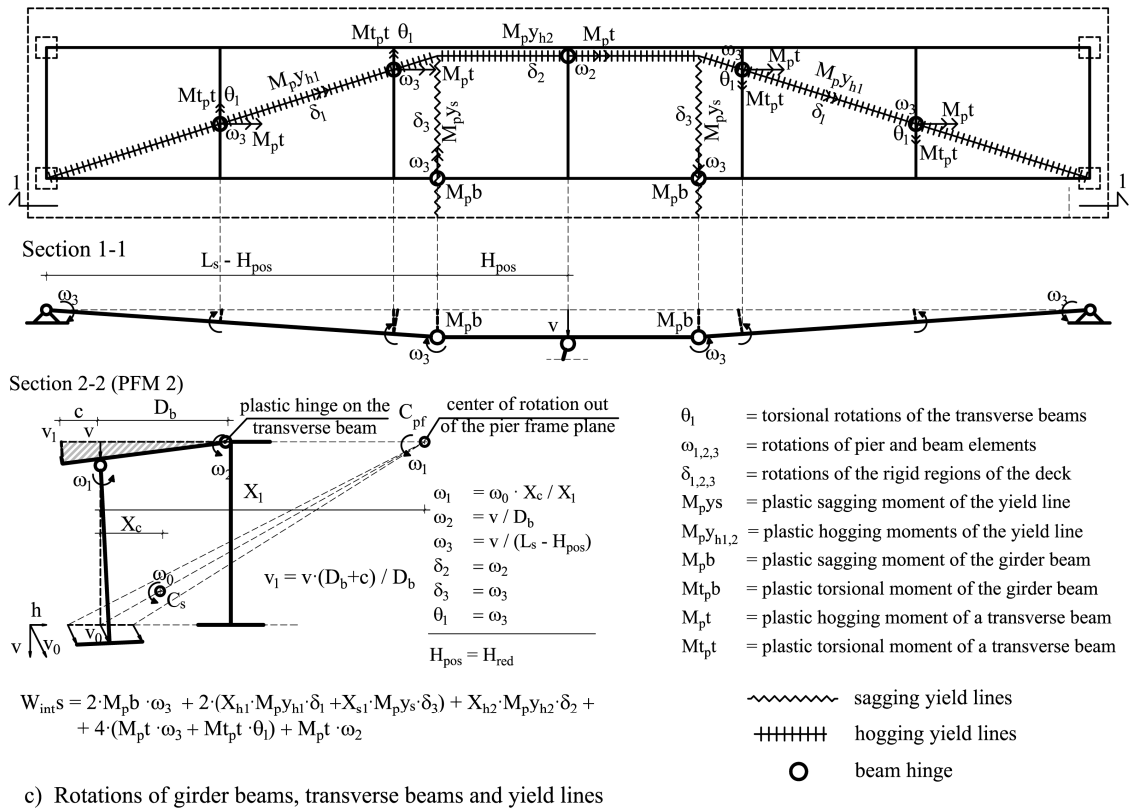


Fig. 5.23 Possible failure pattern of the superstructure - *DFP 2*

The external rate of work W_{extS} is obtained by considering the geometry of the failure pattern in the deck (Fig. 5.23c):

$$W_{extS} = vD_b \left(\frac{L_{pos}}{3} + H_{pos} \right) + cv(L_{pos} + 2H_{pos}) + c(v_1 - v) \left(\frac{L_{pos}}{3} + H_{pos} \right) \quad (5.7)$$

where:

v, v_1 = virtual vertical displacements of the deck

L_{pos}, D_b, c, H_{pos} = dimensions associated to the deforming regions of the deck

5.7 Analysis of a soil-bridge model in the lateral direction – An example

At first, it is not clear which of the two presented *DFP*-s engage more structure's self-weight and dissipate the least amount of internal energy. Thus, the four combined mechanisms are considered and the data used in the optimization procedure is summarized in Table 5.4. The locations of the transverse beams are assumed to be in the thirds of each span, which is the usual practice in Serbia.

Table 5.4 Input data and results of the optimization procedure for the lateral failure modes

Input data							Results					
Main girder		Pier-Foundation system		Plastic strength of bridge elements [kNm] ×			Soil Properties		Bridge type ^{xxx}	S _c [m]	Area %	Fig.
Span L _s [m]	20.0	Pier height H _p [m]	8.0	Top of the column	M _{pj} =	820.1	friction angle φ [°]	25.0	L _t CFM 1 (DFP 1 + PFM 1)	1.45	56.8	5.24
Deck width D [m]	8.0	Column B _c [m]	0.75	Transverse Beam	M _{pt} =	421.4	cohesion c [kN/m ²]	10.0	L _t CFM 2 (DFP 1 + PFM 2)	1.77	66.2	
Deck height d _h [m]	0.2	Column D _c [m]	0.75	Girder beam	M _{pb} =	702.3	weight γ [kN/m ³]	18.0	L _t CFM 3 (DFP 2 + PFM 1)	1.58	60.8	
Beam height h [m]	1.7	Foundation width B _f [m]	3.0	Deck	M _{pt} =	165.4			L _t CFM 4 (DFP 2 + PFM 2)	1.89	69.4	
Beam width b [m]	0.5	Foundation length L _f [m]	3.0	* Based on section 4.5 and minimum reinforcement requirements of a design code; The reinforcement layout corresponds to Fig 5.2a; f _{pc} =2.0 kN/cm ² , f _y =24.0 kN/cm ²								
g [kN/m ²]	7.6	Foundation height H _f [m]	2.0	** The initial factor of safety (FS) is based on the Eq. 4.1 without the surcharge load								
Δg [kN/m ²]	2.0	Self-weight PF _g [kN]	840.0	*** Refer to Figs. 5.22 and 5.23 for deck failure patterns and to Figs. 5.21 for pier frame failure modes								

Based on the given geometry, the *DFP 1* engages the similar amount of the self-weight as *DFP 2*. Nevertheless, the *L_tCFM 1* yields the best results among the analyzed failure modes (Fig. 5.24). It may be concluded that KMS 2 combined with the two assumed failure patterns DFP 1 and DFP 2 give better results when compared to the sinking mechanisms.

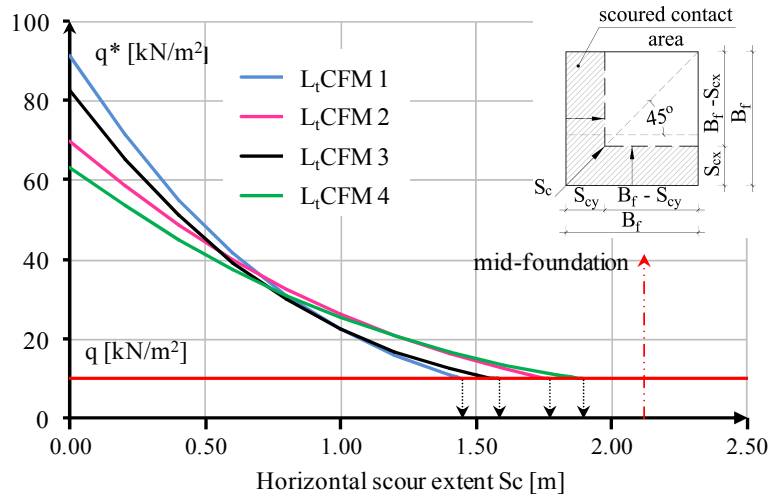


Fig. 5.24 The lateral combined failure modes

The effects of the soil mechanical properties, given by φ and c, on the ultimate horizontal scour extent are given in Figs. 5.25 and 5.26, respectively. The initial safety factors (FS) of bearing capacity are based on the Eq. 4.1 without the surcharge load.

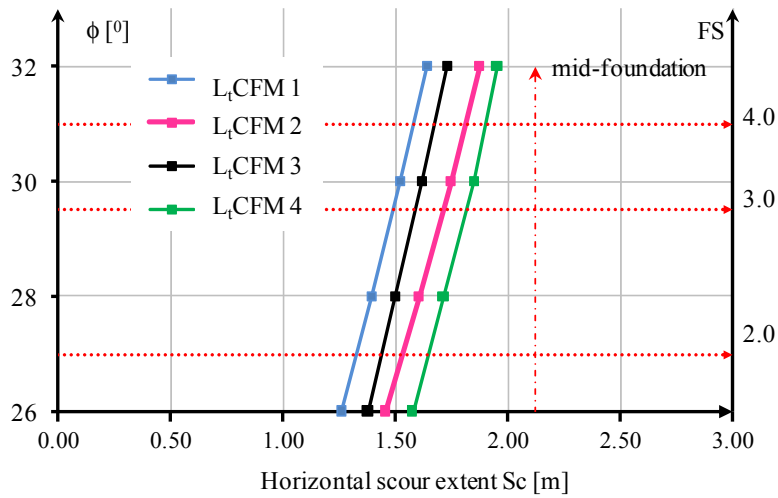


Fig. 5.25 The influence of internal friction angle on the lateral combined failure modes

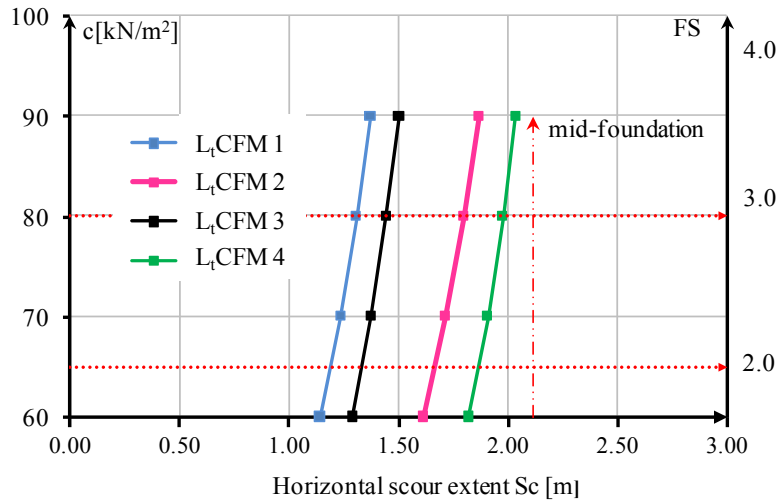


Fig. 5.26 The influence of cohesion on the lateral combined failure modes

The superstructure elements' properties have larger impact on the lateral combined failure modes in comparison to the failure modes in bridge longitudinal direction. The influence of plastic strength of a joint at the pier top, governed by reinforcement ratio of the section (A_s/A_b), on the ultimate scour extent for the critical mechanism is seen in (Fig. 5.27). Furthermore, the plastic strength of transverse beams has a significant role in controlling the failure. The increase of transverse reinforcement favors the $L_tCFM 3$ and $L_tCFM 4$, while for the increase of plastic hogging strength, the $L_tCFM 1$ and $L_tCFM 2$ yield lower ultimate horizontal scour extents. In the given example, for less than two transverse beams in a span (i.e. a short-span bridge) the $L_tCFM 3$ becomes the critical mechanism.

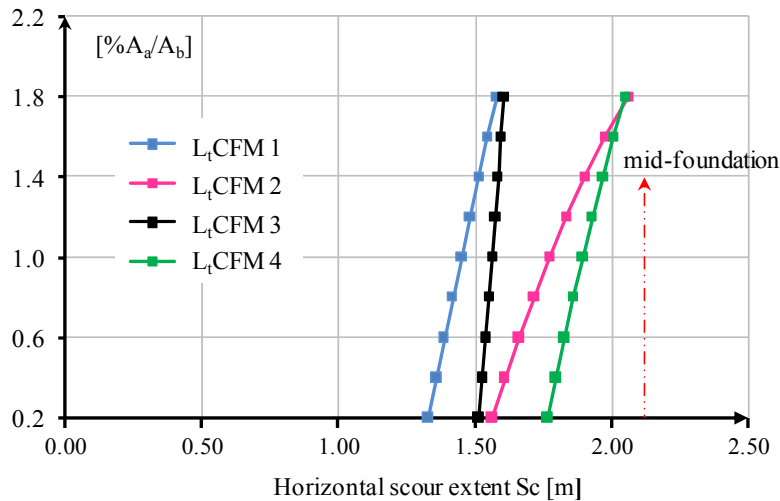


Fig. 5.27 The influence of the pier reinforcement ratio on the lateral combined failure modes

5.8 Failure modes without the soil failure

The case of a pier with double columns on a strip footing affected by the local scour cavity as in Fig. 4.7b is given in Fig. 5.28. The inadequate longitudinal or transverse reinforcement at the foundation may trigger pier vertical displacement. Either the *DFP 1* or *DFP 2* are possible, but this is unimportant as the poor detailing solely govern the critical local scour extent beneath the foundation (S_c in Fig. 5.28). In such situations, the study of the project documentation is crucial for the analysis. The mentioned cases are beyond the scope of the thesis.

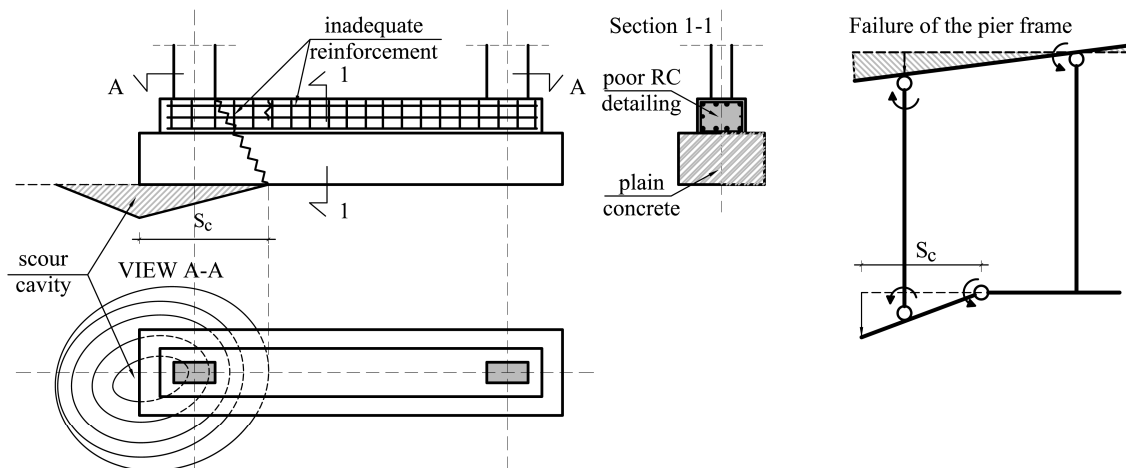


Fig. 5.28 Example of bridge failure solely governed by inadequate reinforcement

Chapter 6. Probability of bridge failure due to local scour action

The goals of the previous sections were to identify possible failure modes of the bridges with shallow foundations affected by a local scour cavity. In this chapter, the modes are used to estimate the probability of a bridge failure in a local scour event. The Quasi Monte Carlo analysis is applied in the example of a four-span continuous bridge crossing a river channel (Fig. 6.7), where the uncertainties connected to the governing parameters necessary for WSB interaction are considered. The chapter ends with a review of the presented approach to estimate probability of a bridge failure and further application of here presented study is briefly discussed (section 6.6).

6.1 The crude Monte Carlo and quasi Monte Carlo analysis

In order to consider the uncertainties involved in predictive models and solve multidimensional integration problems, the Monte Carlo (MC) analysis is applied. This method is a common simulation technique in the structural reliability analysis and is used for the estimation of the probability integral [Faber, 2007]:

$$P_i = \int_{g(x) \leq 0} f_X(x) dx = \int I[g(x) \leq 0] f_X(x) dx \approx \frac{1}{N} \sum_{j=1}^N I[g(x) \leq 0] \quad (6.1)$$

where:

$$P_i = \int_{g(x) \leq 0} f_X(x) dx = \text{the probability integral}$$

$$f_X(x) = \text{joint probability density function of a basic random variable } X$$

$$g(x) = \text{limit state function}$$

$$I[g(x) \leq 0] = \text{indicator function equal to 1 for } g(x) \leq 0 \text{ otherwise equal to 0}$$

$$\frac{1}{N} \sum_{j=1}^N I[g(x) \leq 0] = \text{the unbiased estimator of the failure probability for the } N \text{ realizations of the basic random variable } x, \text{ i.e. } x_j, j=1,2,\dots,N$$

The crude Monte Carlo approach (CMC) is based on the application of the formula in Eq. 6.1. The expected value of failure probability P_i after a large number of simulations N is obtained as $\frac{n_f}{N}$, where n_f is the number of cases where the limit state function $g(x)$ has negative values. The simulation with CMC requires pseudo-random numbers generation from the uniform distribution within the unit interval $[0, 1]$ (i.e. uniform sampling). The values of stochastic variables are obtained from cumulative

distribution function by inverse transformation (Fig. 6.1). This approach is straightforward and its main benefit is applicability to wide range of problems regardless their complexity. However, the drawback of the CMC is the slow convergence of the solution. The large number of simulations is necessary to obtain a sufficiently accurate result for multiple parameter problems, which considerably increase the associated computation time. For example, if the target probability is in the order of 10^{-6} , it is expected that approximately 10^8 simulations are necessary for an estimate with coefficient of variance in order of 10% [Faber, 2007]. In the analysis, the limit state function is non-linear (Eq. 6.5) and implies the optimization problem with variable geometry of a KMS (Eq. 5.5), thus CMC analysis becomes cumbersome tool for estimating the probability.

Various methods such as importance sampling, low-discrepancy sequences (LDS) and Markov chains are applied to decrease the number of simulations and increase the accuracy in the MC analysis. At this point, the application of the importance sampling method is not possible as the governing parameters, which define the limit state function (Eq. 6.5), have different uncertainty (section 6.2). The LDS methods (e.g. Sobol, Halton, Faure, Latin Hypercube) are commonly used to solve multidimensional integration problems and give a finer uniform partitions of the unit interval i.e. a more uniform sample of random generated numbers (i.e. quasi-random numbers) (Fig. 6.2). The MC based on these methods is referred to as quasi Monte Carlo (QMC).

In this analysis, the LDS method given by [Sobol, 1967] is applied. It is based on the algorithm of constructing a sequence of numbers that fill a s-dimensional hypercube $[0, 1]^s$ to obtain the convergence to the exact solution in Eq.6.1 as fast as possible.

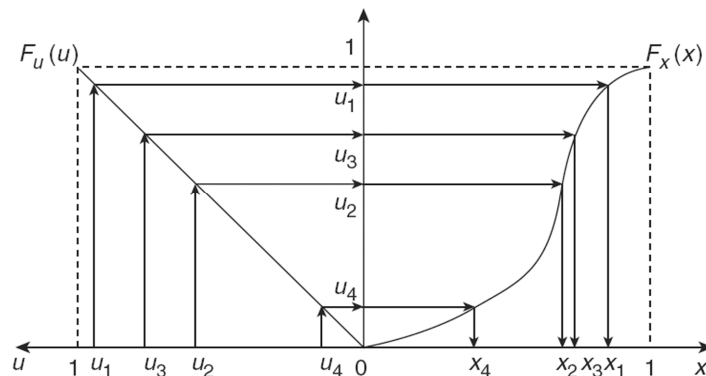


Fig. 6.1 Concept of generation of random variable x_j by uniform random number u_j based on the inverse transformation [Phoon, 2008]

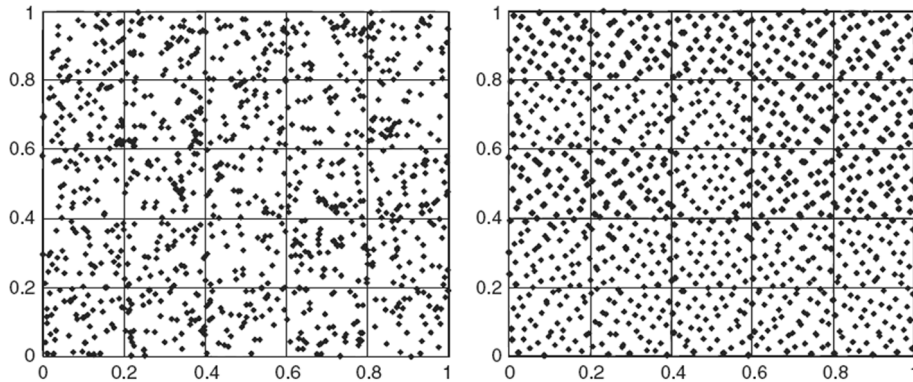


Fig. 6.2 Pseudo number generation (left) compared to quasi random number generation (right) for 1000 random numbers generated in two-dimensional space [Phoon, 2008]

Here, the quasi-random numbers from Sobol sequence are generated in the Matlab script with the function *sobolset* and successively used for the simulation of the stochastic parameters in the QMC analysis. The application of the Sobol sequence is here presented as a convenient tool in the analysis and its efficiency was not compared to the other similar methods. Nevertheless, it has very low standard error in comparison with pseudo-random numbers and other LDS methods. In addition, it gives better performance than typical pseudo-random sequences for all four probabilistic moments as discussed in [Krykova, 2003].

Once the necessary data in QMC is obtained, it should be fitted to a parametric distribution in order to have unambiguous post-processing. Commonly, the result is the model which agrees well with the data in the high density regions and poorly in the “tails” of the simulated data distribution, which affects the accuracy of the probability estimate. The solution to this problem is a non-parametric fit in high density region combined with a Generalized Pareto Distribution. Here, this approximation is preformed with the Matlab function *paretotails* (statistics toolbox).

6.2 The uncertainties in the vulnerability assessment of bridges to local scour

One of the main features of the vulnerability assessment lies in its comprehensive approach to the entire bridge population, which means that data collection at every bridge site is not an acceptable/plausible action. The uncertainties related to estimation of the governing parameters, which are necessary for application of the WBS interaction, control the accuracy of the results in the vulnerability analysis. Thus, the preliminary assessment of the complete bridge population should be based on

the available (i.e. limited) data from the bridge databases, project documentation and hydraulic studies. If necessary, the additional data collection (in-situ and/or laboratory testing, monitoring) and calibration should be performed in order to decrease the levels of parameter uncertainties and obtain results that are more reliable.

The governing parameters, which are used for the estimation of a local scour action at piers and for the related combined resistance of a soil-bridge system, comprise the three sets of input data. The modeling of the uncertainties related to these parameters is beyond the scope of this thesis. Here, the results and conclusions from the state-of-the art research and reliability based design approaches are used.

6.2.1 The uncertainties in the local scour evaluation

The risk based approach in the scour prediction procedures, with primary purpose to analyze the probability of scour depth exceedance is elaborated in [Lagasse et al., 2013]. Here the uncertainties in the local scour evaluation are discussed. There are hydrologic, hydraulic and model uncertainties, which arise owing to unknown characteristics of future extreme flood, variability of river channel properties at a bridge site and an applied local scour formula respectively.

Typically, the scour prediction in risk analysis is associated with a 100-year flood, which represents a hydrologic event that has a 1% chance of being equaled or exceeded in any given year. In general, for the modeling of the recurrence intervals of a peak discharge, the extreme probability distributions such as the *Log-Pearson Type III* (default in the U.S.) or extreme generalized distributions such as *Gumbel* are used [Briaud et al., 2009]. The peak discharge is commonly estimated based on flow records from stream gaging stations adjusted to a bridge location. If this data is unavailable for the investigated location, data from nearby watersheds of similar size and nature to the watershed of interest are used. This is possible if the regional regression relationships are available (e.g. the U.S. Geological Survey - USGS).

In the vulnerability assessment, the fundamental input must comprise an extreme flood hydrograph i.e. the peak discharge Q_{ext} and its associated equivalent time duration t_{eq} for the investigated location (e.g. Eq. 3.12). The extreme flood-hydrographs strongly depend upon the quantity and quality of the available data and commonly the extreme probability distributions are used to model Q_{ext} . For the evaluation of the local scour

magnitude at bridge piers and abutments, the one dimensional analysis and assumption of uniform steady flow is usually sufficient. It is a well known fact that the risk assessment of local scour at a bridge pier foundation may be performed only if the probabilistic distributions of corresponding hydraulic and soil parameters are sufficiently well known [Johnson and Dock, 1998]. The parameters, which define the river channel cross-section: width, depth, and bank inclination, and properties: channel slope S and the Manning roughness coefficient n , possess a level of uncertainty but they may be verified easily at a bridge site. Still, stochastic modeling is necessary since these variables may considerably change over time due to instability of the river channel. In the absence of reliable data for the investigated locations, the Manning coefficient, which cannot be directly measured at a bridge site, may be taken as a log-normally distributed variable, while the normal distribution would be appropriate for modeling of a channel slope [Lagasse, et al., 2013].

When the hydraulic parameters are defined, the unscoured water depth at affected pier y_d associated with Q_{ext} , may be solved from Chézy-Manning equation for the open-channel flow:

$$Q_{ext} = \frac{A_{ch}}{n} R_h^{\frac{2}{3}} S^{\frac{1}{2}} \quad (6.2)$$

where:

Q_{ext} = extreme discharge [m^3/s]

A_{ch} = flow cross-section area [m^2]

R_h = hydraulic radius of the flow cross-section [m]

n = Manning roughness coefficient [$s/m^{1/3}$] - function of river bed type

S = slope of the channel bottom [m/m]

For the trapezoidal channel cross-section (as in Fig. 6.7):

$$A_{ch} = \frac{y_d(B_{ch} + T_{ch})}{2} \quad (6.3)$$

$$R_h = \frac{A_{ch}}{B_{ch} + 2 \left(\left(\frac{T_{ch} - B_{ch}}{2} \right)^2 + y_d^2 \right)^{0.5}} \quad (6.4)$$

where:

B_{ch} = bottom width of the channel [m]

T_{ch} = top width of the flowing water [m]

y_d = unscoured water depth at the affected pier [m]

The approaching velocity of the flow V is assumed to have constant intensity over channel depth and width. It is obtained as the Q_{ext} divided by the flow cross-section area A_{ch} . The y_d and V are the main input for local scour evaluation formulas (section 3.1), which are developed based on the laboratory and field data.

It should be considered that despite controlled conditions, laboratory data have disadvantages, which are small and inconsistent length scales (geometric and sediment) and the predominance of clear-water conditions. On the other hand, the field data are uncontrolled (e.g. large parameter uncertainty and type of scour) and difficult to measure (e.g. scour refill, non-ultimate scour levels).

The model uncertainty of scour evaluation formulas was not considered here and the FDOT and HEC-18 clay formulas (Chapter 3) are applied respectively for the cohesionless and cohesive soil. The critical velocity V_c for the cohesionless soil is the threshold for local scour type in FDOT formula and it is based on the median soil diameter D_{50} (Eq. 3.8). This parameter may be obtained by gathering of soil samples and accounting for soil spatial variability at the investigated location.

The most reliable way to determine the scour evolution in cohesive soils is laboratory testing of extracted undisturbed soil specimens in erodibility measuring devices such as the EFA apparatus. The obtained erosion plots (e.g. Fig. 6.3) define the relationship between values of the erosion rate of a soil sample and associated approaching water velocity. The soil erodibility is generally positively correlated with undrained shear strength (Fig 3.4), but the cohesive soils erode irregularly and this soil property is still not investigated in detail. In the vulnerability assessment a curve fit may be used as an approximation of the plot (Fig. 6.3).

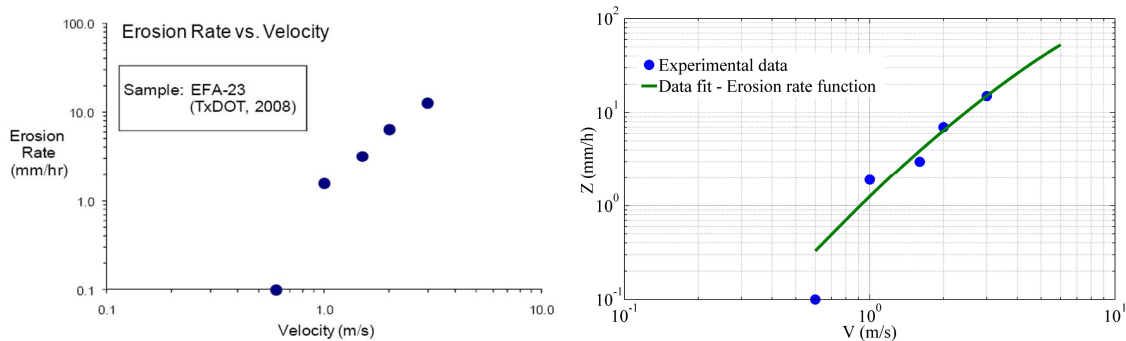


Fig. 6.3 Example of an erosion plot based on velocity [Briaud, 2008] (left); Approximation of the experimental data - the erosion rate function (right)

6.2.2 The uncertainties of soil geotechnical properties

In the evaluation of the soil geotechnical properties - the internal friction angle and undrained shear strength, different types of geotechnical uncertainty arise. According to [Phoon, 2008] these depend on inherent soil variability, degree of equipment and procedural control maintained during site/laboratory investigation. The high reported COV-s in Table 6.1 are mainly due to spatial variation of soil and measurement variability in situ.

Table 6.1 The COV for some common field measurements, adapted from [Phoon and Kulhawy, 1996]

Test type	Property	Soil type	Mean	Units	Cov (%)
CPT (Cone penetration test)	q_t	Clay	0.5-2.5	MN/m ²	< 20
	q_c	Clay	0.5-2	MN/m ²	20-40
	q_c	Sand	0.5-30	MN/m ²	20-60
VST (Vane shear test)	s_u	Clay	5-400	kN/m ²	10-40
SPT (Standard penetration test)	N	Clay and sand	10-70		25-50
	A reading	Clay	10-450	kN/m ²	10-35
	A reading	Sand	60-1300	kN/m ²	20-50
	B reading	Clay	500-880	kN/m ²	10-35
DMT (Dilatometer test)	B reading	Sand	350-2400	kN/m ²	20-50
	I_D	Sand	1-8		20-60
	K_D	Sand	2-30		20-60
	E_D	Sand	10-50	MN/m ²	15-65
	P_L	Clay	400-2800	kN/m ²	10-35
PMT (Pressuremeter test)	P_L	Sand	1600-3500	kN/m ²	20-50
	E_{PMT}	Sand	5-15	MN/m ²	15-65
	w_n	Clay and silt	13-100	%	8-30
	W_L	Clay and silt	30-90	%	6-30
	W_P	Clay and silt	15-15	%	6-30
Lab. Index	PL	Clay and silt	10-40	%	_a
	LI	Clay and silt	10	%	_a
	γ, γ_d	Clay and silt	13-20	kN/m ³	<10
	D_r	Sand	30-70	%	10-40; 50-70 ^b

Notes

^aCOV = (3-12%)/mean

^bThe first range of variable gives the total variability for the direct method of determination, and the second range of values gives the total variability for the indirect determination using SPT values

The major factors influencing the measurements in the laboratory testing occur due to errors in the equipment or human errors as well as from random testing effects that cannot be separately measured (Table 6.2).

Table 6.2 Total measurement error for laboratory-measured properties, adapted from [Phoon and Kulhawy, 1999]

Property (units)	Soil Type	Data groups no.	No. of Tests Per Group		Property Value		Property COV (%)	
			Range	Mean	Range	Mean	Range	Mean
$s_u^{(a)}$ [kPa]	Clay, silt	11	*	13	7 - 407	125	8 - 38	19
$s_u^{(b)}$ [kPa]	Clay, silt	2	13 - 17	15	108 - 130	119	19 - 20	20
$s_u^{(c)}$ [kPa]	Clay	15	*	*	4 - 123	29	5 - 37	13
$\phi^{(a)}$ [°]	Clay, silt	4	9 - 13	10	2 - 27	19.1	7 - 56	24
$\phi^{(b)}$ [°]	Clay, silt	5	9 - 13	11	24 - 40	33.3	3 - 29	13
$\phi^{(b)}$ [°]	Sand	2	26	26	30 - 35	32.7	13 - 14	14
$\tan\phi^{(a)}$	Clay, silt	6	*	*	*	*	2 - 22	8
$\tan\phi^{(b)}$	Clay	2	*	*	*	*	6 - 22	14
w_n [%]	Fine-grained	3	82 - 88	85	16 - 21	18	6 - 12	8
LL [%]	Fine-grained	26	41 - 89	64	17 - 113	36	3 - 11	7
PL [%]	Fine-grained	26	41 - 89	62	12 - 35	21	7 - 18	10
PI [%]	Fine-grained	10	41 - 89	61	4 - 44	23	5 - 51	24
γ [kN/m ³]	Fine-grained	3	82 - 88	85	16 - 17	17	1 - 2	1
* Not reported (a) Triaxial compression test (b) Direct shear test (c) Vane shear test			s_u = undrained shear strength ϕ = internal friction angle γ = specific weight					

The spatial variation of soil properties vertically with depth z , may be represented with a simple model (Fig. 6.4) and the associated formula in Eq. 6.5 [Phoon and Kulhawy, 1999].

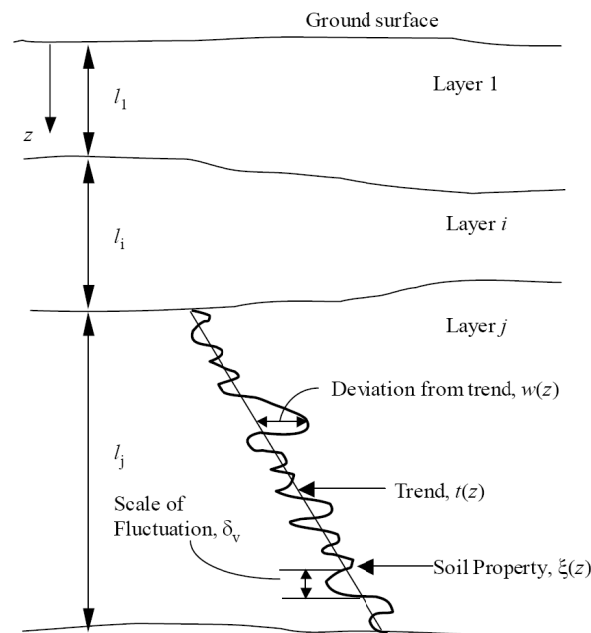


Fig. 6.4 Inherent soil variability [Phoon and Kulhawy, 1999]

$$\xi(z) = t(z) + w(z) + e(z) \quad (6.5)$$

where:

- $\xi(z)$ = insitu soil property
- $t(z)$ = deterministic trend component
- $w(z)$ = random component

Here, the scale of fluctuation indicates how rapidly a soil property varies about the trend. It is generally much higher in horizontal than in vertical direction.

The problem of spatially varying soil properties is commonly solved probabilistically where the model of random fields is used. The difference between uniform and heterogenic soil deposits are presented in Fig. 6.5. It is seen that the geometry of the failure mechanism strongly depends on the assumed random generated soil field. The centrally loaded symmetric foundation experience differential settlements in contrast to the theoretical response for uniform soil. In addition, the presented results (Fig 6.5) indicate considerably lower bearing capacity [Popescu et al., 2005].

The vulnerability assessment would benefit by application of the random field model and it is going to be considered in the future research.

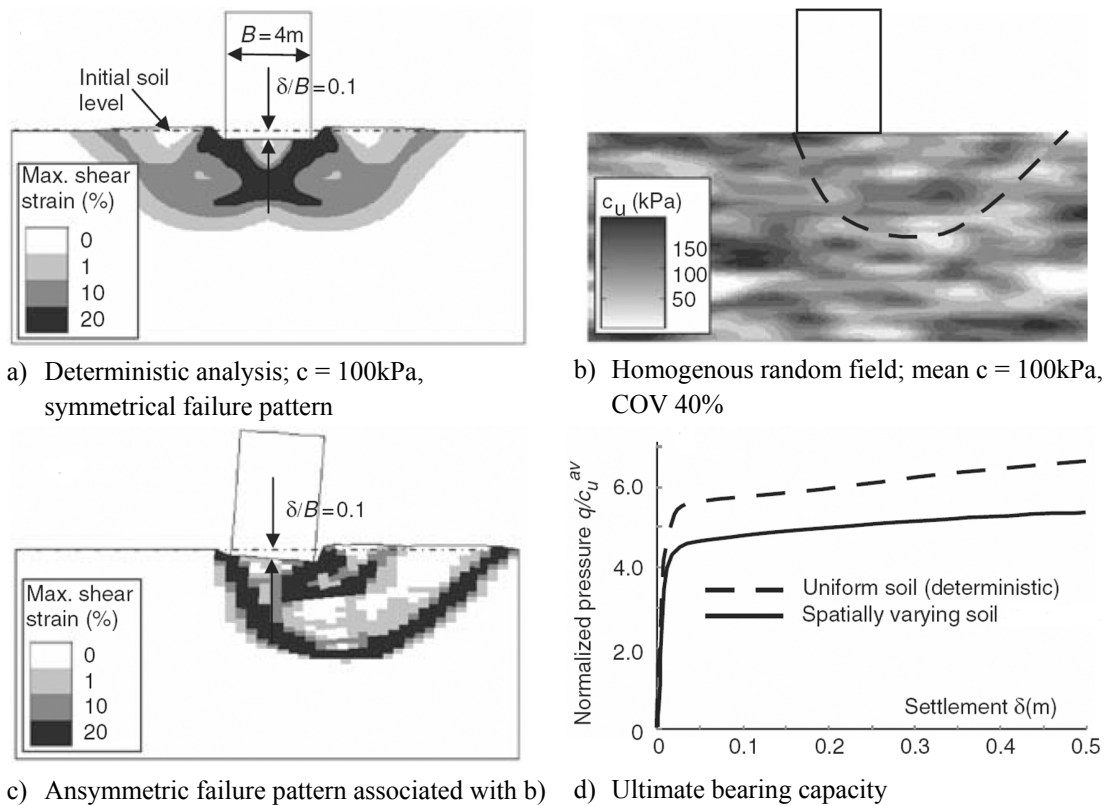


Fig. 6.5 Comparison between finite element computations of bearing capacity for a uniform and heterogeneous soil deposit, adapted from [Popescu et al., 2005]

To achieve reasonably uniform reliability levels in the simple reliability based design, the three ranges of soil property variability are sufficient (Table. 6.3). The ranges of these reported values are wide and are only suggestive of conditions at a specific site.

Table 6.3 The COV of geotechnical parameters, [Phoon et al., 2008]

Geotechnical parameter	Property variability	COV (%)
Undrained shear strength	Low	10-30
	Medium	30-50
	High	50-70
Effective stress friction angle	Low	5-10
	Medium	10-15
	High	15-20
Horizontal stress coefficient	Low	30-50
	Medium	50-70
	High	70-90

Usually in a bridge project documentation the data from only a few boring holes is given, which is generally insufficient for obtaining the reliable soil profile at the scour affected pier. Still, for the preliminary vulnerability analysis the available soil geotechnical properties may be modeled as log-normal, gamma or beta distributed stochastic variables taking into account values from Tables 6.1, 6.2 and 6.3.

6.2.3 The uncertainties related to the bridge structure

The bridge resistance in a scouring event is governed by strength and properties of its elements thus any uncertainty related to them must be properly considered.

According to the [JCSS, 2002], the covariance (COV) for self-weight of concrete bridges may be taken as 0.1 (for the elements cast in-situ) while the COV for additional dead load (e.g. asphalt wearing surface) is 0.25. The information on the preformed remedial works is often not included in the BPM database and this uncertainty can be considerably reduced by reviewing of the available project documentation and/or by surveying of the geometry at the bridge site. The dead load g and the additional dead load Δg may be modeled as stochastic variables with the log-normal probability distributions.

Without the project documentation, there is an unknown level of uncertainty for the reinforcement layout and detailing. When considering the entire population of

bridges from a database, these can be deduced from the design codes and regulations applied in the design phase. At least the minimum amounts of reinforcement should be assumed in bridge elements' sections according to the codes that were valid in the period of the original design. Furthermore, the reinforcement layout in main girder beams should be approximated based on the envelope for bending moments in a simple linear elastic analysis, accounting for self-weight, live load and safety factors as defined in the original design. Here, the half of the maximum bottom reinforcement area in the span may be assumed at the middle supports (common Serbian bridge practice in the past). The actual location of the bar splicing is generally unknown. Since it may affect the optimal position of the hinge in the combined failure modes, it is suggested to be modeled as the uniformly distributed stochastic variable (e.g. $U [3/5, 4/5]$ of a span). Alternatively, the pattern for ultimate moment redistribution as in Fig. 5.2b may be used if there is reliable information on the detailing. In absence of documentation, the plastic strength of a joint at a pier top may be assumed to be equal to the strength of pier's section at the foundation. The latter strength may be calculated based on the braking force, which is common for the aging bridges in the Serbian road network. However, in the light of recent failures (e.g. Figs. 1.15 and 1.17), the assumption of inadequate/minimum reinforcement at pier top should be also considered.

In addition, there is uncertainty related to the inherent material strength and the deterioration of materials over time due to cracking and corrosion. The bridge elements have different rate of deterioration corresponding to their exposure to excess loadings and weather, which may be intensified by the shortcomings in the design and/or inadequate maintenance. These uncertainties differ from case to case and cannot be easily generalized, even if the elements are frequently inspected. The solution for a preliminary vulnerability assessment is to account the observed deteriorated elements, which are reported in a database, in the definition of additional failure mechanisms and scenarios.

Based on the previous discussions, the knowledge on the exact amounts of reinforcement in bridge sections and material properties (concrete plastic strength and steel tensile strength) are desirable. In the analysis example (section 6.4), these parameters (i.e. the bridge elements' plastic strength) and bridge geometry are taken as deterministic values.

6.3 The limit state function

In the up-to-date research and bridge management practice, the limit state function assumed a bridge failure for all scour depths exceeding the foundation depth, which is rather conservative for the vulnerability assessment. The maximum scour depth alone is insufficient for estimation of the valid bounds of the probability of a bridge failure. It is suggested here that the local scour cavity beneath the shallow pier foundation should be taken into account. The limit state function may be defined as:

$$G = R(S_zmax, h_{cov}) - Z_{sc}(t) \quad (6.6)$$

where:

G = limit state function (i.e. margin of safety) [m]

$R(S_zmax, h_{cov})$ = resistance of the adopted soil-bridge model to local scour action at the affected pier [m]

$Z_{sc}(t)$ = time- dependent local scour depth at the affected pier [m]

The value $R(S_zmax, h_{cov})$ is obtained as the sum of the maximum local scour depth beneath the pier foundation level that a soil-bridge model may withstand (S_zmax) and height of the soil cover at the pier h_{cov} (Fig. 6.6). Over the bridge service life, the h_{cov} is affected by general scour. This parameter has to be measured (or monitored) on site or alternatively, in the preliminary analysis, it may be adopted based on the inspection data/project documentation. The ultimate horizontal scour extent beneath the foundation S_cmax depends on the critical combined failure mode of an assumed soil-bridge model, but the connection between the scour depth below the foundation base S_z and related horizontal extent S_c remains unknown (Fig. 6.6). Here, the maximum scour cavities are assumed as discussed in Chapter 5, i.e. the cavity is symmetrical and the slope angles for frictional soils equal the soil internal friction angle, while for the purely cohesive soil they are adopted to be equal 45° .

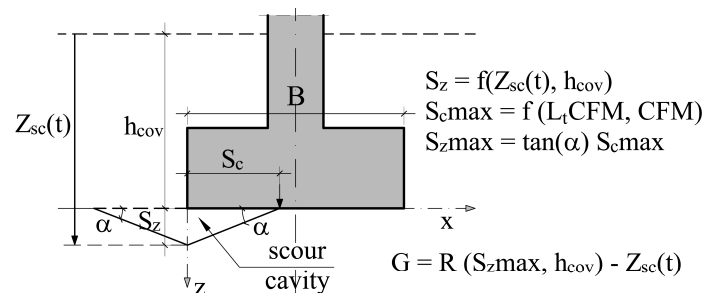


Fig. 6.6 Limit state function for estimation of the probability of bridge failure due to local scour action at shallow foundations

6.4 The probability of bridge failure due to local scour by considering the WSB interaction – An example

In this example, the four-span continuous RC girder bridge (4 x 20m) crossing over the trapezoidal water channel is analyzed (Fig. 6.7a). The local scour action at the **Pier 2** is selected as a possible scenario of a bridge failure in a flooding event. The two cases of pier-foundation system are considered, the one column pier (**case A**) and two-column pier (**case B**) (Fig. 6.7c). Furthermore, the two types of soil are accounted, purely frictional (**sub-cases AI and BI**) and purely cohesive soil (**sub-cases A2 and B2**) for which the erodibility function is assumed (Fig. 6.3). The bridge model **BT 3** (see Table 5.1) is used in the analysis and presented in Fig. 6.7b. The local scour cavities as in Figs. 4.7d and 4.7c are used respectively for the **cases A** and **B**. The most probable scenarios of bridge failure are assumed for the longitudinal and lateral direction for **cases A** and **B** respectively. The longitudinal failure modes were not treated in **case B**, as it is assumed that just one of the columns is severely affected by scour. In **case A**, the three possible failure modes are considered – *CFM 1**, *CFM 3**, *CFM 7**, while in **case B** these are – *L_tCFM 1*, *L_tCFM 2*, *L_tCFM 3**, *L_tCFM 4**. The failure modes in the lateral direction here, in difference to those presented in section 5.7, consider restricted rotation at the adjacent supports (i.e. additional internal work in the superstructure for *L_tCFM 3* and *L_tCFM 4*). The deterministic and stochastic input data used in the analysis are given in the Tables 6.4 and 6.5.

Table 6.4 The deterministic input data used in the analysis (all cases)

Deterministic data *									
Bridge element plastic strength** [kNm]		Pier-Foundation system			Channel geometry		Combined Failure Modes		
Joint at the pier top	$M_{pj}^A =$	1820.1	Pier height [m]	$H_p^A =$	10.0	Bottom width B_{ch} [m]	35.0	CASE A	<i>CFM 1*</i>
	$M_{pj}^B =$	820.1		$H_p^B =$	10.0				
Transverse beam	$M_{pt} =$	421.4	Pier diameter [m]	$D_c^A =$	1.0	Top width T_{ch} [m]	80.0		
	$M_{tp} =$	165.4		$D_c^B =$	0.6				
Girder beam	$0.5M_{ps} =$	702.3	Foundation base [m]	$D_f^A =$	3.5	Height H_{ch} [m]	8.0	CASE B	<i>L_tCFM 2</i>
	$0.5M_{ph} =$	2809.2		$B_f^B/L_f^B =$	3.0 / 3.0				
	$M_{pb} =$	372.2	Alignment to flow	45°		Soil Cover h_{cov} [m]	1.0		
Deck in both directions	$M_{p,xy} =$	19.8	Self-weight [kNm]	$PFg^A =$	824.0			CASE B	<i>L_tCFM 4*</i>
				$PFg^B =$	435.0				

* Data with superscript A or B denote the property associated with the cases A and B

** Main girder geometry given in Table 5.2

Table 6.5 Probability models for the parameters used in the analysis (all cases)

Stochastic parameters	Parameter	Distribution	Mean	COV
<i>Local scour action</i>				
Extreme discharge	Q_{ext} [m ³ /s]	<i>Gumbel</i>	800	0.1
Channel slope	S [m/m]	<i>Normal</i>	0.001	0.1
Manning coeff	n [s/m ^{1/3}]	<i>Log-normal</i>	0.025	0.015
Soil median size diameter	D_{50} [mm]	<i>Log-normal</i>	20	0.1
<i>Soil properties</i>				
internal angle of friction	ϕ [°]	<i>Log-normal</i>	28	0.1
cohesion	c [kPa]	<i>Log-normal</i>	80	0.3
<i>Bridge properties</i>				
Additional dead load	Δg [kN/m ²]	<i>Log-normal</i>	2.00	0.25
Plastic hinge location in span	H_{pos} [m]	<i>Uniform</i>	5.0	0.115

The input for an extreme flooding event is adopted as an impulse hydrograph with an extreme discharge Q_{ext} given by Gumbel extreme distribution (Fig. 6.7d). In general, the duration of the associated flood t_{eq} is also stochastic parameter, which is correlated with the Q_{ext} . Here, it is assumed as the deterministic parameter for which the probability of failure is estimated.

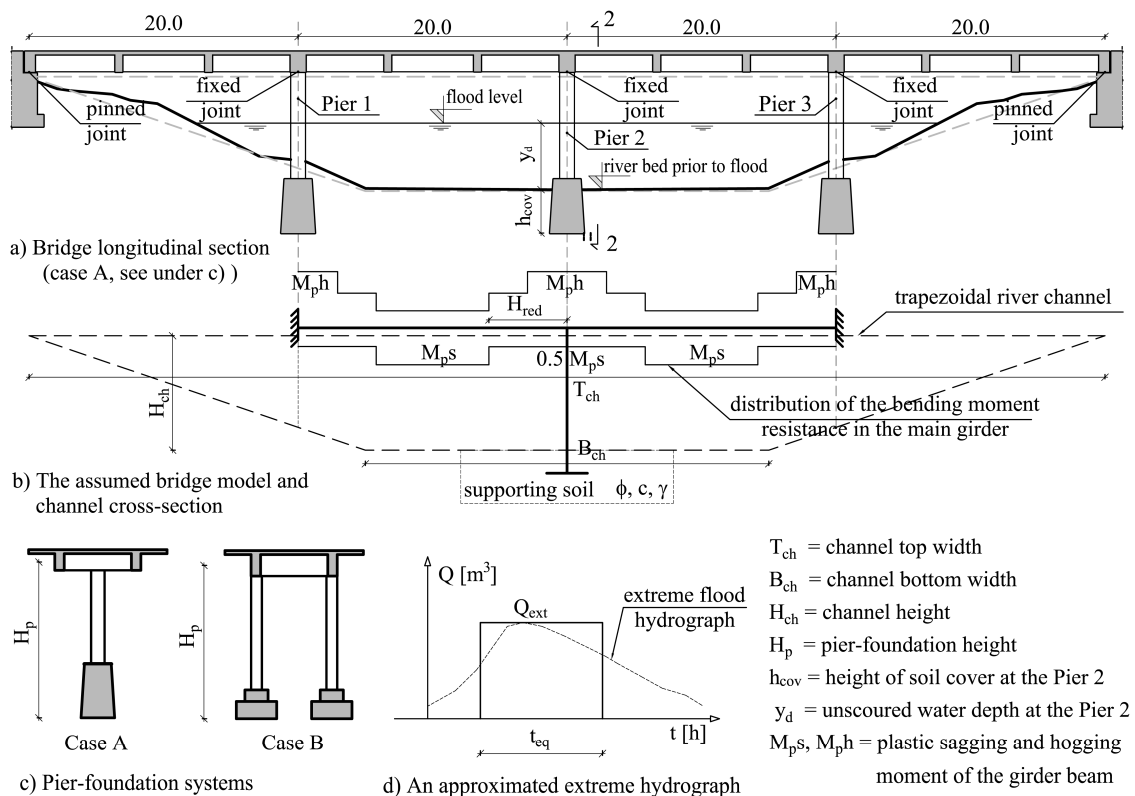


Fig. 6.7 The example of a multiple span continuous girder bridge crossing a trapezoidal water channel

The calculation of the probabilities of failure for the adopted bridge model in the assumed local scour event is performed in a Matlab script. The minimum step for S_c (Fig. 6.6) was adopted to be 0.5 cm for purely cohesive and for purely frictional soil this value was set to D_{50} . The two sets of values for R and Z_{sc} , which define the limit state function (Eq. 6.6), are generated in the QMC based on the input data. The number of simulations per different time duration t_{eq} (3h, 6h, 12h, 24h, 36h, 48h and 60h) of an extreme discharge is set to 10^5 , which was sufficient to achieve accuracy of order 10^{-4} . The probability of bridge failure is calculated using the formula:

$$P_f = \sum_{i=1}^n \frac{1}{n} \frac{n_{G<0}}{n} \quad (6.7)$$

where:

- P_f = probability of the bridge failure in the local scour event
- n = number of simulations in the QMC analysis
- $n_{G<0}$ = number of cases where the limit state function is less than zero i.e. number of cases where the local scour magnitude $Z_{sc}(t)$ exceeds resistance of the soil-bridge model to local scour $R(S_{zmax}, h_{cov})$

Based on the assumed scenarios of failure and fact that the actual correlation between the adopted failure mechanisms is unknown, for each sub-case separately, the simple bounds on the failure probability P_f are estimated by assuming the series system with n elements [Faber, 2007]:

$$\max_{i=1}^n \{P(F_i)\} \leq P_f \leq 1 - \prod_{i=1}^n (1 - P(F_i)) \quad (6.8)$$

where:

- $P(F_i)$ = probability of failure for the failure mode F_i ($i = 1$ to n)
- $\max_{i=1}^n \{P(F_i)\}$ = lower bound corresponds to the case of full correlation
- $1 - \prod_{i=1}^n (1 - P(F_i))$ = upper bound corresponds to the case of zero correlation

The PDF-s (probability density functions) and CDF-s (cumulative distribution functions) of the simulated data for local scour depths are given in Figs. 6.8 to Figs. 6.11. In Figs. 6.12 to 6.15 the simulated data for the resistance of the soil-bridge model are presented.

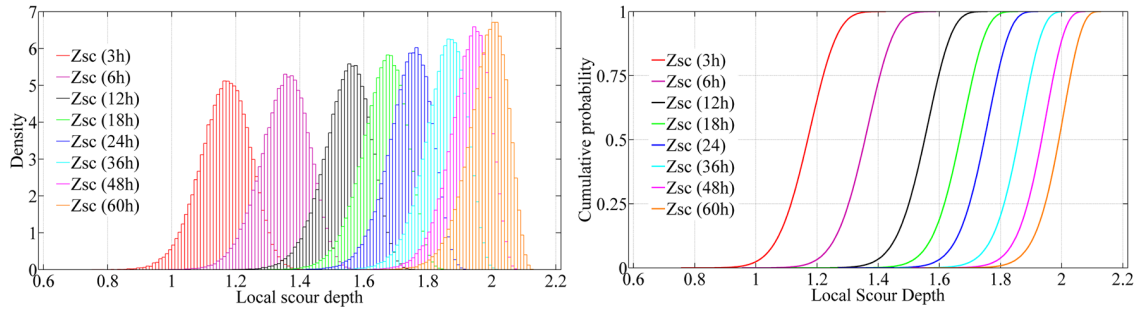


Fig. 6.8 PDF-s and CDF-s of the local scour depths (FDOT) at the Pier 2, sub-case **A1**

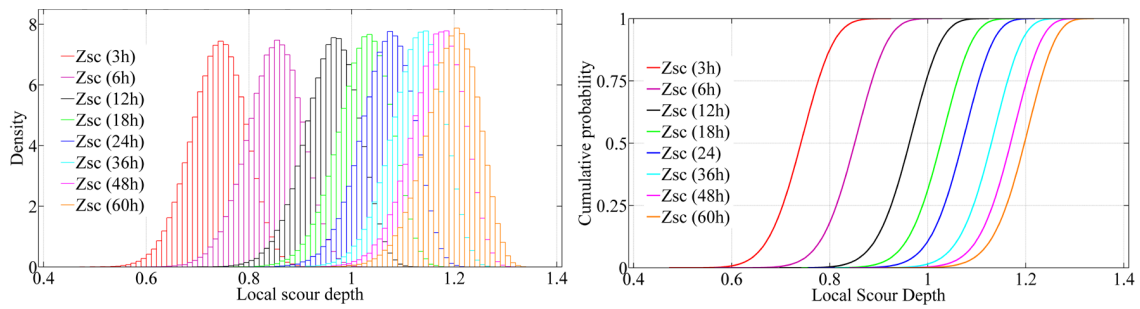


Fig. 6.9 PDF-s and CDF-s of the local scour depths (FDOT) at the Pier 2, sub-case **B1**

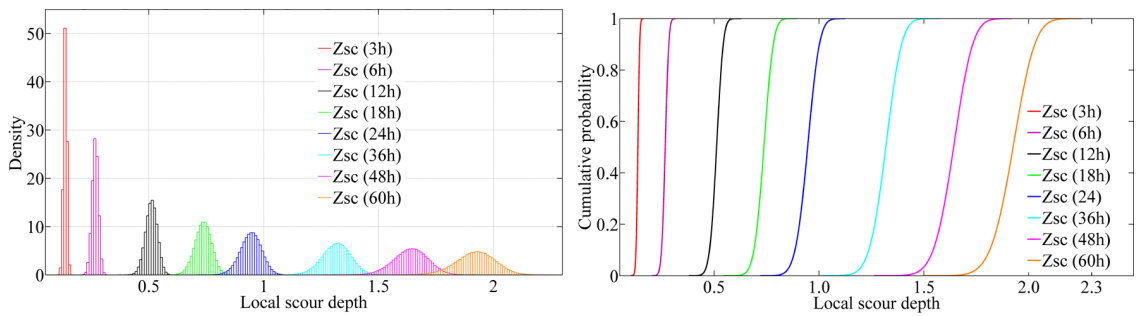


Fig. 6.10 PDF-s and CDF-s of the local scour depths (HEC-18 clay) at the Pier 2, sub-case **A2**

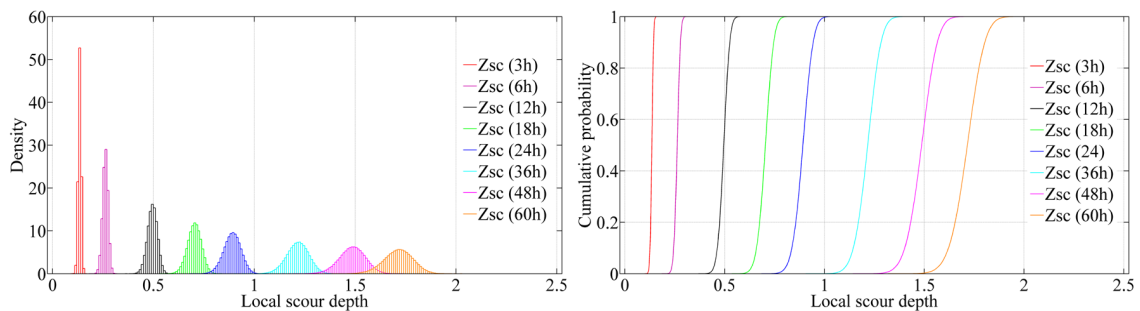


Fig. 6.11 PDF-s and CDF-s of the local scour depths (HEC-18 clay) at the Pier 2, sub-case **B2**

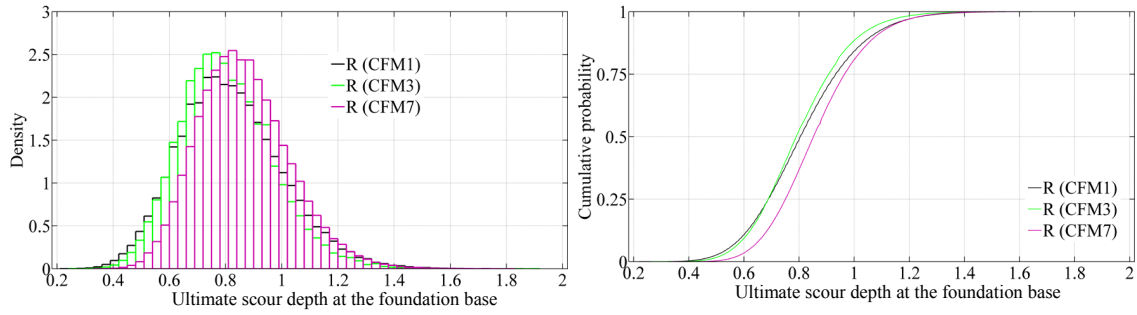


Fig. 6.12 PDF-s and CDF-s of the soil-bridge model resistance at Pier 2, sub-case **A1**

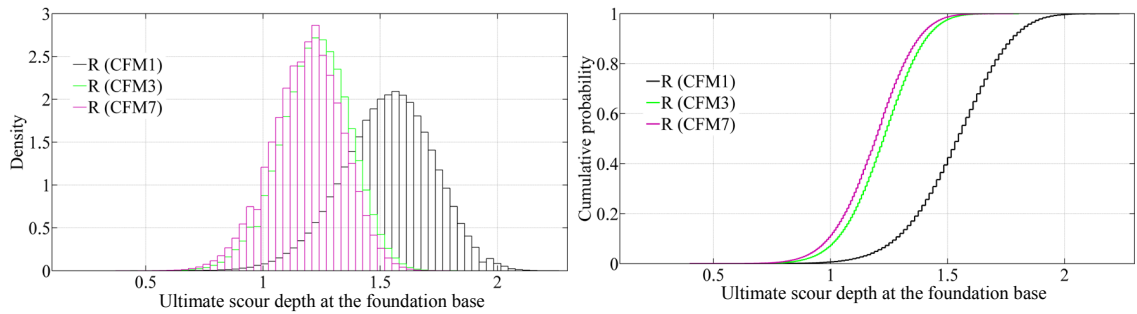


Fig. 6.13 PDF-s and CDF-s of the soil-bridge model resistance at Pier 2, sub-case **A2**

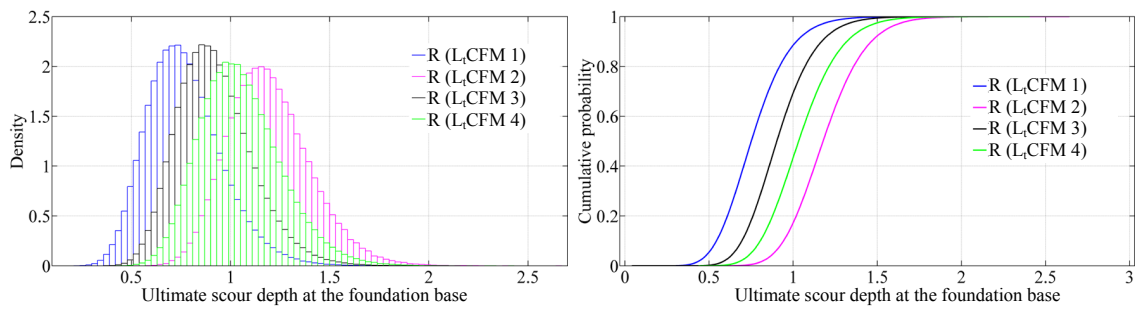


Fig. 6.14 PDF-s and CDF-s of the soil-bridge model resistance at Pier 2, sub-case **B1**

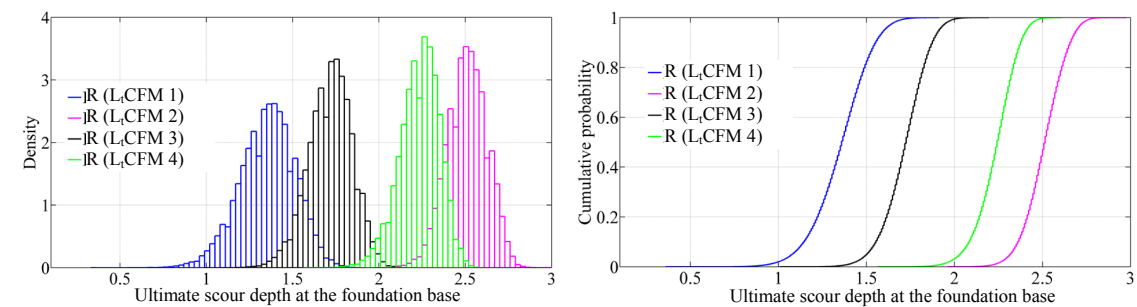
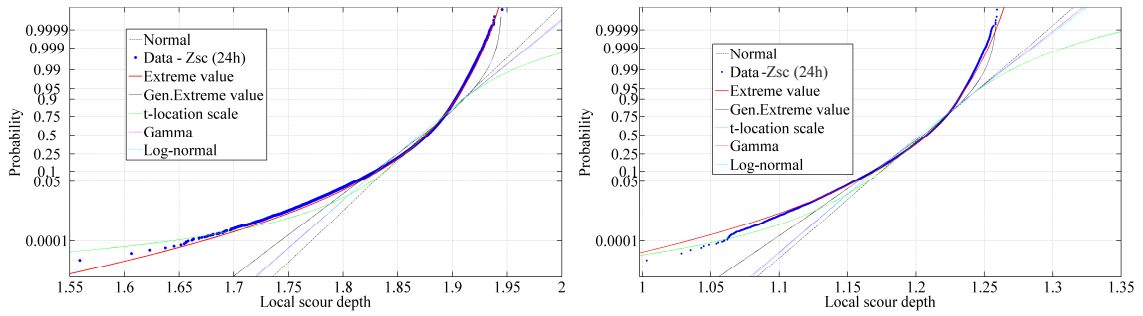
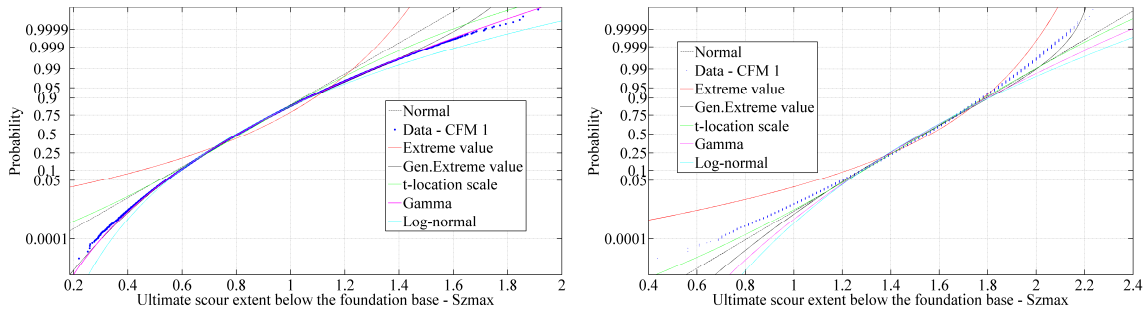


Fig. 6.15 PDF-s and CDF-s of the soil-bridge model resistance at Pier 2, sub-case **B2**

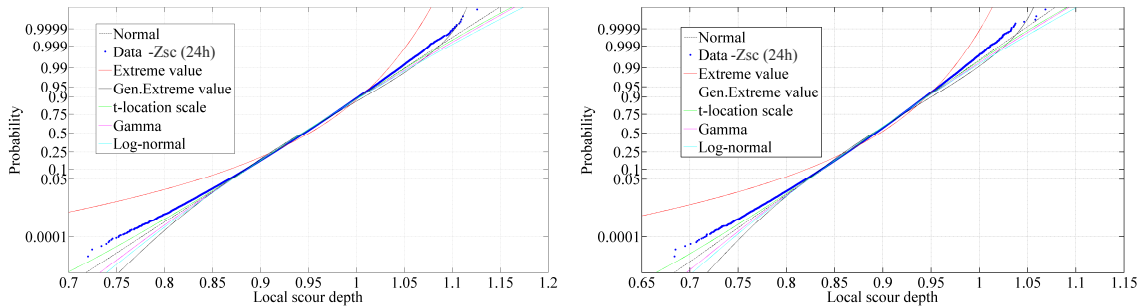
The statistical fitting (maximum likelihood) is performed on the simulated data distributions. As seen from Fig. 6.16, for modeling the local scour depth in frictional soil (sub-cases **A1** and **B1**), the extreme value distribution may be used.



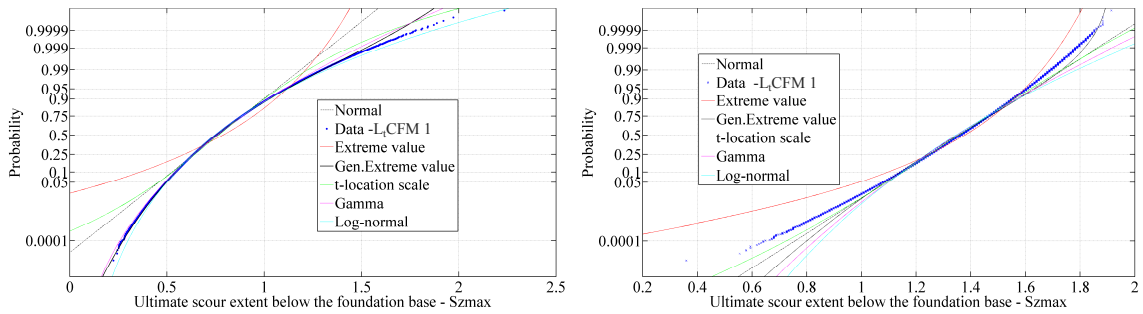
a) Z_{sc} (24h) data fitting, sub-cases A1 (left) and B1 (right), purely frictional soil



b) CFM 1 data fitting, sub-cases A1 (left) and A2 (right) (one column pier)



c) Z_{sc} (24h) data fitting, sub-cases A2(left) and B2 (right), purely cohesive soil



d) L_CFM 1 data fitting, sub-case B1 (left) and B2 (right) (double column pier)

Fig. 6.17 Probability plots - statistical fitting of the generated data

For the resistance of a bridge in longitudinal direction and frictional soil (**sub-case A1**), the generalized extreme value or gamma distribution give good model of the simulated data. Similarity holds for the resistance of the soil-bridge model in lateral direction and frictional soils (**sub-case B1**). The subcases which imply cohesive soil

could not be fitted with standard probabilistic distributions. In general, for all sub-cases, the tails of the simulated data are poorly modeled by standard probabilistic distributions and thus the Generalized Pareto distribution is applied. The probabilities lower than 10^{-8} are neglected.

The results in Tables 6.6 and 6.7 give the variation in the bounds of failure probability as a function of the extreme flood duration. Obviously, the assumption of failure when the local scour reaches the bottom of the shallow foundation gives rather conservative values. In the sub-cases *A1* and *A2* (bridge with one column pier) the larger probabilities of failure are obtained than for the bridge with double column pier due to the fact that it has larger pier diameter (i.e. caisson) thus exposed to larger local scour extents. Also, the difference between failure probabilities for different soil type is obvious (*A1* vs *A2* and *B1* vs *B2*).

Table 6.6 Simple bounds of probability for sub-cases *A1* and *B1* (purely frictional soil)

Flood duration [h]	sub - case A1 / probability of failure					sub - case B1 / probability of failure				
	QMC			Statistical fitting		QMC			Statistical fitting	
	No CFM *	Lower bound	Upper bound	Lower bound	Upper bound	No L _t CFM *	Lower bound	Upper bound	Lower bound	Upper bound
3	0.99999	0.00158	0.00215	0.01159	0.01847	0.00001	0.0	0.0	0.0	0.0
6	1.0	0.04198	0.07999	0.11735	0.24038	0.47086	5.00E-07	5.00E-07	0.0	0.0
12	1.0	0.27083	0.54493	0.36485	0.69253	0.99528	9.58E-06	9.58E-06	2.19E-06	2.19E-06
18	1.0	0.51677	0.84194	0.68642	0.93045	0.99990	9.99E-06	9.99E-06	2.05E-05	2.07E-05
24	1.0	0.67639	0.94615	0.74350	0.97930	1.0	1.00E-05	1.22E-05	1.02E-04	1.71E-04
36	1.0	0.84689	0.99260	0.84442	0.99486	1.0	0.00009	0.00010	2.35E-03	2.66E-03
48	1.0	0.91604	0.99855	0.90309	0.99859	1.0	0.00042	0.00043	0.00765	0.00837
60	1.0	0.94826	0.99962	0.93529	0.99954	1.0	0.00107	0.00108	0.01591	0.01720

* No WSB interaction i.e. bridge failure is assumed for the local scour depth = h_{cov}

Table 6.7 Simple bounds of probability for sub-cases *A2* and *B2* (purely cohesive soil)

Flood duration [h]	sub - case A2 / probability of failure					sub - case B2 / probability of failure				
	QMC			Statistical fitting		QMC			Statistical fitting	
	No CFM *	Lower bound	Upper bound	Lower bound	Upper bound	No L _t CFM *	Lower bound	Upper bound	Lower bound	Upper bound
3	0.0	0.0	0.0	0.0	0.0	0.0	0.0	0.0	0.0	0.0
6	0.0	0.0	0.0	0.0	0.0	0.0	0.0	0.0	0.0	0.0
12	0.0	0.0	0.0	0.0	0.0	0.0	0.0	0.0	0.0	0.0
18	0.0	0.0	0.0	0.0	0.0	0.0	0.0	0.0	0.0	0.0
24	0.1072	0.0	0.0	0.0	0.0	0.00263	0.0	0.0	0.0	0.0
36	1.0	1.15E-06	1.35E-06	6.12E-08	6.86E-08	0.99979	2.25E-08	2.25E-08	0.0	0.0
48	1.0	0.00107	0.00168	0.00547	0.00795	1.0	1.30E-05	1.30E-05	0.00145	0.00145
60	1.0	0.06529	0.10872	0.24966	0.39862	1.0	0.00052	0.00052	0.04574	0.04574

* No WSB interaction i.e. bridge failure is assumed for the local scour depth = h_{cov}

6.5 Review of the governing parameters in the procedure for estimation of the probability of a bridge failure due to local scour action

The current bridge management practices do not account the resistances of supporting soil and bridge structure in a flooding event. The presented procedure in Chapter 5 revealed the combined failure modes, which now allow more realistic vulnerability assessments of bridges with regard to this hazard. The goal in the presented work is definition of the minimum set of governing parameters to account in the WSB interaction. They comprise the three sets of input data and their interdependencies are presented in Fig. 6.16:

- Local scour action
 - Extreme flood hydrograph - Q_{ext} , t_{eq}
 - Channel geometry and properties – slope S , Manning coeff. n
- Soil resistance
 - Type, weight, median soil diameter D_{50} ,
 - Height of soil cover at the pier foundation h_{cov}
 - Erodibility
 - Undrained shear strength i.e. cohesion c
 - Internal friction angle ϕ
- Bridge resistance
 - Main girder type and distribution of plastic bending moment resistance
 - Types of the joint at the pier top and adjacent supports, and their plastic strength to bending and shear
 - Pier-foundation type, geometry and alignment to the flow

Besides hydraulics and geometry of a river channel, the local scour action at bridge piers is directly affected by soil properties, geometry of a pier foundation system and its alignment to the flow as well as with the height of soil cover at the pier. Actually, the soil displays two different types of resistances in a local scouring event. The first is given by yet unclear soil property – the erodibility, which governs the rate and possible extent of local scour action. The second is given by geotechnical properties, which in conjunction with bridge structure properties govern the behavior of a soil-bridge system to the local scour cavity growth at a foundation.

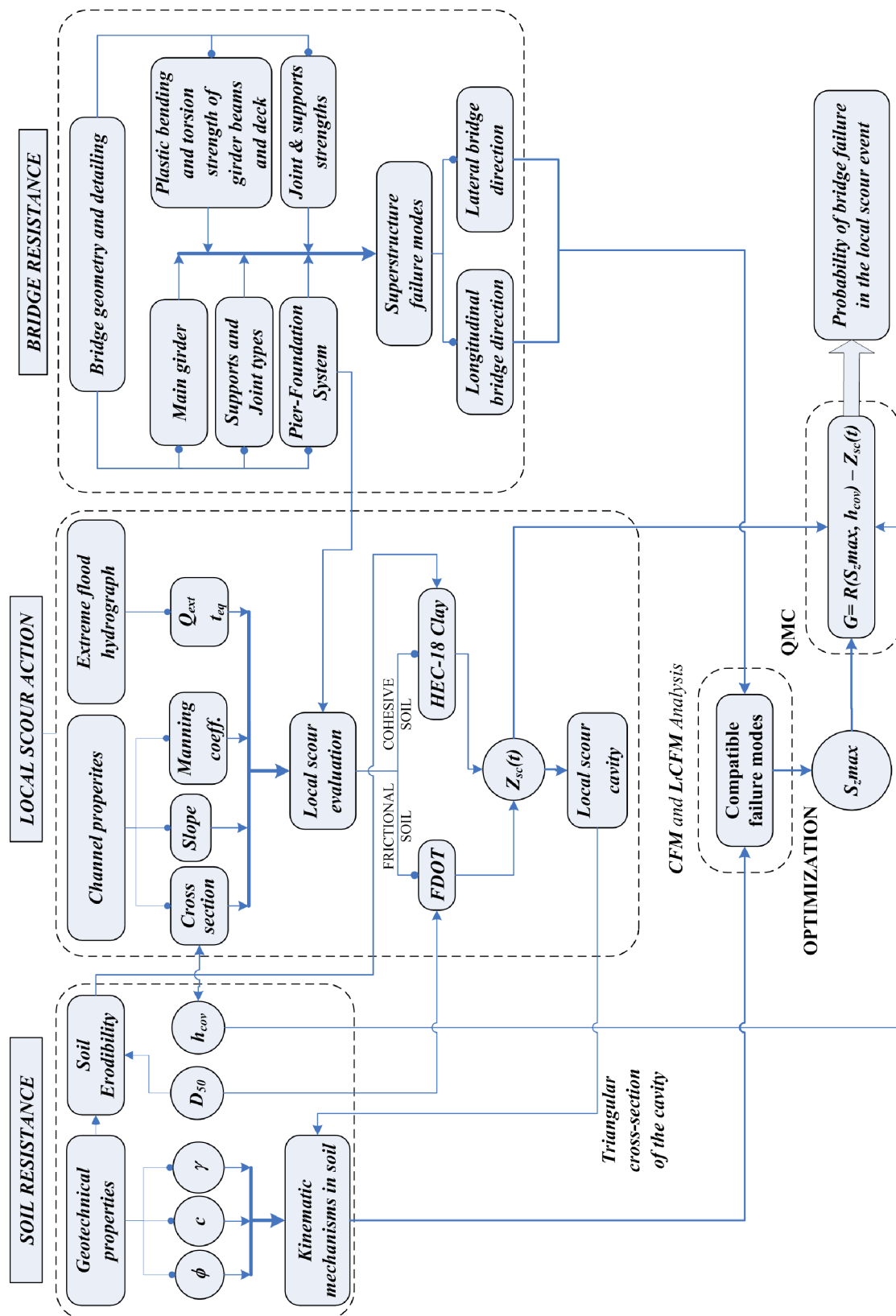


Fig. 6.16 WSB interaction in evaluation of the probability of a bridge failure in a scouring event and interdependencies of the governing parameters

6.6 Application of the presented methodology for quantitative vulnerability assessment

The essential step for completing the vulnerability assessment is estimation of the failure related consequences. The direct consequences comprise costs of repairs or bridge replacement and insurance claims, which may be reliably estimated based on the known bridge failure modes. The time necessary for returning a bridge in a pre-failure state governs the indirect costs. These are cumulative and dependant from a road network topology, affected road links' capacities and the related traffic flow redistribution. Here, the main contribution to the amount of consequences stems from additional travel time/distance and accident costs [Erath et al., 2011]. Generally, the most accurate analysis of the indirect costs for a selected road network is obtained when the monitored traffic volumes are assigned to current transport supply in a traffic simulation model. This well-established methodology of a cost-benefit analysis, which quantifies changes in traffic flows into monetary units, has been given for the entire road network in Switzerland. In Fig. 6.17, the line widths represent the expenditures per hour owing to a severance of a road link.

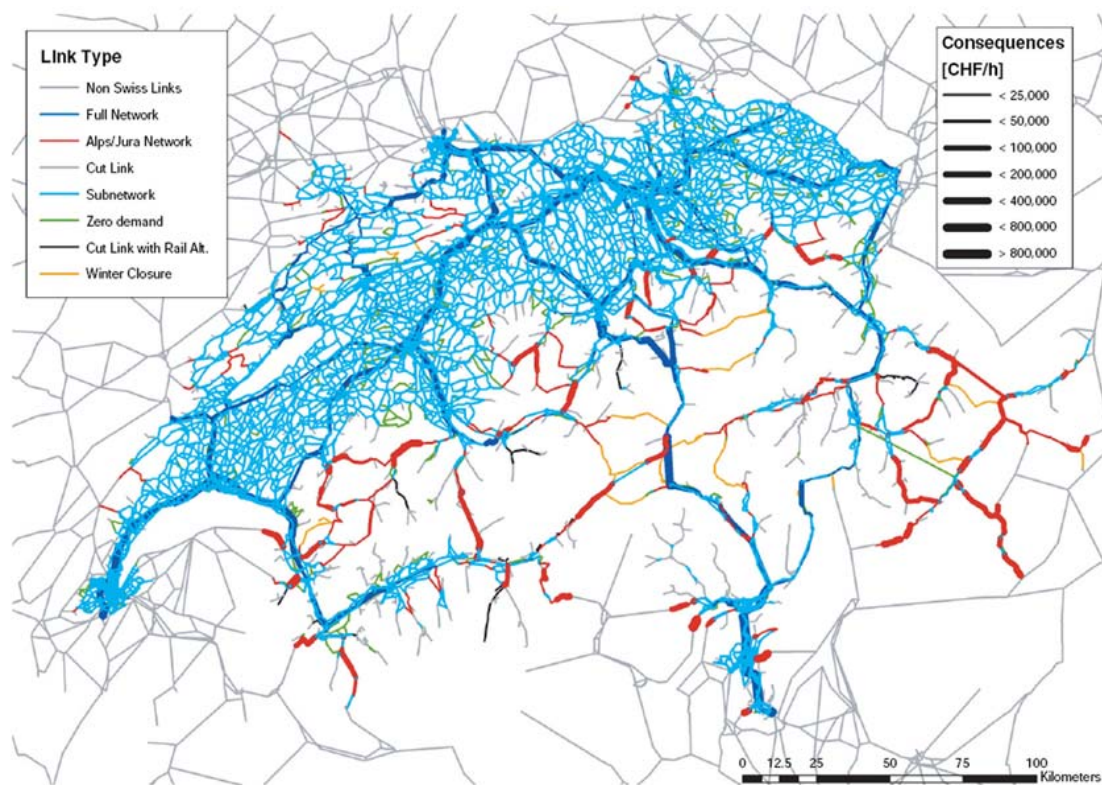


Fig. 6.17 Indirect failure consequences based on the Swiss National Transport Model [Erath et al., 2011]

A similar analysis has been performed in the example of the sub-network which is located around the future expressway in southern Serbia [Tanasic et al., 2013]. Here, the link severance scenarios are considered as full or partial closure of the road links on the four analyzed bridges due to structural damage inflicted by local scour. The outcome of the preformed traffic simulation gives the most vulnerable road links related to a bridge closure in the case of a 200-year flooding event (Fig. 6.18).

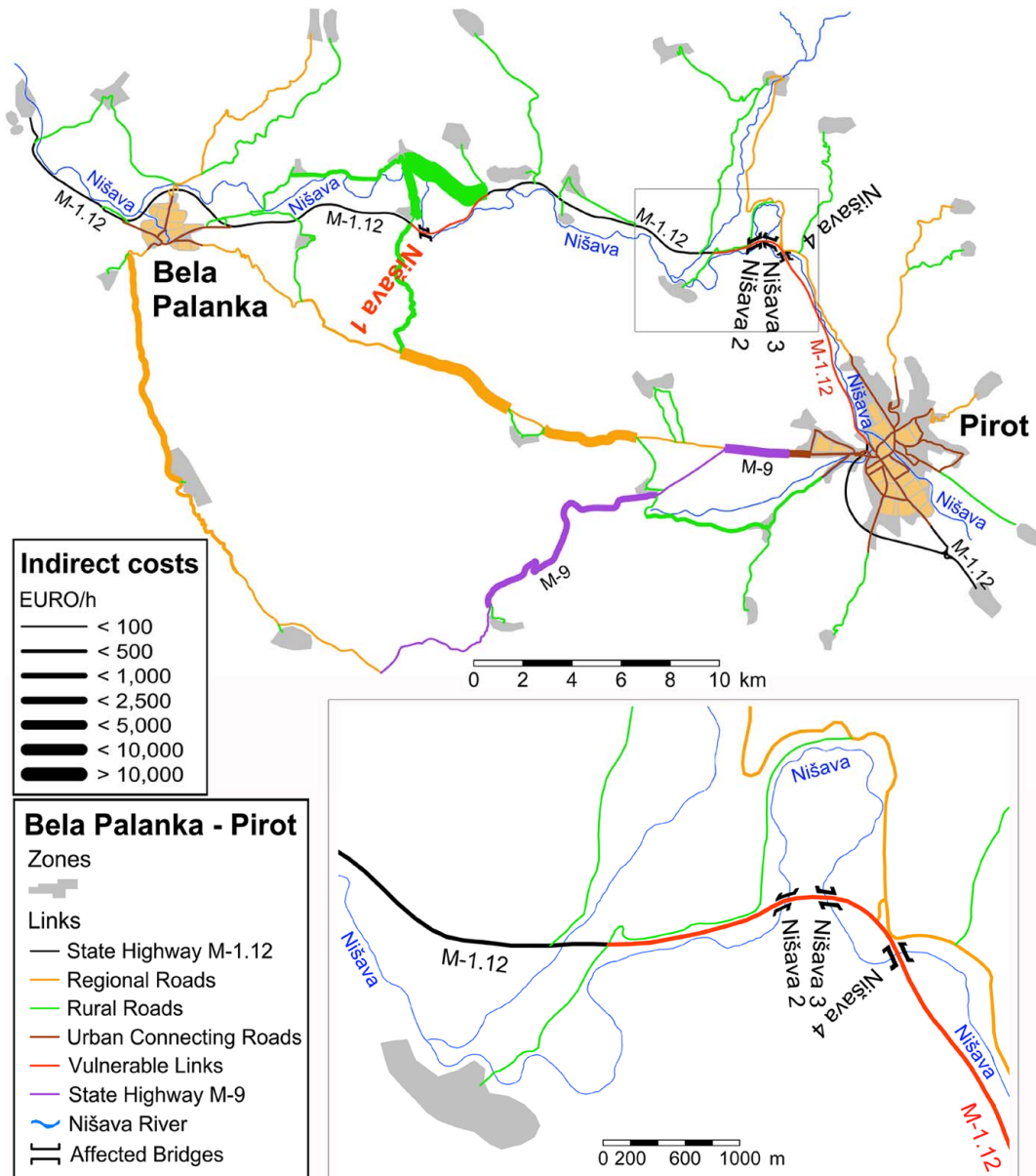
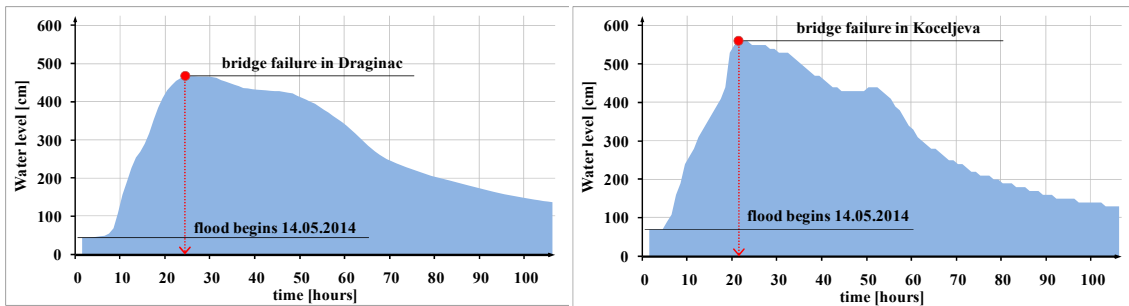


Fig. 6.18 Indirect failure consequences of closing the bridge Nišava 1, [Tanasic et al., 2013]

The latter analysis is a basis for development of the vulnerability maps for Serbian road network in respect to a flooding hazard. The vulnerability maps would

give insight into direct and indirect consequences of a bridge or bridges' failures due to future oncoming flooding events of certain magnitudes. These are going to be especially useful in prioritizing of bridges and funding allocation in bridge management, as well as for emergency planning. In order to develop and use such maps, the traffic counting data for the entire road network should be obtained. The preliminary screening for scour affected bridges should be performed based on the current entries in the BPM, and their project documentation should be reviewed. For the evaluation of the local scour action at the affected bridges extreme flood hydrographs are necessary. When the possible scenarios of the bridges' failures are outlined, the probabilities of failure may be evaluated with the approach presented herein, followed by the consequences analysis.

The hindsight of the flood in Serbia in May 2014 is going to be practically useful both for data collection and processing. In Fig. 6.19, the measured water levels near two bridge sites are presented. The bridge failures at these locations have occurred approximately 18 hours after the beginning of the flood.



a) Bridge failure in Draginac, see Fig. 1.19

b) Bridge failure in Koceljeva, see Fig. 1.20

Fig. 6.19 Measured water levels at rivers Jadar (left) and Tamnava (right), during 4 days of flood, unofficial data from RHMS (Republic Hydrometeorological Service of Serbia)

Chapter 7. Conclusion

7.1 The summary of the realized work

Extreme floods coupled with inadequate maintenance of rivers and bridges still inflict damage to transportation infrastructure all over the world affecting the society in general. The local scour in flooding events represents the main threat to bridges and current procedures in bridge management do not give satisfactory results in planning and scheduling the appropriate risk reducing interventions. The comprehensive quantitative approach for vulnerability assessment of bridges exposed to local scour is deemed necessary and a novel multidisciplinary methodology is suggested in this thesis. The estimation of the probability of bridge failure due to local scour is elaborated as the essential ingredient in this methodology. The consequences associated to failures are beyond the scope of the thesis, and they are briefly discussed.

The presented research is focused on the development of an approach for vulnerability assessment, which targets the largest group of scour critical bridges in Serbian road network. It was essential to define a typical bridge model affected by local scour action and develop a framework with a modest data set for its simple yet accurate analysis. The scope of the research is therefore based on the short to medium multiple span RC girder bridges with shallow foundations. The bridge types considered in the analysis have double-tee main girder combined with the most common type of pier-foundation systems on different types of soil. The bridge geometry, elements' properties, supports and reinforcement layouts are adopted based on the review of the available project documentation of several typical scour affected bridges (Chapter 4).

The water-soil-bridge (WSB) interaction is suggested as the general approach to identify and analyze possible failure modes of the model and consequently obtain the probability of bridge failure in a scouring event (Chapter 2). The first task in the WSB interaction is approximating of the local scour action at bridge piers. The current scour evaluation methods, which completely rely on the empirical formulas, were reviewed without questioning their accuracy and precision within this thesis (Chapter 3). Accounting for river hydraulic properties, soil type and pier geometry, the choice of appropriate local scour formulas for vulnerability analysis is discussed, giving the advantage to those that may consider the temporal aspect of scour. It was necessary to

relate the time-dependent local scour depth, obtained by the formulas, to the ultimate extent of the scour beneath the shallow foundation base, which was not topic of the past research. This relationship is considered essential in the vulnerability analysis as it provides insight of the threat to bridge and public from future oncoming floods. Here, the assumed scour cavities under the foundation base of different pier-foundation types have form of oblique cone with closed-curve basis. The triangular cross-section of these cavities is adopted due to simplicity and the local scour action at bridge piers is simplified to a plane strain problem. The local scour at bridge abutments and scenarios of their failures are beyond the scope of the thesis.

For the second task of the WSB interaction, the investigation of the combined response of a bridge structure and supporting soil to approximated scour cavities is necessary. The perfectly rigid plastic behavior of the soil and bridge elements is assumed to apply the upper bound theorem of the theory of plasticity. The elastic deformations prior to failure were regarded as relatively unimportant. The resistance of supporting soil to local scour cavity growth at a pier foundation is considered on plane strain kinematic mechanisms governed by principal soil geotechnical properties – internal friction angle, cohesion and soil weight. Here, the basic 2D mechanisms, which consider sinking, translation and rotation of a pier-foundation system, are applied. The estimation of the resistances of bridge structural elements is required to evaluate the internal work in the failure mode. In the model, all joints and supports are assumed as: free, pinned or fixed. The plastic strengths of the double-tee main girder and monolithic joint at the pier top are accounted based on the given reinforcement layouts and detailing. The shear failure of model elements was not treated within the thesis.

Based on the given assumptions and approximations, the two-span soil-bridge model is presented in Chapter 5 and its response to the assumed local scour action is investigated separately for the longitudinal and lateral directions. It was essential to define a compatible mechanism i.e. a combined failure mode of the supporting soil and bridge structure. The center of a pier foundation is adopted as the connection between the assumed kinematic mechanisms in soil and bridge structure. This assumption in fact leads to a slight decrease of an actual upper bound solution, which is acceptable at this moment as currently there are no lower bound solutions.

The optimization procedure was required for an estimation of the ultimate horizontal local scour extent beneath a foundation. It is here based on the principle of virtual work, parameters of the adopted kinematic mechanism in soil, superstructure parameters and scour cavity growth. The combined soil-bridge failure modes in the longitudinal direction (*CFM-s*) are investigated for four bridge types by considering simple kinematic and geometrical constraints. For determining the combined failure modes in the lateral bridge direction (*L_rCFM-s*), a bridge with double column pier is investigated. Here, two possible patterns of superstructure failure were reviewed in combination with pier frame failure modes. In the elaborated combined failure modes the pier-foundation system was considered as a rigid body i.e. the local failures were not treated.

The analyses' results revealed that the combined failure modes based on the sinking and translational mechanisms in soil are less sensitive to the local scour action than the rotational mechanisms regardless of the soil type and applied safety factors in bearing capacity design. It is observed that the main resistance of bridge structure to local scour action is given by the restraints of a pier-foundation system displacement. In the bridge longitudinal direction, the soil properties are mainly governing the failure modes, whereas for the lateral direction the properties of the elements that comprise the bridge superstructure are significantly affecting the results. The exact amounts of built-in reinforcement are not crucial for the analysis, but the soil properties are. Nevertheless, the plastic strengths of the main girder sections do affect the ultimate extents of scour, and in the absence of project documentation, it is sufficient to perform a simple linear elastic analysis and assume the minimum reinforcement ratios given by the original design code. The list of possible combined failure modes is not definite as only the basic types of kinematic mechanism in soil are considered, but it represents the basis for further research and comparison to future upper and lower bound solutions.

The three sets of input data are necessary for the probability calculation and they comprise variables for local scour evaluation, soil strength parameters and bridge elements' properties. The uncertainties related to this data have been discussed based on the state-of-the-art documents. The limit state function used for the calculation of probability of failure is comprised from two variables - the time-dependant local scour depth at the affected pier and the ultimate scour extent at a shallow foundation

representing the resistance of an adopted soil-bridge model. The Quasi Monte Carlo simulation is used for the analysis due to faster convergence of the solution than the crude Monte Carlo. The example of a four span continuous bridge is given to present the viability of the assumed soil-bridge model in calculation of the probability of failure.

The suggested WSB interaction represents a straightforward approach for the estimation of the probability of a bridge failure due to local scour. Although the obtained results are by default the upper bound estimates, the clear insight of the resistances of supporting soil and bridge structure to local scour action are presented, which was not clarified up to date. The obtained solutions are yet to be verified by lower bound methods, which will bracket the correct solution. Nevertheless, the presented approach is the basis of the methodology for quantitative vulnerability assessment, which will identify the vulnerable bridges in a road network to be examined in more detail. The ultimate goal of the methodology is update of the existing bridge databases and integration into future Bridge Management Systems.

The necessary input data for the vulnerability assessment are mostly in the BPM database. The rest can be collected during regular inspections and/or estimated based on the available project documentation and monitoring. The following information should be added/updated in the BPM:

- The geometry and quantitative properties of bridge elements (main girder, pier/foundation system, joints, bearings, reinforcement layout and detailing)
- Soil properties at substructures (type, results of geotechnical testing, soil cover at piers and erodibility if possible)
- Extreme flood hydrographs for rivers at bridge sites (extreme discharge and related flood duration)
- Traffic data/studies for the road network

7.2 Potential for further research

The current BMS do not consider the real-time risk of natural hazards, thus the presented methodology is a step forward towards a comprehensive decision-making tool for bridge management. The future development of the suggested approach is justified and the several enhancements that may be readily included are discussed.

The presented soil-bridge model may be easily upgraded to account different geometry of bridge elements, include additional parameters, kinematic mechanisms and combined failure modes. Here, the scope of the future work will be mainly focused on the various types of bridge superstructure and alternate kinematic mechanisms in soil, which may provide better upper bound solutions. The assumption of rigid body behavior of a pier-foundation system may be violated in some cases and will be investigated further for the common solutions of reinforcement detailing. The severe deterioration in strength of bridge elements (e.g. due to fatigue, corrosion or chloride attack) or defects in the design are not discussed in the analysis, but may be considered by applying plastic hinges in critical sections thus yielding additional combined mechanisms. The force redistribution between bridge elements due to scour cavity at a bridge pier may cause bearings/supports to suffer damage, which subsequently affects the realized failure mode. The ultimate capacity of deteriorated bridge bearings is a topic that still waits to be investigated in detail.

The idea given in [Michailowski, 1997], which entails multiple block kinematic mechanisms in soil, would certainly resolve the issue of kinematic admissibility of velocity fields without losing the accuracy. In addition, 3D kinematic soil mechanisms may be applied to improve here obtained solutions. This would be especially important when accounting the local scour cavities at strip foundations and spread footings where the bridge resistance in both longitudinal and lateral directions must be considered. In addition, a general case of multilayered, spatially variable soil should be included in the further research as it would affect the form and growth of local scour cavity in time, as well as the critical kinematic mechanism in soil.

Besides bridge piers, bridge abutments are commonly endangered by local scour. The formulas for evaluation of the maximum scour depths at abutments exist and can be applied in the existing soil-bridge model. This will allow a more accurate estimation of the probability of a bridge failure in the scouring event as different scenarios could be accounted. The temporal aspect of scour is essential in the vulnerability analysis, but it was not among prime objectives in the research of local scour in the past. The actual form of scour cavity and its growth under the base of a shallow foundation in time, wait to be revealed. The duration of the highest flow and shape of flood hydrograph for the particular location is especially important when

analyzing the effect of multiple flood events on the height of soil cover at the pier (h_{cov}). For this case, the approach given in [Briaud et al., 2009] may be considered. The procedure for evaluation of the maximum local scour depth in eroded rock exist [Arneson et al., 2012], and the vulnerability assessments would certainly benefit if it includes the temporal aspect of scour in the future research.

The extent of local scour cavity at shallow foundations when debris is present, for different pier types and bridge openings, is yet another research topic. The local scour formulas to account debris at piers exist, but they do not allow time evaluation of scour. The adverse effect of the horizontal forces exerted by flowing water and floating debris are not considered in the thesis, but may be easily added as horizontal force acting at an affected pier.

The flooding event in Serbia in May 2014 is a tragic reminder of a future threat to transportation networks in the world, but it also emphasizes the importance for the vulnerability assessments of the aging transportation infrastructure in respect to this hazard. The failure modes of the bridges in this event justify the suggested combined failure modes both for longitudinal and lateral direction, which can be seen in Figs. 1.18 and 1.19 / Figs. 1.15 and 1.20, respectively. The collection of the essential data for analysis of the damaged bridges in Serbia is currently underway, and the case studies, which will entail the approach presented in this thesis, are going to be subject of the future research.

References

- [Agrawal et al., 2007] Agrawal A.K., Khan M.A. and Yi Z. Handbook of Scour Countermeasures Designs. Report FHWA-NJ-2005-027, University Transportation Research Center, the City College of New York, Dec. 2007. <http://www.state.nj.us/transportation/refdata/research/reports/FHWA-NJ-2005-027.pdf>
- [Alipour et al., 2013] Alipour A., Shafei B. and Shinozuka M. Reliability-Based Calibration of Load and Resistance Factors for Design of RC Bridges under multiple Extreme Events: Scour and Earthquake. In Journal of Bridge Engineering, Vol. 18(5), pp. 362-371, May 2013.
- [Apaydin, 2010] Apaydin M. MSc Thesis: A study on risk assessment of scour vulnerable bridges, Middle East Technical University, Ankara, Turkey, 2010.
- [Arneson et al., 2012] Arneson L.A., Zevenbergen L.W., Lagasse P.F., and Clopper P.E. Evaluation Scour at Bridges, Fifth Edition, Federal Highway Administration, Report FHWA-HIF-12-003, Hydraulic Engineering Circular No. 18, U.S. Department of Transportation, Washington, D.C. <http://www.fhwa.dot.gov/engineering/hydraulics/pubs/hif12003.pdf>
- [Barnard et al, 2010] Barnard T., Hovell C.G., Sutton J.P., Mouras J.M., Neuman B.J., Samaras V.A., Kim J., Williamson E.B. and Frank K.H. Modeling the Response of Fracture Critical Steel Box-Girder Bridges. CTR Technical Report 9-548-1, Texas Department of Transportation, Austin, 2010. www.utexas.edu/research/ctr/pdf_reports/9_5498_1.pdf.
- [Bebić, 1998] Bebić D. (in Serbian) Osnove inženjersko-tehničkog rešenja, knjiga 1 - Tehničko rešenje baze podataka o mostovima. Institut za puteve, Beograd, 1998.
- [Bebić, 2006] Bebić D. (in Serbian) Analiza ukupnih momenata savijanja od pokretnog opterećenja u glavnim nosačima mostova na putevima. Put i saobraćaj Vol.53 (3), pp. 18-26, 2006.
- [Benn, 2013] Benn, J. Railway bridge failure during flooding in the UK and Ireland. Proceedings of the ICE - Forensic Engineering, Vol. 166(4), pp 163 –170, 2013.
- [Birdsall, 2009] Birdsall J. PhD. Thesis number 4251: The Responsive Approach: an Integrated Socially-Sustainable Technically-Optimal Decision Model. Swiss Federal Institute of Technology, Lausanne, Switzerland, 2009.

- [Bolduc et al., 2008] Bolduc L.C., Gardoni P. and Briaud J.-L. Probability of Exceedance Estimates for Scour Depth around Bridge Piers. *Journal of Geotechnical and Geoenvironmental Engineering*, Vol. 134, No. 2, ASCE, Reston, Virginia, USA. pp. 175-184, 2008.
- [Bransby and Randolph, 1997] Bransby M. F. and Randolph M. F. Shallow foundations subject to combined loadings. In *IACMAG '97: 9th Int. Conf. of the International Association for Computer Methods and Advances in Geomechanics*, Wuhan, China, 27 November 1997, Vol. 3, pp. 1947-1952. The Netherlands: Balkema.
- [Briaud et al., 2003] Briaud J. L., Chen H.C., Li Y., Nurtjahyo P. and Wang J. NCHRP Report 24-15: Complex pier scour and contraction scour in cohesive soils. Transportation Research Board of the National Academies, Washington D.C., 2003. ceprofs.civil.tamu.edu/briaud/SRICOS-EFA/NCHRP_24-15%20as%20printed.pdf
- [Briaud, 2006] Briaud J.-L. Bridge Scour, *Geotechnical News*, Vol. 24(3), September 2006, BiTech Publishers Ltd, 2006.
- [Briaud et al., 2009] Briaud J. L., Govindasamy A. V., Kim D., Gardoni P., Olivera F., Chen H.C., Mathewson C. and Elsbur, K. Report 0-5505-1: Simplified method for estimating scour at bridges, Texas Department of Transportation, Austin, 2009.
- [Briaud et al., 2010] Briaud J. L., Hurlebaus S., Chang K.A., Yao C., Sharma H., Yu O.Y., Darby C., Hunt B. E. and Price G.R. Report 0-6060-1: Realtime monitoring of bridge scour using remote Monitoring technology, Texas Department of Transportation, Austin, 2010. <http://tti.tamu.edu/documents/0-6060-1.pdf>
- [Briaud et al., 2011] Briaud J.L., H.C. Chen K.A. Chang S.J. Oh, S. Chen, J. Wang, Y. Li, K. Kwak, P. Nartjaho, R. Gudaralli, W. Wei, S. Pergu, Y.W. Cao, and F. Ting, Summary Report: The Sricos – EFA Method. Texas A&M University, 2011. ceprofs.civil.tamu.edu/briaud/SRICOS-EFA/Summary%20of%20SRICOS-EFA%20Method.pdf.
- [Bridge over Nišava II -reconstruction, 2010] (in Serbian) Projekat rekonstrukcije mosta preko reke Nišave – Nišava II, deonica 5A: Staničenje - Pirot. Zavod za projektovanje mostova i konstrukcija. Institut za puteve A.D. Beograd, Srbija, 2010.
- [Bridge over Crni Timok, 1968] (in Serbian) Most preko Crnog Timoka na km. 70+467 puta Paraćin-Zaječar. Preduzeće za puteve -Zaječar, Zaječar, Serbia, 1968.
- [Chen, 1975] Chen W.F. Limit analysis and soil plasticity, Amsterdam, Elsevier, 1975.

- [Coleman and Melville, 2001] Coleman S.E. and Melville B. W. Case study: New Zealand Bridge Scour Experiences. *Journal of Hydraulic engineering*, 2001.
- [Donnée, 2008] Donnée N.E. PhD Thesis: Automated screening tool for stability of highway bridges subject to scour. Auburn University, Alabama, USA, 2008.
- [Erath et al., 2011] Erath A., Birdsall J., Axhausen K. W. and R. Hajdin. Vulnerability Assessment Methodology for Swiss Road Network. In *Transportation Research Record: Journal of the Transportation Research Board*, No. 2137, Transportation Research Board of the National Academies, Washington, D.C., 2009, pp. 118-126.
- [Ettema et al., 2011] Ettema R., Constantinescu G., Melville B. Evaluation of Bridge Scour Research: Pier Scour Processes and Predictions. NCHRP Web-Only Document no.175, Transportation Research Board of the National Academies, Washington, D.C., 2011.
http://onlinepubs.trb.org/onlinepubs/nchrp/nchrp_w175.pdf
- [Faber, 2007] Faber M.H. Lecture Notes on Risk and Safety in Civil Engineering. Swiss Federal Institute of Technology Zurich, 2007.
- [FDOT, 2010] Florida Department of Transportation Bridge Scour Manual. Tallahassee, Florida, USA, 2010. www.oea-inc.com/FDOTScourManual_March2010.pdf.
- [FEMA, 2007] FEMA. HAZUS-MH MR3 - Multi-Hazard Loss Estimation Methodology - Flood Model - Technical Manual. Federal Emergency Management Agency, Washington D.C., 2007.
- [Figueiredo et al., 2013] Figueiredo E., Moldovan I. and Marques M.B. Condition Assessment of Bridges: Past, Present and Future, a Complementary Approach. Universidade Católica Editora Palma de Cima, Lisboa, 2013.
- [Federico et al. 2003] Federico F., Silvagni G. and Volpi F. Scour Vulnerability of River Bridge Piers. *ASCE Journal of Geotechnical and Geoenvironmental Engineering*, Vol. 129(10), pp. 890–899, Oct. 2003.
- [Federico, 2010] Federico, F. Mechanical effects of floods on river bridge pier foundations. Presented at the 34th international symposium on bridge and structural engineering, Venice, 2010.
- [Fukui and Nishitani, 2002] Fukui J. and Nishitani M. Survey of Bridge Damages due to a Heavy Rain in the Northern Part of Kanto Region, Japan. Presented at the First

- International Conference on Scour of Foundations, TexasA&MUniversity, College Station, Texas, USA, November 17-20, pp. 47-56, 2002.
- [Gouvernec, 2007], Gouvernec S. Failure envelopes for offshore shallow foundations under general loading. *Geotechnique* 57(9), pp. 715–728, 2007.
- [Govindasamy et al., 2013] Govindasamy A.V., Briaud J.L., Kim D., Oliveira F., Gardoni P. and Delphia J. Observation Method for Estimating Future Scour depth at Existing Bridges. *Journal of Geotechnical and Geoenvironmental Engineering*. Vol.139 (7), pp.1165-1175, 2013.
- [Ghosn et al., 2003] Ghosn M., Moses F. and Wang J. Design of Highway Bridges for Extreme Events. NCHRP Report 489. Transportation Research Board of the National Academies, Washington, D.C., 2003.
- [Hajdin, 2008] Hajdin R. KUBA 4.0 – The Swiss road structure management system. International Bridge and Structure Management: 10th International Conference on Bridge and Structure Management, Buffalo, IBSMC08-027, pp. 47-62, 2008.
- [Hansen, 1970] Hansen, J. B. A revised and extended formula for bearing capacity. *Geoteknisk Inst., Bulletin*, Vol. 28, pp.5-11, 1970.
- [Hsieh et al., 2010] Hsieh K.H., Lee W.F. and Wang C.C. Bridge Foundation Failures During Typhoon Morakot in Taiwan. Presented at the 4th Japan-Taiwan Joint Workshop on Geotechnical Hazards from Large Earthquakes and Heavy Rain falls, Sendai, Japan, October 25-28, 2010.
- [Hsu and Mo, 2010] Hsu T.T.C. and Y.L. Mo. Unified theory of concrete structures. John Wiley & Sons Inc., United Kingdom, 2010.
- [Imhof, 2004] Imhof D. Risk assessment of existing bridge structures. PhD Thesis. University of Cambridge, UK, 2004.
- [JBA, 2004] JBA Consulting. Scour & Flood Risk at railway structures Report prepared for Railway Safety & Standards Board, Project No. T112, Skipton, North Yorkshire, U.K., 2004.
- [Ji and Julien, 2005] Ji U., Julien P. Typhoon Maemi and Impacts on Lower Nakdong River, South Korea, *Proc. Hydrology Days*, pp. 103–110, 2005.
- [Johnson and Ayyub, 1992] Johnson P. A. and Ayyub, B. M. Assessing time-variant bridge reliability due to pier scour. *Journal of Hydraulic Engineering ASCE*, 118(6), pp. 887-903, 1992.

- [Johnson and Dock, 1998] Johnson P.A. and Dock A.D. Probabilistic bridge scour estimates. *Journal of Hydraulic Engineering ASCE* 124(7): pp. 750–754, 1998.
- [Jovanović, 2006] Jovanović, M. Risk assessment of pier scour, *Vodoprivreda*, Vol. 38, no. 4-6, 2006, pp. 167-179, 2006.
- [JCSS, 2002] The Joint Committee on Structural Safety. Probabilistic Model Code 2002. http://www.jcss.byg.dtu.dk/Publications/Probabilistic_Model_Code.
- [Khelifa et al., 2013] Khelifa A., Garrow L.A., Higgins M.J. and Meyer M.D. Impacts of climate change on scour-vulnerable bridges: Assessment based on Hyrisk. *Journal of infrastructure systems* (19): pp. 138 – 146, 2013.
- [Ko et al., 2012] Ko Y.Y., Chiou J.S., Tsai Y.C. and Chen C.H. An Evaluation on Flood Resistant Capacity of Scoured Bridges A Case Study of the Shuang-Yuan Bridge in Taiwan. ICSE6 Paris - August 27-31, 2012.
- [Kothyari et al., 2007] Kothyari U. C., Hager W. H., and Oliveto G. Generalized approach for clear-water scour at bridge foundation elements. *J. Hydr. Engng.*, Vol.133(11), 1229–1240, 2007.
- [Krykova, 2003] Krykova I. Msc. Thesis: Evaluating of path-dependent securities with Low discrepancy methods. Worcester Polytechnic institute, December 2003.
- [Lagasse et al., 2010] Lagasse P. F., Clopper P. E., Zevenbergen L. W., Spitz W. J. and Girard L. G. Effects of debris on bridge pier scour, NCHRP Report 653, Transportation Research Board of the National Academies, Washington, D.C., 2010. onlinepubs.trb.org/onlinepubs/nchrp/nchrp_rpt_653.pdf.
- [Lagasse et al., 2013] Lagasse P. F., Ghosn M., Johnson P.A., Clopper P. E. and Zevenbergen L. W. NCHRP Report 24-34: Risk-based approach for bridge scour. Transportation Research Board of the National Academies, Washington, D.C., 2011. http://onlinepubs.trb.org/onlinepubs/nchrp/docs/NCHRP24-34_FR.pdf.
- [Lee et al., 2013] Lee W. F., Cheng T. T., Huang C. K., Yen C. I., Mei H. T., Performance of A Highway Bridge under Extreme Natural Hazards – A Case Study on Bridge Performance during 2009 Typhoon Morakot, special issue on Performance of Bridge under Critical Natural Hazards, *Journal of Performance of Constructed Facilities*, ASCE, 2013.
- [Li, 2013] Li X. Bearing Capacity Factors for Eccentrically Loaded Strip Footings Using Variational Analysis. Hindawi Publishing Corporation Mathematical

- Problems in Engineering Volume 2013, Article ID 640273, 17 pages.
<http://dx.doi.org/10.1155/2013/640273>
- [Maddison, 2012] Maddison B. Scour failure of bridges. Proceedings of the Institution Civil Engineers Forensic Engineering, Vol. 165, Issue FE1, pp 39–52, 2012.
<http://dx.doi.org/10.1680/feng.2012.165.1.39>
- [Mašović and Hajdin, 2014] Mašović S. and Hajdin R. Modelling of bridge elements deterioration for Serbian bridge inventory, Structure and Infrastructure Engineering: Maintenance, Management, Life-Cycle Design and Performance, Vol. 10 (8), pp. 976-987, 2014.
- [May et al., 2002] May R.W.P., Ackers J.C. and Kirby A.M. Manual on scour at bridges and other hydraulic structures, C551, CIRIA, London, 2002.
- [Melville and Coleman, 2000] Melville B. W., Coleman S.E. Bridge scour. Water Resources Publications, Littleton, CO., 2000.
- [Meyerhof, 1953] Meyerhof G. G. The Bearing Capacity of Foundations under Eccentric and Inclined Loads. Proc., 3rd Int. Conf. on Soil Mechanics and Foundation Engineering, Vol. 1, Zürich, 440–445, 1953.
- [Michailowski, 1997] Michailowski R.L. An estimate of the influence of soil weight on the bearing capacity using limit analysis, Soils and Foundations, Japanese Geotechnical Society, Vol. 37(4), pp. 57-64, 1997.
- [Michailowski and You, 1998] Michailowski R.L. and You L. Non-Symmetrical limit loads on strip footings, Soils and Foundations, Japanese Geotechnical Society, Vol. 38(4), pp. 195-203, 1998.
- [Mlakar et al., 2000] Mlakar P.F., Velasquez G.I., Combs P.G. and Collingsworth S.R. Bridge Performance in Hurricane Mitch. Forensic Engineering, pp. 244-252, 2000. doi: 10.1061/40482(280)27.
- [Monotti, 2004] Monotti M.N. Reinforced concrete slabs – compatibility limit design. Institute of structural engineering Swiss Federal Institute of Technology Zurich, 2004.
- [Mtenga, 2007] Mtenga P.V. Elastomeric Bearing Pads Under Combined Loading. FDOT-FHWA sponsored research project no. BC352-16, Tallahassee, Florida, USA, 2007.

- [Mulla, 2014] Mulla M.A. Evaluating Bridges with Unknown Foundations for Vulnerability to Scour: North Carolina Applies Risk-Based Guidelines. In TR News, No. 291. Transportation Research Board of the National Academies, Washington D.C., pp. 43-45, March 2014.
- [Narita et al., 1989] Narita K. and Yamaguchi H. Analysis of bearing capacity for log-spiral sliding surfaces, *Soils and Foundations*, Vol. 29(2), pp. 85-98, 1989.
- [NYSDOT, 2003] New York State Department of Transportation. Hydraulic Vulnerability Manual. New York, USA, 2003. www.dot.ny.gov/divisions/engineering/structures/manuals/hydraulics
- [Nielsen, 1984] Nielsen M.P. Limit Analysis and Concrete Plasticity, Prentice-Hall Series in Civil Engineering, Englewood Cliffs, New Jersey, 1984.
- [Oliveto, et al., 2007] Oliveto G., Di Domenico A., and Comuniello V. Temporal development of live-bed scour at bridge piers. Proc. 32nd Congress of International Association of Hydraulic Engineering Research, Venice, Italy, 2007.
- [Park et al., 2012] Park J.H., Kwak K., Lee J.H. and Chung M. Scour vulnerability evaluation of pile foundations during floods for national highway bridges. Presented at 6th ICSE, Paris, 27-31 August, 2012.
- [Palmer et al., 1999] Palmer R., Turkiyah G., Harmsen P. NCHRP Report 426: CAESAR- An Expert System for Evaluation of Scour and River Stability. Transportation Research Board of National Academies, Washington D.C., 1999
- [Pearson et al., 2002] Pearson D., Stein S. and Jones J. S. Hyrisk methodology and User Guide. Report FHWA-RD-02-XXX. Federal Highway Administration, Washington, 2002.
- [Phoon and Kulhawy, 1996] Phoon K. K. and Kulhawy F. H. On quantifying inherent soil variability. Uncertainty in the Geologic Environment, ASCE specialty conference, Madison, WI. ASCE, Reston, VA, pp. 326–40, 1996.
- [Phoon and Kulhawy, 1999] Phoon K. and Kulhawy F.H. Characterization of geotechnical variability," *Canadian Geotechnical Journal*, Vol. 36, pp. 625-639, 1999.
- [Phoon, 2008] Phoon K.K., Editor. Reliability-Based Design in Geotechnical Engineering: Computations and Applications, Taylor & Francis, London, 2008.

- [Popescu et al., 2005] Popescu R., Deodatis R. and Nobahar A. Effects of soil heterogeneity on bearing capacity. *Probabilistic Engineering Mechanics*, Vol. 20(4), pp. 324–341, 2005.
- [Prandtl, 1921] Prandtl, L. (in German) Ueber die Eindringfestigkeit (Haerte) plastischer Baustoffe und die Festigkeit von Schneiden. *Zeitschrift für angewandte Mathematik und Mechanik* 1, Band 1, 15–20, 1921.
- [Ramey and Brown, 2004] Ramey G. E. and Brown D. A. Research Project 930-585: Stability of highway bridges subject to scour, Alabama Department of Transportation, Department of Civil Engineering, Auburn University, Sept. 2004. www.eng.auburn.edu/files/centers/hrc/930-585.pdf.
- [Richardson and Davis, 2001] Richardson E.V. and Davis S.R. Evaluating Scour at Bridges, Fourth Edition. *Hydraulic Engineering Circular No.18*, FHWA–NHI–01–001–HEC–18, Washington, D.C., 2001.
- [Salençon and Pecker, 1995] Salençon J., Pecker A. - Ultimate Bearing Capacity of shallow foundations under inclined and eccentric loads. Part I: Purely Cohesive Soil. *European Journal of Mechanics*, Vol.14 (3), pp. 349-375, 1995.
- [Sheppard and Miller, 2006] Sheppard D.M. and Miller W. Live-bed Local Pier Scour Experiments, *Journal of Hydraulic Engineering - ASCE*, Vol. 132(7), pp. 635-642, 2006.
- [Sheppard et al., 2011] Sheppard D.M., Melville B.W. and Deamir H. NCHRP Report 682: Scour at Wide Piers and Long Skewed Piers, Transportation Research Board, National Academy of Science, Washington D.C, 2011. onlinepubs.trb.org/onlinepubs/nchrp/nchrp_rpt_682.pdf.
- [Sobol, 1967] Sobol I.M. Distribution of points in a cube and approximate evaluation of integrals. *U.S.S.R Comput. Maths. Math. Phys.* Vol. 7, pp. 86–112 (in English), 1967.
- [Stein et al., 2006] Stein S., Sedemera K. and GKY & Associates, Inc. Springfield, VA. Risk-Based Management Guidelines for Scour at Bridges with Unknown Foundations. NCHRP Web-Only Document no.107, Transportation Research Board of the National Academies, Washington D.C., 2006. onlinepubs.trb.org/onlinepubs/nchrp/nchrp_w107.pdf.

- [Sousa and Bastos, 2013] Sousa J.J. and Bastos L. Multi-temporal SAR interferometry reveals acceleration of bridge sinking before collapse. Published in *Natural Hazards Earth Syst. Sci.*, Vol. 13, pp. 659–667, 2013.
- [Sullivan, 2005] Sullivan M. NYDOT national bridge failure database. Structures Division of the New York State Department of Transportation, USA, 2005.
- [Taiebat and Carter, 2002] Taiebat H.A. and Carter J.P., Numerical studies of the bearing capacity of shallow foundations on cohesive soil subjected to combined loading. *Geotechnique*, Vol. 50(4), pp. 409–418, 2002.
- [Tanasić et al. 2013] Tanasic N., Ilic V. and Hajdin R. Vulnerability assessment of bridges exposed to scour. In *Transportation Research Record: Journal of Transportation Research Board*, Vol. 2360, pp. 36-44, TRB of the National Academies, Washington D.C, 2013. <http://trb.metapress.com/content/18rjl2732q50/?sortorder=asc>
- [Tanasić and Hajdin, 2014] Tanasic N. and Hajdin R. Bridge failure modes due to local scour. Presented at the 7th International Conference on Bridge Maintenance, Safety and Management IABMAS China 7-11 July, 2014. <http://www.crcnetbase.com/doi/abs/10.1201/b17063-220>
- [Terzaghi, 1943] Terzaghi, K. *Theoretical Soil Mechanics*. Wiley, New York, 1943.
- [Thompson et al., 1998] Thompson P.D., Small E.P., Johnson M. and Marshal A.M. The Pontis bridge management system. *Structural engineering International*, Vol.8, pp. 303-308, 1998.
- [Ukritchon et al., 1998] Ukritchon B., Whittle A. J. and Sloan S. W. Undrained limit analysis for combined loading of strip footings on clay. *Journal of Geotechnical and Geoenvironmental Engineering ASCE*, Vol. 124(3), pp. 265–276, 1998.
- [Vesic, 1975] Vesic A. Bearing Capacity of Shallow Foundations. In *Foundation Engineering Handbook*, H. F. Winterkorn and H. Y. Fang, eds., Van Nostrand Reinhold, New York, pp. 121–147, 1975.
- [Vrouwenvelder and Witteveen, 2003] Vrouwenvelder A.C.W.M. and Witteveen J. Plasticity Ct 4150. The plastic behavior and the calculation of the plates subjected to bending. Technical University Delft Faculty of Civil Engineering and Geosciences, 2003. homepage.tudelft.nl/p3r3s/contentsplates.pdf

- [Wu et al., 2012] Wu T-R., Wang H., Ko Y-Y., Chiou J-S., Hsieh S-C., Chen C-H., Lin C., Wang C-Y., and Chuang M-H. Forensic Diagnosis on Flood-Induced Bridge Failure, Part II- Framework of Quantitative Assessment. *Journal of Performance of Constructed Facilities*, September 10, 2012. doi:10.1061/(ASCE)CF.1943-5509.0000393.
- [Yanmaz, 2006] Yanmaz A. M. Temporal variation of clear water scour at cylindrical bridge piers. *Canadian Journal of Civil Engineering*, Vol. 33(8), pp. 1098–1102, 2006.
- [Yao et al., 2010] Yao C., Darby C., Yu O.Y., Hurlbauss S., Chang K.A., Price J., Hunt B. and Briaud. J.L. Motion Sensors for Scour Monitoring: Laboratory Experiment with a Shallow Foundation. *Proceedings of GeoFlorida 2010*, West Palm Beach, Florida. February 20–24, 2010. ASCE.

Web sources:

- [Curtis, 2011] The Dawson trail Dispatch, Curtis Marianne. “St. Adolphe bridge finally reopened“. Published 1st April 2011. <<http://mariannecurtis.wordpress.com/2011/04/01/st-adolphe-bridge-finally-reopened/>>. Accessed on 15th May 2012.
- [DisasterRelief, 2003]. DisasterRelief.org. “Massive Typhoon Maemi pounds South Korea”. Published 15th September 2003. <<http://reliefweb.int/report/republic-korea/massive-typhoon-maemi-pounds-south-korea>>. Accessed 20th April 2011.
- [Manitoba, n.d.] Government of Manitoba (Canada) website. <<http://www.gov.mb.ca/flooding/history/index.html>>. Accessed 10th May 2014.
- [RoadRisk, n.d.] Swiss Federal roads office – ASTRA <<http://www.roadrisk.ch>>
- [TKIC, n.d.] Türkiye Köprü ve İnşaat Cemiyeti website. <<http://www.tkic.org.tr/documents/caycuma.pdf>>. Accessed 10th May 2014.
- [Wairoa, n.d.]. Wairoa.net. “Cyclone Bola March 1988”. <<http://wairoa.net/bola1.htm>>. Accessed 15th March 2012.

Curriculum vitae

Nikola Tanasić was born on 16th of February 1984 in Belgrade, Serbia. He completed elementary and grammar school in Valjevo, Serbia. As the first in his class he graduated in the field of reinforced concrete bridges at the University of Belgrade, Faculty of Civil Engineering (2002 – 2007). During the last year of graduate studies he was a student demonstrator for course Soil mechanics at the Chair for Geotechnics.



Since 2007 he is a PhD student and works as a teaching assistant at the Chair for concrete structures, Institute for materials and structures at the Faculty of Civil Engineering in Belgrade. Over six years he has participated in the preparation and implementation of classes for several courses in the field of concrete structures on the undergraduate studies. He has co-supervised twenty seven bachelor graduate projects in course Design of concrete structures.

In October 2010 he has started the research on his PhD thesis with a topic “Vulnerability of reinforcement concrete bridges exposed to local scour in bridge management” as a part of the project TR36002 (2011 – 2014) founded by the Serbian Ministry of Education, Science and Technological Development.

He has co-authored one scientific paper published in international journal and one in domestic journal. He participated in the 92nd and 94th Transportation Research Board Annual Conferences in Washington D.C. in 2013 and 2015, and 7th IABMAS Conference in Shanghai 2014, with presentations of three scientific papers on the topic of his thesis.

He passed Civil engineering state exam and has six years of engineering experience. He had been assistant structural designer on several domestic projects including residential buildings, kindergarten, foundations of industrial facilities and water purification plants.

Nikola Tanasić is fluent in written and spoken English, and he is novice in German. He is married and has no children yet.

Биографија аутора

Никола Танасић је рођен 16.02.1984. у Београду у Србији. Основну и средњу школу је завршио у Ваљеву. На Грађевинском факултету Универзитета у Београду (2002 - 2007) дипломирао је као први у генерацији, на тему армиранобетонских мостова. Током последње године студија био је студент демонстратор на предмету Механика тла на катедри за Геотехнику.



Од 2007. године је студент докторских студија и ради као асистент на катедри за Бетонске конструкције на Институту за материјале и конструкције на Грађевинском факултету у Београду. Активно учествује у припреми и извођењу вежби као и консултацијама на предметима са групације бетонске конструкције. Био је коментор приликом израде 27 синтезних пројеката студената на предмету Пројектовање и грађење бетонских конструкција.

У октобру 2010 године је почео рад на својој докторској тези чија је тема „Управљање армиранобетонским мостовима у контексту њихове угрожености локалном ерозијом речног дна“ која је део пројекта ТР36002 (2011 – 2014) финансираног од стране Министарства образовања, науке и технолошког развоја Републике Србије.

Био је коаутор на једном научном чланку објављеном у интернационалном часопису и једном чланку у домаћем часопису. Учествовао је на 92-гој и 94-тој годишњој конференцији „TRB“ у Вашингтону јануара 2013 и 2015 год., и на 7-мој конференцији „IABMAS“ у Шангају у јулу 2014 године, са презентацијама три научна чланка на тему своје дисертације.

Има положен стручни испит за грађевинске инжењере за пројектовање конструкција. Током 6 година инжињерске праксе учествује на изради пројектне документације, графичких прилога, идејних и главних пројеката конструкција у Србији међу којима су стамбене зграде, обданиште, фундаменти индустријских објеката, постројења за пречишћавање воде.

Никола Танасић течно говори и прича енглески језик и има почетни ниво немачког језика. Ожењен је и тренутно нема деце.

Прилог 1.

Изјава о ауторству

Потписани: Никола Танасић, дипл.грађ.инж.

Број уписа: 2/07

Изјављујем

да је докторска дисертација под насловом:

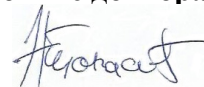
VULNERABILITY OF REINFORCED CONCRETE BRIDGES TO LOCAL SCOUR
IN BRIDGE MANAGEMENT

(на српском језику: УПРАВЉАЊЕ АРМИРАНОБЕТОНСКИМ МОСТОВИМА У
КОНТЕКСТУ ЊИХОВЕ УГРОЖЕНОСТИ ЛОКАЛНОМ ЕРОЗИЈОМ
РЕЧНОГ ДНА)

- резултат сопственог истраживачког рада,
- да предложена дисертација у целини ни у деловима није била предложена за добијање било које дипломе према студијским програмима других високошколских установа,
- да су резултати коректно наведени и
- да нисам кршио ауторска права и користио интелектуалну својину других лица.

У Београду, јануар 2015.

Потпис докторанда



Прилог 2.

Изјава о истоветности штампане и електронске верзије докторског рада

Име и презиме аутора: Никола Танасић, дипл.грађ.инж.

Број уписа: 2/07

Студијски програм: Докторске студије - Грађевинарство

Наслов рада: VULNERABILITY OF REINFORCED CONCRETE BRIDGES TO LOCAL SCOUR IN BRIDGE MANAGEMENT

Наслов рада на српском језику: УПРАВЉАЊЕ АРМИРАНОБЕТОНСКИМ МОСТОВИМА У КОНТЕКСТУ ЊИХОВЕ УГРОЖЕНОСТИ ЛОКАЛНОМ ЕРОЗИЈОМ РЕЧНОГ ДНА

Ментор: Др Раде Хајдин, ванредни професор
Грађевински факултет, Универзитет у Београду,

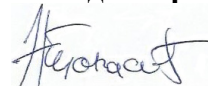
Потписани: Никола Танасић, дипл.грађ.инж.

Изјављујем да је штампана верзија мог докторског рада истоветна електронској верзији коју сам предао за објављивање на порталу Дигиталног репозиторијума Универзитета у Београду.

Дозвољавам да се објаве моји лични подаци везани за добијање академског звања доктора наука, као што су име и презиме, година и место рођења и датум одбране рада.

Ови лични подаци могу се објавити на мрежним страницама дигиталне библиотеке, у електронском каталогу и у публикацијама Универзитета у Београду.

Потпис докторанда



У Београду, јануар 2015.

Прилог 3.

Изјава о коришћењу

Овлашћујем Универзитетску библиотеку „Светозар Марковић“ да у Дигитални репозиторијум Универзитета у Београду унесе моју докторску дисертацију под насловом: VULNERABILITY OF REINFORCED CONCRETE BRIDGES TO LOCAL SCOUR IN BRIDGE MANAGEMENT (на српском језику: УПРАВЉАЊЕ АРМИРАНОБЕТОНСКИМ МОСТОВИМА У КОНТЕКСТУ ЊИХОВЕ УГРОЖЕНОСТИ ЛОКАЛНОМ ЕРОЗИЈОМ РЕЧНОГ ДНА) која је моје ауторско дело.

Дисертацију са свим прилозима предао сам у електронском формату погодном за трајно архивирање.

Моју докторску дисертацију похрањену у Дигитални репозиторијум Универзитета у Београду могу да користе сви који поштују одредбе садржане у одабраном типу лиценце Креативне заједнице (Creative Commons) за коју сам се одлучио.

1. Ауторство

2. Ауторство - некомерцијално

3. Ауторство – некомерцијално – без прераде

4. Ауторство – некомерцијално – делити под истим условима

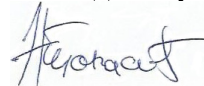
5. Ауторство – без прераде

6. Ауторство – делити под истим условима

(Молимо да заокружите само једну од шест понуђених лиценци, кратак опис лиценци дат је на полеђини листа).

У Београду, јануар 2015.

Потпис докторанда



1. Ауторство - Дозвољавате умножавање, дистрибуцију и јавно саопштавање дела, и прераде, ако се наведе име аутора на начин одређен од стране аутора или даваоца лиценце, чак и у комерцијалне сврхе. Ово је најслободнија од свих лиценци.

2. Ауторство – некомерцијално. Дозвољавате умножавање, дистрибуцију и јавно саопштавање дела, и прераде, ако се наведе име аутора на начин одређен од стране аутора или даваоца лиценце. Ова лиценца не дозвољава комерцијалну употребу дела.

3. Ауторство - некомерцијално – без прераде. Дозвољавате умножавање, дистрибуцију и јавно саопштавање дела, без промена, преобликовања или употребе дела у свом делу, ако се наведе име аутора на начин одређен од стране аутора или даваоца лиценце. Ова лиценца не дозвољава комерцијалну употребу дела. У односу на све остале лиценце, овом лиценцом се ограничава највећи обим права коришћења дела.

4. Ауторство - некомерцијално – делити под истим условима. Дозвољавате умножавање, дистрибуцију и јавно саопштавање дела, и прераде, ако се наведе име аутора на начин одређен од стране аутора или даваоца лиценце и ако се прерада дистрибуира под истом или сличном лиценцом. Ова лиценца не дозвољава комерцијалну употребу дела и прерада.

5. Ауторство – без прераде. Дозвољавате умножавање, дистрибуцију и јавно саопштавање дела, без промена, преобликовања или употребе дела у свом делу, ако се наведе име аутора на начин одређен од стране аутора или даваоца лиценце. Ова лиценца дозвољава комерцијалну употребу дела.

6. Ауторство - делити под истим условима. Дозвољавате умножавање, дистрибуцију и јавно саопштавање дела, и прераде, ако се наведе име аутора на начин одређен од стране аутора или даваоца лиценце и ако се прерада дистрибуира под истом или сличном лиценцом. Ова лиценца дозвољава комерцијалну употребу дела и прерада. Слична је софтверским лиценцама, односно лиценцама отвореног кода.